

## Continuous Fractionation of Polymers in Solution by Thermal Diffusion

IVO KÖSSLER and HELENA KRAUSEROVÁ,  
*Institute of Physical Chemistry, Czechoslovak Academy of Sciences and Institute of Physical Chemistry, Charles University, Prague, Czechoslovakia*

### Synopsis

The possibility of carrying out continuous fractionation of polymers by the thermodiffusion method was investigated. From the working space of a plate-type column, fractions of polymer were continuously withdrawn simultaneously with filling of the column with fresh solution from a storage vessel. After equilibrium had been established, the distributions of molecular weights of the fractions were determined by a modified Baker and Williams method. In the same apparatus, and at constant temperature and concentration, fractionation, which may be characterized by a limiting viscosity number, is dependent on the total rate of withdrawal and on the ratios of amounts of polymer withdrawn in various places on the column.

### INTRODUCTION

After the first papers on thermal diffusion of polymers in solution, the separation of polymers according to molecular weight by thermal diffusion was investigated in order to explore the possibility of establishing distribution curves of molecular weights<sup>1-6</sup>. The method, based on the dependence of the thermal diffusion coefficient on molecular weight,<sup>7-9</sup> is not as successful as the method of column fractionation.<sup>10</sup>

In this paper the use of thermal diffusion for the continuous fractionation of polymers is discussed.<sup>11</sup>

### EXPERIMENTAL

#### Polymers

A 1.1% solution in benzene of a poly(methyl methacrylate) with limiting viscosity number at 25°C. of  $[\eta] = 1.34$  was used.

#### Apparatus

For the thermal diffusion, a plate-type apparatus without reservoirs was used;<sup>4</sup> the height of its working space was 150 cm., the width 7.35 cm., and the thickness 0.05 cm., the total volume thus being 55 cm.<sup>3</sup>. It was possible to introduce the solution of the polymer continuously at different

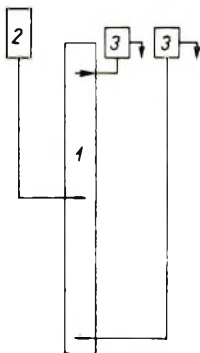


Fig. 1. Apparatus for continuous fractionation: (1) working space; (2) storage vessel; (3) pump.

points into the working space or continuously to withdraw the polymer solution (Fig. 1). The withdrawal was performed by means of small pumps using all-glass syringes with a valve system. The levels of the solution in the storage vessel and in the pumps were maintained equal to the level of the liquid in the working space. The take-off could be varied from 0.5 to 40 cm.<sup>3</sup>/hr. The same amount of original solution as that taken from the column was supplied from the storage vessel containing the storage solution of the polymer. It was also possible to add a definite quantity of pure solvent at an arbitrary place in the working space.

#### Determination of the Limiting Viscosity Numbers and Distribution of Molecular Weights

Samples of the polymer solution withdrawn from various places of the apparatus (denoted as fractions 1-6) were characterized by limiting viscosity numbers and distribution curves. The distribution of molecular weights was determined by the method of Baker and Williams<sup>11</sup> as modified by Poláček.<sup>12</sup>

A solution of poly(methyl methacrylate) at a concentration of 1.1 g./100 ml. was fractionated in the described apparatus with wall temperatures of 15 and 50°C. respectively, i.e. with a temperature gradient of 700° C./cm. In experiment 1, the fractions were withdrawn at the rate of 5 ml./hr. in the upper part of the column and at 14 ml./hr. at the bottom, or 19 ml./hr. total; the polymer solution from the storage vessel was introduced into the working space to a height of 90 cm. In experiment 2 the fractions were withdrawn from six places on the column at heights of 0, 18, 36, 60, 114, and 150 cm., at rates of 2.2, 2.5, 2.2, 2.2, 2.4, and 2.8 ml./hr., respectively, or 14.3 ml./hr. total. The inlet was at a height of 90 cm.

### RESULTS

Figure 2 presents the curves of the polymer-solvent and polymer-polymer separation in experiment 1 from the beginning up to the time at

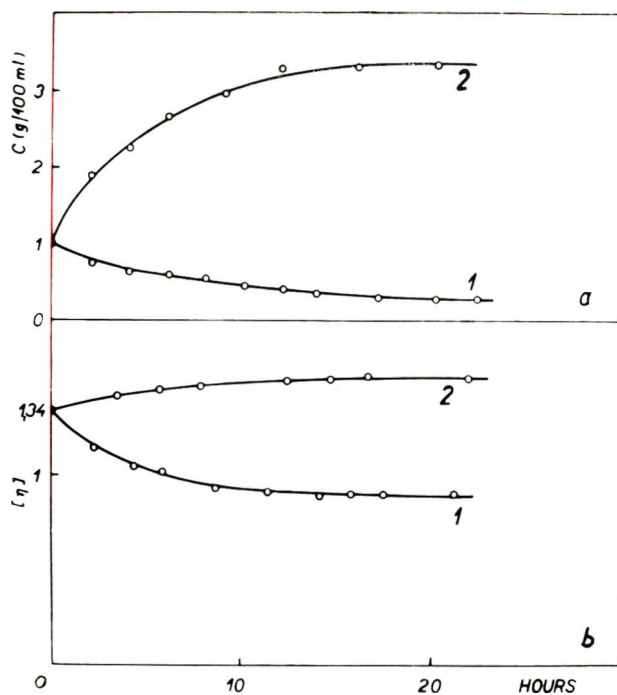


Fig. 2. Equilibration of (a) polymer-solvent separation and (b) polymer fractionation processes: (1) upper fraction (2) bottom fraction.

which a stationary state of the continuous process was reached. Differential distribution curves of the fractions from experiment 1 are presented in Figure 3 and of fractions 2, 3, and 6 from experiment 2 in Figure 4. The distribution curves of fractions 4 and 5 lie between the curves of fractions 3 and 6. The values characterizing the fractions are summarized in Table I.

TABLE I

Expt. no.	Fraction	Levels of inlet and outlet, cm.	Concn., g./100 ml.	$[\eta]_{ar}$	Amount of polymer, g./hr.	% of total
I	Original solution	90	1.100	1.34	—	100
	1	150	0.0302	0.92	0.0423	20
	2	0	3.352	1.45	0.1676	80
II	Original solution	90	1.100	1.34	—	100
	1	150	0.0197	0.70	0.0004	0.28
	2	114	0.160	1.02	0.0038	2.4
	3	60	0.702	1.13	0.0154	9.5
	4	36	0.762	1.19	0.0168	10.27
	5	18	1.33	1.28	0.0332	20.5
6	0	4.153	1.56	0.0914	57.0	

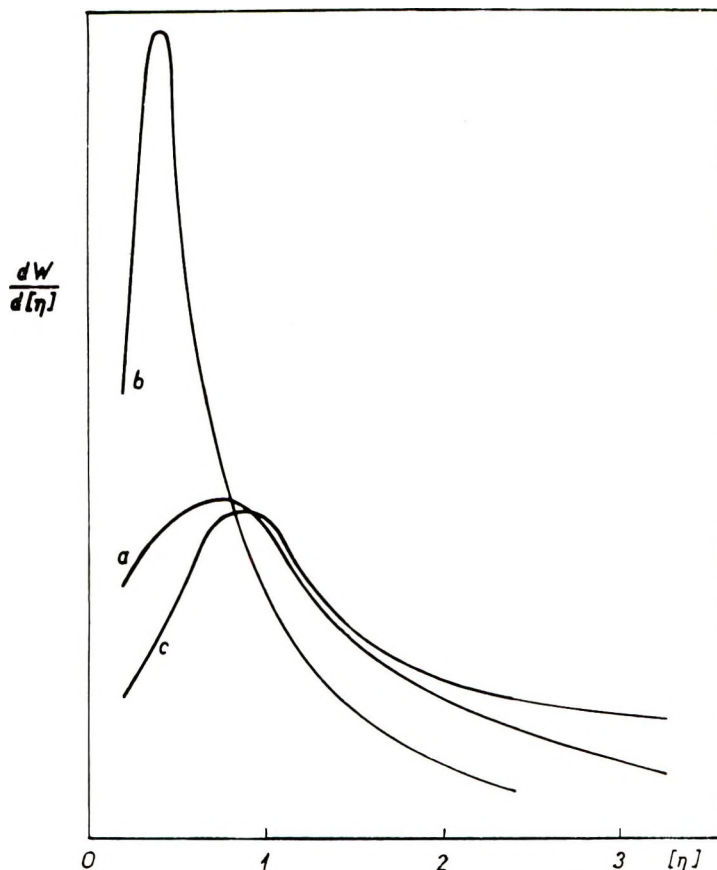


Fig. 3. Differential distribution curves of: (a) original polymer; (b) fraction 1 (upper); (c) fraction 2 (lower).

With the arrangement of experiment 1 the dependence of the fractionation coefficient (defined as the ratio of limiting viscosity number of the fraction  $[\eta]$  to limiting viscosity number of the original polymer  $[\eta]_0$ ) on the total take-off was measured. The dependence of the fractionation coefficient of the upper fraction on total take-off rate of the polymer at a constant ratio of take-off rates from the top and bottom parts is shown in Figure 5.

### DISCUSSION

The continuous thermal diffusion process in polymer solutions is from several points of view, analogous to that of oil separations.<sup>13,14</sup> Both cases involve systems of  $n$  components. In the case of polymer fractionation, however, one component (solvent) is in excess and has a markedly lower molecular weight than the other components. Thus, in the thermodiffusion of polymers, two effects are recognized: polymer-solvent separation and



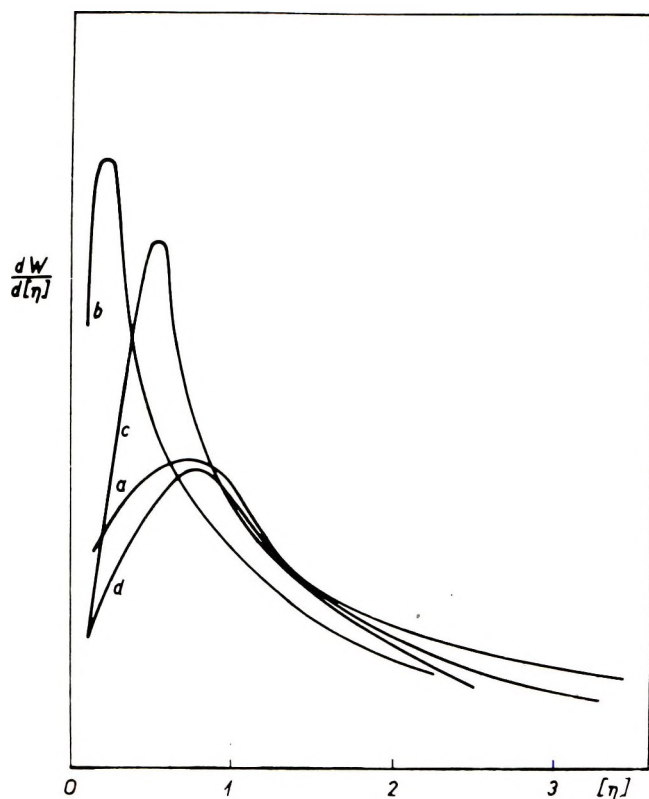


Fig. 4. Differential distribution curves of: (a) original polymer; (b) fraction 2; (c) fraction 3; (d) fraction 6.

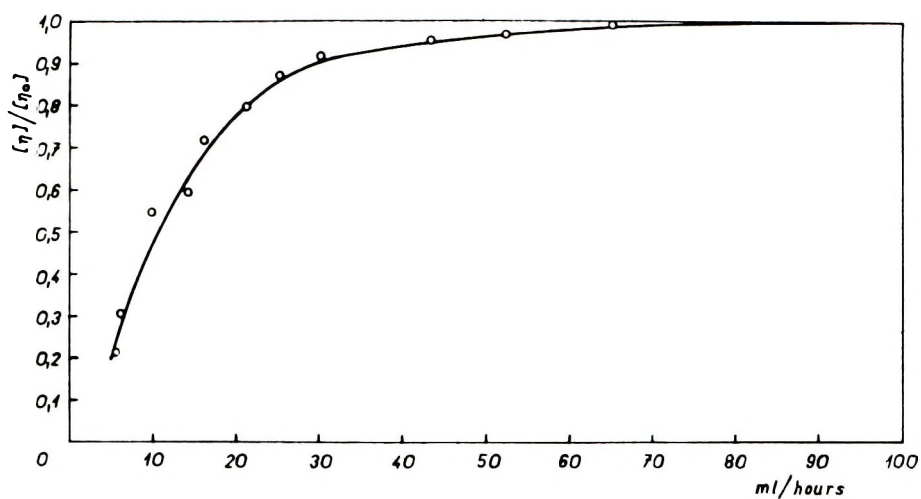


Fig. 5. Dependence of fractionation coefficient  $[\eta]/[\eta]_0$  on the total rate of withdrawal.

polymer-polymer fractionation. Great variations in solution viscosities along the column exist as a result of the polymer-solvent separation effect. Another complication may arise from the observed inversion effect.<sup>9</sup>

The degradation and decomposition of macromolecules may also take place during thermodiffusion fractionation. These processes occur especially with polymers capable of oxidative degradation. A small amount of degradation was, however, also observed in the case of poly(methyl methacrylate). The decrease in molecular weights of the last fractions removed, using the modified Baker-Williams fractionation method, is evidence of a degradation process involving formation of peroxide-bonded crosslinks with successive decomposition steps.<sup>15</sup>

The molecular weight distributions of individual fractions in experiments 1 and 2 are relatively broad and asymmetrical. The fractions contain a progressively increasing amount of macromolecules of higher molecular weight, as is evident from both the values of limiting viscosity numbers at the maxima of the curves  $[\eta]_{\max}$  and from the average limiting viscosity number  $[\eta]_{\text{av}}$  (see Table I).

Both separation and fractionation are at constant temperature and concentration, dependent on the number of outlets and the ratio of withdrawal rates of individual fractions. At total withdrawal rates close to zero both separation and fractionation effectiveness are determined by the column dimensions, wall temperatures, and concentration. With increasing rate of withdrawal the value of fractionation coefficient (Fig. 5) increases; with a withdrawal rate of 100 ml./hr., as in experiment 1, the coefficient is close to 1.

The total input of energy in the thermodiffusion process is very large. With a temperature difference of 35°C. and a mean temperature of 32.5°C., it was about 17,000 kcal./g. polymer with a molecular weight distribution as in Figure 4.

The results indicate that the efficiency for continuous fractionation of polymers by thermal diffusion is low in comparison with other methods of polymer fractionation. Molecular weight distributions of fractions obtained in a one-stage fractionation are broad. From the analogy with attempts to separate oils, it may be concluded that a multistage fractionation would lead to more homogeneous fractions but that the efficiency would be very low.

## References

1. Debye, P., and A. M. Bueche, in *High Polymer Physics*, H. A. Robinson, Ed. Chemical Publishing Co., New York 1948.
2. Langhammer, G., H. Pfenig, and K. Quitzch, *Z. Elektrochem.*, **62**, 458 (1958).
3. Kössler, I., and J. Krejsa, *J. Polymer Sci.*, **35**, 308 (1959).
4. Kössler, I., and M. Štolka, *J. Polymer Sci.*, **44**, 213 (1960).
5. Krejsa, J., *Makromol. Chem.*, **33**, 244 (1959).
6. Kössler, I., and J. Krejsa, *J. Polymer Sci.*, **57**, 509 (1962).
7. Ham, J. S., *J. Appl. Phys.*, **31**, 1853 (1960).
8. Khazanovich, T. N., *Dokl. Akad. Nauk SSSR*, **157**, 165 (1964).

9. Kössler, I., and J. Krejsa, *J. Polymer Sci.*, **29**, 69 (1958).
10. Baker, C. A., and R. J. P. Williams, *J. Chem. Soc.*, **1956**, 2352.
11. Krauserová, H., Dissertation, Chemical Department of Charles University, Prague, 1962.
12. Poláček, J., *Collection Czech. Chem. Commun.*, **28**, 1838 (1963).
13. Frazier, D., *Ind. Eng. Chem., Proc. Design Devel.*, **1**, 237 (1962).
14. Graselli, R., and D. Frazier, *Ind. Eng. Chem., Proc. Design Devel.*, **1**, 241 (1962).
15. Poláček, J., I. Kössler, and J. Vodenhual, *J. Polymer Sci. A*, **3**, 2511 (1965).

### Résumé

On examine la possibilité d'effectuer un fractionnement continu des polymères en employant une méthode de thermodiffusion. En travaillant avec une colonne à plateaux, les fractions de polymère sont continuellement éliminées pendant que la colonne est remplie avec une solution fraîche à partir d'un récipient de stockage, lorsque l'équilibre est atteint, on a déterminé le poids moléculaire des fonctions par une méthode modifiée de Baker et Williams. Dans le même appareil, à température et concentration constantes, le fractionnement, qui peut être caractérisé par un indice viscosimétrique limite, dépend de la vitesse totale de prélèvement et des rapports des quantités de polymères soutirées à divers endroits de la colonne.

### Zusammenfassung

Die Möglichkeit, eine kontinuierliche Fraktionierung von Polymeren nach der Thermodiffusionsmethode auszuführen, wurde untersucht. Aus dem Arbeitsraum einer Säule vom Plattentyp wurden kontinuierliche Polymerfraktionen entnommen, während gleichzeitig die Säule aus einem Vorratsgefäß mit frischer Lösung gefüllt wurde. Nach der Gleichgewichtseinstellung wurde das Molekulargewicht der Fraktionen nach einer modifizierten Baker-Williams-Methode bestimmt. Im gleichen Apparat und bei konstanter Temperatur und Konzentration ist die Fraktionierung, welche durch eine Grenzviskositätszahl charakterisiert werden kann, von der totalen Entnahmegeschwindigkeit und dem Verhältnis der an verschiedenen Stellen der Säule entnommenen Polymermenge abhängig.

Received January 28, 1965

Revised June 22, 1965

Prod. No. 4775A

## Polymerization of $\alpha$ -Halogenated *p*-Xylenes With Base

H. G. GILCH\* and W. L. WHEELWRIGHT, *Research and Development Department, Plastics Division, Union Carbide Corporation, Bound Brook, New Jersey*

### Synopsis

Various  $\alpha$ -halo-*p*-xylenes have been polymerized with base yielding *p*-xylylene polymers. The reaction involves a 1,6-dehydrohalogenation to give a xylylene which then polymerizes.  $\alpha, \alpha'$ -Dichloro-*p*-xylene forms poly- $\alpha$ -chloro-*p*-xylylene and polymers containing stilbene units;  $\alpha, \alpha, \alpha', \alpha'$ -tetrachloro-*p*-xylene gives poly- $\alpha, \alpha, \alpha', \alpha'$ -trichloro-*p*-xylylene; alkyl, aryl, and halogen ring-substituted  $\alpha$ -chloro-*p*-xylenes give the corresponding ring-substituted poly-*p*-xylylenes. The more halogens in the  $\alpha$  positions (up to five), the weaker the base necessary for dehydrohalogenation. Sodium hydroxide in methanol will polymerize tetrachloro-*p*-xylene, while potassium *tert*-butoxide in refluxing *p*-xylene is necessary to polymerize  $\alpha$ -chloro-*p*-xylenes. Stilbenes are formed when  $\alpha$ -halo-*p*-xylenes are reacted with potassium *tert*-butoxide in polar solvents such as dimethyl sulfoxide.

### INTRODUCTION

Thiele and Balhorn<sup>1</sup> prepared the first poly-*p*-xylylenes more than sixty years ago. Since Szwarc's<sup>2</sup> discovery of the formation of *p*-xylylene by the pyrolysis of *p*-xylene, the chemistry of *p*-xylylenes has been more thoroughly investigated. The field has been reviewed by Errede and Szwarc.<sup>3</sup> Recently Gorham<sup>4</sup> showed a commercially interesting method for the production of poly-*p*-xylylene films and coatings. However, as far as is known, no systematic investigation of the reaction of  $\alpha$ -halo-*p*-xylenes with base has been reported.

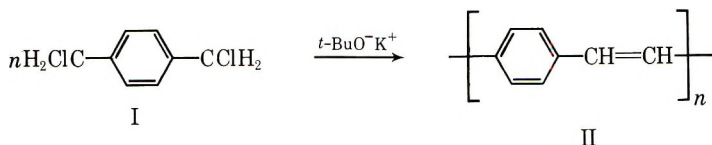
### DISCUSSION AND RESULTS

#### Reactions of $\alpha, \alpha'$ -Dihalo-*p*-Xylenes with Base

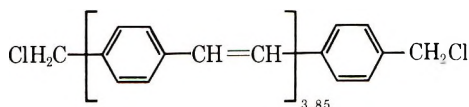
During an investigation of the reaction of halogenated hydrocarbons with base,  $\alpha, \alpha'$ -dichloro-*p*-xylene (I) was reacted with potassium *tert*-butoxide. The rapid exothermic reaction yielded a bright yellow solid (II) which was insoluble in all common solvents and exhibited remarkable heat stability. No color change was observed when the product was heated to 280°C.; between 280 and 320°C. the product darkened; at higher

\* Present address: Farbenfabriken Bayer A.G., Werk Uerdingen, Wissenschaftliches Hauptlaboratorium, Krefeld, Germany.

temperatures the product turned brown without melting. The bright yellow color, strong ultraviolet fluorescence, the ultraviolet and infrared spectra were consistent with the conjugated structure II. McDonald

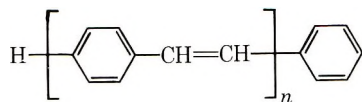


and Campbell<sup>5</sup> have prepared polymer II by a Wittig reaction; this material has identical properties to our product. After extraction with refluxing xylene to remove all starting material, the product contained 12.5% chlorine. If the chlorine content were due to endgroups, the average structure should be:



III

Recently Zidaroff<sup>6</sup> suggested a similar structure for a reaction product from I and sodium amide in liquid ammonia. Drefahl and Ploetner<sup>7</sup> have prepared polyphenylpolyenes of the general structure IV. For  $n = 3$ ,

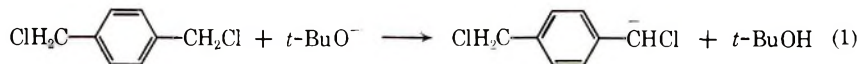


IV

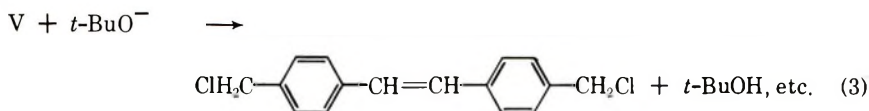
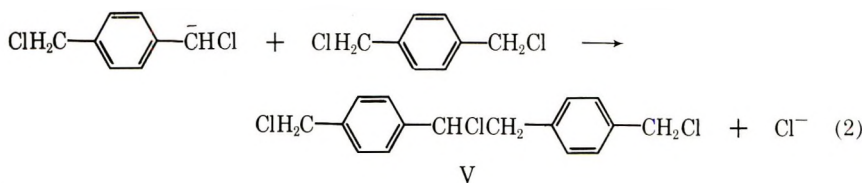
the compound is yellow (m.p. 330°C.); for  $n = 4$ , it is orange (m.p. 350°C.).

Polymer III can be formed by the coupling of carbenes<sup>8,9</sup> or by the condensation of a carbanion with a benzyl chloride group.<sup>10</sup> If the polymer is formed via a carbene, one should be able to trap the carbene intermediate with cyclohexene or tetramethylethylene. Reactions carried out with a large excess of these trapping agents did not yield any cyclopropane derivatives.

Hauser<sup>10</sup> has shown that benzyl chloride can be coupled in the presence of sodium amide in liquid ammonia. A bifunctional compound such as  $\alpha, \alpha'$ -dichloro-*p*-xylene could react in a similar manner to form polymer III as shown in eqs. (1)–(3). This polycondensation is a stepwise reac-

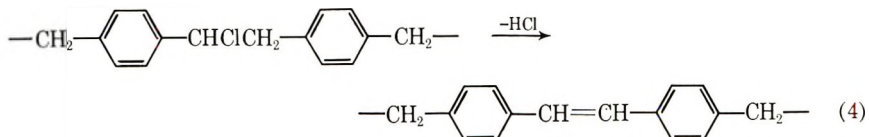


tion; therefore, the polymer molecular weight should depend upon conversion. If a small percentage of the theoretical amount of base were reacted, oligomers should be formed. To distinguish between addition polymerization and stepwise polycondensation, a solution of  $\alpha, \alpha'$ -dichloro-

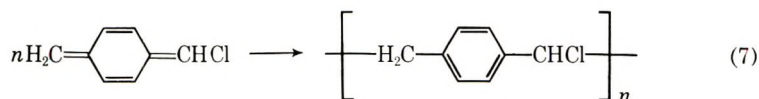
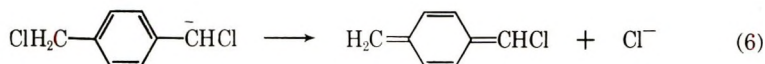
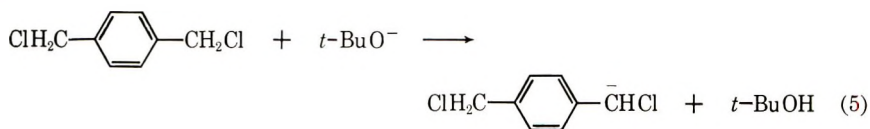


*p*-xylene was reacted with 30% of the theoretical amount of potassium-*tert*-butoxide. The reaction yields the same insoluble product (III) as with a large excess of base. This indicates that a polycondensation reaction can be excluded.

When a dilute solution of potassium *tert*-butoxide in *tert*-butanol is slowly added to an excess of a solution of  $\alpha, \alpha'$ -dichloro-*p*-xylene, a white solid is formed which analyzes correctly for poly- $\alpha$ -chloro-*p*-xylylene. When the polymer is heated or treated with additional base, it turns bright yellow and eliminates hydrogen chloride [eq. (4)]. The resulting product has the same physical properties as III and contains 12.8% chlorine.



The formation of poly- $\alpha$ -chloro-*p*-xylylene is consistent with the mechanism shown in eqs. (5)–(7). The anion formed by reaction of I



with base eliminates a chloride ion in the 6 position, forming the relatively stable chloro-*p*-xylylene which in turn polymerizes.

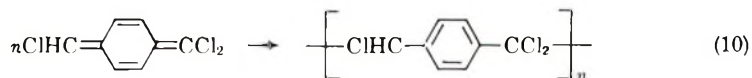
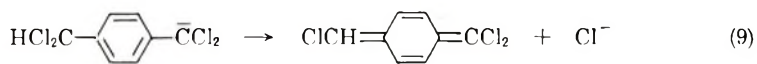
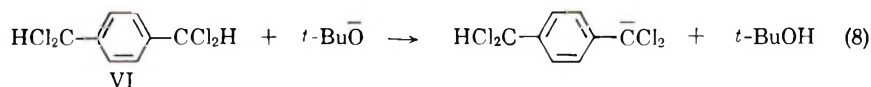
$\alpha, \alpha'$ -Dichloro-*p*-xylene has been reacted with weaker bases than potassium *tert*-butoxide. With sodium methoxide the dimethyl ether of *p*-xylenediol is isolated. A yellow solid identical with III is isolated when  $\alpha, \alpha'$ -dichloro-*p*-xylene is reacted in a 50/50 (w/w) melt of NaOH-KOH at 300°C.



Reactions of  $\alpha, \alpha'$ -dibromo- and  $\alpha, \alpha'$ -diiodo-*p*-xylene and their ring-substituted derivatives with potassium *tert*-butoxide yield poly-*p*-xylylenes as well.

### Reactions of $\alpha, \alpha, \alpha', \alpha'$ -Tetrachloro-*p*-Xylene with Base

$\alpha, \alpha, \alpha', \alpha'$ -Tetrachloro-*p*-xylene (VI) reacts more rapidly with base than  $\alpha, \alpha'$ -dichloro-*p*-xylene. When the reaction is run so that there is never a large excess of potassium *tert*-butoxide present, a colorless product, soluble in hot chloronaphthalene and analyzing correctly for poly-trichloro-*p*-xylylene, can be isolated [eqs. (8)–(10)]. When the polymer is prepared

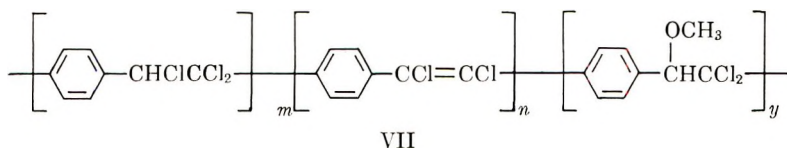


with an excess of base, it is yellowish, insoluble in chloronaphthalene, and analyzes for 1–2% less chlorine, presumably due to dehydrochlorination.

Sodium methoxide and sodium hydroxide in methanol also polymerize tetrachloro-*p*-xylene. Here a tetrahydrofuran-soluble polymer is obtained.

When the polymerization is carried out in mixtures of *tert*-butanol and methanol, reduced viscosities and conversions increase with higher concentrations of *tert*-butanol. The decrease at 100% *tert*-butanol can be caused by the low solubility of sodium hydroxide. The results are shown in Table I.

The chlorine analyses of these polymers are low and the carbon contents high compared to poly- $\alpha, \alpha, \alpha'$ -trichloro-*p*-xylylene, as shown in Table II. This can be explained by partial substitution of chlorine atoms with methoxy groups or by elimination of hydrogen chloride to form stilbene units. It was shown by the Zeisel method that methoxy groups are present (about 1% for polymer 1), but the exact chemical structure of these polymers has not been determined. The structure VII is consistent with experimental results:



where  $n$  and  $y$  are small. Clear films of polymer 2 (Table I) were cast from tetrahydrofuran. These films have a glass transition of 160°C. (determined by subjecting the samples to a 1% stress cycle and heating at 1.5°C./min., using an Instron tensile tester), a room temperature modulus of 350,000 psi, and a tensile strength of 6,500 psi. Films compression-



TABLE I  
 Polymerization of  $\alpha, \alpha', \alpha', \alpha'$ -Tetrachloro-*p*-Xylene with Sodium Hydroxide

Polymer	Solvent ratio (volume)		Yield of polymer, %	Reduced viscosity <sup>a</sup>
	MeOH, %	<i>t</i> -BuOH, %		
Equimolar amount of base				
1	100	0	20	1.2
2	95	5	24	1.1
3	90	10	24	1.1
4	40	60	48	2.4
5	20	80	48	3.4
6	10	90	53	3.2
7	5	95	58	3.4
8	0	100	17	Insoluble
Double molar amount of base				
9	100	0	40	1.0
10	50	50	73	1.1
11	10	90	82	0.8
12	0	100	12	Insoluble

<sup>a</sup> 0.2% solution in tetrahydrofuran at 20°C.

TABLE II  
 Elemental Analyses

Polymer	C, %	H, %	Cl, %
1	50.57	2.36	45.07
3	50.55	2.60	45.10
7	49.84	2.44	47.28
8	45.90	2.71	50.54
PTX <sup>a</sup>	46.30	2.43	51.27

<sup>a</sup> Calcd. for polytrichloro-*p*-xylylene.

molded at 190°C. are slightly discolored and have properties similar to those of cast films.

### Reaction of $\alpha$ -Halo-*p*-Xylenes with Base

If  $\alpha$ -chloro-*p*-xylene (VIII) is reacted with potassium *tert*-butoxide in a polar solvent such as dimethyl sulfoxide, a transient orange-red color is observed, indicating carbanion formation. 4,4'-Dimethylstilbene is isolated, indicating the reaction to proceed as shown in eqs. (11)–(13). The stilbenes listed in Table III were formed under the same reaction conditions.

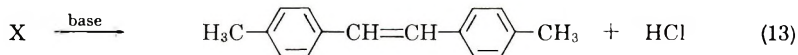
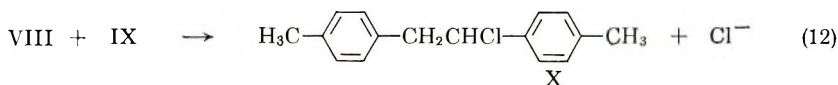
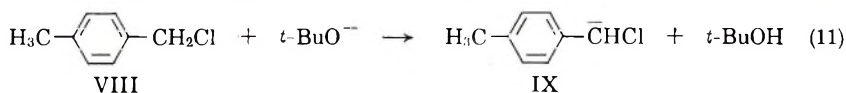


TABLE III  
Stilbenes from Benzyl Chloride Derivatives, Dimethyl  
Sulfoxide with Potassium *tert*-Butoxide

Starting material	Reaction product	Yield, %	Melting point, °C.	
			Found	Lit.
Benzyl chloride	<i>trans</i> -Stilbene	51	123–124	124 <sup>a</sup>
$\alpha$ -Chloro- <i>p</i> -xylene	4,4'-Dimethylstilbene	36	181–182	180 <sup>b</sup>
Diphenylchloromethane	Tetraphenylethylene	61	220–221	221 <sup>c</sup>
1-Chloro-5-chloromethyl-2-methylbenzene	3,3'-Dichloro-4,4'-dimethylstilbene	6	147–148	—

<sup>a</sup> Data of Michaelis.<sup>11</sup>

<sup>b</sup> Data of Wislicenus.<sup>12</sup>

<sup>c</sup> Data of Behr.<sup>13</sup>

TABLE IV  
Conversion of 1-Chloromethyl-3,4-Dimethylbenzene to  
Poly-2-Methyl-*p*-Xylylene

Reaction time, min.	Monomer charged, mole	<i>tert</i> -Butoxide charged, mole <sup>a</sup>	Polymer recovered, %	Reduced viscosity of polymer <sup>b</sup>
1.5	0.0873	0.0873	13.3	0.40
2.5	0.0872	0.0872	16.7	0.50
5.0	0.0873	0.0873	22.7	0.46
10.0	0.0872	0.0872	25.4	0.46
20.0	0.0871	0.0871	25.5	0.27
30.0	0.0869	0.0869	26.8	0.28

<sup>a</sup> Based on titration of the base in water with standard HCl.

<sup>b</sup> 0.2% solution in benzene at 50°C.

TABLE V  
Conversion of 1-Chloro-5-Chloromethyl-2-Methylbenzene to  
Poly-2-Chloro-*p*-Xylylene

Base charged, mole	Monomer charged, mole	Polymer recovered, %	Reduced viscosity of polymer <sup>a</sup>
0.1898	0.1000	47.9	0.25
0.0872	0.1000	36.3	0.61
0.0742	0.1000	28.1	0.65
0.0561	0.1000	19.8	0.44
0.0371	0.1000	8.0	0.44
0.0180	0.1000	1.3	0.20

<sup>a</sup> 0.2% solution in 1-chloronaphthalene at 170°C.

If  $\alpha$ -chloro-*p*-xylene or ring-substituted derivatives are reacted with potassium *tert*-butoxide in a nonpolar solvent, such as *p*-xylene, poly-*p*-xylylenes are formed. A kinetic investigation of the polymerization was carried out. Two series of experiments were run to obtain polymers at various degrees of conversion. The first series was with 1-chloromethyl-3,4-di-

TABLE VI  
 Polymers Prepared from  $\alpha$ -Chloro-*p*-Xylene Derivatives with *tert*-Butoxide in *p*-Xylene

Starting material	Polymer	Yield, %	Softening temp., °C.
		78	Dec. at 340 without melting
		55	250-270
		50	340 (dec.)
		24	60
		14	100
		0	
		16	155
		1	Viscous oil
		30	320-340

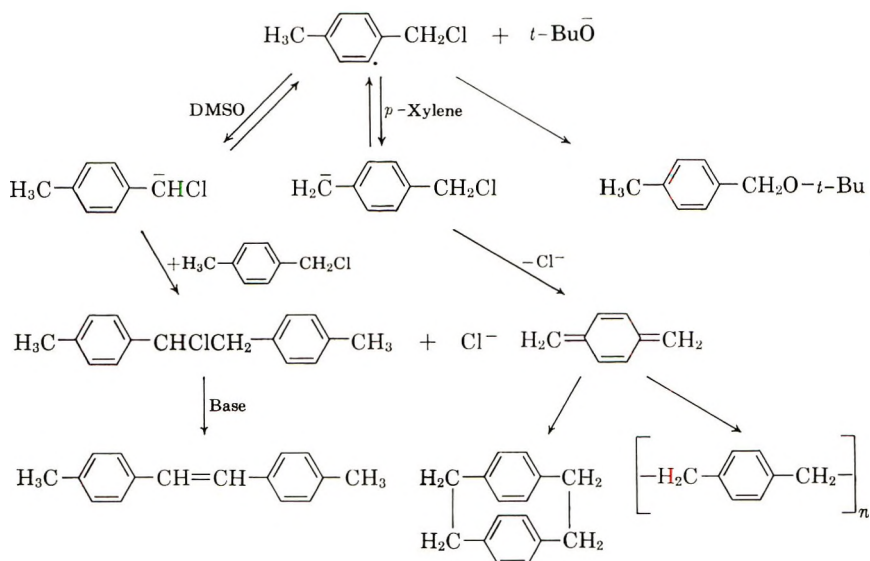
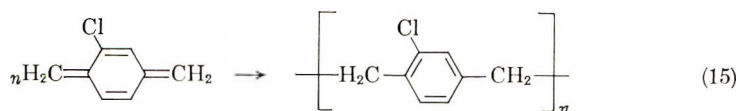
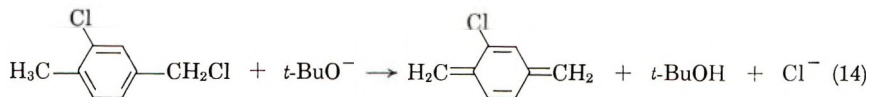


Fig. 1. Reaction of  $\alpha'$ -chloro-*p*-xylene with potassium *tert*-butoxide.

methyl benzene (XI); the second with 1-chloro-5-chloromethyl-2-methylbenzene (XII). The polymerization with XI was carried out with equimolar amounts of base. Table IV shows polymer yields after various reaction times. As the viscosity measurements show, the molecular weight does not increase with the extent of the reaction. This is consistent with an addition rather than a condensation polymerization.

It is desirable to have a very low conversion in order to obtain good evidence about the polymerization mechanism. Since the polymerization occurs rapidly, the interruption of the reaction at low conversion is difficult. Therefore, the monomer was reacted with deficient amounts of base. For this investigation XII was chosen as the starting material because it undergoes a relatively clean reaction and the polymer is soluble. Table V shows the results. Even with a large excess of monomer, polymers of relatively high molecular weight are formed. It is concluded that a reactive intermediate, *p*-xylylene, is formed and this undergoes addition polymerization, as shown in eqs. (13) and (14).



Along with polymer, the reaction mixtures contained 1,2-ditolylethane (up to 8%), *p*-xylyl-*tert*-butyl ether (up to 19%), and the cyclic dimer of

2-chloro-*p*-xylylene (about 2%). The ratio of these compounds seems dependent upon base concentration. An exact correlation was not established.

TABLE VII  
Mechanical Properties of Polymethyl- and Polydimethyl-*p*-Xylylenes

	Tensile modulus, psi	Tensile strength, psi	Elongation, %	Impact ft.-lb./in. <sup>3</sup>	$T_g$ , °C.	Softening temp., °C.
Polymethyl- <i>p</i> -xylylene	275,000	4600	1-6	8-23	50-55	60
Polydimethyl- <i>p</i> -xylylene	260,000	2200	1	Low	90-100	100

TABLE VIII  
Copolymers of *p*-Xylylene and 2-Methyl-*p*-Xylylene

$\alpha$ -Chloro- <i>p</i> -xylylene charged, mole-%	Softening temp., °C.	Reduced viscosity
0	60	0.72 <sup>a</sup>
25	150-160	0.33 <sup>a</sup>
50	175-185	0.30 <sup>b</sup>
100	360	Insoluble

<sup>a</sup> 0.2% solution in benzene at 50°C.

<sup>b</sup> 0.2% solution in 1-chloronaphthalene at 170°C.

TABLE IX  
Copolymers of 2-Chloro-*p*-Xylylene and 2-Methyl-*p*-Xylylene

Monomers charged mole-%		Tensile modulus, psi	Tensile strength, psi	Elongation, %	Impact ft.-lb./in. <sup>3</sup>	$T_g$ , °C.	Softening temperature, °C.
Chloro	Methyl						
100	0	350,000	—	—	—	70	270
77	23	330,000	7,000	9	10	65	200
65	35	320,000	7,000	9	10	60-65	200
38	62	275,000	5,700	2-7	7-22	60	165
0	100	275,000	4,600	1-6	8-23	50-55	60

TABLE X  
Orientation of 77/23 Copolymer of 2-Chloro-*p*-Xylylene and 2-Methyl-*p*-Xylylene

	Compression-molded film	Stretch-oriented fiber
$T_m$ , °C.	200	200
$T_g$ , °C.	65	65
Tensile modulus, psi	330,000	750,000
Tensile strength, psi	7,000	30,000
Elongation, %	9	10

TABLE XI  
Properties of Copolymers of Benzo-*p*-Xylylene and 2-Methyl-*p*-Xylylene

Monomers charged, mole-%		Tensile modulus, psi	Tensile strength, psi	Elongation, %	Impact, ft.-lb./in. <sup>3</sup>	$T_g$ , °C.	Softening temp., °C.	Reduced viscosity
Benzo	Methyl							
100	0	—	—	—	—	160	320	—
25	75	380,000	8,600	3-5	Low	90	110	0.45 <sup>a</sup>
10	90	290,000	5,500	2-3	8	75	80	0.38 <sup>a</sup>
5	95	280,000	5,300	2-11	13	65	65	0.53 <sup>a</sup>
0	100	275,000	4,600	1-6	8-23	50-55	60	0.72 <sup>b</sup>

<sup>a</sup> 0.2% solution in 1-chloronaphthalene at 170°C.

<sup>b</sup> 0.2% solution in benzene at 50°C.

TABLE XII  
Properties of a Methyl-*p*-Xylylene-Dimethyl-*p*-Xylylene Copolymer

Monomers charged, mole-%		Tensile modulus, psi	Tensile strength, psi	Elongation, %	Impact, ft.-lb./in. <sup>3</sup>	$T_g$ , °C.	Softening temp., °C.	Reduced viscosity
Methyl	Dimethyl							
0	100	260,000	2,200	1	Low	90-100	100	0.40 <sup>a</sup>
50	50	285,000	4,400	2-3	11	75	75	0.66 <sup>b</sup>
100	0	275,000	4,600	1-6	8-23	50-55	60	0.72 <sup>b</sup>

<sup>a</sup> 0.2% solution in benzene at 25°C.

<sup>b</sup> 0.2% solution in benzene at 50°C.

Figure 1 summarizes the reactions which  $\alpha$ -chloro-*p*-xylene gives with potassium *tert*-butoxide. The polymers which have been prepared from  $\alpha$ -chloro-*p*-xylene derivatives and potassium *tert*-butoxide in *p*-xylene are shown in Table VI.

### Mechanical Properties

Many of the polymers reported in this paper are insoluble, infusible, and cannot be fabricated by molding or casting. Compression-molded films can be prepared from poly-2-methyl- and poly-2,5-dimethyl-*p*-xylylenes, and their mechanical properties are shown in Table VII.

2-Methyl-*p*-xylylene copolymerizes with *p*-xylylene; the properties are shown in Table VIII.

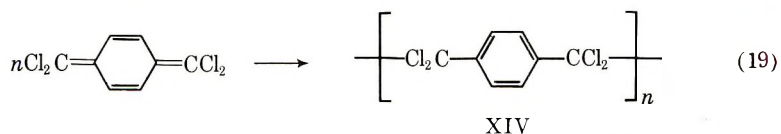
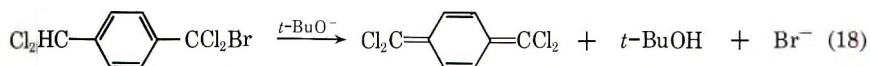
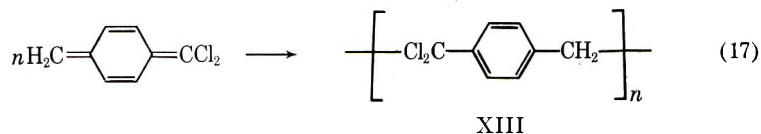
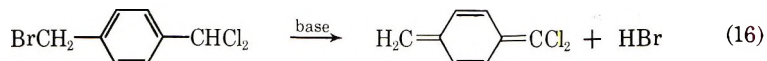
Copolymers of 2-chloro-*p*-xylylene and 2-methyl-*p*-xylylene could be compression-molded. The properties are shown in Table IX. The copolymer containing 77% chloro-*p*-xylylene was oriented to give increased tensile properties, as shown in Table X.

The copolymers prepared from benzo-*p*-xylylene (from 1-chloromethyl-4-methylnaphthalene) and methyl-*p*-xylylene are shown in Table XI.

Table XII shows properties of methyl-*p*-xylylene-dimethyl-*p*-xylylene copolymer.

### Reaction of Tri- and Pentahalo-*p*-Xylenes with Base

It has been shown that  $\alpha$ -halo-,  $\alpha, \alpha'$ -dihalo-, and  $\alpha, \alpha, \alpha', \alpha'$ -tetrahalo-*p*-xylenes can be polymerized by a 1,6 elimination of hydrogen halide in the presence of base. Tri- and pentahalo-*p*-xylenes also polymerize via a 1,6 elimination reaction, as shown in eqs. (16)–(19). No change is observed



when poly tetrachloro-*p*-xylylene (XIV) is heated to 250°C.

## EXPERIMENTAL

### Reaction of $\alpha, \alpha'$ -Dichloro-*p*-Xylene with Potassium *tert*-Butoxide

Potassium *tert*-butoxide (16 g.) is added to 10 g.  $\alpha, \alpha'$ -dichloro-*p*-xylene in 40 ml. of benzene. A yellow solid is formed. The mixture is refluxed



for 15 min. with stirring. The solid is filtered off and washed thoroughly with benzene, ethanol, and water; yield, 4.5 g. of a bright yellow powder.

Potassium (1 g.) in 50 ml. *tert*-butanol is slowly added to 88 g.  $\alpha,\alpha'$ -dichloro-*p*-xylene in 225 ml. *tert*-butanol at reflux with stirring. The white product is filtered, washed with benzene, ethanol, and water.

Anal. Calcd. for polychloro-*p*-xylylene: C, 69.31%; H, 5.05%; Cl, 25.63%. Found: C, 69.1%; H, 5.2%; Cl, 26.0%.

The polymer turns yellow when heated.

#### Preparation of $\alpha,\alpha,\alpha',\alpha'$ -Tetrachloro-*p*-Xylene

Terephthalaldehyde, (200 g.) is added to a stirred suspension of 600 g. phosphorus pentachloride in 1500 ml. carbon tetrachloride. The mixture is refluxed 1 hr. The solvent and most of the phosphorus oxychloride is distilled off and the residue reacted with ice. The  $\alpha,\alpha,\alpha',\alpha'$ -tetrachloro-*p*-xylene is isolated by filtration and recrystallized from heptane; yield, 269 g. (74%); m.p. 92–93°C.<sup>14</sup>

#### Preparation of Poly- $\alpha,\alpha,\alpha',\alpha'$ -trichloro-*p*-xylylene

A solution of 24.4 g. of  $\alpha,\alpha,\alpha',\alpha'$ -tetrachloro-*p*-xylene (0.1 mole) in 200 ml. *tert*-butanol is stirred at reflux under nitrogen. A solution of potassium *tert*-butoxide in *tert*-butanol prepared by dissolving 1.9 g. potassium (0.05 mole) in 70 ml. *tert*-butanol is added within 30 min. The polymer is isolated by filtration, washed with methanol and water, and dried under vacuum at 40°C.; yield, 81 g.

Anal. Calcd. for poly-trichloro-*p*-xylylene: C, 46.26%; H, 2.41%; Cl, 51.32%. Found: C, 46.20%; H, 2.43%; Cl, 51.28%.

#### Reaction of $\alpha,\alpha,\alpha',\alpha'$ -Tetrachloro-*p*-Xylene with Sodium Hydroxide

A mixture of 4.88 g.  $\alpha,\alpha,\alpha',\alpha'$ -tetrachloro-*p*-xylene, 0.8 g. sodium hydroxide, 30 ml. 50/50 methanol–butanol is stirred at reflux for 1 hr. The reaction mixture is poured into 200 ml. methanol, filtered, and washed with methanol and water. The polymer is dried under vacuum at 40°C. Yields are reported in Table I.

#### Preparation of Stilbenes

A 0.12-mole portion of the benzyl chloride derivative is slowly added to 13.5 g. (0.12 mole) of potassium *tert*-butoxide in 300 ml. dimethyl sulfide. An orange color and exotherm are noted. The reaction is stirred at 20°C. until the color disappears. The mixture is poured into water and the stilbene filtered off. Yields are listed in Table III.

#### Reaction of $\alpha$ -Chloro-*p*-Xylene with Potassium *tert*-Butoxide

Potassium *tert*-butoxide (9 g., 0.08 mole) and 500 ml. *p*-xylene is brought to reflux under nitrogen; 0.08 mole of the  $\alpha$ -chloro-*p*-xylene is added and

the reaction refluxed 1 hr. The polymer is precipitated in alcohol and washed with water.

### References

1. Thiele, J., and H. Balhorn, *Ber.*, **37**, 1463 (1904).
2. Szwarc, M., *Discussions Faraday Soc.*, **2**, 46 (1947); *J. Polymer Sci.*, **6**, 319 (1951).
3. Errede, L. A., and M. Szwarc, *Quart. Rev.*, **12**, 301 (1958).
4. Gorham, W., paper presented at 149th American Chemical Society Meeting, Detroit, April 1965.
5. McDonald, R. N., and T. W. Campbell, *J. Am. Chem. Soc.*, **82**, 4669 (1960).
6. Zidaroff, E., and D. Ivanoff, *Naturwiss.*, **52**, 13 (1965).
7. Drefahl, G., and G. Ploetner, *Ber.*, **91**, 1274 (1958).
8. Chinoporos, E., *Chem. Rev.*, **63**, 235 (1963).
9. Kirmse, W., *Angew. Chem.*, **73**, 161 (1961).
10. Hauser, C. R., *J. Am. Chem. Soc.*, **78**, 1653 (1956).
11. Michaelis, A., *Ber.*, **8**, 1314 (1875).
12. Wislicenus, W., *Ber.*, **38**, 506 (1905).
13. Behr, R., *Ber.*, **3**, 752 (1870).
14. Colson, A., *Ann. Chim. Phys.*, **11**, 24 (1887).

### Résumé

Divers  $\alpha$ -halogéno-*p*-xylènes ont été polymérisés en présence des bases avec formation des polymères *p*-xylyliques. La réaction consiste en une déshydrohalogénéation en 1,6 qui forme un xylylène; ce dernier polymérise en suite. L' $\alpha, \alpha'$ -dichloro-*p*-xylène forme le poly- $\alpha$ -chloro-*p*-xylène et des polymères contenant des unités stilbéniques; l' $\alpha, \alpha, \alpha', \alpha'$ -tetrachloro-*p*-xylène conduit au poly- $\alpha, \alpha, \alpha', \alpha'$ -trichloro-*p*-xylylène; les  $\alpha$ -chloro-*p*-xylènes avec substituants alcoyle, aryle ou halogène dans les noyaux, fournissent les poly-*p*-xylylènes substitués correspondants. L'accroissement du nombre des atomes d'halogène en position  $\alpha$  (5 au maximum) nécessite une base de plus en plus faible pour la déshydrohalogénéation. L'hydroxyde de sodium dans du méthanol est effectif pour la polymérisation du tetrachloro-*p*-xylène; d'autre part, la polymérisation des  $\alpha$ -halogéno-*p*-xylènes nécessite le butylate tertiaire de potassium dans du xylène à reflux. La réaction des  $\alpha$ -halogéno-*p*-xylènes avec le butylate tertiaire de potassium dans des solvants polaires, p. ex. le diméthyl sulfoxyde, conduit aux stilbènes.

### Zusammenfassung

Verschiedene  $\alpha$ -Halogeno-*p*-xylol wurden mit Basen unter Bildung von *p*-Xylylenpolymeren polymerisiert. Die Reaktion verläuft über eine 1,6-Dehydrohalogenierung zu einem Xylylen, welches dann polymerisiert.  $\alpha, \alpha'$ -Dichlor-*p*-xylol bildet Poly( $\alpha$ -chlor-*p*-xylylen) und Polymere mit Stilbenbausteinen;  $\alpha, \alpha, \alpha', \alpha'$ -Tetrachlor-*p*-xylyl bildet Poly( $\alpha, \alpha, \alpha', \alpha'$ -Trichlor-*p*-xylylen); Alkyl-, Aryl- und Halogenring-substituierte  $\alpha$ -Chlor-*p*-xylyl bilden die entsprechenden ringsubstituierten Poly(*p*-xylylene). Je mehr Halogene sich in den  $\alpha$ -Stellungen befinden (bis zu fünf), umso schwächer kann die für die Dehydrohalogenierung notwendige Base sein. Natriumhydroxyd in Methanol bringt Tetrachlor-*p*-xylyl zur Polymerisation, während zur Polymerisation von  $\alpha$ -Chlor-*p*-xylylen *tert*-Butoxyd in *p*-Xylol unter Rückfluss notwendig ist. Bei der Reaktion von  $\alpha$ -Halogenoxylylen mit Kalium-*tert*-butoxyd in polaren Lösungsmitteln wie Dimethylsulfoxyd werden Stilbene gebildet.

Received June 1, 1965

Revised October 1, 1965

Prod. No. 4915A



## Preparation of Poly-*p*-Xylylenes by Electrolysis

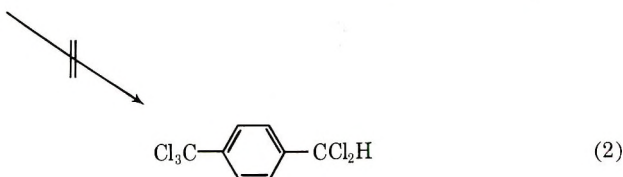
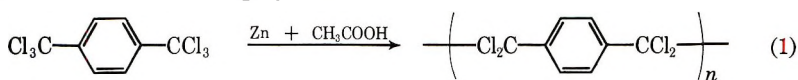
H. G. GILCH,\* *Research and Development Department, Plastics Division, Union Carbide Corporation, Bound Brook, New Jersey*

### Synopsis

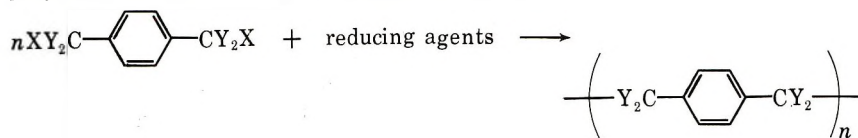
Poly-*p*-xylylenes were prepared by electrolytic reduction of  $\alpha, \alpha'$ -dihalo-*p*-xylenes at controlled cathode potentials (c.p.). Polymers and halides are formed at the cathode; at the anode the halide is oxidized to halogen. Poly-*p*-xylylene was prepared from  $\alpha, \alpha'$ -dichloro-*p*-xylene (c.p. -1.2 v.) and  $\alpha, \alpha'$ -dibromo-*p*-xylene (c.p. -1.2 v.); poly-*p*-2-chloroxylylene from  $\alpha, \alpha'$ -2-trichloro-*p*-xylene (c.p. -1.4 v.) and  $\alpha, \alpha'$ -dibromo-2-chloro-*p*-xylene (c.p. -1.2 v.); poly- $\alpha, \alpha, \alpha', \alpha'$ -tetrachloro-*p*-xylylene from  $\alpha, \alpha, \alpha, \alpha', \alpha', \alpha'$ -hexachloro-*p*-xylene (c.p. -0.7 v.), and poly- $\alpha, \alpha, \alpha', \alpha'$ -tetrafluoro-*p*-xylylene from  $\alpha, \alpha'$ -dibromo- $\alpha, \alpha, \alpha', \alpha'$ -tetrafluoro-*p*-xylene (c.p. -1.1 v.). The cathode potentials were measured and controlled with respect to a saturated calomel electrode. Current efficiencies up to 96% were observed.  $\alpha, \alpha, \alpha', \alpha'$ -Tetrachloro-*p*-xylylene was identified as an intermediate in the reduction of  $\alpha, \alpha, \alpha, \alpha', \alpha', \alpha'$ -hexachloro-*p*-xylene. A general mechanism for these reactions is suggested and discussed. It involves elimination of halide by a two-electron charge transfer with formation of a xylyl anion, followed by an elimination of halide in  $\alpha'$ -position yielding xylylenes which then polymerize.

### INTRODUCTION

In an attempt to prepare  $\alpha, \alpha, \alpha, \alpha', \alpha'$ -pentachloro-*p*-xylene from hexachloro-*p*-xylene by reduction with zinc and acetic acid, polytetrachloro-*p*-xylylene was isolated in high yield.

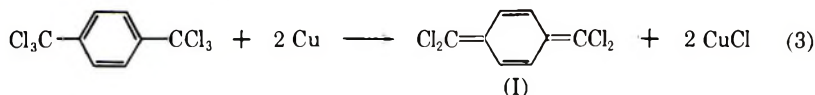


This is a general type of reaction in which  $\alpha, \alpha'$ -dihalo-*p*-xylenes can be polymerized by a variety of reducing agents:



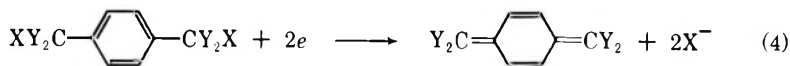
\* Present address: Farbenfabriken Bayer A.G., Werk Uerdingen, Wissenschaftliches Hauptlaboratorium, Krefeld, Germany.

where X is chlorine, bromine, or iodine and Y is halogen and/or hydrogen. Polymerizations with zinc,<sup>1</sup> copper,<sup>2</sup> phenyllithium,<sup>3</sup> sodium,<sup>4</sup> and iron<sup>5</sup> have been reported. In case of the gas-phase reduction of hexachloro-*p*-xylene with copper, it has been possible to isolate and identify  $\alpha, \alpha', \alpha', \alpha'$ -tetrachloro-*p*-xylylene (I).<sup>6</sup>



In the other cases, no attempts have been made to isolate the xylylene intermediates; nevertheless, results of kinetic investigations are consistent with an addition polymerization of a reactive intermediate which is formed by reduction. It has now been found that the polymerization of hexachloro-*p*-xylene can also be achieved with stannous chloride or hydrogen on a platinum surface.

The widely different nature of the reducing agents forces the conclusion that the key step in these reactions does not seem to be the formation of an intermediate between the reducing agents and the haloxylenes, but only a transfer of electrons:



## RESULTS

It should be possible to carry out these reactions by electrolytic reduction, if the key step in these polymerizations of  $\alpha, \alpha'$ -dihalo-*p*-xylenes were the transfer of electrons. Attempts to polymerize  $\alpha, \alpha'$ -dihalo-*p*-xylenes in a solution of tetrahydrofuran and hydrochloric acid with the use of platinum electrodes failed; only hydrogen formed on the cathode. However, when cathodes of lead or mercury were used (these exhibit a high enough overvoltage for hydrogen), polymers were isolated in excellent yields.

In most of the experiments a mercury pool was used as cathode. In some cases the polymer formed as a film on the mercury and insulated the cathode. Therefore, a magnetic stirrer, floating on the mercury surface, was used for most of the electrolyses. The cathode potential was measured against a calomel electrode and was kept constant during the entire electrolysis.

Table I shows starting materials, isolated polymers, yields, and experimental conditions. Some of the polymers were also isolated as coherent films. In these cases the mercury pool was not stirred. The polymers were identified by elemental analysis and by comparison of their infrared spectra with the spectra of the same polymers prepared by classical means.

The reduced viscosity of an 0.2% solution in chloronaphthalene at 170°C. of poly-2-chloro-*p*-xylylene prepared from  $\alpha, \alpha'$ -dibromo-2-chloro-*p*-xylene was 0.78, that from  $\alpha, \alpha'$ -2-trichloro-*p*-xylene 0.68. This compares with a

TABLE I  
 Polymerization Conditions for  $\alpha,\alpha'$ -Halo-*p*-Xylylenes<sup>a</sup>

Starting material	Polymer	Cathode potential, v.	Cathode-anode potential, v.	Current density, ma./cm. <sup>2</sup>	Current efficiency, %
		-1.2	3.0-3.5	1.4-2.7	35
		-0.7	3.0-6.0	2.0-5.5	95
		-1.4	3.4-4.0	1.3-3.2	65
		-1.2	2.5-4.5	1.2-3.5	90
		-1.2	2.3-4.2	1.0-3.5	90
		-1.1	4.9-6.0	3.0-6.0	96

<sup>a</sup> All polymerizations were carried out as described for dibromotetrafluoro-*p*-xylylene except hexachloro-*p*-xylylene.



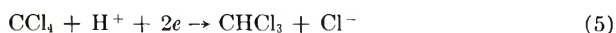
reduced viscosity of 0.65 of the same polymer prepared by the reaction of  $\alpha, \alpha'$ -dichloro-*p*-xylene with potassium butoxide. The remaining polymers in Table I are insoluble.

The formation of xylylenes as intermediates in the polymerization of  $\alpha, \alpha'$ -dihalo-*p*-xylenes with reducing agents was consistent with all the experimental facts.<sup>6</sup> It was therefore assumed that in the electrolytic polymerization xylylene intermediates were formed as well. As shown earlier,<sup>6</sup> I has a relatively long half-life at lower temperatures. Therefore, in order to isolate the theoretically resulting I, hexachloro-*p*-xylene was electrolyzed at  $-10^\circ\text{C}$ .

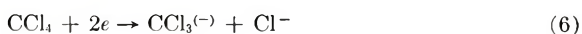
The cathodic potential was kept at  $-0.70$  v. Yellow crystals of I were isolated from the catholyte, which was concentrated at low temperature. These crystals were dissolved in tetrahydrofuran at room temperature. After a few minutes the solution became cloudy, and poly- $\alpha, \alpha', \alpha', \alpha'$ -tetrachloro-*p*-xylylene precipitated. A few crystals of I were reacted with bromine, and the resulting  $\alpha, \alpha'$ -dibromo- $\alpha, \alpha', \alpha', \alpha'$ -tetrachloro-*p*-xylene was identified by its infrared spectrum and its melting point.<sup>6</sup>

## DISCUSSION

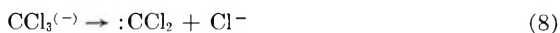
According to Stackelberg<sup>7</sup> and Wawzonek<sup>8</sup> the reduction of alkyl halides at the dropping mercury electrode consists of a two-electron charge transfer:



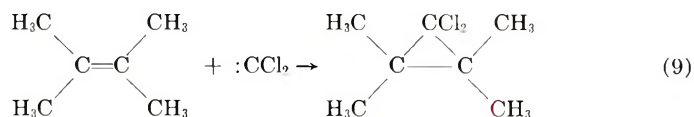
This equation can be separated into two steps:



It is well known that anions such as  $\text{CCl}_3^{(-)}$  can eliminate chloride ion and form carbenes in the absence of protons:<sup>9</sup>



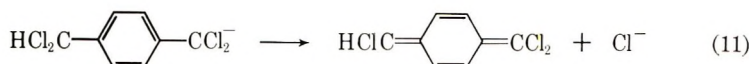
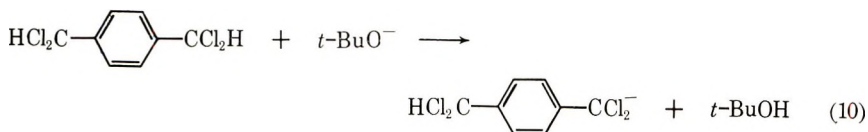
Wawzonek<sup>10</sup> was able to trap the dichlorocarbene with tetramethylethylene in an electrolytic reduction of carbon tetrachloride in acetonitrile.



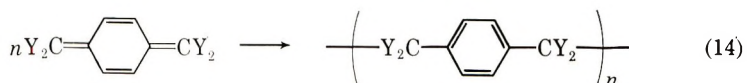
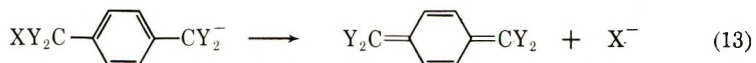
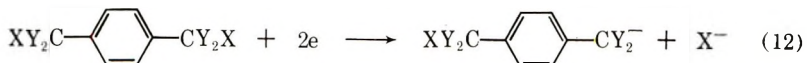
The isolation of the tetramethyldichlorocyclopropane can be considered as evidence for the presence of the trichloromethyl anion as an intermediate.

It is shown elsewhere<sup>11</sup> that  $\alpha$ -halo-*p*-xylyl anions do not eliminate chloride ion from the  $\alpha$ -position to form carbenes but eject chloride ion from the  $\alpha'$ -position to yield the more stable xylylenes, as shown in eqs. (10) and (11).





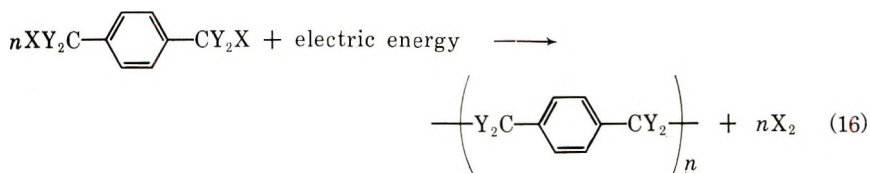
Thus, for the electrolytic polymerization of  $\alpha, \alpha'$ -dihalo-*p*-xylenes the reaction mechanism of eqs. (12)–(14) is consistent with experimental results.



The first step consists of a two-electron charge transfer as in eq. (6), the second one is a loss of halide ion from the  $\alpha'$ -position, followed by polymerization of the xylene. These reactions occur at the cathode or in the solution; at the anode, halide ions are oxidized to halogen.



The overall reaction, is as given in eq. (16).



## EXPERIMENTAL

### Electrolysis of $\alpha, \alpha'$ -Dibromo- $\alpha, \alpha', \alpha', \alpha'$ -Tetrafluoro-*p*-Xylene

$\alpha, \alpha'$ -Dibromo  $\alpha, \alpha', \alpha', \alpha'$ -tetrafluoro-*p*-xylene (2 g.) was dissolved in a mixture of 50 ml. dioxane, 10 ml. water, and 2 ml. concentrated hydrochloric acid. The solution was electrolyzed under a blanket of nitrogen, a mercury pool being used as cathode and a carbon rod as anode. The electrodes were separated by a ceramic diaphragm. The surface of the mercury was stirred by a magnetic stirrer floating on the mercury. The cathode potential was measured against a calomel reference electrode; it was kept at 1.10 v. by an Anotrol 4000 constant potential power supply (Anotrol Division, Continental Oil Co., Ponca City, Okla.). The electric

current increased from 3 ma./cm.<sup>2</sup> at the beginning to 6 ma./cm.<sup>2</sup> after 2.5 hr.

The polymer was isolated by filtration, washed with dioxane, and dried in vacuum for 15 hr. at 120°C.; 0.7116 g. of polymer was isolated. The current efficiency was 95%.

ANAL. Calcd. for C<sub>8</sub>H<sub>4</sub>F<sub>4</sub>: C, 54.54%; H, 2.27%; F, 43.18%. Found: C, 54.25%; H, 2.56%; F, 43.11%.

### Electrolysis of $\alpha,\alpha,\alpha',\alpha',\alpha',\alpha'$ -Hexachloro-*p*-Xylene

**At Room Temperature.** A solution of 2 g. of  $\alpha,\alpha,\alpha',\alpha',\alpha',\alpha'$ -hexachloro-*p*-xylene in 100 ml. dioxane, 10 ml. water, and 2 ml. hydrochloric acid is electrolyzed in a cell described above. The cathodic potential was kept at -0.70 v. Current densities of 2.0-5.5 ma./cm.<sup>2</sup> at a voltage between cathode and anode of 3-6 v. were measured.

The electrolysis was carried out under a blanket of nitrogen. After about 3 min. white polymer precipitated, after about 1 hr. yellow crystals of I were observed. After 2.5 hr. the electrolysis was interrupted and in order to complete the polymerization of tetrachloro-*p*-xylylene, the catholyte was stirred at room temp. and under nitrogen for another 2 hr. The polymer was isolated by filtration, washed with tetrahydrofuran, and dried under reduced pressure at 110°C.; yield 304.3 mg.; current efficiency 95%.

**At -10°C.**  $\alpha,\alpha,\alpha',\alpha',\alpha',\alpha'$ -Hexachloro-*p*-xylene (2 g.) was dissolved in a mixture of 100 ml. tetrahydrofuran, 20 ml. water, and 4 ml. concentrated hydrochloric acid. The cathodic potential was kept at -0.70 v. The electrolysis was carried out at a voltage between anode and cathode of 3.5-4.5 v. and a current density of 1.5-4.5 ma./cm.<sup>2</sup>. After 62 min. the electrolysis was interrupted and the catholyte, which contained large amounts of crystalline tetrachloro-*p*-xylylene, was concentrated at -10°C. A very small amount of these crystals was isolated and reacted with bromine, yielding  $\alpha,\alpha'$ -dibromo- $\alpha,\alpha',\alpha',\alpha'$ -tetrachloro-*p*-xylene, which was identified by its melting point<sup>6</sup> and infrared spectrum.

The remaining catholyte was dissolved in 300 ml. of tetrahydrofuran to yield a clear solution. After standing for about 5 min. at room temperature, polytetrachloro-*p*-xylylene precipitated. The polymer was isolated after 14 hr. by filtration, washed with tetrahydrofuran, and dried; yield 0.1454 g.

### References

1. Thiele, J., and H. Balhorn, *Ber.*, **37**, 1463 (1904).
2. Yagupol'skii, L. M., and B. F. Malichenko, *J. Gen. Chem. USSR Eng. Transl.*, **32**, 2985 (1962).
3. Golden, J. H., *J. Chem. Soc.*, **1961**, 1604.
4. Brown, C. J., and A. C. Farthing, *J. Chem. Soc.*, **1953**, 3270.
5. Sisido, K., N. Kusano, R. Noyori, Y. Nozaki, M. Simosaka, and H. Nozaki, *J. Polymer Sci. A*, **1**, 2101 (1963).
6. Gilch, H. G., *Angew. Chem.*, **77**, 592 (1965); *Angew. Chem. Intern. Ed.*, **4**, 598 (1965).

7. Stackelberg, M., and W. Stracke, *Z. Electrochem.*, **53**, 118 (1949).
8. Wawzonek, S., *Anal. Chem.*, **24**, 32 (1952).
9. Hine, J., *J. Am. Chem. Soc.*, **72**, 2438 (1950).
10. Wawzonek, S., *J. Electrochem. Soc.*, **108**, 1135 (1961).
11. Gilch, J. G., and W. L. Wheelwright, *J. Polymer Sci. A-1*, **4**, 1329 (1966).

### Résumé

Des poly-*p*-xylylènes ont été préparés par réduction électrolytique à potentiel cathodique contrôlé des  $\alpha, \alpha'$ -dihalo-*p*-xylylènes. Les polymères et les halogénures sont formés à la cathode; à l'anode les halogénures sont oxydés en halogènes. C'est ainsi que le poly-*p*-xylylène a été préparé à partir du  $\alpha, \alpha'$ -dichloro-*p*-xylylène (potentiel cathodique  $-1.24$ ) ou a parti du  $\alpha, \alpha'$ -dibromo-*p*-xylylène (potentiel cathodique  $-1.2$  v); le poly-*p*-2-chloroxylylène au départ de l' $\alpha, \alpha'$ -2-trichloro-*p*-xylylène (p.e.  $-1.4$  v) du l' $\alpha, \alpha'$ -dibromo-2-chloro-*p*-xylylène (p. e.  $-1.2$  v); le poly- $\alpha, \alpha, \alpha', \alpha'$ -tétra-chloro-*p*-xylylène au départ de l' $\alpha, \alpha, \alpha, \alpha', \alpha', \alpha'$ -hexachloro-*p*-xylylène (p. e.  $-0.7$  v) et le poly- $\alpha, \alpha, \alpha', \alpha'$ -tétrafluoro-*p*-xylylène à partir du  $\alpha, \alpha'$ -dibromo- $\alpha, \alpha, \alpha', \alpha'$ -tétrafluoro-*p*-xylylène (p. e.  $-1.1$  v). Les potentiels cathodiques ont été mesurés et contrôlés par rapport à une électrode calomel saturée. Des efficacités de courant atteignant 96% étaient observées. L' $\alpha, \alpha, \alpha', \alpha'$ -tétrachloro-*p*-xylylène a été identifié comme intermédiaire dans la réduction de l' $\alpha, \alpha, \alpha, \alpha', \alpha', \alpha'$ -hexachloro-*p*-xylylène. Un mécanisme général de ces réactions est proposé et discuté. Il comporte une élimination de l'halogène par un transfert de charge à deux électrons avec formation d'un anion xylylique, suivie d'une élimination de l'halogénure de la position  $\alpha$ -formant ainsi les xylylènes qui polymérisent ultérieurement.

### Zusammenfassung

Poly-*p*-Xylylene wurden durch elektrolytische Reduktion von  $\alpha, \alpha'$ -Dihalogeno-*p*-xylylen bei kontrollierten Kathodenpotentialen dargestellt. An der Kathode werden Polymere und Halogenide gebildet; an der Anode wird das Halogenid zu Halogen oxydiert. Poly-*p*-xylylen wurde aus  $\alpha, \alpha'$ -Dichlor-*p*-xylyl (Kathodenpotential  $-1,2$ ) und  $\alpha, \alpha'$ -Dibrom-*p*-xylyl (C.P.  $-1,2$ ), Poly-*p*-2-chloroxylylen aus  $\alpha, \alpha'$ -2-Trichlor-*p*-xylyl (C.P.  $-1,4$ ) und  $\alpha, \alpha'$ -Dibrom-2-chlor-*p*-xylyl (C.P.  $-1,2$ ), Poly- $\alpha, \alpha, \alpha', \alpha'$ -Tetrachlor-*p*-xylylen aus  $\alpha, \alpha, \alpha, \alpha', \alpha', \alpha'$ -Hexachlor-*p*-xylyl (C.P.  $-0,7$  V) und Poly- $\alpha, \alpha, \alpha', \alpha'$ -tetrafluor-*p*-xylylen aus  $\alpha, \alpha'$ -Dibrom- $\alpha, \alpha, \alpha', \alpha'$ -tetrafluor-*p*-xylyl (C.P.  $-1,1$  V). Das Kathodenpotential wurde gegen eine gesättigte Kalomelektrode gemessen. Stromausbeuten bis zu 96% wurden beobachtet.  $\alpha, \alpha, \alpha', \alpha'$ -Tetrachlor-*p*-xylylen wurde als Zwischenstoff bei der Reduktion von  $\alpha, \alpha, \alpha, \alpha', \alpha', \alpha'$ -Hexachlor-*p*-xylyl identifiziert. Ein allgemeiner Mechanismus für diese Reaktionen wird vorgeschlagen und diskutiert. Dabei wird die Eliminierung eines Halogenids durch eine Zwei-Elektronen-Ladungs-übertragung unter Bildung eines Xylylanions und darauffolgend eine Eliminierung von Halogenid in  $\alpha'$ -Stellung unter Bildung von Xylylenen angenommen, welche dann polymerisieren.

Received June 1, 1965

Revised October 1, 1965

Prod. No. 4916A

## Polymerization of Lactam Ethers

NAOYA OGATA,\* TOMOHIKO ASAHARA, and SYUNROKU TOHYAMA, *Basic Research Laboratories, Toyo Rayon Company, Ltd., Tebiro, Kamakura, Japan*

### Synopsis

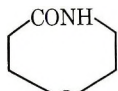
Preparation and polymerization of lactam ethers which contain an amide and an ether group in the same ring are described. Seven-membered lactam ethers give relatively low molecular weight polymers with an anionic or cationic catalyst, while with diethylzinc as catalyst, the 2,7-dimethyl lactam ether of a seven-membered ring gives a crystalline polymer having a melting point of 220°C. A polymerization mechanism is discussed.

### INTRODUCTION

The ring-opening polymerization of monofunctional cyclic compounds has been widely studied on lactams, lactones, cyclic ethers, etc., while cyclic compounds with bifunctional groups such as lactam ether or lactone ether have not been extensively investigated. A cyclic lactam ether has two opening points for polymerization, that is, an amide and an ether group.

Lactams require a relatively high activation energy for ring-opening polymerization owing to the resonance stabilization of an amide group, and especially when the conformation of the amide group is *trans*, it becomes quite stable.<sup>1</sup> For instance, lactams high in the series, such as laurolactam, polymerize much more slowly than  $\epsilon$ -caprolactam and require three times as long a period of heating for the completion of polymerization.<sup>2</sup>

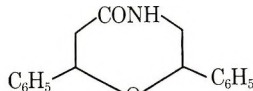
On the other hand, cyclic ethers can be polymerized very easily by an anionic or cationic catalyst, and the polymerizability of the cyclic ethers is greatly influenced by the basicity of the ether group and hence by the substituent on the  $\alpha$ -carbon atom, since the polymerization proceeds through successive opening of the carbon-oxygen bond of an oxonium ion intermediate.<sup>3</sup> However, the polymerizability of lactam ethers may be different from that of lactams or cyclic ethers, since it is expected that the



I



II



III

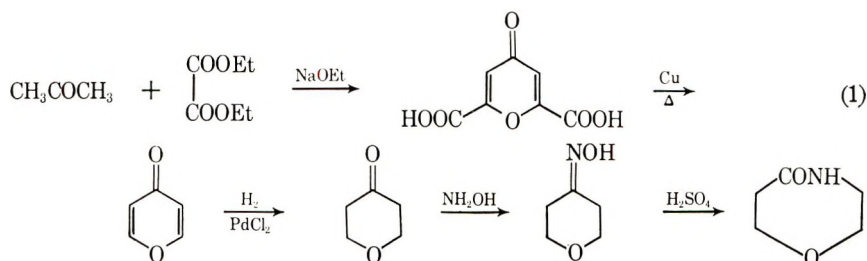
\* Present address: Chemistry Department, Sophia University, Chiyoda-ku, Tokyo, Japan.

reactivity of an amide and ether group might influence each other through the ring. Therefore the polymerization of the lactam ethers I, II, and III has been investigated.

## EXPERIMENTAL

### Preparation of Lactam Ethers

**Tetrahydro-1,4-oxazepin-5(4H)-one.** Synthesis was carried out by the route shown in eq. (1).<sup>4-6</sup>

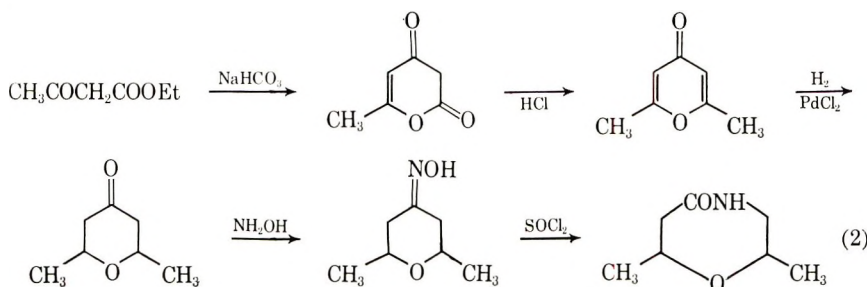


$\gamma$ -Pyrylone, which was obtained by the pyrolysis of cheridonic acid in the presence of metallic copper powder, was hydrogenated under a pressure of 1 atm. of hydrogen at room temperature in the presence of palladium(II) chloride to give tetrahydro- $\gamma$ -pyrylone (b.p. 50°C./8 mm. Hg).

The lactam ether was synthesized from the oxime of tetrahydro- $\gamma$ -pyrylone (m.p. 78–79°C.), through Beckmann rearrangement with sulfuric acid at 120°C.; m.p. 77–78°C.

ANAL. Calcd.: C, 52.2%; H, 7.8%; N, 12.2%. Found: C, 51.1%; H, 8.2%; N, 12.4%.

**Tetrahydro-2,7-dimethyl-1,4-oxazepin-5(4H)-one.** The route for the synthesis is given in eq. (2).<sup>7</sup>



The hydrogenation of 2,6-dimethyl- $\gamma$ -pyrylone took about 2 weeks under a pressure of 1 atm. because of the steric hindrance of methyl groups.<sup>6</sup> Selective hydrogenation of the double bonds was carried out under a hydrogen pressure of 50–60 kg./cm.<sup>2</sup> at 50°C. for 1 or 2 days in the presence of PdCl<sub>2</sub> catalyst. Beckmann rearrangement of the oxime by sulfuric acid or polyphosphoric acid<sup>8</sup> gave a poor yield, since considerable quantities of a

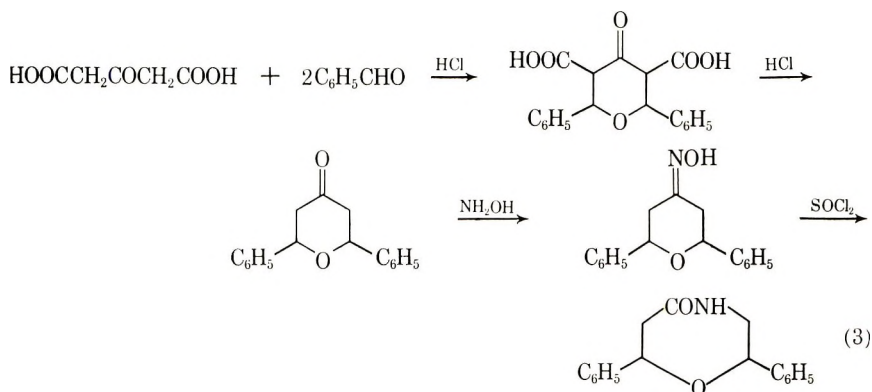


ring-fission product were obtained, and it was found that with thionyl chloride the oxime rearranged smoothly to the corresponding lactam at low temperature.

For instance, 3 g. of the oxime was dissolved in 40 ml. of benzene and 3 ml. of thionyl chloride was added from a dropping funnel, the temperature being maintained at 0–10°C. After stirring for 5 hr., a small amount of water was added to decompose excess thionyl chloride, and the solution was neutralized with potassium bicarbonate. The lactam ether was extracted with dichloromethane and purified by recrystallization from toluene; m.p. 125°C.; b.p. 125°C./5 mm.

ANAL. Calcd.: N, 9.8%;  $M_w = 143$ . Found: N, 9.79%;  $M_w = 143$ .

**Tetrahydro-2,7-diphenyl-1,4-oxazepin-5(4H)-one.** The route for the synthesis was as shown in eq. (3).<sup>10,11</sup>



Freshly prepared acetone dicarboxylic acid (200 g.) obtained by the method of Ingold<sup>9</sup> reacted with benzaldehyde at –20°C. for 4 hr. in the presence of dry hydrogen chloride. The pH value of the solution was adjusted at 9–10 by adding sodium bicarbonate so that the excess benzaldehyde was separated in the upper layer. After the aqueous solution was neutralized by HCl, a semisolid substance was separated from the solution. The substance decomposed slowly, evolving carbon dioxide gas. It was a mixture of *cis* and *trans* isomers of tetrahydro-2,6-diphenyl- $\gamma$ -pyrone. After standing overnight, a considerable amount of a white mass was precipitated from the aqueous solution, which was a mixture of *cis* and *trans* isomers. Fractional recrystallization from isopropyl alcohol separated the isomers; *trans*-lactam ether, m.p. 199–203°C.; *cis*-lactam ether, m.p. 130–133°C.

ANAL. Calcd.: C, 76.38%; H, 6.41%; N, 5.24%. Found: C, 76.3%; H, 6.40%; N, 5.25%.

**Tetrahydro-4H-1,3-oxazin-4-one.** The route tried for the synthesis<sup>12–15</sup> is shown in eq. (4). Beckmann rearrangement of the oxime of





## RESULTS

**Polymerization of Tetrahydro-1,4-oxazepin-5(4H)-one**

A soft, yellowish polymer was obtained from the unsubstituted lactam ether as shown in Table I. Neither water nor anionic catalyst gave a high polymer and the infrared spectrum (Fig. 2) showed that the polymer has a structure of poly(amide ether). The melting point of the polymer is not sharp, but the polymer becomes sticky at about 100°C.

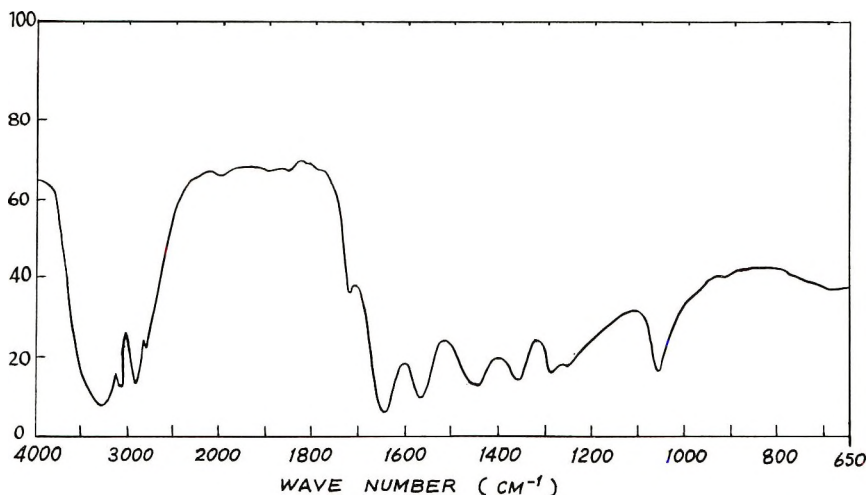


Fig. 2. Infrared spectrum of poly[tetrahydro-1,4-oxazepin-5(4H)-one].

Copolymerization with  $\epsilon$ -caprolactam at a molar ratio of 50/50 was tried in the presence of 5 mole-% of sodium metal on heating at 200°C. for 1 hr. A yellowish soft polymer having  $\ln(\eta_r/c) = 0.20$  in DMF was obtained at 95% conversion of monomers.

**Polymerization of Tetrahydro-2,7-dimethyl-1,4-oxazepin-5(4H)-one**

Results in the presence of several catalysts are summarized in Table II. Cationic catalysts such as  $H_3PO_4$ ,  $FeCl_3$ , and  $AlCl_3$  gave a polymer in a good yield at relatively low temperature, while complexes such as  $BF_3$  or  $PF_5$  etherates and  $(C_6H_5)_3P$  did not catalyze the polymerization. A hydrolytic polymerization in the presence of water resulted in a poor yield of polymer. Alkali metals gave a low polymer in a good yield, while  $Et_2Zn$  gave a film-forming high polymer of  $\ln(\eta_r/c) = 0.65$  (in formic acid, 25°C., 0.5 g./dl.). Infrared spectra of the polymers are shown in Figure 3.

An x-ray diffraction pattern of the polymer obtained in the presence of  $Et_2Zn$  showed a highly crystalline structure (Fig. 4), and the melting point of this polymer was 210°C. by differential thermal analysis. The high melting point and high crystallinity of the substituted polyamide ether are

TABLE I  
 Polymerization of Tetrahydro-1,4-oxazepin-5(4H)-one

Catalyst	Catalyst, mole-%	Solvent	Monomer concn., mole/l.	Temp., °C.	Time, hr.	Polymer	
						Yield, %	$(\eta_{sp}/c)^a$
H <sub>2</sub> O	10	None	—	180	30	90	0.10
H <sub>3</sub> PO <sub>4</sub>	3	None	—	207	24	80	0.05
BF <sub>3</sub>	1	Dioxane	2.9	100	50	9.0	—
AlCl <sub>3</sub>	1	Dioxane	2.9	100	50	9.3	—
PF <sub>5</sub> ·THF	1	Dioxane	2.9	100	50	Trace	—
Na	5	None	—	180	30	80	0.10

<sup>a</sup> In dimethylformamide, 25°C.,  $c = 0.5$  g./dl.

TABLE II  
 Polymerization of Tetrahydro-2,7-dimethyl-1,4-oxazepin-5(4H)-one

Catalyst	Catalyst, mole-%	Solvent	Monomer concn., mole/l.	Temp., °C.	Time, hr.	Polymer	
						Yield, %	M.p., °C. $\ln(\eta_r/c)^a$
H <sub>3</sub> PO <sub>4</sub>	8	None	—	207	44.5	95	—
BF <sub>3</sub> -ether	5	None	—	180	30	0	—
"	4.4	Toluene	20	180	50	0	—
FeCl <sub>3</sub>	5	None	—	180	30	99	0.07
"	11.5	Toluene	20	100	50	57.5	0.03
AlCl <sub>3</sub>	29.1	Toluene	20	100	50	85	0.04
PF <sub>5</sub> -THF	2.5	Toluene	20	100	50	0	—
(C <sub>6</sub> H <sub>5</sub> ) <sub>3</sub> P	5	Toluene	20	100	50	0	—
Na	1	None	—	140	0.25	70	0.03
"	8	Toluene	20	100	50	70	0.03
K	10	Toluene	20	100	50	85	0.03
Et <sub>2</sub> Zn	10	None	—	140	0.25	80	0.65 <sup>b</sup>
Et <sub>2</sub> Zn/H <sub>2</sub> O	10	None	—	140	0.25	0	—
Et <sub>3</sub> Al	1	None	—	140	0.25	0	—
H <sub>2</sub> O	1	None	—	140 <sup>c</sup> 207	24 <sup>c</sup> 48	44	0.08

<sup>a</sup> In dimethylformamide, 25°C.,  $c = 0.5$  g./dl.

<sup>b</sup> In formic acid, 25°C.,  $c = 0.5$  g./dl.

<sup>c</sup> 24 hr. at 140°C. and then 48 hr. at 207°C.

remarkable, since a substituent on lactam ring tends to reduce the crystallinity and hence to lower the melting point, as in the case of  $\epsilon$ -caprolactam.

Several cocatalysts for  $\text{Et}_2\text{Zn}$  were investigated. Results were not satisfactory as far as the polymer yield is concerned (Table III), and reproducibility of the experiment was poor.

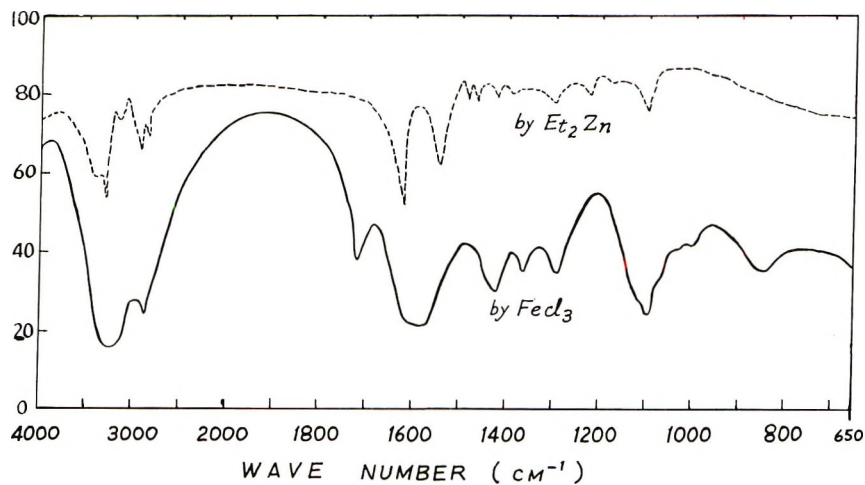


Fig. 3. Infrared spectrum of poly[tetrahydro-2,7-dimethyl-1,4-oxazepin-5(4H)-one] obtained in the presence of  $\text{ZnEt}_2$  (film).

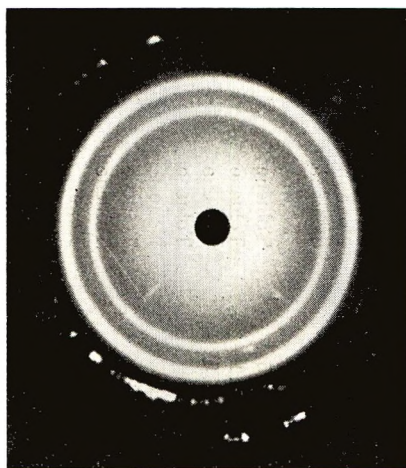


Fig. 4. X-ray diffraction pattern of poly[tetrahydro-2,7-dimethyl-1,4-oxazepin-5(4H)-one].

Copolymerization with  $\epsilon$ -caprolactam in the presence of potassium resulted in lower molecular weight polymer with increasing amounts of dimethyl lactam ether as shown in Table IV.

TABLE III  
 Polymerization of Tetrahydro-2,7-dimethyl-1,4-oxazepin-5(4H)-  
 one in the Presence of  $ZnEt_2$  and Co catalysts

Co-catalyst	Cocatalyst, mole-% <sup>a</sup>	Solvent	Temp., °C.	Time, min.	Polymer	
					Yield, %	M.p., °C.
None	10	None	207	15	80	210
H <sub>2</sub> SO <sub>4</sub>	1	None	207	15	18	—
Ac <sub>2</sub> O	1	None	207	15	33	200
CH <sub>3</sub> CHO	1	None	207	15	33	—
$\beta$ -Alanine	0.5	None	207	15	4	261
PCl <sub>3</sub>	1	None	207	15	54	208

<sup>a</sup> Percentage relative to monomer. Equimolar amount of cocatalyst used relative to the catalyst.

### Polymerization of Tetrahydro-2,7-diphenyl-1,4-oxazepin-5(4H)-one

Polymerization of the diphenyl lactam ether yielded a low polymer, as seen in Table V.

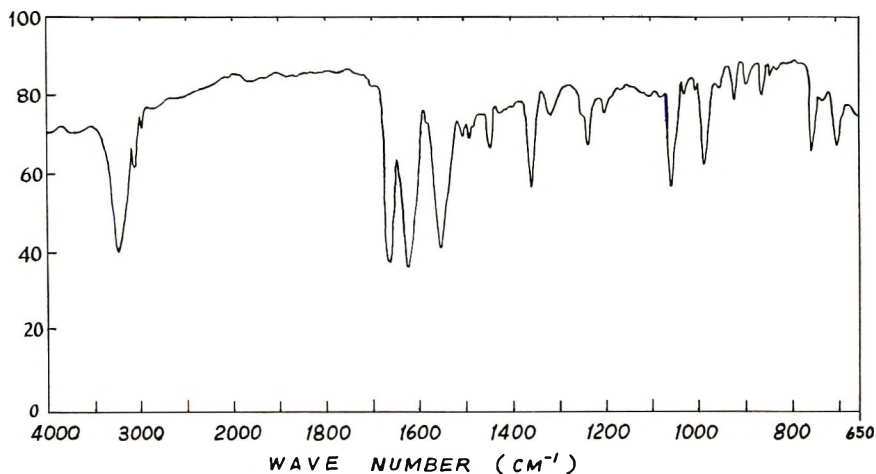


Fig. 5. Infrared spectrum of poly[tetrahydro-2,7-diphenyl-1,4-oxazepin-5(4H)-one].

Generally speaking, anionic catalysts gave a better yield of polymer than cationic catalysts, and the *cis* isomer gave a better yield of polymer than the *trans* isomer in the presence of  $BF_3$ -ether catalyst. All of these polymers have melting points around 180°C. and the polymerization degrees are low, as estimated by viscosity data. The infrared spectrum of the polymer is indicative of poly(amide-ether) structure (Fig. 5).

TABLE IV  
 Copolymerization of Tetrahydro-2,7-dimethyl-1,4-oxazepin-5(4H)-one and  $\epsilon$ -Caprolactam (H<sub>2</sub>O; 1 mole-%)

$\epsilon$ -Caprolactam, mole-%	Dimethyl lactam ether, mole-%	Temp., °C.	Time, hr.	Yield, %	M.p., °C.	Polymer	
						In ( $\eta_r/c$ ) <sup>a</sup>	Character
100	0	230	50	70	215	0.80	White solid
90	10	"	"	97	205	0.15	Yellow solid
80	20	"	"	90	182	0.09	Dark brown solid
70	30	"	"	99	150	0.07	Brown powder
60	40	"	"	99	Soft	0.09	Brown grease
50	50	"	"	90	Soft	0.04	"
40	60	"	"	96	Soft	0.04	"

<sup>a</sup> In dimethylformamide, 25°C.,  $c = 0.5$  g./dl.



TABLE V  
 Polymerization of Tetrahydro-2,7-diphenyl-1,4-oxazepin-5(4H)-one

Expt. no.	Monomer	Catalyst	Catalyst concn., mole/l.	Solvent	Monomer concn., mole/l.	Temp., °C.	Time, hr.	Polymer	
								Yield, %	$\ln \eta_r/c^a$
1	<i>trans</i>	Na	5	None	—	230	0.25	15	0.034
2	<i>trans</i>	BF <sub>3</sub> Et <sub>2</sub> O	5	None	—	230	4.5	0	—
3	<i>cis</i>	ZnEt <sub>2</sub>	16	None	—	230	0.25	18	0.023
4	<i>cis</i>	ZnEt <sub>2</sub>	9.6	Benzene	0.25	78	24	26	0.025
5	<i>cis</i>	BF <sub>3</sub> Et <sub>2</sub> O	5.5	Benzene	0.25	78	24	35	0.023
6	<i>cis</i>	BF <sub>3</sub> Et <sub>2</sub> O	12	Benzene	0.25	78	24	38	—
7	Mix. <sup>b</sup>	H <sub>3</sub> PO <sub>4</sub>	10	None	—	207	20	0	—
8	Mix.	ZnEt <sub>2</sub>	10	None	—	207	20	10.6	0.020
9	Mix.	Na	5	None	—	230	1	50	0.037
10	Mix.	K	5	None	—	230	1	55	0.035
11	Mix.	Li	5	None	—	230	1	23	0.038
12	Mix.	K/Ac <sub>2</sub> O	1	None	—	230	1	4	—
13	Mix.	K/Ac <sub>2</sub> O	5	None	—	230	1.5	6	—

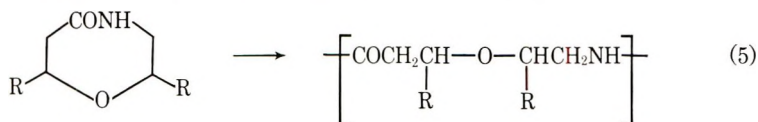
<sup>a</sup> In dimethylformamide, 25°C.,  $c = 0.5$  g./dl.

<sup>b</sup> Mixture of both isomers, ratio unknown.

## DISCUSSION

It is known that the equilibrium of  $\epsilon$ -caprolactam polymerization between ring and chain forms shifts toward ring form when a substituent is introduced into the lactam ring, and that a disubstituted  $\epsilon$ -caprolactam does not polymerize at all in the presence of water.<sup>16</sup> The shift of the polymerization equilibrium is not attributed to ring strain, but to the difference in thermodynamical character caused by intramolecular rotational isomers.<sup>17, 18</sup> Substitution on the poly- $\epsilon$ -caproamide chain results in low crystallinity and hence a lower melting point.

It is seen from the above results that the polymerizability of the lactam ether is remarkably different from that of the lactam, since disubstituted lactam ethers polymerize into crystalline polymers [eq. (5)].



Complexes such as  $\text{BF}_3$  or  $\text{PF}_5$  etherates, which are strong cationic catalysts, do not catalyze polymerization of the dimethyl lactam ether, while Lewis acids such as  $\text{FeCl}_3$  or  $\text{AlCl}_3$  accelerate the polymerization at  $100^\circ\text{C}$ . ( $\epsilon$ -Caprolactam does not polymerize under the similar condition with these catalysts.)

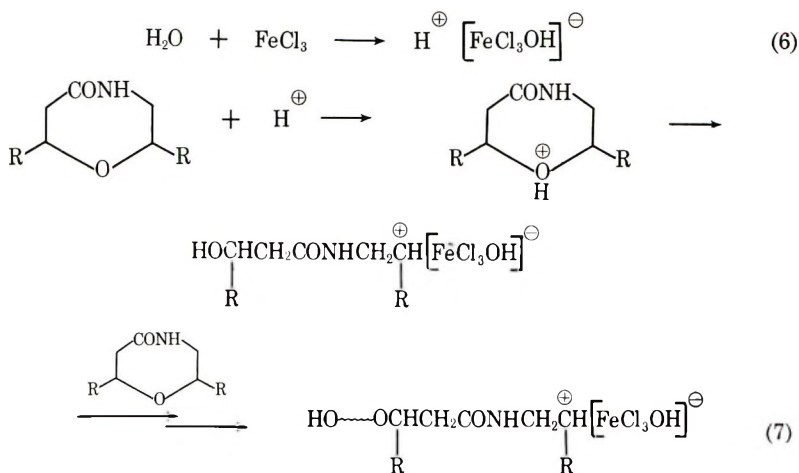
The steric conformation of the dimethyl lactam ether around an oxygen atom might hinder coordination of the complex catalyst, resulting in a poor catalytic effect. The greater polymerizability of the disubstituted lactam ether compared to the lactam ether in the presence of  $\text{FeCl}_3$  or  $\text{AlCl}_3$  catalyst shows that the carbonium ion intermediate which is produced by breaking of the C—O bond of an oxonium ion might be stabilized by the methyl group.

The result that the *trans* isomer of the diphenyl lactam ether gave a better yield of polymer than the *cis* isomer might indicate steric hindrance around an ether oxygen for the coordination of catalysts.

From these results, it is assumed that the cationic polymerization of the lactam ether proceeds through formation of an oxonium ion, followed by breakage of the C—O bond, since lactams do not give polymer under the same conditions. The infrared spectrum of the poly(amide ether) obtained in the presence of  $\text{FeCl}_3$  shows a broad peak at  $3300\text{ cm}^{-1}$ , which suggests the existence of an OH group. The polymerization may proceed through the mechanism shown in eqs. (6) and (7).

The polymerization of the dimethyl lactam ether in the presence of alkali metal or organometallic compounds may proceed through splitting off of an amide group, since a gas evolution was noted during the reaction. Sodium or diethylzinc reacts with equimolar quantities of lactam ether, giving a nearly theoretical amount of hydrogen or ethane.

The high yield and degree of polymerization of the polymer in the case of  $\text{ZnEt}_2$  catalyst require a further elucidation of the reaction mechanism.



Alkali metal polymerizes the lactam ether very rapidly, while the degree of polymerization of the polymer is very low. It is generally known that acyl compounds have a cocatalytic effect on the polymerization of lactams. However, experimental results show that acyl compounds have an inhibiting effect in the case of the lactam ether, as shown in Tables III and V. The carbonyl absorption of  $\epsilon$ -caprolactam appears at  $1650 \text{ cm.}^{-1}$ , while dimethyl or diphenyl lactam ethers show an absorption at  $1670\text{--}1680 \text{ cm.}^{-1}$ . This carbonyl shift indicates that the polarization of the carbonyl group is reduced by an electronic interaction induced by the ether oxygen atom.

The low degree of polymerization of the polymers may be attributed to the monomer transfer reaction, in which the lactam anion reacts exclusively with the monomer and for which the propagation reaction may be very slow. Therefore, it is expected that a cationic or coordinating catalyst may give a high polymer since such catalysts could open an ether linkage.

The authors wish to thank Dr. T. Hoshino for permission to publish this report. We also thank Mr. H. Hirai for assisting in some of the experimental work.

### References

1. N. Ogata, *J. Polymer Sci. A*, **1**, 3151 (1963).
2. T. I. Shein and L. N. Vlasova, *Polymer Sci. U.S.S.R.*, **5**, 564 (1964).
3. S. Iwatsuki et al., *J. Polymer Sci. B*, **2**, 549 (1964).
4. *Organic Synthesis*, Coll. Vol. II, Wiley, New York, 1963, p. 126.
5. R. Willstatter and R. Pummer, *Ber.*, **37**, 3740 (1904); *ibid.*, **38**, 1461 (1905).
6. W. Borsche, *Ber.*, **48**, 682 (1915); *ibid.*, **56**, 2012, 2132 (1923); *ibid.*, **59**, 237 (1926).
7. F. Arndt et al., *Ber.*, **69**, 2373 (1936).
8. C. Barkenbus, J. F. Diehl, and G. R. Vogel, *J. Org. Chem.*, **20**, 871 (1955).
9. C. K. Ingold and L. C. Nickolls, *J. Chem. Soc.*, **121**, 1642 (1922).
10. P. Petrenko and D. Platnippoff, *Ber.*, **30**, 2801 (1897).
11. R. Cornubert and P. Robinet, *Bull. Soc. Chim. France*, **1**, 90 (1934).
12. H. Wynsberg and A. Bantijes, in *Organic Synthesis*, Coll. Vol. IV, Wiley, New York, 1963, p. 534.
13. J. H. Weiland et al., *Rec. Trav. Chim.*, **82**, 651 (1963).

14. I. K. Korobitsyana, Yu. K. Yurev, and E. Lukina, *Zh. Obshch. Khim.*, **25**, 531 (1955).
15. R. C. Elderfield et al., *J. Org. Chem.*, **26**, 1703 (1961).
16. H. Yumoto, K. Ida, and N. Ogata, *Bull. Chem. Soc. Japan*, **31**, 249 (1958).
17. H. Yumoto, *J. Chem. Phys.*, **29**, 1234 (1958).
18. R. C. P. Cubbon, *Makromol. Chem.*, **80**, 44 (1964).

### Résumé

La préparation et la polymérisation d'éther lactamique qui contient un groupe éther et un groupe amide dans le même cycle sont décrites. Les lactames-éthers à sept atomes donnent des polymères de poids moléculaires relativement bas en présence d'un catalyseur anionique ou cationique, alors que la lactame éther 2,7-diméthyle d'un cycle à sept atomes fournit un polymère cristallin d'un point de fusion de 220°C en présence d'un catalyseur à base de diéthylzinc. Le mécanisme de polymérisation est soumis à discussion.

### Zusammenfassung

Darstellung und Polymerisation von Lactamäthern mit einer Amid- und einer Äthergruppe im selben Ring werden beschrieben. Siebengliedrige Lactamäther liefern mit einem anionischen oder kationischen Katalysator verhältnismässig niedermolekulare Polymere, während 2,7-Dimethylactamäther mit einem siebengliedrigen Ring mit Diäthylzink als Katalysator kristalline Polymere mit einem Schmelzpunkt von 220°C geben. Ein Polymerisations-mechanismus wird diskutiert.

Received August 9, 1965

Revised October 10, 1965

Prod. No. 4942A

## Spectroscopic Studies of Poly(vinyl Chloride) and Its Deuterated Derivatives

S. ENOMOTO and M. ASAHINA, *Tokyo Research Laboratory, Kureha Chemical Industry Co. Ltd., Hyakunin-cho, Shinjuku-ku, Tokyo, Japan*, and S. SATOH, *Takatsuki Research Institute, Kureha Spinning Co. Ltd., Nishiamakawa, Osaka-fu, Japan*

### Synopsis

Poly(vinyl chloride) (PVC) and all its deuterated derivatives were prepared by variation of the polymerization method and polymerization temperature to study the structure of PVC and the mechanism of addition polymerization by infrared spectroscopy and high resolution NMR spectroscopy. The CH and CH<sub>2</sub> stretching modes of PVC were assigned completely from the infrared spectra of PVC- $\alpha d_1$ , PVC- $\beta, \beta d_2$  and PVC- $d_3$ . The frequencies of the CCl stretching modes of the polymers depended not only on the substituents in the *trans* position to the Cl atom across both adjacent C—C bonds, but also on the atom attached to the C atom of the C—Cl bond. The frequency shifts were used to assign the CCl stretching modes of PVC- $\beta d_1$  and PVC- $\alpha, \beta d_2$  and to study the opening of the double bond of VC in the addition polymerization. The differences of the chemical shifts of the  $\alpha$  and  $\beta$  protons of PVC due to the tacticity were determined experimentally by PVC- $\beta, \beta d_2$  and PVC- $\alpha d_1$  without using the spin-decoupling technique. With PVC- $\alpha, \beta d_2$ , the conception of the tetrad was required to interpret the four observed peaks whose intensities changed with the polymerization temperature and the *trans-cis* composition of the monomer used.

### INTRODUCTION

Infrared spectroscopy and high-resolution NMR spectroscopy are effective methods for elucidating the complicated structure of PVC. Assignments in the infrared spectrum have been made by use of the deuterated derivatives<sup>1-3</sup> and a normal coordinate analysis has been carried out for some of their spectra with the transferred force constants obtained from low molecular organic chlorine compounds.<sup>4</sup> After Shimanouchi and his co-workers pointed out that the CCl stretching modes of PVC were sensitive to the chain conformation,<sup>5</sup> various low molecular organic chlorine compounds were studied intensively to understand more clearly the relation between their CCl stretching modes and chain conformations.<sup>6-8</sup> These results were applied to the quantitative analysis of the tacticity,<sup>9,10</sup> the change of the conformation caused by stretching and heat set,<sup>11</sup> and the effect of plasticizer upon the chain.<sup>8</sup>

NMR spectroscopy is a convenient method for determining the tacticity. The NMR spectrum of PVC has been analyzed by numerous workers.<sup>12-18</sup>

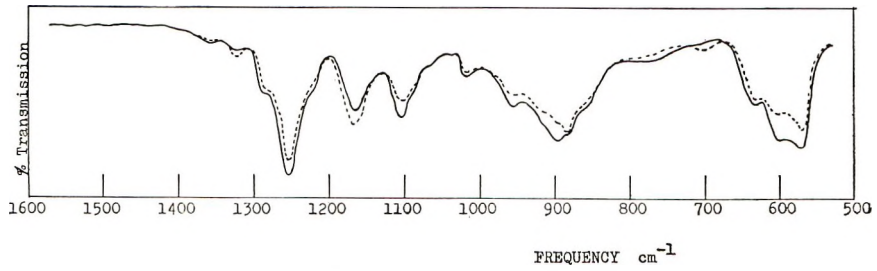


Fig. 1. Infrared spectra of PVC- $\beta,\beta d_2$  from 1600 to 500  $\text{cm}^{-1}$ : (—) with electric vector perpendicular to orientation; (- -) with electric vector parallel to orientation direction.

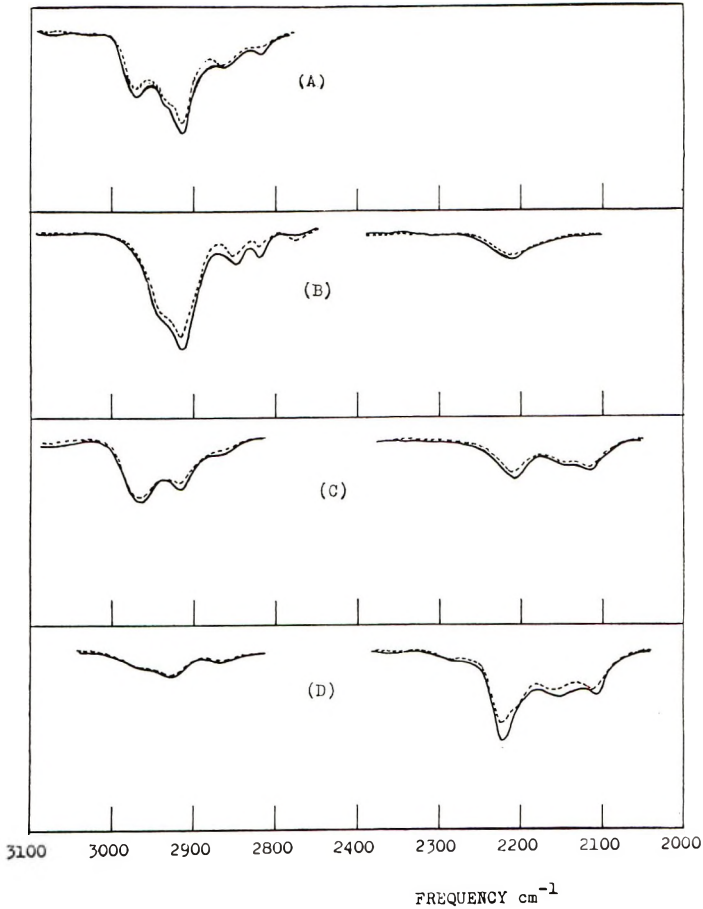


Fig. 2. Infrared spectra of (A) PVC, (B) PVC- $\alpha d_1$ , (C) PVC- $\beta,\beta d_2$ , and (D) PVC- $d_3$  from 3100 to 2000  $\text{cm}^{-1}$ : (—) with electric vector perpendicular to orientation direction; (- -) with electric vector parallel to orientation direction.



The meso 2,4-dichloropentane and the racemic compound have been studied to help in the analysis of PVC,<sup>19,20</sup> and studies with model compounds of PVC have been extended recently to 2,4,6-trichloroheptane, for which syndiotactic, isotactic, and heterotactic parts of PVC are expected.<sup>16</sup> An attempt has been by the spin-decoupling technique<sup>21,22</sup> to observe the NMR lines of the  $\beta$ -protons and these of the  $\alpha$ -proton separately without the interactions between them, and the NMR spectrum of the  $\beta$ -protons decoupled from the  $\alpha$ -proton was consistent with that of PVC- $\alpha d_1$ .<sup>23</sup>

The NMR spectra of PVC- $\beta, \beta d_2$ , PVC- $\beta d_1$ , and PVC- $\alpha, \beta d_2$  are desired for analysis of the spectrum of PVC in detail because they will give more refined information with respect to the chemical shifts and the spin-spin coupling constants of PVC than the spin-decoupling method. Especially, PVC- $\beta, \beta d_2$  which has not been reported is of great interest in making assignments of infrared spectrum of PVC completely and for confirmation of the chemical shift of the  $\alpha$ -proton.

Another point of interest is study of the opening of the double bond of VC in the addition polymerization. If only *trans* opening or *cis* opening occurs in the polymerization of *trans* or *cis*  $\alpha, \beta$ -disubstituted vinyl chloride, the CCl stretching modes assigned to the isotactic PVC- $\beta d_1$  and PVC- $\alpha, \beta d_2$  will depend upon the substituents in the positions *trans* to the Cl atom across both adjacent C—C bonds.

This paper will describe the points above mentioned.

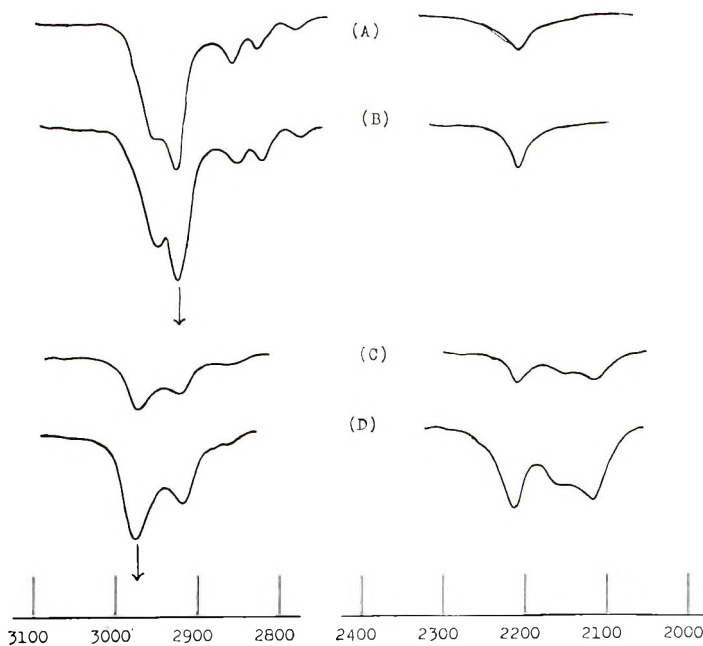


Fig. 3. Crystalline bands of CH and CH<sub>2</sub> stretching modes: (A) 50°C., PVC- $\alpha d_1$ ; (B) -30°C., PVC- $\alpha d_1$ ; (C) 50°C., PVC- $\beta, \beta d_2$ , (D) -30°C., PVC- $\beta, \beta d_2$ . The spectra were obtained with unoriented films.

## EXPERIMENTAL

## Preparation of Samples

The spectroscopic study showed the monomers used in this work to be very pure. While VC- $\beta d_1$  contained only the *trans* form, VC- $\alpha, \beta d_2$  contained both *cis* and *trans* components, and the monomers A and B were different compositions.<sup>24</sup> The three recipes I, II, and III listed in Table I were used to polymerize the monomers. The interesting recipe III was used for the polymerizations of VC- $\beta d_1$  and VC- $\alpha, \beta d_2$  to study the polymerization mechanism by a modified Ziegler-type catalyst.<sup>25</sup>

TABLE I  
Polymerization Conditions

Polymer	Polymerization temperature, °C.	Recipe <sup>a</sup>	Monomer
PVC	50	I	
	-30	II	
PVC- $\alpha d_1$	50	I	
	-30	II	
PVC- $\beta, \beta d_2$	50	I	
	-30	II	
PVC- $\beta d_1$	58	I	
	30	III	
	-30	II	
PVC- $\alpha, \beta d_2$	50	I	
A	30	III	87.3%;  12.7%
	-30	II	
	50	I	
B	30	III	55.6%;  44.4%
	-30	II	

<sup>a</sup> Recipes: (I) ordinary suspension polymerization with lauroyl peroxide; (II) photosensitized polymerization in methanol solution with uranyl nitrate.<sup>28</sup> (III) solution polymerization with  $\text{AlCl}_3\text{Et}$  (1 mole/l.) and  $\text{Ti}(\text{O}i\text{Bu})_4$  (0.5 mole/l.) in *n*-hexane.<sup>25</sup>

## Infrared Spectra

A Nihon Bunko 402G type grating spectrometer was used for the measurements. Only new results obtained are shown here, as most of the in-

frared spectra at solid state have already been reported.<sup>3</sup> The infrared spectrum of PVC- $\beta,\beta d_2$  is shown in Figure 1 and listed in Table II. Figures 2 and 3 show the infrared spectra in the region of from 3200–2000  $\text{cm.}^{-1}$  to assign completely the CH and  $\text{CH}_2$  stretching modes of PVC. The samples were dissolved in carbon disulfide-acetone mixed solvent to observe their CCl stretching modes in solution, and the spectra are shown in Figures 4 and 5.

TABLE II  
Infrared Spectrum of PVC- $\beta,\beta d_2$

Frequency, $\text{cm.}^{-1}$	Relative intensity <sup>a</sup>	Polarization	Assignment
2962	w	$\perp$	CH stretch. ( $A_1$ ), ( $B_1$ )
2915	w	$\perp$	
2855	vvw	$\perp$	amorphous
2210	w	$\perp$	$\text{CD}_2$ antisymm. stretch. ( $B_1$ ), ( $B_2$ )
2150	sh	$\perp$	
2112	w	$\perp$	$\text{CD}_2$ symm. stretch. ( $A_1$ )
1356	vvw	?	
1325	vw	.	CII bend. ( $B_2$ )
1286	vvw	$\perp$	CH bend. ( $A_1$ )
1275	vvsh	?	
1252	vs	$\perp$	CII bend. ( $B_1$ )
1225	wsh	?	
1167	m	.	CC stretch., $\text{CD}_2$ wag ( $B_2$ )
1105	m	$\perp$	CC stretch., $\text{CD}_2$ wag ( $B_1$ )
1090	sh	?	
1063	sh	?	skeletal mode
1032	vvwsh	?	
1020	w	$\perp$	$\text{CD}_2$ bend. ( $A_1$ )
955	sh	$\perp$	$\text{CD}_2$ twist. ( $A_1$ ), CC stretch, $\text{CD}_2$ wag ( $B_1$ )
917	vwsh	?	
900	s	$\perp$	$\text{CD}_2$ rock. ( $B_1$ )
885	sh	.	$\text{CD}_2$ wag, CC stretch. ( $B_2$ )
855	sh	?	
709	sh	.	$\text{CD}_2$ rock. ( $B_2$ )
639	s	$\perp$	S. . (CHCl)
599	s	$\perp$	S. . ( $A_1$ )
572	s	$\perp$	S. . amorphous
572	s	$\perp$	S. . amorphous
565	s	$\perp$	S. . (CHCl) ( $B_1$ )

<sup>a</sup> w = weak, m = medium, s = strong, sh = shoulder.

### NMR Spectra

All samples were dissolved in *o*-dichlorobenzene to give about 10% concentration. NMR spectra were measured at 170°C. with a Varian Model V-4311 spectrometer operating at a fixed frequency of 60 Mc./sec. and equipped with a variable temperature accessory, Model V-4340. In partic-

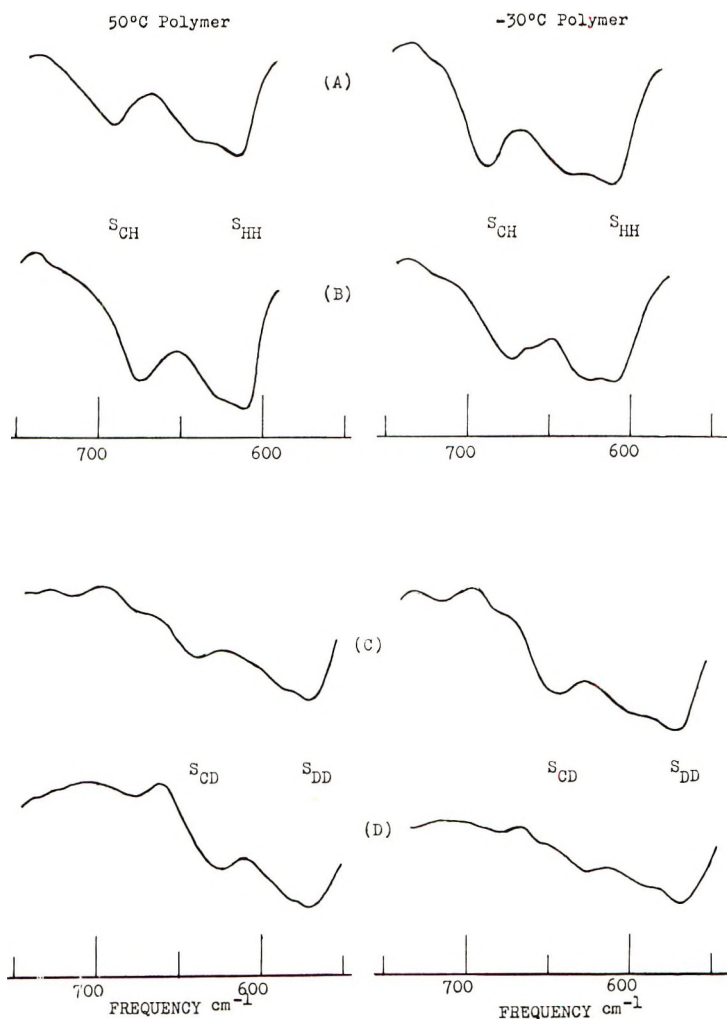


Fig. 4. Infrared spectra of PVC, PVC- $\alpha d_1$ , PVC- $\beta, \beta d_2$  and PVC- $d_3$  in solution: (A) PVC, (B) PVC- $\alpha d_1$ , (C) PVC- $\beta, \beta d_2$ , (D) PVC- $d_3$ .

ular with PVC- $\alpha d_1$ , the experiment was performed up to 200°C. in order to investigate the change in line widths. A Japan Electronic Company Model JNH-4H-100 spectrometer operating at 100 Mc./sec. was also used to observe the spectrum of PVC polymerized at 50°C. A spin-decoupling experiment was performed by the side-band method.

NMR spectra are reproduced in Figure 6. The spectra of PVC and PVC- $\alpha d_1$  are, respectively, the same as those already reported.<sup>14,15,22</sup> Three peaks are observed in the spectrum of PVC- $\beta, \beta d_2$ . They may be ascribed to the signals due to the protons on the isotactic, heterotactic, and syndiotactic parts, respectively. The spectrum of PVC- $\beta d_1$  consists of two groups of incompletely resolved multiplets. It is easily shown by the

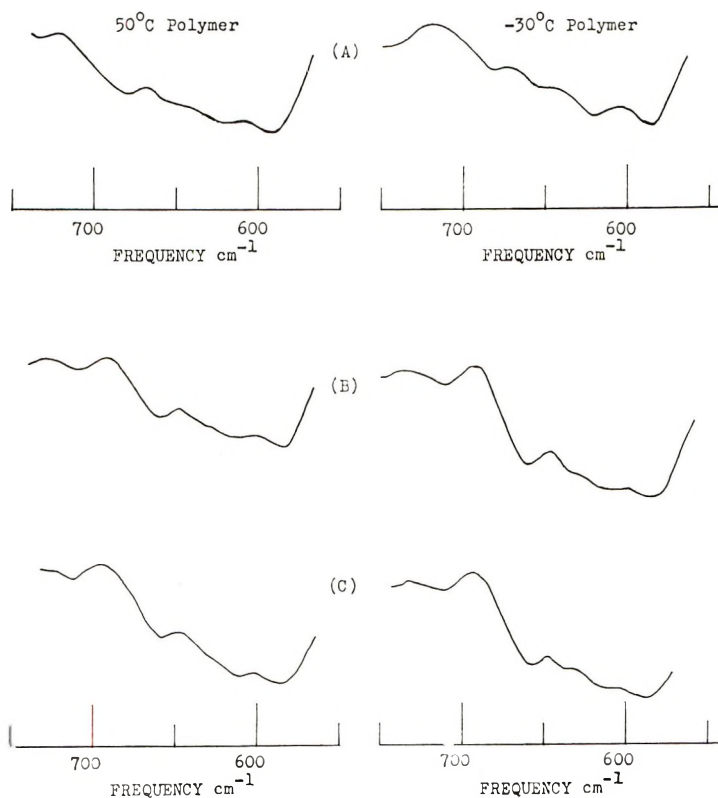


Fig. 5. Infrared spectra of PVC- $\beta d_1$  and PVC- $\alpha, \beta d_2$ : (A) PVC- $\beta d_1$  from *trans* VC- $\beta d_1$ , (B) PVC- $\alpha, \beta d_2$  from *trans* VC- $\alpha, \beta d_2$  87% and *cis* VC- $\alpha, \beta d_2$  13%; (C) PVC- $\alpha, \beta d_2$  from *trans* VC- $\alpha, \beta d_2$  55.6% and *cis* VC- $\alpha, \beta d_2$  44.4%.

spin-decoupling method that the multiplets are due to the indirect spin-spin interactions between  $\alpha$ - and  $\beta$ -protons. The spin-decoupled spectrum is reproduced in Figure 6. Four peaks, at least, are distinguished in the spectrum of PVC- $\alpha, \beta d_2$ , and their relative intensities vary, as illustrated in Figure 8, with polymerization temperature and with the *cis* and *trans* content of vinyl chloride- $\alpha, \beta d_2$ .

## RESULTS AND DISCUSSION

### Interpretation of Infrared Spectra

**The CH and CH<sub>2</sub> Stretching Modes of PVC.** A treatment of normal coordinate analysis is required to assign the infrared spectra of the deuterated polymers, as their CD and CD<sub>2</sub> modes are coupled with each other and are associated with the skeletal modes.<sup>4</sup> The assignments of the infrared spectrum of PVC- $\beta, \beta d_2$  in Table II are based on the calculations which Prof. Shimanouchi kindly made available to us.<sup>26</sup>

However, the infrared spectra of some deuterated polymers facilitate complete assignment of the CH and CH<sub>2</sub> stretching modes of PVC because

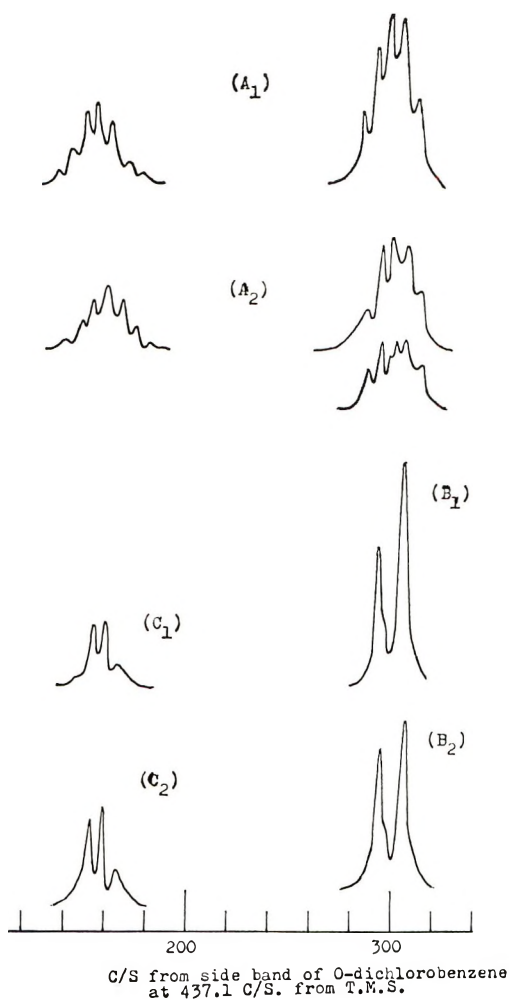


Fig. 6. NMR spectra of PVC, PVC- $\alpha d_1$ , and PVC- $\beta, \beta d_2$ . ( $A_1$ )  $-30^\circ\text{C}$ ., PVC; ( $A_2$ )  $50^\circ\text{C}$ ., PVC (upper) operating at 60 Mc., (lower) operating at 100 Mc.; ( $B_1$ )  $-30^\circ\text{C}$ ., PVC- $\alpha d_1$ , ( $B_2$ )  $50^\circ\text{C}$ ., PVC- $\alpha d_1$ , ( $C_1$ )  $-30^\circ\text{C}$ ., PVC- $\beta, \beta d_2$ , ( $C_2$ )  $50^\circ\text{C}$ ., PVC- $\beta, \beta d_2$ .

they are shifted largely to lower frequency by the substitution of a D atom on a specific H atom. Figure 2 shows such spectra. According to the normal coordinate analysis, both CH stretching modes of PVC ( $A_1$  and  $B_1$ ) should appear at around  $2970\text{ cm}^{-1}$ , and this assignment seems to be reasonable from the fact that only one band which is assignable to the CD stretching mode appears at  $2207\text{ cm}^{-1}$  in the infrared spectrum of PVC- $\alpha d_1$ . On the other hand, three bands appear at  $2962$ ,  $2915$ , and  $2855\text{ cm}^{-1}$  in the infrared spectrum of PVC- $\beta, \beta d_2$  and they should be assigned to the CH stretching modes. The relative intensity ratio between the band at  $2962\text{ cm}^{-1}$  and that at  $2915\text{ cm}^{-1}$  increases with decreasing polymerization temperatures, as shown in Figure 3, and the band at  $2962\text{ cm}^{-1}$  is



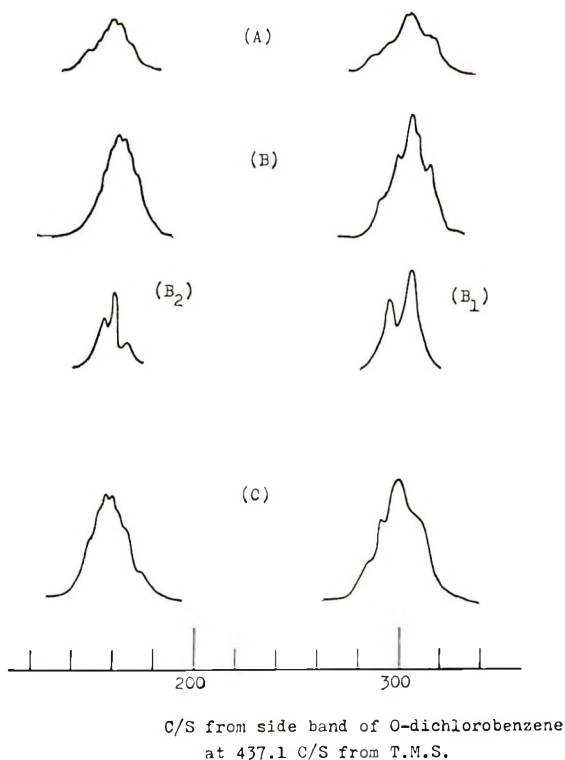


Fig. 7. NMR spectra of PVC- $\beta$ - $d_1$ : (A)  $-30^\circ\text{C}$ ., PVC- $\beta$ - $d_1$ ; (B)  $30^\circ\text{C}$ ., PVC- $\beta$ - $d_1$ ; (B<sub>1</sub>) decoupled lines of  $\beta$ -protons from  $\alpha$ -proton with  $30^\circ\text{C}$ . polymer; (B<sub>2</sub>) decoupled lines of  $\alpha$ -proton from  $\beta$ -protons with  $30^\circ\text{C}$ . polymer; (C)  $50^\circ\text{C}$ ., PVC- $\beta$ - $d_1$ .

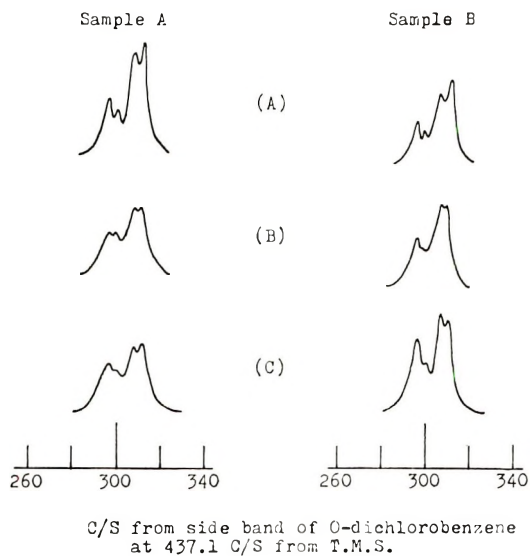


Fig. 8. NMR spectra of PVC- $\alpha,\beta$ - $d_2$ : (A)  $-30^\circ\text{C}$ ., PVC- $\alpha,\beta$ - $d_2$ ; (B)  $30^\circ\text{C}$ ., PVC- $\alpha,\beta$ - $d_2$ ; (C)  $50^\circ\text{C}$ ., PVC- $\alpha,\beta$ - $d_2$ . Sample A prepared from monomer 87.3% *trans* and 12.7% *cis*; sample B prepared from monomer 55.6% *trans* and 44.4% *cis*.

assigned to the CH stretching mode of the syndiotactic crystalline part. The band at  $2855\text{ cm.}^{-1}$  will be assigned to the mode of the amorphous part or to impurity because of its weak intensity, and the rather strong intensity of the band at  $2915\text{ cm.}^{-1}$  may be due to Fermi resonance. The  $\text{CH}_2$  stretching modes of PVC are easily understood from the infrared spectrum of PVC- $\alpha d_1$ , and four bands are observed at 2935, 2915, 2850, and  $2822\text{ cm.}^{-1}$ . Factor group analysis predicts that three  $\text{CH}_2$  stretching modes are associated with the  $A_1$ ,  $B_1$  and  $B_2$  species, and the  $B_2$  mode should show parallel dichroism; however, no parallel band is observed in this region. As the intensity of the band at  $2935\text{ cm.}^{-1}$  is increased with decreasing polymerization temperature, this band is assigned to the crystalline one. The complete assignments of the CH and  $\text{CH}_2$  stretching modes of PVC are summarized in Table III.

**The CCl Stretching Modes.** Detailed studies of a series of secondary alkyl halide revealed that the frequency of the CCl stretching mode depends in particular on the substituents which are *trans* to the Cl atom across both adjacent C—C bonds.<sup>7</sup> A convenient notation was proposed to classify the modes.  $S_{XY}$  expresses the CCl stretching mode of secondary chloride, where X is one substituent *trans* to the Cl atom and Y is the other. In case of PVC, the modes in the region from  $600$  to  $640\text{ cm.}^{-1}$  are  $S_{HH}$  and  $S_{CH}$  appears at  $690\text{ cm.}^{-1}$ .

The CCl stretching modes of PVC- $\beta, \beta d_2$  appear at 639, 599, 570, and  $565\text{ cm.}^{-1}$ . Among them, the bands at 599 and  $565\text{ cm.}^{-1}$  are assigned to the CCl stretching modes of the crystalline region because of their absences in the infrared spectrum at solutional state.

The existence of an amorphous band assigned to a modified  $S_{HH}$  of the nonplanar chain conformation was pointed out in the infrared spectrum of PVC, as a weak shoulder was still observed near the crystalline band at  $640\text{ cm.}^{-1}$  in solution, and this crystalline band became weaker than the

TABLE III  
Assignments of the Bands in the Region of CH Stretching Modes  
and CD Stretching Modes

PVC	Frequency, $\text{cm.}^{-1}$			Assignments of PVC and PVC- $d_3$
	PVC- $\alpha d_1$	PVC- $\beta, \beta d_2$	PVC- $d_3$	
2970		2962		CH stretch.
2935	2933			$\text{CH}_2$ antisym. stretch.
2913	2915	2915		CH stretch. $\text{CH}_2$ sym. stretch.
2856	2850	2855		CH stretch, $\text{CH}_2$ stretch
2823	2822			$\text{CH}_2$ stretch
	2207	2210	2222	CD stretch, $\text{CD}_2$ antisym. stretch
		2150	2148	$\text{CD}_2$ stretch
		2112	2110	$\text{CD}_2$ stretch

amorphous band at  $615\text{ cm.}^{-1}$  after stretching the unoriented film.<sup>3,11</sup> The same amorphous bands which are probably assignable to the modified  $S_{\text{HH}}$  or  $S_{\text{DD}}$  exist in the infrared spectra of PVC- $\beta,\beta d_2$ , and PVC- $d_3$  shown in Figure 4.

The frequencies of the  $S_{\text{HH}}$  and  $S_{\text{CH}}$  modes in the infrared spectrum of PVC are higher than these of PVC- $\alpha d_1$  and the same tendency is observed for  $S_{\text{DD}}$  and  $S_{\text{CD}}$  modes of PVC- $\beta,\beta d_2$  and PVC- $d_3$ . Then, the atom in the  $\alpha$  position affects the frequencies of the CCl stretching modes as well as the substituents in *trans* positions to the Cl atom across both adjacent C—C bonds; this relation is listed in Table IV.

TABLE IV  
Assignments of CCl Stretching Modes at the  
Amorphous States of PVC and the Deuterated Derivatives

Polymer	Frequency, cm. <sup>-1</sup>	Assignment
PVC	690	$S_{\text{CH}}(\text{CHCl})$
	640	Modified $S_{\text{HH}}(\text{CHCl})$
	615	$S_{\text{HH}}(\text{CHCl})$
PVC- $\alpha d_1$	675	$S_{\text{CH}}(\text{CDCl})$
	625	Modified $S_{\text{HH}}(\text{CDCl})$
	610	$S_{\text{HH}}(\text{CDCl})$
PVC- $\beta,\beta d_2$	640	$S_{\text{CD}}(\text{CHCl})$
	584	Modified $S_{\text{DD}}(\text{CHCl})$
	571	$S_{\text{DD}}(\text{CHCl})$
PVC- $d_3$	625	$S_{\text{CD}}(\text{CDCl})$
	582	Modified $S_{\text{DD}}(\text{CDCl})$
	570	$S_{\text{DD}}(\text{CDCl})$
PVC- $\beta d_1$	680	$S_{\text{CH}}(\text{CHCl})$
	653	$S_{\text{CD}}(\text{CHCl})$
	620	$S_{\text{HH}}(\text{CHCl}) + \text{modified } S_{\text{HD}}(\text{CHCl})$
PVC- $\alpha,\beta d_2$	585	$S_{\text{HD}}(\text{CHCl}) + S_{\text{DD}}(\text{CHCl})$
	660	$S_{\text{CH}}(\text{CDCl})$
	630	$S_{\text{CD}}(\text{CDCl})$
	612-608	$S_{\text{HH}}(\text{CDCl}) + \text{modified } S_{\text{HD}}(\text{CDCl})$
	585	$S_{\text{HD}}(\text{CDCl}) + S_{\text{DD}}(\text{CDCl})$

The CCl stretching modes assigned to the isotactic part of  $\alpha,\beta$ -disubstituted poly(vinyl chloride)  $(\text{CXY}-\text{CX Cl})_n$ , where X and Y refer to H or D atoms, will be more complicated because both  $S_{\text{CX}}(\text{CX Cl})$  and  $S_{\text{CY}}(\text{CX Cl})$  are anticipated. The modes  $S_{\text{XX}}(\text{CX Cl})$ ,  $S_{\text{YY}}(\text{CX Cl})$  and  $S_{\text{XY}}(\text{CX Cl})$  should be also considered for the syndiotactic part.

Those of PVC- $\beta d_1$  and PVC- $\alpha,\beta d_2$  are assigned easily from the spectra of PVC, PVC- $\alpha d_1$ , PVC- $\beta,\beta d_2$  and PVC- $d_3$  and the  $S_{\text{XY}}$  modes will appear between the  $S_{\text{XX}}$  modes and  $S_{\text{YY}}$  modes as shown in Table IV. The modified  $S_{\text{XX}}$ ,  $S_{\text{XY}}$ , and  $S_{\text{YY}}$  modes are not assigned from the present work because they overlap with the pure  $S_{\text{XX}}$ ,  $S_{\text{YY}}$ , and  $S_{\text{XY}}$  modes in solution.

### Interpretation of NMR Spectra

**PVC- $\beta,\beta d_2$ .** Three resonance lines are observed in the spectrum of this polymer at  $\tau = 5.28, 5.38,$  and  $5.50$ . The patterns are quite consistent with those of the resonance lines corresponding to the  $\alpha$ -protons in PVC decoupled from  $\beta$ -protons,<sup>15,22</sup> and they may be ascribed to the  $\alpha$ -protons in the isotactic, heterotactic, and syndiotactic units. As listed in Table V, the relative intensities of these peaks vary with polymerization

TABLE V  
Tacticity of PVC- $\beta,\beta'-d_2$

Polymerization temp., °C.	Isotactic, %	Heterotactic, %	Syndiotactic, %
-30	10	44	46
58	17	48	35

temperature. The syndiotactic part is increased by lowering the polymerization temperature. Table VI shows the values of chemical shifts  $\tau$  of  $\alpha$ -protons in PVC, PVC- $\beta,\beta d_2$ , and three isomers of the model compound, 2,4,6-trichloroheptane. Though the magnitudes of the chemical shifts in these compounds do not always show complete coincidence, the relative chemical shifts between syndiotactic and heterotactic  $\alpha$ -protons and between heterotactic and isotactic ones show good agreement. This result seems to confirm the validity of the assumption<sup>12</sup> that the resonance field of meso methylene protons is lower than that of isotactic polymer.

TABLE VI  
Chemical Shifts of  $\alpha$ -Protons

	$\tau^a$		
	Syndiotactic	Heterotactic	Isotactic
2,4,6-Trichloroheptane	5.65	5.79	5.92
PVC	5.43	5.53	5.69
PVC- $\beta,\beta d_2$	5.28	5.38	5.50

<sup>a</sup> Against tetramethylsilane.

**PVC- $\alpha,\beta d_2$ .** Four peaks at least, are distinguished in the spectrum of PVC  $\alpha,\beta d_2$  and can be roughly classified into two groups: one consists of two rather weak lines at lower field (group 1) and the other of two rather strong at higher field (group 2). As shown in Figure 7 and Table VII, the polymerization conditions have a greater effect upon their intensities than the composition of *trans* and *cis* monomers used. While both components of group 1 are increased by elevating polymerization temperatures, the component at  $\tau = 7.77$  of group 2 keeps an almost constant intensity and the highest one becomes weak. The indirect spin-spin interaction between the  $\beta$ -proton and  $\alpha$ - and  $\beta$ -deuterons probably give no observable fine

TABLE VII  
 NMR Spectra of PVC- $\alpha,\beta d_2$ 

Polymerization temperature, °C.	Peak intensity, %			
	Group 1 $\left\{ \begin{array}{l} \tau = 7.60 \\ \tau = 7.66 \end{array} \right.$		Groups 2 $\left\{ \begin{array}{l} \tau = 7.77 \\ \tau = 7.85 \end{array} \right.$	
	Sample A	Sample B	Sample A	Sample B
-30	32.8 $\left\{ \begin{array}{l} 18.5 \\ 14.3 \end{array} \right.$	31.7 $\left\{ \begin{array}{l} 17.3 \\ 14.4 \end{array} \right.$	67.2 $\left\{ \begin{array}{l} 32.3 \\ 34.9 \end{array} \right.$	68.3 $\left\{ \begin{array}{l} 30.7 \\ 37.6 \end{array} \right.$
+30	36.8 $\left\{ \begin{array}{l} 18.4 \\ 18.4 \end{array} \right.$	35.9 $\left\{ \begin{array}{l} 19.5 \\ 16.4 \end{array} \right.$	$\left\{ \begin{array}{l} 31.2 \\ 32.0 \end{array} \right.$	64.1 $\left\{ \begin{array}{l} 31.2 \\ 32.9 \end{array} \right.$
50	39.8 $\left\{ \begin{array}{l} 21.9 \\ 17.9 \end{array} \right.$	38.6 $\left\{ \begin{array}{l} 22.9 \\ 15.7 \end{array} \right.$	60.2 $\left\{ \begin{array}{l} 29.2 \\ 30.6 \end{array} \right.$	61.4 $\left\{ \begin{array}{l} 31.4 \\ 30.0 \end{array} \right.$

structure of the spectrum, since the gyromagnetic ratio of deuteron is much smaller than that of proton. The magnitude of the relative chemical shift between two  $\beta$ -protons is not clear in PVC; however, the possibility that two lines corresponding to the difference in chemical shift can be observed for  $\beta$ -protons in meso units may not be neglected in this polymer. Two possibilities can be considered for the origin of fine structure of the spectrum; either the polymer forms a ditactic structure or these peaks are due to tetrads of monomer units. The former possibility is ruled out, since ditactic polymer has only three stereoregular structures, that is, disyndiotactic, *threo*-diisotactic and *erthro*-diisotactic. Yoshino and Komiyama<sup>17</sup> examined the NMR spectrum of low molecular weight PVC- $\alpha$ , *cis*- $\beta d_2$  in various solvents and successfully observed eight fairly well resolved lines at a frequency of 100 Mc./sec. in chloroform solution. They interpreted this fine structure in terms of tetrads of monomer units. The persistence length for the meso unit  $\langle m \rangle$  may be smaller than two, while that for a racemic unit may be larger than two. The fractions of the units such as imi, hrh in tetrads are expected to be small compared with other units in the statistical sense. This is also expected if the polymerization process in a stereochemical sense is described by single parameter. The observed four peaks seem to be roughly assigned to the units imh, hmh, hrs, and srs and the residual two units imi and hrh may overlap with other peaks. Since a well-resolved spectrum was not obtained in the present study, it is not clear which peaks correspond to what kind of species in tetrads. On the basis of the relative intensity and the chemical shift, however, the assumption that group 1 corresponds to the meso protons and group 2 to the racemic ones may be reasonable. Variation in relative intensity of each peak may result from the difference in mechanism of opening of the double bond during the polymerization.



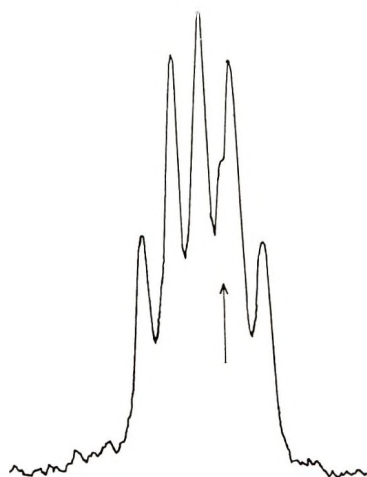


Fig. 9. Methylene resonance lines of PVC polymerized at 120°C. Arrow indicates extra line in question.

**PVC- $\alpha d_1$ .** As already reported, only two peaks are observed in the spectrum of this polymer. The peak at lower field has a somewhat smaller line width than that at higher field. The magnitudes of full width of half intensity at 170°C. are  $4.2 \pm 0.5$  and  $5.6 \pm 0.5$  cps, respectively. These line widths decrease with rising temperature; however, no structure can be observed in both peaks. This result suggests that the magnitude of the spin coupling constant between the two methylene protons is larger than, or at least comparable, with that of the relative chemical shift between them, and that each resonance line corresponding to the meso and to the racemic units in tetrads is concentrated around some two points. The difference in line widths of these two lines seems to originate from the difference in mode and degree of freedom of molecular motion.

**PVC- $\beta d_1$ .** Two unresolved multiplets are observed in the spectrum of PVC- $\beta d_1$ . The multiplets which complicate the spectrum originate from indirect spin-spin interactions between the  $\alpha$ - and  $\beta$ -protons as confirmed by the spin-decoupling method. Spin-decoupled lines corresponding to the  $\alpha$ -protons are identical with those of PVC- $\beta, \beta d_2$ ; decoupled lines due to the  $\beta$ -protons are more similar to those due to PVC- $\alpha d_1$  than those to PVC- $\alpha, \beta d_2$ . This result seems unreasonable since this polymer contains only one  $\beta$ -proton in a repeating unit. Since the line widths are larger than those of PVC- $\alpha d_1$ , this may be due to large line width of each component peak or to difference in mode of molecular motions. Information on indirect spin-spin interaction between  $\alpha$ - and  $\beta$ -protons should become clear if a well resolved spectrum could be obtained. The present study, however, cannot clarify the interactions.

**PVC.** The information obtained from the NMR spectra of above four partially deuterated PVC's provides a key for interpretation of the spectrum. Resonance lines due to methylene protons consist of five peaks at



60 Mc./sec. and of six at 100 Mc./sec. This apparent difference can be interpreted in the difference of relative chemical shift between meso and racemic methylene protons. In the carefully measured spectrum, however, an extra line is observed as a shoulder, as illustrated in Figure 9. Irregularities in polymer chain such as branching,<sup>18</sup> head-to-head bonding, and others may be considered as the origin of this line. Recently, Abe and his co-workers<sup>27</sup> tried to interpret the methylene resonance lines in terms of tetrads assuming the small difference in chemical shifts between the methylene protons in each unit of tetrads, and obtained fairly good qualitative agreement between observed and calculated lines. Since the difference in chemical shifts assumed is too small to distinguish the lines by spin-decoupling techniques, it cannot be decided whether the analysis based on tetrads of monomer units is uniquely correct or not. Though magnetic nonequivalence of the two methylene protons in meso units is clear, and though the spectrum of PVC- $\alpha,\beta d_2$  can be interpreted by tetrads, so long as the spectra at 60 and 100 Mc./sec. are concerned, it may be safely said that the resonance lines due to methylene protons in PVC are composed of two triplets besides the small extra line mentioned above. The resonance lines corresponding to  $\alpha$ -protons can be interpreted with the superposition of three quintets whose relative intensities are equal to those of isotactic, heterotactic, and syndiotactic sequences.

### Mechanism of Polymerization of Vinyl Chloride

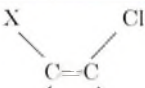

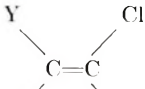
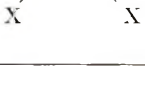
The opening of the double bonds in the polymerization of ethylene and propylene with Ziegler-type catalysts has been successfully studied by experimental and theoretical studies of infrared spectroscopy. However, the same treatment cannot simply be applied to the radical polymerization of vinyl chloride because the single polymer molecule is composed of syndiotactic, heterotactic, and isotactic parts and these components are not separated by usual methods such as extraction. An  $\alpha,\beta$ -disubstituted vinyl chloride is an interesting monomer for studying the polymerization mechanism of vinyl chloride. The relation between the CCl stretching modes and the openings of the double bond in Table VIII shows the possibility that the  $S_{CX}$  mode of the isotactic part should be a key to the mechanism, while only the  $S_{XY}$  mode may appear in the syndiotactic part when a single opening of the double bond occurs in the polymerization. When both *trans* and *cis* openings occur in the polymerization, the  $S_{CX}$  and  $S_{CY}$  modes are in the isotactic part and the  $S_{XY}$ ,  $S_{XX}$  and  $S_{YY}$  modes in the syndiotactic part. Further, if the monomer contains both *trans* and *cis* forms and the both openings are possible, all of the CCl stretching modes are expected.

From the viewpoint of NMR spectroscopy, two  $\beta$ -protons in the meso unit are expected to give two resonance lines corresponding to their difference in chemical shifts. The geminal coupling yields fusion of these lines into a single line in PVC- $\alpha d_1$  at 60 Mc./sec., however, they are probably observed separately in PVC- $\alpha,\beta d_2$ , since the spin coupling constant

between  $\beta$ -protons and  $\beta$ -deuterons is much smaller. If the opening of the double bond is limited to either *cis*- or *trans* opening, one of lines in meso units such as imi, hmh should not be observed.

As shown in Figures 4 and 5 and Table IV, PVC- $\beta d_1$  polymerized from the *trans* form has the  $S_{CH}(CHCl)$ ,  $S_{CD}(CHCl)$ ,  $S_{HH}(CHCl)$ ,  $S_{HD}(CHCl)$ , and  $S_{DD}(CHCl)$  modes. The infrared spectrum of the polymer prepared by a modified Ziegler-type catalyst does not show any significant difference from those obtained by the usual radical polymerization. The same relation is observed in their NMR spectra and the two broad peaks of the  $\beta$ -proton and the  $\alpha$ -proton indicate that their configurations are quite complicated. As three peaks assigned to the  $\alpha$ -proton in the syndiotactic, heterotactic, and isotactic part are observed in the decoupled spectrum of

TABLE VIII  
CCl Stretching Modes of  $\alpha,\beta$  Disubstituted Poly(vinyl Chloride)

Monomer	Opening	Tacticity	$\nu(CCl)$
	<i>trans</i>	S I	$S_{XY}(CXCl)$ $S_{CY}(CXCl)$
	<i>cis</i>	S I	$S_{XY}(CXCl)$ $S_{CX}(CXCl)$
	<i>trans</i>	S I	$S_{XY}(CXCl)$ $S_{CX}(CXCl)$
	<i>cis</i>	S I	$S_{XY}(CXCl)$ $S_{CY}(CXCl)$

the polymer obtained with modified Ziegler-type catalyst, isotactic poly(vinyl chloride) is not so easily prepared by this catalyst as polymers of  $\alpha$ -olefins.

A more complicated situation is expected in PVC- $\alpha,\beta d_2$  than in PVC- $\beta d_1$ , as the monomer used contained *trans* and *cis* forms. We used two monomers of different composition ratios, and no difference is observed in the infrared spectra depending on the polymerization method, and the five CCl stretching modes appear in solutions. The two peaks of group 2 assigned to the racemic  $\beta$ -proton in the NMR spectra change their relative intensity with variation of the polymerization temperature, and this change is not so much due to the monomer composition ratio. This suggests the possibility that the transformation between the *trans* and *cis* forms at the end of the growing chain radical depends on the polymerization temperature.

The above data indicate that both *trans* and *cis* opening of the double bond occur in the polymerization of vinyl chloride. In particular, with  $\alpha,\beta$ -disubstituted vinyl chloride, the transformation between the *trans* and *cis* forms will occur at the end of the growing chain radical even if a single monomer is used in the polymerization.

The authors are greatly indebted to Professor N. Yamazaki of Tokyo Institute of Technology for the preparation of PVC- $\beta d_1$  and PVC- $\alpha, \beta d_2$  by a modified Ziegler type catalyst and also thank Mr. T. Kuroda of Kureha Spinning Co. Ltd., Takatsuki Research Institute for carrying out the NMR spectroscopy.

### References

1. S. Narita, S. Ichinohe, and S. Enomoto, *J. Polymer Sci.*, **37**, 281 (1959).
2. M. Asahina and S. Enomoto, *Nippon Kagaku Zasshi*, **81**, 1374 (1960).
3. S. Krimm, V. L. Folt, J. J. Shipman, and A. R. Berens, *J. Polymer Sci. A*, **1**, 2621 (1963).
4. T. Shimanouchi and M. Tasumi, *Bull. Chem. Soc. Japan*, **34**, 359 (1961).
5. T. Shimanouchi, S. Tsuchiya, and S. Mizushima, *J. Chem. Phys.*, **30**, 1365 (1959), *Kobunshi Kagaku*, **8**, 202 (1959).
6. T. Shimanouchi and M. Tasumi, *Spectrochim. Acta*, **17**, 755 (1962).
7. J. J. Shipman, V. L. Folt, and S. Krimm, *Spectrochim. Acta*, **18**, 1603 (1963).
8. S. Enomoto, M. Koguro, and M. Asahina, *J. Polymer Sci. A*, **2**, 5355 (1964).
9. M. Asahina and S. Enomoto, *Nippon Kagaku Zasshi*, **81**, 1011 (1960).
10. J. W. L. Fordham, P. H. Burleigh, and C. L. Sturm, *J. Polymer Sci.*, **41**, 73 (1959).
11. S. Krimm and S. Enomoto, *J. Polymer Sci. A*, **2**, 669 (1964).
12. U. Johnsen, *J. Polymer Sci.*, **54**, S6 (1961).
13. W. C. Tincher, *J. Polymer Sci.*, **62**, S148 (1962).
14. F. A. Bovey, *Chem. Ind. (London)*, **1962**, 1826.
15. F. A. Bovey, E. W. Anderson, and D. C. Douglass, *J. Chem. Phys.*, **39**, 1199 (1963).
16. S. Satoh, R. Chujo, E. Nagai, Y. Abe, M. Tasumi, and T. Shimanouchi, *Rept. Progr. Polymer Phys. Japan*, **8**, 311 (1965).
17. T. Yoshino and J. Komiyama, *J. Polymer Sci. B*, **3**, 311 (1965).
18. W. C. Tincher, *Makromol. Chem.*, **85**, 20 (1965).
19. S. Satoh, R. Chujo, and E. Nagai, *Rept. Progr. Polymer Phys. Japan*, **7**, 299 (1964).
20. Y. Fujiwara and S. Fujiwara, *Bull. Chem. Soc. Japan*, **37**, 1005 (1964).
21. S. Satoh, R. Chujo, and E. Nagai, *Rept. Progr. Polymer Phys. Japan*, **7**, 301 (1964).
22. F. A. Bovey, E. W. Anderson, D. C. Douglass, and J. A. Manson, *J. Chem. Phys.*, **39**, 1199 (1963).
23. S. Enomoto and M. Asahina, *J. Mol. Spectry.*, **19**, No. 2 (1966).
24. N. Yamazaki, K. Sasaki, and S. Kambara, *J. Polymer Sci. B*, **2**, 487 (1964).
25. T. Shimanouchi and M. Tasumi, University of Tokyo, private communication.
26. Y. Abe, M. Tasumi, T. Shimanouchi, S. Satoh, and R. Chûjô, *J. Polymer Sci. A-1*, **4**, 1413 (1966).
27. H. Watanabe and Y. Amagi, *Kogyo Kagaku Zasshi*, **61**, 888 (1958).

### Résumé

Le chlorure de polyvinyle et toutes sortes de ses dérivés deutérés ont été préparés en variant la méthode de polymérisation et la température de polymérisation afin d'étudier la structure du PVC et le mécanisme de polymérisation par addition au moyen de spectroscopie infra-rouge et par spectroscopie NMR à haute résolution. Les modes d'étirement CH et CH<sub>2</sub> du PVC ont été attribués complètement au départ de spectres infra-rouge du PVC- $\alpha d_1$ , PVC- $\beta, \beta d_2$  et PVC- $d_3$ . Les fréquences des modes d'étirement CCl de s polymères dépendent non seulement des substituants en position trans par rapport aux atomes de chlore de chaque côté d'un lien C—C mais également de l'atome attaché à l'atome de carbone du lien CCl. Les variations de fréquence ont été appliquées pour attribuer les modes d'étirement CCl au PVC- $\beta d_1$ , et PVC- $\alpha, \beta d_2$  et pour étudier l'ouverture de la double soudure du chlorure de vinyle au cours de la polymérisation par addition. Les différences de glissements chimiques des protons  $\alpha$  et  $\beta$  du PVC par

suite de la tacticité ont été déterminées expérimentalement par le PVC- $\alpha,\beta d_2$ , et PVC- $\alpha d_1$  sans user la technique de découplage de spin. Avec le PVC- $\alpha,\beta d_2$ , la conception de tétrade est nécessaire pour interpréter les 4 pics observés dont les intensités variaient avec la température de polymérisation et la composition *trans* et *cis* du monomère utilisé.

### Zusammenfassung

Polyvinylchlorid (PVC) und alle möglichen deuterierten Derivate wurden nach verschiedenen Polymerisationsmethoden und bei verschiedenen Polymerisationstemperaturen zur Untersuchung der Struktur von PVC und des Mechanismus der Additions-polymerisation durch Infrarotspektroskopie und Hochauflösungs-NMR-Spektroskopie dargestellt. Die CH- und die CH<sub>2</sub>-Valenzfrequenzen von PVC wurden anhand der Infrarotspektren von PVC- $\alpha d_1$ , PVC- $\beta,\beta d_2$  und PVC- $d_3$  vollständig zugeordnet. Die CCl-Valenzfrequenzen der Polymeren hängen nicht nur von den Substituenten in *trans*-Stellung zum Chloratom über beide benachbarte C—C-Bindungen, sondern auch von dem am C-Atom der CCl-Bindung befindlichen Atom ab. Die Frequenzverschiebungen wurden zur Zuordnung der CCl-Valenzfrequenzen von PVC- $\beta d_1$  und PVC- $\alpha,\beta d_2$  sowie zur Untersuchung der Öffnung der Doppelbindung von VC-(Vinylchlorid) bei der Additionspolymerisation verwendet. Die auf der Taktizität beruhenden Unterschiede in der chemischen Verschiebung der  $\alpha$ - und  $\beta$ -Protonen von PVC wurden experimentell an PVC- $\beta,\beta d_2$  und PVC- $\alpha d_1$  ohne Anwendung des Spinentkopplungsverfahrens bestimmt. Bei PVC- $\alpha,\beta d_2$  war die Aufstellung einer Tetrade zur Interpretation der vier beobachteten Maxima notwendig, deren Intensität von der Polymerisationstemperatur und der *trans*- und *cis*-Zusammensetzung des verwendeten Monomeren abhängig war.

Received September 27, 1965

Revised October 21, 1965

Prod. No. 4943A

## Synthesis and Characterization of Branched Polystyrene. Part I. Synthesis of Four- and Six-Branch Star Polystyrene

J. A. GERVASI and A. B. GOSNELL, *Camille Dreyfus Laboratory, Research Triangle Institute, Durham, North Carolina*

### Synopsis

The synthesis of very well defined four- and six-branched polystyrene has been carried out. Anionic polymerization initiated by butyllithium in benzene-tetrahydrofuran medium gave single chains of narrow distribution. Coupling this living polystyryllithium with bis(trichlorosilyl)ethane gave a maximum of four branches. Coupling with the cyclic trimer of phosphonitrilic chloride gave a maximum of six branches. The reaction procedures have been discussed and mechanisms suggested for some of the reactions.

### Introduction

It has long been known that branching occurs in polymer chains, often from random and uncontrolled side reactions during polymerization. It has also been known that branching can exert a marked influence on polymer solution properties. One of the efforts to place this influence on a quantitative basis was the theoretical approach of Zimm and Kilb.<sup>1</sup> They concluded that, for star-shaped polymers, wherein all the branches radiate from a single point,

$$[\eta]_{\text{branched}}/[\eta]_{\text{linear}} = g' \cong g^{1/2}$$

where  $[\eta]_{\text{branched}}$  is the intrinsic viscosity of the branched polymer,  $[\eta]_{\text{linear}}$  is the intrinsic viscosity of linear polymer of the same molecular weight, and  $g$  is the ratio of their mean-square radii of gyration.

Obviously, it would be desirable to provide experimental verification for this theoretical conclusion. Such verification would require the synthesis of star-shaped branched polymers in which the number and length of the branches were extremely well defined. An approach to this synthesis originally suggested by Szwarc,<sup>2</sup> makes use of anionic polymerization, followed by a coupling reaction to attach several branches to a common center. The very narrow molecular weight distribution from the polymerization defines the length of the branches, and the functionality of the coupling agent defines the number of branches.

This problem has been investigated by Morton et al.<sup>3</sup> who used a modification of techniques devised by Wenger and Yen.<sup>4</sup> Thus, Morton em-



ployed anionic polymerization of styrene followed by reaction of the "living polymer"<sup>5</sup> with silicon tetrachloride. The reaction product contained star polymers with three and four branches. Intrinsic viscosity measurements on these polymers apparently confirmed the Zimm and Kilb relationship.

It was of interest both from the synthetic and from the solution property standpoint to extend this investigation to the synthesis of star polystyrene with six branches to determine if the Zimm and Kilb theory applied as well at the higher degree of branching.

The synthesis of the branched polymers will be described below and the fractionation procedure employed to isolate the branched species is described in the following paper.<sup>6</sup> The characterization studies will be reported in a later communication.

### Experimental

The overall synthetic approach was the anionic polymerization of styrene initiated by butyllithium in benzene-tetrahydrofuran medium. This gave living polymer of very narrow molecular weight distribution, which then underwent a substitution reaction with a hexafunctional chloride to yield the branched star polymer. The extreme sensitivity of anionic polymerization demanded, as nearly as possible complete removal of reactive impurities from reagents and apparatus. Therefore, the procedures and apparatus described were adopted or devised to permit the elimination of these impurities.

### Reagents and Apparatus

The reactor was a 500-ml. round-bottomed Pyrex flask. Several reagent chambers were sealed to the reactor but separated by break-seals so that reagents could be added when desired by pouring or condensing the chamber

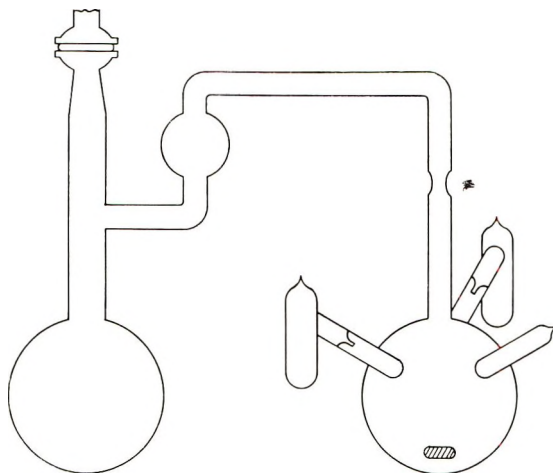


Fig. 1. Reagent purification vessel and reactor.



contents into the reactor. The stirrer was a stainless steel enclosed magnet which was also used as the hammer to smash the break-seals. A diagram of this apparatus is shown in Figure 1. Glassware was cleaned by rinsing in order with hydrofluoric acid solution, water, and methanol, then dried. The glass apparatus was then sealed together and evacuated to  $10^{-6}$  Torr while heating with a hot air blower. This cleaning procedure was found to be useful as a preliminary measure, but entirely inadequate for final elimination of impurities.

At first the purging technique of Wenger<sup>7</sup> was used for the final *in situ* reagent cleaning. Purging was found not to be necessary, however, if the glass walls were rinsed by condensing the contained reagent on all the glass surfaces, then transferring the condensate back into a sodium and benzophenone solution. This procedure apparently dislodged impurities from the glass and destroyed them. After several such transfer cycles the desired volume of reagent was condensed in the chamber and the chamber sealed off. Thus, by transferring small portions of reagent back and forth several times between the reactor chamber and the sodium-benzophenone solution, the reagents and glassware could be cleaned simultaneously.

The polymerization diluent was reagent grade benzene, from various sources, which was further treated essentially according to Bywater.<sup>8</sup> It was stirred with several batches of concentrated sulfuric acid until fresh acid was not discolored, washed with water, dried over phosphorus pentoxide, distilled in a nitrogen atmosphere from the blue complex of sodium and benzophenone, and stored over calcium hydride. Immediately before polymerization the benzene was siphoned into a flask which had been sealed to the reactor, degassed, distilled from sodium and benzophenone, and 250 ml. sealed off in the reactor.

Styrene was obtained from Eastman and subjected to a preliminary rectification to remove the inhibitor. This styrene was stored over calcium hydride at  $-15^{\circ}\text{C}$ . and remained substantially free of polymer for several weeks. Immediately before polymerization, the monomer was degassed and 15 ml. distilled from sodium and benzophenone directly into a reactor chamber and sealed off.

Small amounts (1–10 ml.) of tetrahydrofuran were used to narrow the molecular weight distribution as discussed below.<sup>9,10</sup> The quantity was chosen to provide a molar ratio of approximately 100:1 tetrahydrofuran:butyllithium. Fisher Certified Reagent grade was stored over calcium hydride and, after degassing, distilled from sodium and benzophenone into a reactor chamber and sealed off.

The butyllithium initiator was obtained from Foote Mineral Company as a 15% solution in hexane and was used without further treatment. Small quantities of the solution (0.1–1.0 ml.) were transferred by hypodermic syringe to a chamber on the reactor and diluted with benzene, aliquots were removed for titration, and the chamber degassed and sealed off. Direct acid titration was found to be adequate for control of polymer molecular weight in the desired 25,000–30,000 range.<sup>11</sup>

Two different coupling agents were used as the central hub of the star polymers, as discussed below. These were bis(trichlorosilyl)ethane and the cyclic trimer of phosphonitrilic chloride.

The silylethane obtained from Peninsular ChemResearch was fractionated on a spinning-band-column, and the fraction which distilled at 90°C./13.5 mm. was collected in an ampule and sealed off. The expected boiling point was 84°C./13.5 mm.<sup>12</sup> but the difference cannot be explained at present. The ampule was opened under nitrogen, and a sample was titrated with sodium hydroxide (found, 70.17% Cl; calculated, 71.65% Cl). The titration was complicated by the immediate precipitation of silica so that the 98% purity appeared to be satisfactory. A 0.35-ml. portion of the silyl halide was withdrawn by hypodermic syringe and added to 100 ml. of benzene. Several portions of the benzene solution were then transferred to ampules, degassed, and sealed off under vacuum. All the ampules had been evacuated to  $10^{-6}$  Torr, flamed, and refilled with nitrogen before receiving the solutions. For the coupling reaction the ampules were opened under nitrogen, the required amount of silyl halide solution transferred by hypodermic to a reactor chamber, degassed, and sealed off. The silyl halide solution remaining in the opened ampule was discarded.

The solid phosphonitrilic compound could not, of course, be transferred in a pure state as easily as the liquid silicon compound. The procedure finally used was to accomplish the purification essentially in a closed system. Thus, a weighed amount of the solid cyclic trimer of phosphonitrilic chloride was placed in a reactor chamber which was then sealed to a flask. Benzene, sodium, and benzophenone were placed in the flask, some benzene condensed in the chamber with the solid, and the assembly degassed. Benzene was distilled back and forth from flask to chamber until returning benzene did not discolor the blue complex. Then 5 ml. of benzene was condensed in the reactor chamber and the chamber sealed off. By this means any volatile reactive impurities could be removed from the coupling agent without pumping directly on the solid.

After the benzene, tetrahydrofuran, styrene, and butyllithium had been sealed in their chambers the polymerization was carried out.

First, the tetrahydrofuran and styrene were distilled into the benzene in the reactor and the mixture was frozen. The chamber which had contained the styrene was cut off, but the chamber which had contained the tetrahydrofuran was retained for later sampling. The initiator solution was then poured into the reactor and stirred, just as the reactor contents thawed. The initiator chamber was then removed. It was necessary to follow this order of addition because in the absence of styrene, butyllithium reacted with tetrahydrofuran and was destroyed. In the presence of styrene, however, initiation was apparently straightforward.

After 2 hr. reaction at room temperature the polymerization was assumed to be complete.<sup>10</sup> A 20-ml. sample was withdrawn and the chamber removed. The sample was precipitated in methanol, dried in a vacuum oven at 60°C., and its molecular weight measured by a single-point in-

trinsic viscosity determination. The relationships used<sup>13,14</sup> were:  $[\eta] = \eta_{sp}/[c(1 + 0.28 \eta_{sp})]$  and  $[\eta] = 1.04 \times 10^{-4} M^{0.73}$ . From the molecular weight and the known volume of styrene, the concentration of active chains could be calculated as a check on the measured initiator volume. The required amount of coupling agent solution was then sealed in a chamber as described above. The quantity was chosen so as to maintain approximately a 20% excess of polystyryl anions. The coupling reaction was allowed to proceed for at least 48 hr. at room temperature, then 24 hr. further at 50°C. The reactor was then opened and its contents poured into approximately 3 liters of methanol. The precipitated polymer was filtered, washed with 300 ml. of methanol and dried in a vacuum oven at 60°C. The polymer was then fractionated to isolate the branched species as will be described in the following paper.<sup>6</sup>

### Results and Discussion

The synthesis of the desired branched polymers required first the preparation of single chains with the narrowest possible molecular weight distribution and second the addition of six of these chains to a central hub to form the six-branch star polymer. Anionic polymerization was employed to minimize the molecular weight distribution and also to provide a reactive polymer. Polystyrene was chosen because of the well worked-out characterization procedures.

For the anionic polymerization the simplest system appeared to be styrene monomer with butyllithium initiator in benzene medium. This has the advantages of a convenient polymerization temperature and homogeneous solution of all the components. A disadvantage of this system is the unfavorable kinetic balance whereby the rate of propagation is faster than the rate of initiation, which tends to broaden the molecular weight distribution.

Wenger and Yen<sup>4</sup> and Morton<sup>3</sup> overcame the unfavorable kinetics by using as initiator not butyllithium but a seed solution of butyllithium-polystyryllithium. The fractionation curves<sup>4</sup> indicate that this worked well, which means that virtually all of the initiation was effected by the short-chain polystyryllithium.

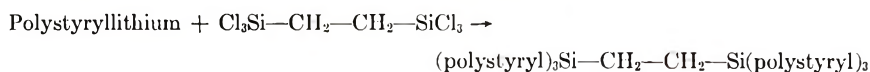
An alternate method of overcoming the kinetic difficulty was to add small amounts of tetrahydrofuran to the polymerization medium.<sup>9,10</sup> By this means, initiation was essentially instantaneous, which eliminated the kinetic problem. The use of tetrahydrofuran also eliminated the presence of unreacted butyllithium after polymerization. This was fortunate because residual butyllithium could complicate the polymer characterization if it reacted later with coupling agent to give an occasional butyl branch instead of the expected polystyryl branch. Therefore, the tetrahydrofuran addition was used, and gave quite narrow molecular weight distribution, as predicted by Bywater<sup>10</sup> and found by Altares and Wyman.<sup>15</sup> The ratio of  $\bar{M}_w/\bar{M}_n$ , for example, was 1.06, as will be shown in the following paper.<sup>6</sup>

A vital part of any anionic polymerization is the elimination of reactive impurities. High vacuum techniques were generally used in this work and reagent transfers accomplished through break-seals. After preliminary rectification, the styrene, tetrahydrofuran, and benzene were distilled under vacuum from the blue complex of sodium and benzophenone directly into the reactor or reactor chambers and sealed off. Initially, the purging technique of Wenger<sup>7</sup> was used in which excess initiator was provided to titrate the remaining contaminants. Purging was found to be unnecessary, however, if the glass surfaces were rinsed with distillate, and the distillate recondensed in the sodium and benzophenone solution as described above. This cleaning procedure is probably not quite as effective as rinsing the glassware directly with sodium-benzophenone solution. The narrow molecular weight distribution and the immediate initiation, however, indicated that impurities were effectively destroyed. Furthermore, this condensation technique has the advantages of greatly simplified apparatus design and reduced handling.

Initiation was accomplished by pouring butyllithium solution from a graduated chamber into the reactor containing benzene, styrene, and tetrahydrofuran near the freezing point. This rough measurement was adequate for control of the desired 25,000–30,000 molecular weight range, because molecular weight equals grams styrene/moles butyllithium. After 2 hr. polymerization a sample was taken from the reactor and its molecular weight measured by a single-point intrinsic viscosity determination.<sup>13</sup> The amount of coupling agent needed could then be calculated because the concentration of living polymer was identical with the concentration of active initiator.

In order to favor complete reaction, the concentrations were adjusted to provide a 20% excess of active chains. After coupling, the product was fractionated, and selected cuts were combined and refractionated. This procedure employed a column elution technique and was satisfactory for the isolation of the branched polymers.

The first coupling agent examined was bis(trichlorosilyl)ethane. The expected reaction<sup>16</sup> was a direct substitution:



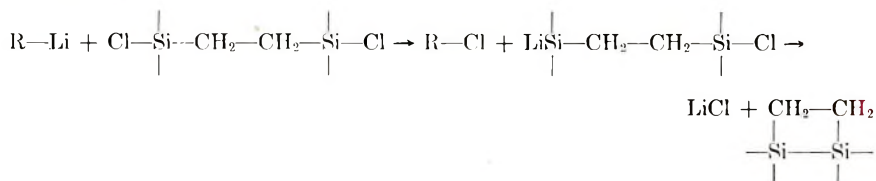
Although various conditions of time and temperature of the coupling reaction were tried, the maximum attained was only four branches. Some crowding was expected, but this result was surprising, because six chains should add to the hexachloro compound as easily as four chains added to the silicon tetrachloride.<sup>3</sup>

These observations prompted an investigation of the reaction of butyllithium with bis(trichlorosilyl)ethane in hopes that the butyl adducts would be easier to separate and identify than the polystyryl adducts. The detailed study of these reaction products will be reported elsewhere.<sup>17</sup> Briefly, the reaction mixture was found to contain roughly equal amounts of six-branch and four-branch products. These apparently formed by



competing reactions rather than a 50% impurity in the original silyl ethane, because no higher than four-branch polystyrene could be observed, and the bis(trichlorosilyl)ethane was at least 98% pure by titration. Furthermore, if there were competing reactions, the bulky polystyryllithium should favor the course leading to less crowding, i.e., four chains, as was observed.

This result cannot yet be accounted for, nor a structure assigned to the product. Gilman has shown, however, that exchange reactions can occur between silicon halides and lithium reagents to give silyl lithium compounds.<sup>13</sup> This could reduce the functionality of the silicon compound to 4, perhaps by a subsequent cyclization:

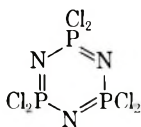


where R is polystyryl. Thus far, no example of the suggested cyclic structure has been found in the literature. It is unlikely, therefore, that this hypothetical structure, if it existed, would survive intact through the polymer isolation procedures.

As can be seen from the equation, an exchange would also produce RCl, where R is polystyryl. This should then couple very rapidly with RLi to give R<sub>2</sub>. Therefore, there should be a significant amount of polystyrene in the coupled product which is exactly twice the molecular weight of the single chains. There was at first no evidence of this "two-branch" polystyrene except for the lower region in the refractionation curve, which had an intrinsic viscosity of 0.34 whereas the higher portion had an intrinsic viscosity of 0.38. This small difference had been considered an artifact. However, the molecular weight of samples from both regions of the curve were determined by light scattering and found to be 60,500 and 121,000 for the lower and higher regions, respectively, which corresponded to two and four of the single chains. The appearance of the two-branch polystyrene, then, is consistent with the possible exchange reaction. This also illustrates the inability of viscosity to give meaningful molecular weight values for branched polymers.

Although the star polymer had only four instead of the expected six branches, the four-branch was isolated from the single-chain and two-branch products, and has been characterized for comparison with the six-branch polymer.

Inasmuch as six-branch polymer could not be synthesized with the bis-(trichlorosilyl) ethane, several other coupling agents were evaluated. The most successful was the cyclic trimer of phosphonitrilic chloride:



Reactions of this compound with organometallic reagents are known to be feasible. With *n*-butyllithium for example, the degree of butylation, Bu:P, varied from 1:1 to 2:1. There was reason to believe, therefore, that fully substituted product could be prepared.<sup>19</sup>

The polymerization and coupling reactions were carried out as before, with special precautions for the removal of reactive impurities from the solid coupling agent. In this case the reaction proceeded at least in small yield to the formation of the expected six-branch star polystyrene.

Once again, however, a quantity of single-chain, of two-branch, and of four-branch polymer could also be isolated. The fractionation curve showed distinct steps at molecular weight multiples of 1, 2, and 4, and a maximum of 6 as measured with an osmometer. The refractionation gave approximately 30% of the highest fraction, which was six times the molecular weight of the single-chain precursor.

The appearance of these branched species cannot be rigorously accounted for. From the work with butyllithium quoted above, however, they are not surprising. It is probable that the two-branch material came from dissociation of the substituted cyclic trimer, and that the six-branch was simply the fully substituted compound. The appearance of four branches was probably not due only to incomplete reaction, because there was no evidence of three or five branches. Therefore, the four-branch polymer may have resulted from a Li-Cl exchange as postulated above for the silicon compound, or perhaps from incomplete dissociation of the fully substituted trimer. Inasmuch as the desired six-branch polymer was isolated, however, no further investigation of the other branched species was pursued.

Further studies of branched polymers are under way, including the synthesis and characterization of higher molecular weight star polymers.

The authors are pleased to acknowledge the financial support of the Celanese Corporation of America which made this work possible. We are also indebted to Dr. V. T. Stannett for his valuable suggestions.

### References

1. B. H. Zimm and R. W. Kilb, *J. Polymer Sci.*, **37**, 19 (1959).
2. M. Szwarc, *Advan. Chem. Phys.*, **2**, 147 (1959).
3. M. Morton et al., *J. Polymer Sci.*, **57**, 471 (1962).
4. F. Wenger and S.-P. S. Yen, paper presented at the 141st American Chemical Society Meeting, Washington, D. C., March 1962.
5. M. Szwarc, *Nature*, **178**, 1168 (1956).
6. A. B. Gosnell, J. A. Gervasi, and A. Schindler, *J. Polymer Sci. A-1*, **4**, 1401 (1966).
7. F. Wenger, *J. Am. Chem. Soc.*, **82**, 4281 (1960).
8. D. J. Worsfold and S. Bywater, *Can. J. Chem.*, **38**, 1891 (1960).
9. F. J. Welch, *J. Am. Chem. Soc.*, **82**, 6000 (1960).
10. S. Bywater and D. J. Worsfold, *Can. J. Chem.*, **40**, 1564 (1962).
11. C. W. Kamienski and D. L. Esmay, *J. Org. Chem.*, **25**, 115 (1960).
12. A. C. Jenkins and G. F. Chambers, *Ind. Eng. Chem.*, **46**, 2367 (1954).
13. G. V. Schulz and G. Sing, *J. Prakt. Chem.*, **161**, 161 (1942).
14. S. Bywater et al., *Trans. Faraday Soc.*, **57**, 705 (1961).



15. T. Altares, Jr. and D. P. Wyman, paper presented at the 145th American Chemical Society Meeting, New York, September 1963.
16. H. Gilman et al., *J. Org. Chem.*, **27**, 1023 (1962).
17. To be published.
18. D. Wittenberg and H. Gilman, *Quart. Rev.*, **13**, 116 (1959).
19. R. A. Shaw et al., *Chem. Rev.*, **62**, 247 (1962).

### Résumé

La synthèse de polystyrène à quatre ou six branches bien définies a été effectuée. La polymérisation anionique initiée par le butyllithium en solution benzène-tétrahydrofurane donne des chaînes simples de distribution étroite. L'accouplement de ce polystyryllithium vivant avec l'éthane-bis-trichlorosylé fournit au maximum un système à quatre branches. L'accouplement du trimère cyclique du chlorure phosphonitrique donne au maximum six branches. Les processus de réaction sont soumis à discussion et des mécanismes suggérés pour certaines de ces réactions.

### Zusammenfassung

Die Synthese gut definierter Polystyrole mit vier und sechs Verzweigungen wurde durchgeführt. Butyllithiumgestartete anionische Polymerisation in Benzol-Tetrahydrofuran lieferte einfache Ketten mit enger Verteilung. Die Kopplung dieses lebenden Polystyryllithiums mit Bis(trichlorsyl)-äthan lieferte ein Maximum von vier Verzweigungen. Kopplung mit dem zyklischen Trimeren von Phosphonitridchlorid lieferte ein Maximum von sechs Verzweigungen. Die Reaktionsführung für einige dieser Reaktionen wurde diskutiert und ein Mechanismus vorgeschlagen.

Received August 18, 1965

Prod. No. 4945A

## Synthesis and Characterization of Branched Polystyrene. Part II. Fractionation

A. B. GOSNELL, J. A. GERVASI, and A. SCHINDLER, *Camille Dreyfus Laboratory, Research Triangle Institute, Durham, North Carolina*

### Synopsis

Fractionations have been carried out by a column-elution method on mixtures of linear and branched polystyrene. These had been prepared by anionic polymerization followed by a coupling reaction to form star-shaped branched polymers. Therefore, the components of the mixture were each of narrow distribution, and their molecular weights differed from each other as multiples of the original single chain length. For single chains in the 25,000-30,000 molecular weight range, separations were accomplished in which the multiples (number of branches) were 1, 2, 4, and 6. By this means, virtually monodisperse samples of the branched polymers could be isolated.

### Introduction

The synthesis of branched polystyrene, reported in the preceding paper,<sup>1</sup> always resulted in a mixture of polymers with a different number of branches. It was necessary to isolate as nearly as possible monodisperse samples from these mixtures, so that extensive fractionation work was required. The polymers were prepared by careful anionic polymerization, followed by a coupling reaction which attached the polymer chains to a common center. Thus, the major polydispersity encountered was not the usual continuous variation of molecular weight, but rather a stepwise transition of discrete molecular weight groupings. That is, the polymerization gave a product with narrow distribution, and the coupling reaction then assembled the polymer chains into groups, each with a narrow distribution but different from each other in the degree of coupling. The separations, therefore, were concerned with molecular species which were a simple multiple of the single-chain length, as well as the polydispersity within the species.

There is precedent in the literature to show that such polymers could be isolated by precipitation methods.<sup>2</sup> Ostensibly, a column-elution technique<sup>3</sup> should be as effective as well as somewhat easier from the manipulation standpoint. The results of the column fractionation of the branched polymer mixtures comprise the subject of this communication.

### Experimental

The fractionation apparatus, shown in Figure 1, was a column assembly similar to one used for the fractionation of polyethylene.<sup>4</sup> It consisted of

a glass tube, about 100 cm. long and of 4 cm. diameter, with a ball-and-socket joint on the top which carried the inlets for nitrogen and eluent, and closed at the bottom by a needle valve with a Teflon stem. About 20 cm. from the bottom, the tube had a ring indentation on which a perforated Teflon disk rested. In the center of the Teflon disk a narrow stainless steel tube was attached which led up to the top of the column. The entire column was surrounded by a jacket which allowed thermostating by refluxing solvents.

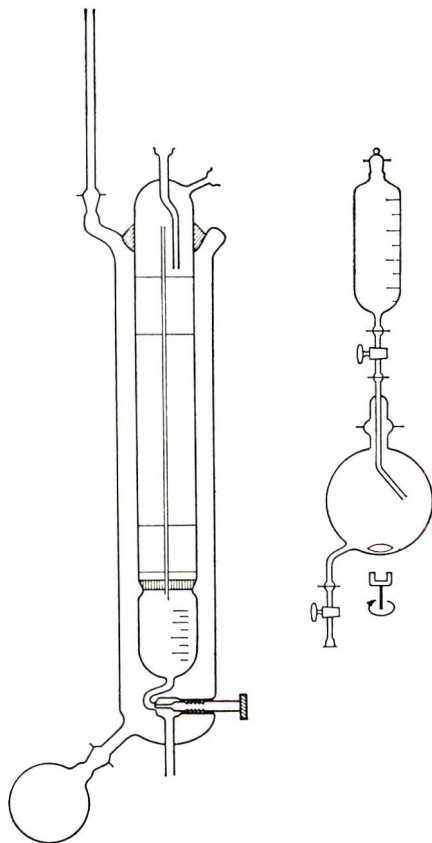


Fig. 1. Fractionation apparatus.

In operation, the top vessel contained the solvent, the next vessel, the mixing vessel of constant mixing volume, contained a mixture of solvent and nonsolvent which drained into the column. The column was filled with a Celite packing coated uniformly with polymer. The graduated receiving chamber below the Teflon disk was either drained manually or the fractions were collected automatically by a fraction collector working on a time base. A volumetric device for the fraction collector proved unsatisfactory, because polymer tended to deposit in the siphon tube and contaminate successive fractions.

Aside from collecting fractions a few features of the apparatus design permitted unattended operation. The continuous mixing of solvent with nonsolvent occurred via the following steps: as nonsolvent drained into the column the pressure was reduced in the vessel. This caused solvent to flow in from above, which, in turn, reduced the pressure in that vessel. This vacuum was then relieved by nitrogen rising through both vessels to the vapor space above each. Inasmuch as this process repeated continuously by gravity, the system operated continuously without the need for mechanical pumps to transfer the solvents. Also, the solvent flow shut off automatically if the bottom valve was left closed. In this case, as the receiving chamber filled with solution the liquid level would rise until it covered the tip of the pressure equalizing central tube. This built up a pressure against which the solvent could not flow and thus the system operated like a check-valve. Later, when the receiving chamber was drained, the solvent flow would resume.

For polystyrene, a maximum of 3 g. of polymer was fractionated in a given run. To prepare the packing, the polymer was first dissolved in 500 ml. of benzene and slurried with 200 g. of Celite (Johns-Manville Hyflo Super-Cel). Then, 500 ml. of methanol was added and the solvents removed by vacuum stripping in a rotary evaporator at a maximum temperature of 40°C. The Celite and polymer mixture was then dried overnight at 60°C. in a vacuum oven. After cooling, the column was packed from the bottom up in order with approximately 1/2 in. of asbestos fiber, 2 in. of untreated Celite, the Celite-polymer mixture, 2 in. of untreated Celite, 1/2 in. of asbestos fiber, and 1 in. of clean sand.

The lower vessel which drained directly into the column at first was filled with nonsolvent (methanol), while the upper vessel which drained into the lower vessel was filled with solvent (butanone). Several hours could be saved, however, if the lower vessel was filled with a mixture of methanol and butanone, which did not dissolve any of the polymer. The separation was improved by using as solvent a 95:5 mixture of butanone and methanol in place of pure butanone.

The procedure after the column was packed was to fill the column with methanol, from the bottom up, in order to displace air and voids. Methylene chloride was refluxed in the jacket to maintain a constant temperature of 40°C. After the column was filled, the methanol was drained from the receiving chamber and, as the level in the column fell, nonsolvent from the lower vessel was admitted into the top of the column. When the nonsolvent began to drain into the column, the solvent from the upper vessel was admitted into the lower vessel. Thereafter the mixing of solvent with nonsolvent and draining into the column proceeded automatically.

Eluent was withdrawn from the receiving chamber in 250-300 ml. batches until the first trace of polymer was observed on pouring into 2 liters of methanol. After that the eluent was usually collected continuously by an automatic fraction collector. A time cycle of 17 min. was employed which delivered 20-30 ml. of eluent. The fractionation was considered

complete when no precipitate could be observed on pouring the eluent into methanol. At this point the fractionation was discontinued and the column flushed with undiluted benzene. As a double check, this benzene was also poured into methanol, but no more polymer was ever found.

The polymer samples were precipitated in methanol, filtered, and washed in weighed sintered glass funnels. The polymer was dried at 60°C. in a vacuum oven while still in the funnels. The latter were then weighed again to determine the weight of the polymer samples.

The molecular weights of the fractions were usually measured by a single-point intrinsic viscosity determination<sup>5</sup> by using the relationship

$$[\eta] = \eta_{sp}/c(1 + 0.28\eta_{sp})$$

This worked well for linear polymers but was misleading for the branched polymers. In later work a single-point osmotic pressure determination was employed. This was made possible by an automatic membrane osmometer which required only 5 ml. of solution for a measurement (Stabin-Shell automatic osmometer, manufactured by Dohrmann Instruments Co.). The osmometer was calibrated by measuring several molecular weight ranges by the standard dilution method, and plotting  $(\Delta h/c)^{1/2}$  versus  $c$  for each, where  $\Delta h$  is the observed difference in pressure between solution and solvent and  $c$  is concentration. Thereafter, the single concentration measurements were located on the graph, and the slope assumed to be parallel with the nearest dilution line.

The data from the preliminary fractionations were treated by plotting the concentration of polymer versus volume of eluent as shown in Figures 3 and 4 below. Because the polymer samples generally fell into fairly well defined molecular weight groups, this plot permitted the identification of the main groups. The fractions falling within a group were then recombined and refractionated to isolate the narrowest possible samples. The refractionation data were treated according to Schulz,<sup>6</sup> as shown in the tables and plots, by using the relationship

$$I(w_n) = \sum^n w_i - w_i/2$$

where  $I(w_n)$  is the integral weight per cent and  $w_i$  is the weight per cent of the  $i$ th fraction.

## Results and Discussion

As a part of a program on the synthesis and characterization of branched polystyrene, fractionation was employed both as an analytical and preparative tool. The overall procedure was the polymerization of styrene by anionic initiation, followed by a coupling reaction to form star-shaped branched polymers.<sup>1</sup> The product was then fractionated to determine the number of branches, and also to isolate monodisperse samples for characterization studies.



TABLE I  
 Fractionation of Linear Polystyrene<sup>a</sup>

Fraction	$m_i$ , g.	$w_i$ , %	$I(w_n)$	$[\eta]^b$	$M_i^c$
1	0.0085	0.99	0.50	0.060	6,000
2	0.0199	2.33	2.17	0.110	13,800
3	0.0302	3.53	5.11	0.128	17,100
4	0.0125	1.46	7.61	0.136	18,500
5	0.0293	3.42	10.05	0.161	23,400
6	0.0357	4.17	12.85	0.161	23,400
7	0.0428	5.00	16.44	0.165	24,100
8	0.0494	5.77	21.83	0.174	26,100
9	0.0274	3.20	26.32	0.185	28,300
10	0.0315	3.68	29.76	0.186	28,400
11	0.0345	4.03	33.62	0.184	28,100
12	0.0396	4.63	37.96	0.197	30,800
13	0.0401	4.69	42.63	0.198	31,200
14	0.0439	5.13	47.55	0.193	29,900
15	0.0497	5.81	53.03	0.194	30,200
16	0.0513	6.00	58.94	0.190	29,400
17	0.0548	6.40	65.14	0.182	27,700
18	0.0528	6.17	71.43	0.196	30,700
19	0.0548	6.40	77.72	0.178	26,900
20	0.0572	6.69	84.28	0.194	30,200
21	0.0430	5.03	90.16	0.193	29,900
22	0.0467	5.46	95.41	0.217	35,200
	0.8556 <sup>d</sup>				

<sup>a</sup>  $M_w = \Sigma w_i M_i = 27,600$ ;  $\bar{M}_n = 1/\Sigma(w_i/M_i) = 26,000$ ;  $\bar{M}_w/\bar{M}_n = 1.06$ .

<sup>b</sup> Single-point intrinsic viscosity determination from  $[\eta] = \eta_{sp}/c(1 + 0.28 \eta_{sp})$ .

<sup>c</sup>  $[\eta] = 1.04 \times 10^{-4} M^{0.73}$  (relation of Bywater<sup>8</sup>).

<sup>d</sup> Recovery =  $0.8556/0.8608 \times 100 = 99.4\%$ .

As a first step, the single-chain polystyrene precursor was fractionated to ensure that the polymerization was giving the hoped-for product of narrow distribution. Figure 2 and Table I show that the polymer was indeed of narrow distribution, with  $\bar{M}_w/\bar{M}_n = 1.06$ .

Polystyrene prepared in this fashion was then subjected to a coupling reaction with bis(trichlorosilyl)ethane in order to synthesize the branched polymer. Fractionation showed that the crude product contained a mixture of molecular weights, as can be seen in Figure 3. In order to isolate a sufficient quantity of polymer for characterization studies, another sample of crude product was fractionated. Selected cuts from both fractionations were then recombined and refractionated as a means of obtaining maximum monodispersity.<sup>7</sup>

Throughout this work the complete data were treated according to Schulz.<sup>6</sup> When it became necessary to run both preliminary and refractionations, however, a complete description of the former did not appear to be warranted. A rapid and useful treatment was obtained by plotting polymer concentration versus volume of eluent. This approach is based on the view that changes in the degree of coupling are accompanied by



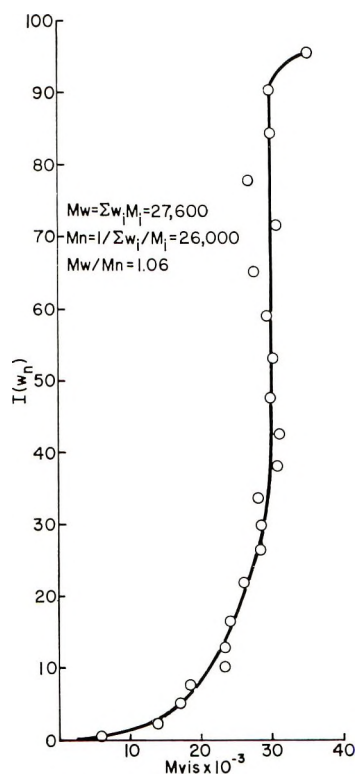


Fig. 2. Integral molecular weight distribution of linear polystyrene.

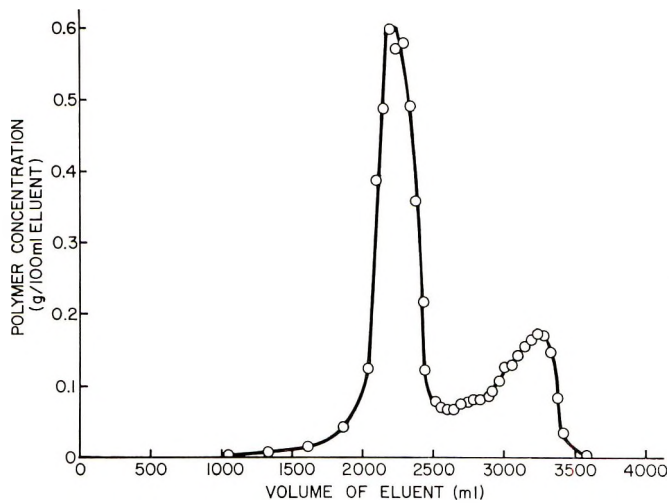


Fig. 3. Approximate molecular weight distribution; mixture of linear and branched polystyrene from bis(trichlorosilyl)ethane.

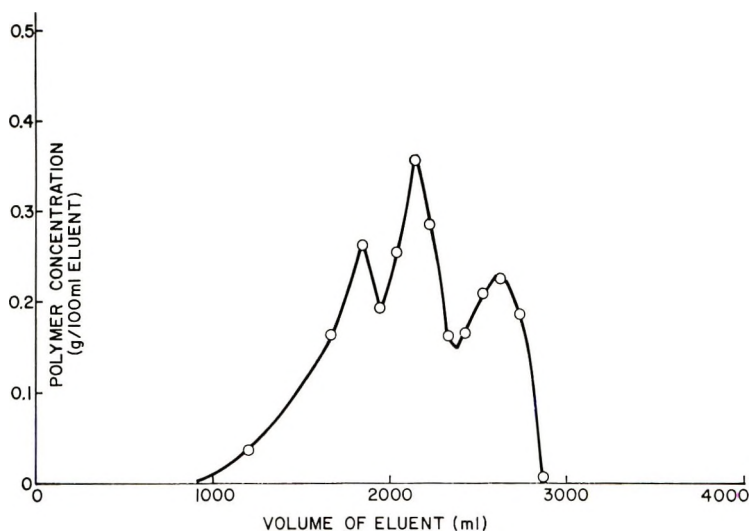


Fig. 4. Approximate molecular weight distribution; mixture of linear and branched polystyrene from phosphonitrilic chloride trimer.

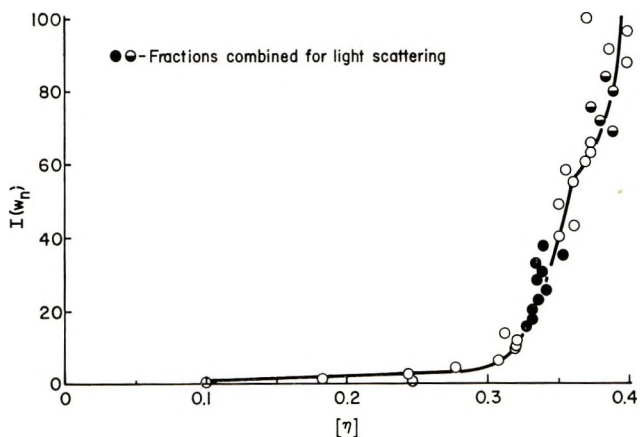


Fig. 5. Integral refractionation curve of "two-branch" and four-branch polystyrene from bis(trichlorosilyl)ethane.

changes in the solubilities, the latter being sufficiently larger than those resulting from the inherent inhomogeneity of the initial polymer. Thus, groupings of narrow distribution should appear as peaks in the plot. Examples of this are shown in Figures 3 and 4. The peaks in the concentration plot, therefore, permitted the selection of polymer samples of high and of intermediate degrees of branching for refractionations.

Despite the narrow distribution of the precursor, the refractionation curve in Figure 5 did not show the expected very narrow distribution plot. Fractions were combined from the lower region of the curve and from the upper region and subjected to a light scattering molecular weight deter-

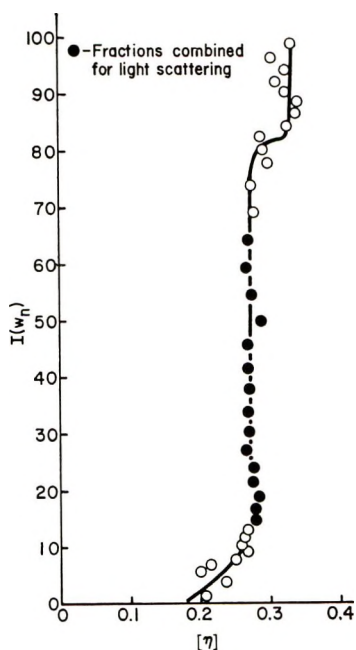


Fig. 6. Integral refractionation curve of two-branch polystyrene from phosphonitrilic chloride trimer.

mination. Although the difference in intrinsic viscosity was small (0.34 versus 0.38 for the lower and upper regions), the molecular weights were 60,500 and 121,000, respectively, which corresponded to two and four of the single chains.

Thus, the normal treatment of the data with the use of intrinsic viscosity as the abscissa was found to be misleading when applied to branched polymers because the small change in viscosity did not adequately reflect the large change in molecular weight. These results suggested that the polymers were separable but that viscosity measurements were unable to discern the separations.

A different branched polymer was synthesized by using the cyclic trimer of phosphonitrilic chloride as coupling agent. Figures 6 and 7 show the refractionation curves for the intermediate and high molecular weight groups for this polymer. In this case, the viscosity gave essentially vertical plots on refractionation perhaps because of improved separation. The precursor molecular weight was 24,000, the intermediate was 48,000, and the high was 137,200 as measured by light scattering. Evidently, therefore, the intermediate was a "two-branch" product, and the high was largely a six-branch polymer. It will be shown below that the polymer in Figure 7 was almost certainly a mixture of branched species undetected by the viscosity.

In the course of characterization studies, however, it became evident that the six-branch polymer had been degraded. That is, successive osmotic pressure measurements showed  $\bar{M}_n$  of 110,500 and 88,800. There-

fore, two more samples of the crude polymer were fractionated, one of which is shown in Table II and Figures 4 and 8. The combined high molecular weight portions, including the degraded sample above, were re-fractionated as shown in Figure 9. In order to minimize possible degradation, these fractions were subjected to the least possible mechanical and thermal abuse. Thus, only eight fractions were taken in Figure 9 instead of the usual 20-30.

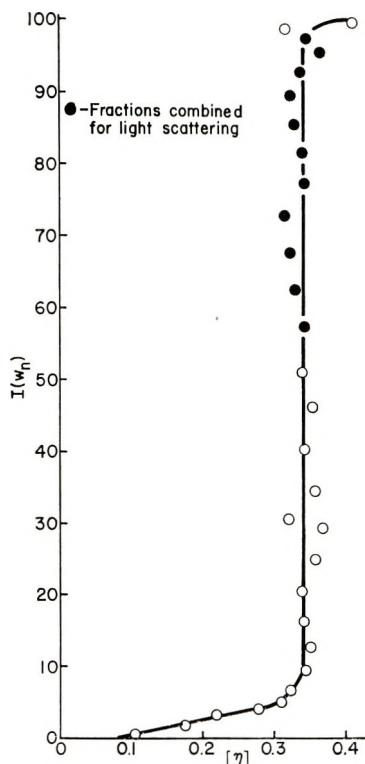


Fig. 7. Integral refractionation curve of four-branch and six-branch polystyrene from phosphonitrilic chloride trimer.

For this series the molecular weights were measured with a membrane osmometer, which permitted a more detailed examination of the fractionation results. Accordingly, the preliminary fractionation of crude polymer was plotted both by the Schulz treatment in Figure 8 and by the concentration method in Figure 4. The Schulz treatment demonstrated that the crude polymer consisted of single chains, "two-branch," four-branch, and six-branch species which were separable. In contrast, the concentration method was able to distinguish three main groupings, corresponding to single-chain, two-branch, and higher branched polymer, but was not sensitive to detailed variations within the groupings. This method, therefore, appeared suitable as an approximation of the distribution, but cannot

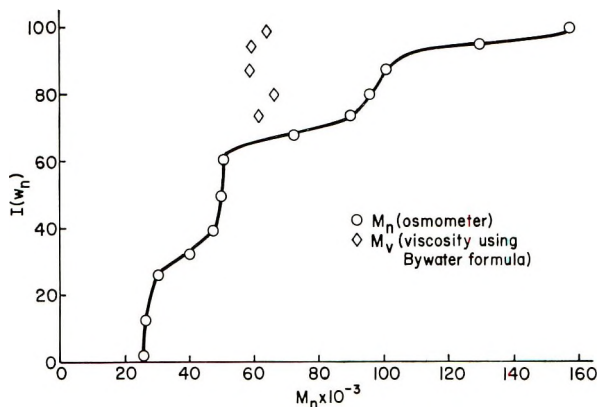


Fig. 8. Integral molecular weight distribution; mixture of linear and branched polystyrene from phosphonitrilic chloride trimer.

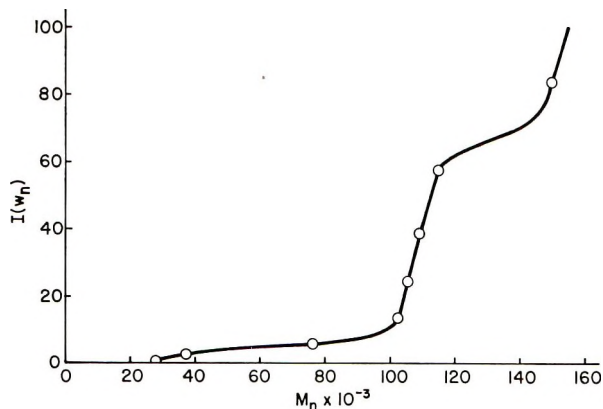


Fig. 9. Integral molecular weight distribution; refractionated four-branch and six-branch polystyrene from phosphonitrilic chloride trimer.

replace the more rigorous treatment if detailed examination is needed, especially with a small number of fractions.

The inability of viscosity measurements to distinguish between branched polymers is further shown in Table II and in Figure 8 by plotting  $M_{vis}$  for the branched fractions on the same scale. Here the viscosity shows only a minor change from the two-branch polymer of 50,000 molecular weight while the osmometry shows a threefold rise.

Another feature of these separations may be observed by comparison of Figures 8 and 9. The latter represents approximately the least soluble 30% of the crude polymer. Yet on refractionation, the shape of the whole curve in Figure 9 was very similar to the corresponding portion of Figure 8. This indicates that the preliminary fractionation was quite efficient and also suggests that extensive degradation did not occur during refractionation. The 10% of the polymer below molecular weight 100,000 may be due to the earlier sample which was known to have degraded.

TABLE II  
Preliminary Fractionation of Branched Polystyrene (Fig. 8)

Frac- tion	$m_i$ , g.	$w_i$ , %	$I(w_n)$	$M_i^a$	$[\eta]^b$	$M_{vis}^c$
1	0.1156	3.88	1.94	25,900		
2	0.4931	16.57	12.17	26,500		
3	0.2622	8.81	24.87	30,900		
4	0.1621	5.45	32.01	40,600		
5	0.2550	8.57	39.03	47,700		
6	0.3565	11.98	49.31	50,400		
7	0.2855	9.59	60.10	51,600		
8	0.1620	5.44	67.62	73,300		
9	0.1646	2.77	73.11	90,600	0.329	62,400
10	0.2087	3.55	79.44	96,500	0.349	67,600
11	0.2264	3.86	86.85	101,800	0.320	60,000
12	0.2047	3.44	94.15	130,700	0.322	60,500
13	0.0794	1.34	98.93	158,500	0.340	65,200
	2.9758 <sup>d</sup>					

<sup>a</sup> Single-point number-average molecular weight determined on Stabin-Shell automatic osmometer.

<sup>b</sup> Single-point viscosity determination from  $[\eta] = \eta_{sp}/c(1 + 0.28 \eta_{sp})$ .

<sup>c</sup>  $[\eta] = 1.04 \times 10^{-4} M^{0.73}$  (relation of Bywater<sup>8</sup>).

<sup>d</sup> Recovery =  $2.9758/3.0063 \times 100 = 98.9\%$ .

In Figure 9, the last fraction had a molecular weight of 151,000. Inasmuch as the single-chain precursor had an  $\bar{M}_n$  of about 25,000, the last fraction was clearly a pure sample of six-branch polystyrene. Although the overall yield of the latter was low, by fractionating, combining cuts, and refractionating, a reasonable amount (0.5–1 g.) of the six-branch polymer could be isolated. The procedures described, therefore, appear to have been satisfactory for the efficient separation of branched species and, when used with osmometry, for a true description of the molecular weight distribution.

The authors are pleased to acknowledge the financial support of the Celanese Corporation of America which made this work possible. We are also indebted to Mrs. Jane Graper for her valuable technical assistance.

### References

1. J. A. Gervasi and A. B. Gosnell, *J. Polymer Sci. A-1*, **4**, 1391 (1966).
2. F. Wenger and S.-P. S. Yen, paper presented at the 141st American Chemical Society Meeting, Washington, D. C., March 1962.
3. C. A. Baker and R. J. P. Williams, *J. Chem. Soc.*, **1956**, 2352.
4. A. Schindler, *Monatsh. Chem.*, **95**, 868 (1964).
5. G. V. Schulz and G. Sing, *J. Prakt. Chem.*, **161**, 161 (1942).
6. G. V. Schulz, in *Die Physik der Hochpolymeren*, H. A. Stuart, Ed., Vol. 2, p. 726.
7. G. M. Guzmán, in *Progress in High Polymers*, J. C. Robb, and F. W. Peaker, Eds., Vol. 1, p. 113.
8. S. Bywater et al., *Trans. Faraday Soc.*, **57**, 705 (1961).



### Résumé

Des fractionnements ont été effectués, utilisant l'éluion sur colonne pour des mélanges de polystyrènes linéaires et branchés. Ceux-ci avaient été préparés par polymérisation anionique suivie d'une réaction d'accouplement en vue de former des polymères branchés sous forme d'étoiles. À cet effet, les composants du mélange étaient chacun d'étroite distribution et le poids moléculaire différait entre eux comme des multiples de la longueur de chaîne de départ. Pour les simples chaînes d'un poids moléculaire de 25000-30000, les séparations ont été accomplies dans lesquelles les multiples (le nombre de branches) s'élevaient à 1, 2, 4, 6. De cette façon, on a obtenu des échantillons virtuellement monodispersés de ces polymères ramifiés.

### Zusammenfassung

An Mischungen von linearem und verzweigtem Polystyrol wurden Fraktionierungen mit einer Säulenclüierungsmethode ausgeführt. Die Polystyrole wurden durch anionische Polymerisation und eine darauffolgende Kupplungsreaktion unter Bildung sternförmiger verzweigter Polymerer dargestellt. Die Komponenten der Mischung besaßen daher jede eine enge Verteilung, und ihre Molekulargewichte unterschieden sich um Vielfache der Länge der ursprünglichen einfachen Ketten. Für einfache Ketten im Molekulargewichtsbereich von 25.000-30.000 wurden Trennungen erreicht, bei welchen die Vielfachen (Anzahl der Zweige) 1, 2, 4, und 6 betragen. Auf diese Weise konnten praktisch monodisperse Proben der verzweigten Polymeren isoliert werden.

Received August 18, 1965

Prod. No. 4946A

## NMR Spectra of Model Compounds of Poly(vinyl Chloride)

YASUAKI ABE, MITSUO TASUMI, and TAKEHIKO SHIMANOUCI, *Department of Chemistry, Faculty of Science, The University of Tokyo, Bunkyo-ku, Tokyo, Japan*, and SHIROH SATOH and RIICHIRO CHŪJŌ, *The Research Institute, Kureha Spinning Company, Ltd., Takatsuki, Osaka, Japan*

### Synopsis

The NMR spectra of three stereoisomers of 2,4,6-trichloroheptane as model compounds of poly(vinyl chloride) have been studied. Spectra were observed at 60 and 100 Mc./sec., both at room temperature and at high temperatures. A spin-decoupling experiment was performed. Computational analysis of the spectra was carried out on an IBM 7090 computer. The difference of the chemical shifts of the two *meso* methylene protons at 60 Mc./sec. was found to be ca. 7 cps. for the isotactic three-unit model while it was ca. 16 cps. for the isotactic two-unit model or heterotactic three-unit model. The spectra of poly(vinyl chloride) were interpreted reasonably on the basis of this result. Observed values of vicinal coupling constants of model compounds were interpreted as the weighted means of those for several conformations, and the stable conformations of the models were determined.

### INTRODUCTION

Recently NMR studies on model compounds of vinyl polymers have been widely carried out.<sup>1-13</sup> Although the magnetic fields experienced by protons in these low molecular weight model compounds may be somewhat different from those in polymers, there are still many characteristics similar to those of the polymers, and the study of these compounds may offer useful information for the analysis of polymer spectra.

The model compounds so far studied are confined to two-unit models. We have extended this study to the three-unit models of poly(vinyl chloride) (PVC), i.e., syndiotactic, isotactic, and heterotactic isomers of 2,4,6-trichloroheptane ( $\text{CH}_3\text{CHClCH}_2\text{CHClCH}_2\text{CHClCH}_3$ ) (Fig. 1); we discuss mainly the correlation between the configuration and conformation of the model compounds and PVC on the basis of infrared spectra, NMR spectra, and dipole moment measurements reported in previous papers.<sup>1,2</sup> In those papers, simple first-order analysis of the NMR spectra was carried out. In this paper we wish to present more refined analysis of the NMR spectra of these model compounds. On this basis the NMR spectra of PVC are analyzed and the stable conformation for the models determined.

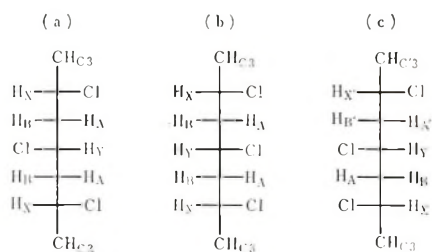


Fig. 1. Structural formulas of stereoisomers of 2,4,6-trichloroheptane: (a) syndiotactic isomer (synd-TCH); (b) isotactic isomer (iso-TCH); (c) heterotactic isomer (hetero-TCH).

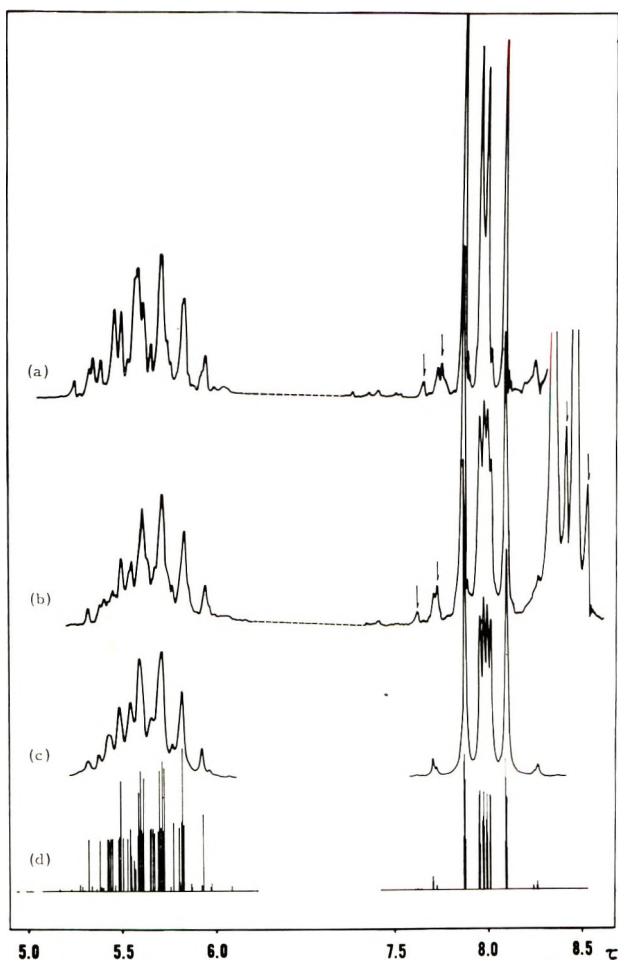


Fig. 2. NMR spectra of syndiotactic 2,4,6-trichloroheptane at 60 Mc./sec.: (a) observed at 120°C. (in  $\text{CCl}_4$ ); (b) observed at 25°C. (in  $\text{CCl}_4$ ); (c) calculated with the parameter set I in Table I with linewidth: 0.8 cps for  $\text{H}_{\text{A}}$  and  $\text{H}_{\text{B}}$ , 1.2 cps for  $\text{H}_{\text{X}}$ , 1.5 cps for  $\text{H}_{\text{Y}}$  protons; (d) stick spectra corresponding to (c). Peaks marked with arrows are due to hetero-TCH.

## EXPERIMENTAL

The method of the preparation of the model compounds was reported in a previous paper.<sup>1</sup>

The NMR spectra at 60 Mc./sec. were measured on a Varian V-4311 spectrometer equipped with a variable temperature probe accessory Model

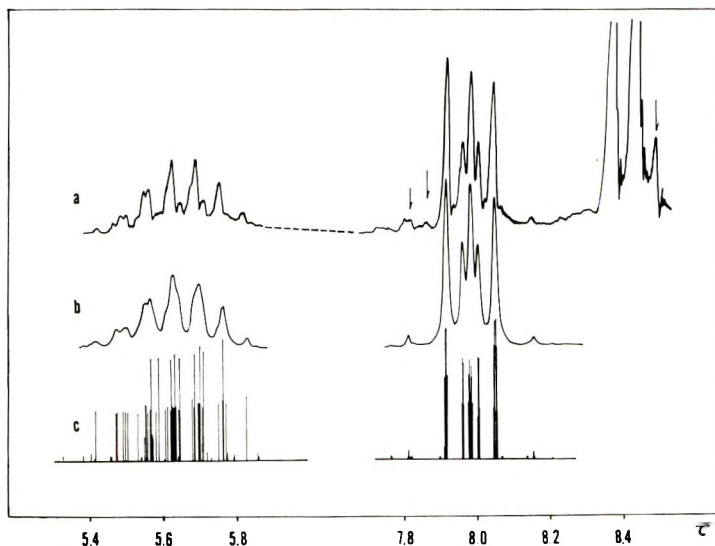


Fig. 3. NMR spectra of syndiotactic 2,4,6-trichloroheptane at 100 Mc./sec.: (a) observed at 25°C. (in  $\text{CCl}_4$ ); (b) calculated with the parameter set I in Table I with line-width: 1.0 cps for  $\text{H}_A$  and  $\text{H}_B$ , 1.5 cps for  $\text{H}_X$ , 2.0 for  $\text{H}_Y$  protons; (c) stick spectra corresponding to (b). Peaks marked with arrows are due to hetero-TCH.

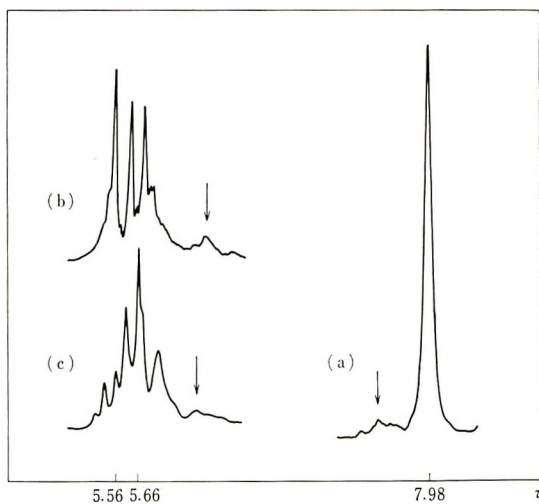


Fig. 4. NMDR spectra of syndiotactic 2,4,6-trichloroheptane at 60 Mc./sec.: (a)  $\text{CH}_2$  proton spectrum decoupled from CH protons; (b) CH proton spectrum decoupled from  $\text{CH}_2$  protons. (c) CH proton spectrum decoupled from  $\text{CH}_3$  protons.

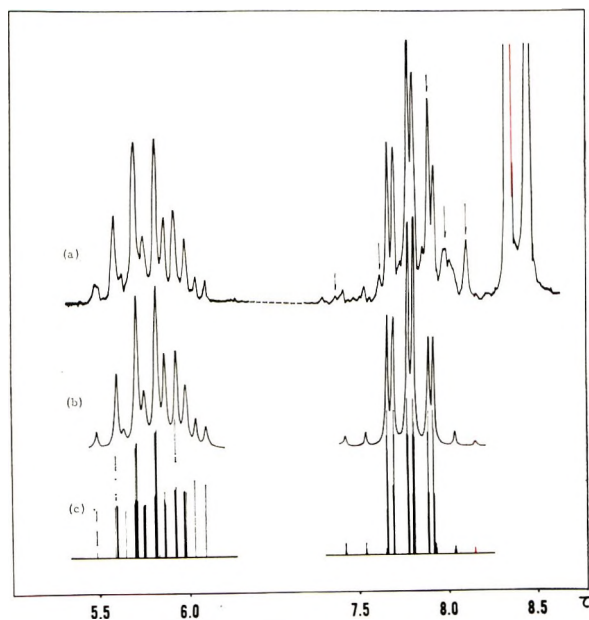


Fig. 5. NMR spectra of isotactic 2,4,6-trichloroheptane at 60 Mc./sec.: (a) observed at 25°C. (in  $\text{CCl}_4$ ); (b) calculated with the parameter set in Table I with linewidth: 0.8 cps for  $\text{H}_A$  and  $\text{H}_B$ , 1.2 cps for  $\text{H}_X$ , 1.5 cps for  $\text{H}_Y$  protons; (c) stick spectra corresponding to (b). Peaks marked with arrows are due to hetero-TCH.

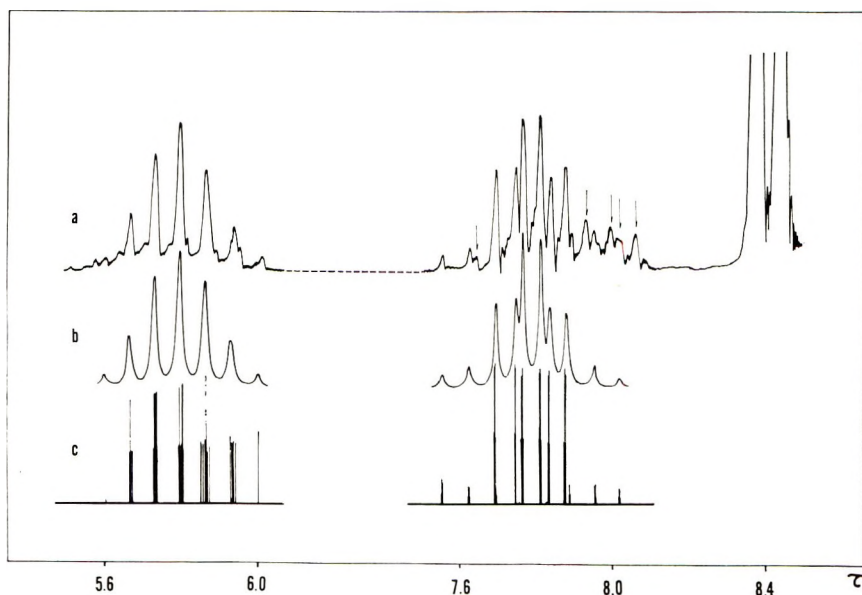


Fig. 6. NMR spectra of isotactic 2,4,6-trichloroheptane at 100 Mc./sec.: (a) observed at 25°C. (in  $\text{CCl}_4$ ); (b) calculated with the parameter set in Table I with linewidth: 1.0 cps for  $\text{H}_A$  and  $\text{H}_B$ , 1.5 cps for  $\text{H}_X$ , 2.0 cps for  $\text{H}_Y$  protons; (c) stick spectra corresponding to (b). Peaks marked with arrows are due to hetero-TCH.

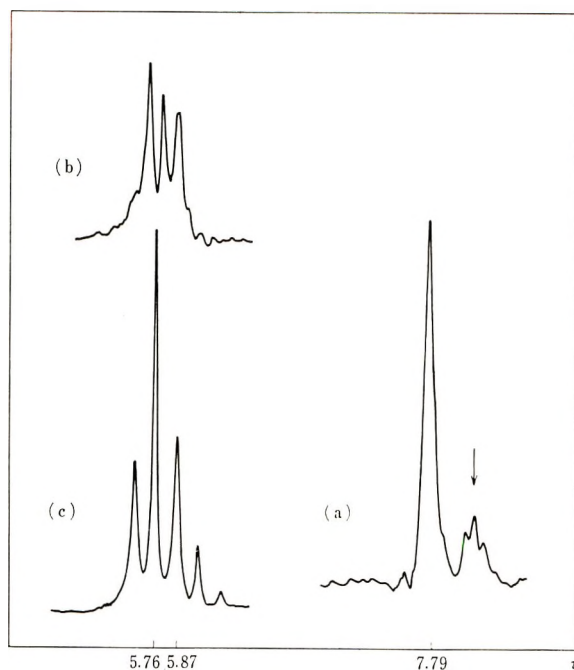


Fig. 7. NMR spectra of isotactic 2,4,6-trichloroheptane at 60 Mc./sec.: (a)  $\text{CH}_2$  proton spectrum decoupled from CH protons; (b) CH proton spectrum decoupled from  $\text{CH}_2$  protons; (c) CH proton spectrum decoupled from  $\text{CH}_3$  protons. Peaks marked with arrows are due to hetero-TCH.

V-4340 and also on a Varian A-60 spectrometer at room temperature and at high temperatures. Spin-decoupling experiments were performed by the side-band method with sweeping field. The spectra at 100 Mc./sec. were measured on a Varian HR-100 spectrometer. We are greatly indebted to Dr. K. Nukada of The Research Laboratory of Toyo Rayon Co., Ltd. for the measurement of the spectra at 100 Mc./sec. All spectra were obtained on ca. 30% solutions in carbon tetrachloride, and peak positions were determined by the side-band method with tetramethylsilane as internal reference.

The spectra are shown in Figures 2-10. The spectra of iso-TCH (isotactic isomer) at high temperatures are not given since they are not markedly different from the spectra at room temperature. The synd-TCH (syndiotactic isomer) and iso-TCH prepared by us contained a small amount of impurity (hetero-TCH: heterotactic isomer), but this mixing yielded no difficulty in the analysis; the peaks due to this impurity are marked with an arrow in Figures 2-10.

### ANALYSIS OF THE SPECTRA

The spin system of the model compounds is shown in Figure 11; couplings other than those represented by the line are neglected. Analysis of



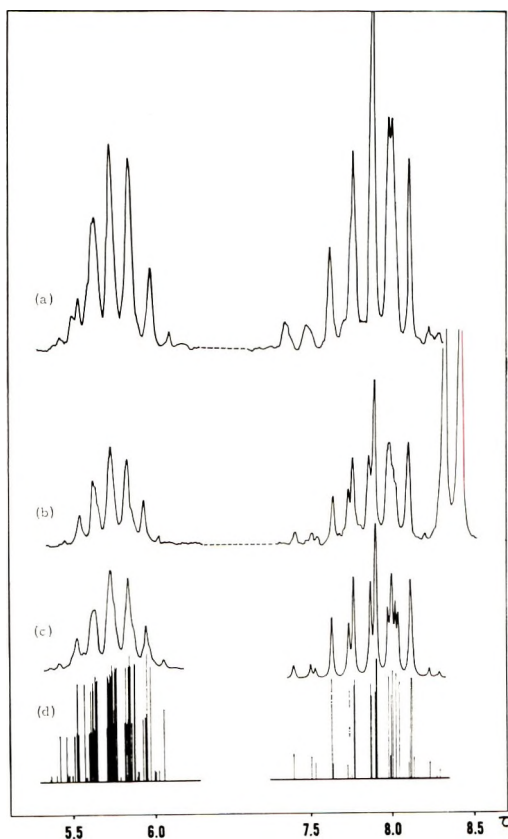


Fig. 8. NMR spectra of heterotactic 2,4,6-trichloroheptane at 60 Mc./sec.: (a) observed at 120°C. (in  $\text{CCl}_4$ ); (b) observed at 25°C. (in  $\text{CCl}_4$ ); (c) calculated with the parameter set I in Table I with linewidth: 0.8 cps for  $\text{H}_A$  and  $\text{H}_B$ , 1.2 cps for  $\text{H}_X$ , 1.5 cps for  $\text{H}_Y$  protons; (d) stick spectra corresponding to (c).

this complete spin system is, however, very complicated, since the system is composed of thirteen spins in all. As the difference of the chemical shifts between the CH protons and the  $\text{CH}_3$  or  $\text{CH}_2$  protons is large enough, it is possible to analyze, to a good approximation, the  $\text{CH}_3$ ,  $\text{CH}_2$ , and CH proton resonances separately. The following computation was carried out on an IBM 7090 computer using Fortran programs.<sup>14</sup> Parameters were refined by the method of least squares. The experimental data at both 60 and 100 Mc./sec. were used as the observed values.

### Methyl Protons

The  $\text{CH}_3$  protons exhibit a strong doublet at the highest field in all isomers and the parameters associated with them,  $\tau_{\text{CH}_3}$  and  $J_{\text{CH}_3-\text{CH}}$ , were easily determined, as given in Table I. The values for them are almost the same for all isomers. As shown in Figures 2 and 3, the  $\text{CH}_3$  resonance of hetero-TCH as a contamination in synd-TCH is seen largely separated

TABLE I  
Chemical Shifts and Coupling Constants of 2,4,6-Trichloroheptane and *meso* 2,4-Dichloropentane<sup>a</sup>

Isomer <sup>b</sup>	Chemical shifts						Coupling constants, cps												
	CH <sub>3</sub>	CH	CH <sub>2</sub>	CH <sub>2</sub>	CH <sub>3</sub> -CHCH <sub>2</sub>	CH <sub>2</sub> -CH	$\tau_C$	$\tau_X$	$\tau_Y$	$\tau_A$	$\tau_B$	$\nu_A - \nu_B$ , <sup>c</sup>	$J_{CX}$	$J_{AB}$	$J_{AX}$	$J_{AY}$	$J_{BX}$	$J_{BY}$	
Synd-TCH at 20°C.																			
Set I	8.41	5.66	5.56	8.00	7.96	7.96	2.44	2.44	6.4	-14.94	10.55	2.39	2.73	2.39	2.73	2.39	2.73	10.98	
Set II	8.41	5.66	5.56	7.96	8.00	7.96	2.44	2.44	6.4	-14.94	10.98	2.73	2.39	2.73	2.39	2.73	2.39	10.98	
Synd-TCH at 120°C.																			
Set I	—	—	—	—	—	—	0.0	0.0	6.4	-14.70	10.20	2.50	2.50	2.50	2.50	2.50	2.50	10.20	
Iso-TCH at 20°C.	8.42	5.76	5.87	7.73	7.85	7.85	7.44	7.44	6.4	-14.09	7.36	7.37	6.26	7.37	6.26	7.37	6.26	6.24	
Hetero-TCH at 20°C.																			
Racemic																			
Set I	8.42	5.71	5.76	8.03	7.99	7.99	2.59	2.59	6.4	-14.91	10.28	1.98	2.06	1.98	2.06	1.98	2.06	10.81	
Set II	8.42	5.71	5.76	7.99	8.03	7.99	2.59	2.59	6.4	-14.91	10.81	2.06	1.98	2.06	1.98	2.06	1.98	10.28	
<i>meso</i>																			
Set I	8.42	5.79	5.76	7.68	7.95	7.95	16.58	16.58	6.4	-13.95	6.25	8.45	7.57	8.45	7.57	8.45	7.57	5.34	
Set II	8.42	5.79	5.76	7.95	7.68	7.95	16.58	16.58	6.4	-13.95	5.32	7.59	8.46	7.59	8.46	7.59	8.46	6.24	
Hetero-TCH at 120°C.																			
Racemic	—	—	—	—	—	—	0.0	0.0	6.4	-14.70	9.59	3.38	3.38	3.38	3.38	3.38	3.38	9.59	
<i>meso</i>	—	—	—	—	—	—	17.25	17.25	6.4	-15.16	7.91	8.87	6.23	8.87	6.23	8.87	6.23	6.10	
<i>meso</i> -DCP at 20°C.	8.49	5.93	—	7.75	8.05	8.05	17.80	17.80	6.4	-14.14	7.67	7.67	6.57	7.67	6.57	7.67	6.57	6.57	

<sup>a</sup> Designations of protons refer to the structural formulae in Figure 1.

<sup>b</sup> Set I is obtained assuming  $\nu_A < \nu_B$ ; set II is obtained assuming  $\nu_A > \nu_B$ .

<sup>c</sup> cps at 60 Mc./sec.

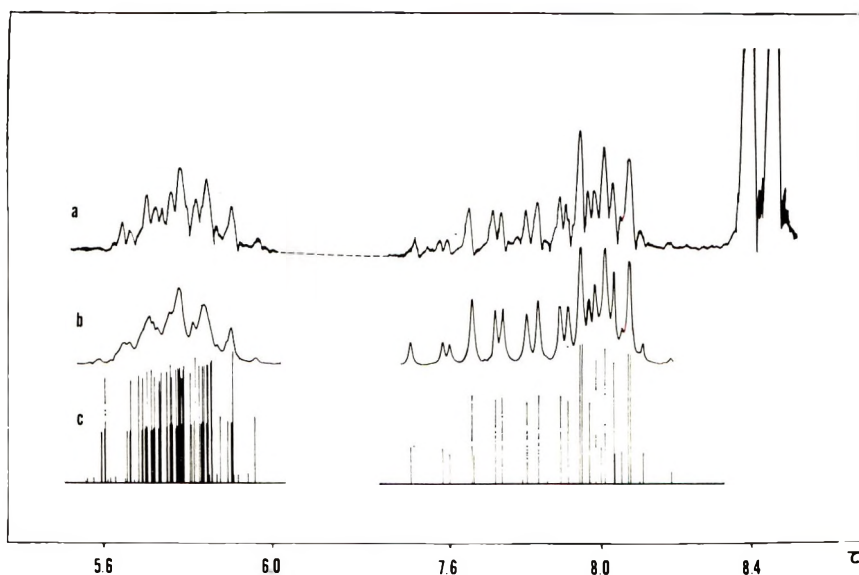


Fig. 9. NMR spectra of heterotactic 2,4,6-trichloroheptane at 100 Mc./sec.: (a) observed at 25°C. (in  $\text{CCl}_4$ ); (b) calculated with the parameter set I in Table I with linewidth: 1.0 cps for  $\text{H}_A$  and  $\text{H}_B$ , 1.5 cps for  $\text{H}_X$ , 2.0 for  $\text{H}_Y$  protons; (c) stick spectra corresponding to (b).

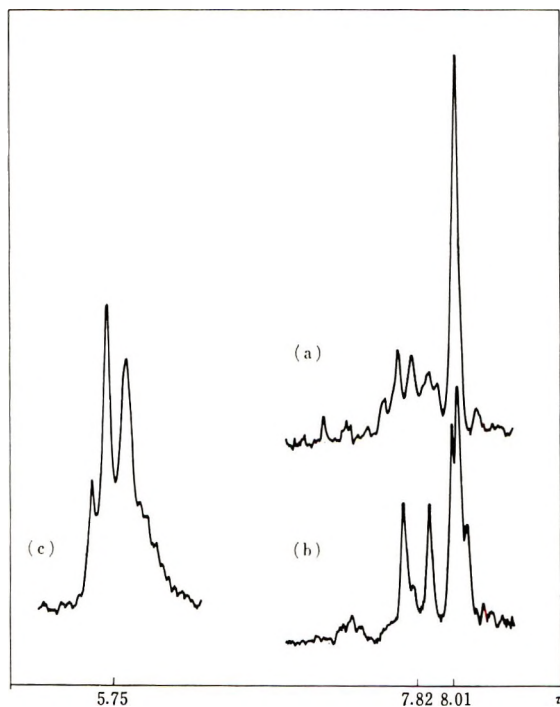


Fig. 10. NMR spectra of heterotactic 2,4,6-trichloroheptane at 60 Mc./sec.: (a) racemic  $\text{CH}_2$  proton spectrum decoupled from CH protons; (b) *meso*  $\text{CH}_2$  proton spectrum decoupled from CH protons; (c) CH proton spectrum decoupled from  $\text{CH}_3$  protons.

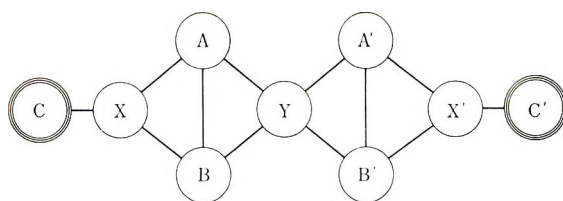


Fig. 11. Spin system of the model compounds.

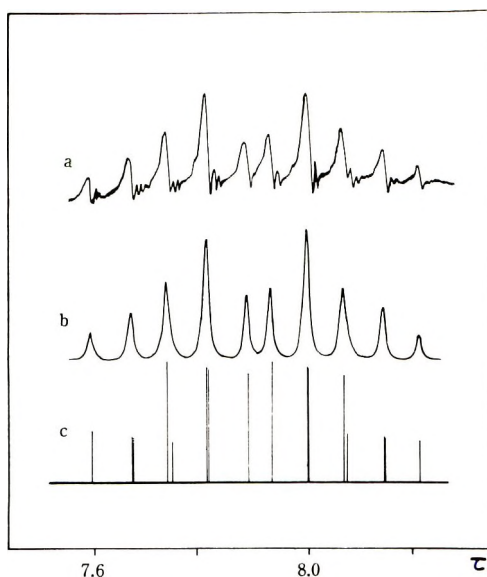


Fig. 12. Methylene proton spectra of *meso* 2,4-dichloropentane at 60 Mc./sec.: (a) observed at 25°C. (in  $\text{CCl}_4$ ); (b) calculated with the parameter set in Table I with linewidth = 0.8 cps; (c) stick spectrum corresponding to (b).

from that of synd-TCH. This may be due to some intermolecular effect, since this resonance in the spectra of pure hetero-TCH appears at nearly the same position as other isomers (Figs. 8 and 9).

### Methylene Protons

The peaks at the left of the  $\text{CH}_3$  strong doublet arise from the  $\text{CH}_2$  protons. We analyzed the  $\text{CH}_2$  proton resonances most extensively since they can be definitely interpreted and offer interesting information in many respects. Although the chemical shift of the  $\text{CH}_3$  protons is rather close to that of the  $\text{CH}_2$  protons, these two groups are separated by the CH proton whose chemical shift is greatly different, and we may disregard the  $\text{CH}_3$  group when we treat the  $\text{CH}_2$  group. Further, the values of the chemical shifts of the CH protons were fixed to those obtained by simple first-order analysis or from the double-resonance spectra. This simplification would not affect the results of analysis.

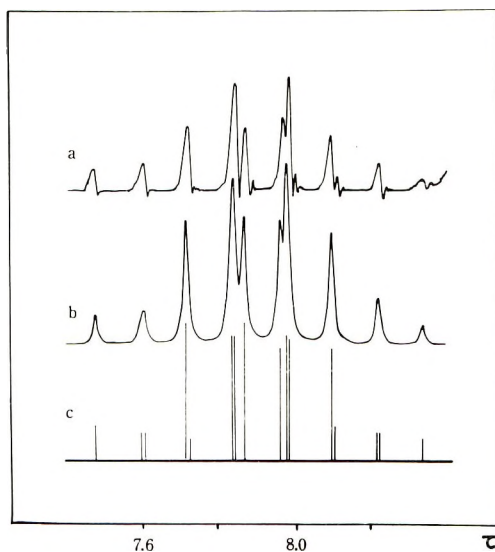


Fig. 13. Methylene proton spectra of *meso* 2,4-dichloropentane at 100 Mc./sec.: (a) observed at 25°C. (in  $\text{CCl}_4$ ); (b) calculated with the parameter set in Table I with linewidth = 1.0 cps; (c) stick spectrum corresponding to (b).

The  $\text{CH}_2$  protons of synd-TCH were analyzed as an AB part of an  $(\text{AB-X})_2\text{Y}$  spin system (where A, B, X, and Y refer to the protons shown in Figs. 1 and 11) by using the symmetrized basic functions for this system. In this case the situation is somewhat different from the case of *dl*-DCP (racemic 2,4-dichloropentane<sup>4,5,10,15</sup>), and there is a slight difference in the chemical shift between the two geminal  $\text{H}_\text{A}$  and  $\text{H}_\text{B}$  methylene protons at room temperature and between the  $\text{H}_\text{X}$ 's and  $\text{Y}_\text{Y}$  methine protons as well. These differences  $|\nu_\text{A} - \nu_\text{B}|$  and  $|\nu_\text{X} - \nu_\text{Y}|$  are, however, very small compared with  $|\nu_\text{X} - \nu_\text{A}|$ ,  $|\nu_\text{X} - \nu_\text{B}|$ ,  $|\nu_\text{Y} - \nu_\text{A}|$ , and  $|\nu_\text{Y} - \nu_\text{B}|$ , and it was impossible to determine which resonance of the two  $\text{CH}_2$  protons,  $\text{H}_\text{A}$  and  $\text{H}_\text{B}$  in Figure 1, appears at higher field. Refinement of parameters was carried out for both of the two possible cases  $\nu_\text{A} < \nu_\text{B}$  and  $\nu_\text{A} > \nu_\text{B}$ , but the thus obtained two sets (given as sets I and II, respectively, in Table I) gave nearly the same calculated spectra which could not be distinguished definitely by our experiment and analysis.

The  $\text{CH}_2$  protons of iso-TCH were analyzed also as an AB part of an  $(\text{ABX})_2\text{Y}$  spin system. Naturally there is a considerable difference between the chemical shifts of the two geminal protons, and it was impossible to determine whether  $\nu_\text{A} > \nu_\text{B}$  or  $\nu_\text{A} < \nu_\text{B}$ . Iso-TCH did not exhibit any appreciable temperature dependence and the spectra at high temperatures were not considered.

The two groups of  $\text{CH}_2$  protons of hetero-TCH, i.e., racemic and *meso*  $\text{CH}_2$ , can be treated as AB parts of two independent XABY four-spin systems, as the separation of the two parts in the spectra is ca. 11 cps at 60 Mc./sec. and the couplings between them are negligible. In the case of

hetero-TCH also, there are two possibilities for the sign of  $(\nu_A - \nu_B)$  with respect to the racemic and *meso* CH<sub>2</sub> protons as well, and parameters for both cases were obtained. The four vicinal coupling constants associated with the *meso* CH<sub>2</sub> protons of hetero-TCH are considerably different, and the situation is different from the case of *meso*-DCP (*meso* 2,4-dichloropentane<sup>4,5,10,15</sup>) and iso-TCH. The spectra of *meso* CH<sub>2</sub> of hetero-TCH and *meso*-DCP at 60 Mc./sec. are quite similar, but a remarkable difference appears at 100 Mc./sec. (Figs. 8, 9, 12, and 13). For comparison the spectra of *meso*-DCP were also analyzed. Spin decoupling was useful for determining each center of the racemic and *meso* CH<sub>2</sub> parts in the spectra. In addition, when the *meso* CH<sub>2</sub> protons were decoupled from the CH protons, the former showed a simple quartet for an AB system, and  $|\nu_A - \nu_B|$  and  $J_{AB}$  were easily determined (Fig. 10).

### Methine Protons

There are two or three different CH protons, i.e., H<sub>X</sub>, H<sub>X'</sub>, and H<sub>Y</sub> protons (Fig. 11). (In synd- and iso-TCH the H<sub>X</sub> and H<sub>X'</sub> protons are equivalent, whereas in hetero-TCH they are not.) Their signals which appear at the lowest field in Figures 2-10 overlap these different CH proton resonances. As the coupling constants associated with the CH protons are more easily determined from the analysis of the CH<sub>3</sub> or CH<sub>2</sub> proton resonances, the spectra of the CH protons were analyzed only to determine the chemical shifts.

The chemical shifts of the CH protons of synd-TCH were determined from the double resonance spectra. In Figure 4*b*, where the CH protons are decoupled from the CH<sub>2</sub> protons, three prominent peaks are seen, of which the two at the higher field are the central two components of a quartet due to the H<sub>X</sub> protons and another peak at the lower field results from the H<sub>Y</sub> proton. (These protons are partially decoupled also from the CH<sub>3</sub> protons and the splitting is rather small.) In Figure 4*c*, where the CH protons are decoupled from the CH<sub>3</sub> protons, six peaks are seen. The stronger three at the higher field construct a triplet due to the H<sub>X</sub> protons, though in this case also the splitting is small owing to partial decoupling from the CH<sub>2</sub> protons. The remaining three at the lower field, which are much weaker than the former, belong to a quintet due to the H<sub>Y</sub> proton. From these two spectra the required parameters were obtained. Calculation of the undecoupled spectra with thus obtained parameters was carried out by treating each of the three CH protons independently as an X in an ABXC<sub>3</sub> six-spin system or as a Y in an ABYBA five-spin system.

As for iso-TCH, the analysis is very simple. In the undecoupled spectrum at 60 Mc./sec. (Fig. 5*a*), two groups of signals are seen at the lowest field, which can be clearly discriminated: a quintet at the higher field results from the H<sub>Y</sub> proton and a sextet at the lower field from the H<sub>X</sub> protons. This interpretation is strongly supported by the double resonance spectra shown in Figures 7*b* and 7*c*.



It was not so easy to obtain these parameters of hetero-TCH, since the two  $H_X$  and  $H_X'$  protons are not equivalent and the double resonance spectra are complicated owing to the presence of the two chemically different  $CH_2$  groups. However, it was possible to get values shown in Table I from the analysis of the spectra decoupled from the  $CH_3$  protons (Fig. 10c) and repeated calculations of the spectra with several sets of parameters.

The obtained parameters are given in Table I and the spectra calculated by using parameter set I are shown in Figures 2-13, both as "stick" spectra and with Lorentzian line shape. (In each case set I gives better results in the calculation of the CH spectra.)

## DISCUSSION

### Analysis of the NMR Spectra of PVC

There have been several studies of the NMR spectra of PVC, although the observed data have been interpreted differently. Johnsen regarded the two *meso*  $CH_2$  protons equivalent without any explanation.<sup>16</sup> On the other hand, Tincher<sup>17</sup> regarded the two protons nonequivalent as expected theoretically, and this analysis was supported by Satoh et al. and Doskocilova from the study on an isotactic two-unit model, i.e., *meso*-DCP, as the difference of the chemical shift between the two *meso*  $CH_2$  protons in this model was 15.1 cps at 60 Mc./sec.<sup>4,5,9</sup> The double resonance spectra of PVC, however, have shown that Johnsen's interpretation is more plausible, since when the CH proton was irradiated, only one peak appeared for the *meso*  $CH_2$  protons.<sup>5,18,19</sup>

An interesting result was obtained from the study on the model compounds. In the isotactic three-unit model the difference between the chemical shifts of the two *meso*  $CH_2$  protons is much smaller than in the two-unit model, whereas it is still large in the heterotactic three-unit model. This indicates that the  $CH_2$  resonances of PVC may not be explained in terms of the diad, but the more distant substituents should be considered, as suggested by Yoshino et al.<sup>20</sup> from a study on  $\alpha,\beta$ -deuterated PVC. When the configurations of the next-nearest neighboring substituents are taken into account, that is, when the tetrad is employed as a unit, we get six kinds of  $CH_2$  groups.<sup>19</sup> *imi*, *imh*, *hmh*, *srs*, *srh*, and *hvh*, where *i*, *h*, *s*, *m*, and *r* follow the notation defined by Bovey and Tiers.<sup>21</sup> We tried to calculate the spectra corresponding to these six tetrads using the information on the model compounds and to add them in the suitable ratio. One of the calculated spectra and the observed spectrum are shown in Figure 14. The parameter set and the ratio of each tetrad used in the calculation are listed in Table II. In this table the ratio was deduced from a polymerization process with a single- $\sigma$  propagation<sup>5,18,21</sup> ( $\sigma$  was determined from the double-resonance spectra); the differences of the chemical shifts of the two  $CH_2$  protons,  $|\nu_A - \nu_B|$ , were estimated from those of the model compounds; and the mean values of the chemical shifts of the two protons,  $(\tau_A + \tau_B)/2$ , were adjusted to get the best agreement between the observed

TABLE II  
Chemical Shifts and Coupling Constants of Poly(vinyl Chloride) in *o*-Dichlorobenzene and Tetrachloroethylene<sup>a</sup>

Tetrad	Concentration <sup>b</sup>	Chemical shifts			Coupling constants, cps					
		$(\tau_A + \tau_B)/2$	$\tau_X$	$\tau_Y$	$ \nu_A - \nu_B $ , cps	$J_{AB}$	$J_{AX}$	$J_{AY}$	$J_{BX}$	$J_{BY}$
<i>imi</i>	$\sigma^3$	7.75	5.69	5.69	3.5	-14.0	6.6	6.6	6.6	6.6
<i>imh</i>	$2\sigma^2(1 - \sigma)$	7.75	5.69	5.53	7.0	-14.0	6.6	6.6	6.6	6.6
<i>hmh</i>	$\sigma(1 - \sigma)^2$	7.78	5.53	5.53	15.0	-14.0	6.6	6.6	6.6	6.6
<i>spS</i>	$(1 - \sigma)^3$	7.95	5.43	5.43	0.0	-14.5	10.0	3.0	3.0	10.0
<i>srh</i>	$2\sigma(1 - \sigma)^2$	7.99	5.43	5.53	2.0	-14.5	10.0	3.0	3.0	10.0
<i>hrh</i>	$\sigma^2(1 - \sigma)$	8.00	5.53	5.53	0.0	-14.5	10.0	3.0	3.0	10.0

<sup>a</sup> Designations of protons are identical with those for models.

<sup>b</sup>  $\sigma$  is the probability that a polymer chain will add a monomer unit to give the same configuration as that of the last unit at its growing end.

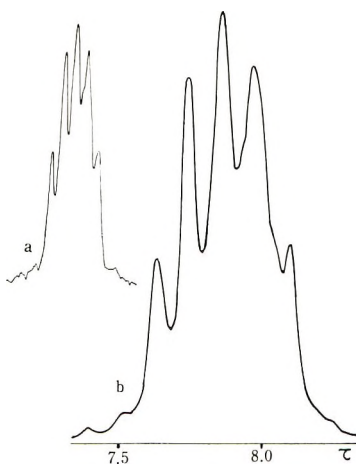


Fig. 14. NMR spectra of poly(vinyl chloride) at 60 Mc./sec.: (a) observed at 120°C. (in *o*-dichlorobenzene and tetrachloroethylene); (b) calculated with the parameters in Table II with linewidth = 3.0 cps and  $\sigma = 0.4$ .

and the calculated spectra. However, the analysis of the NMR spectra of PVC in terms of tetrad has some ambiguities and the set of parameters in Table II is not conclusive. Nevertheless, we may say definitely that it is unreasonable to interpret the  $\text{CH}_2$  proton resonances of PVC in terms of the diad.

Another interesting fact obtained from the spectra of the three-unit models is concerned with the CH resonances. When, in the polymer, the CH proton was decoupled from the  $\text{CH}_2$  protons, three peaks were seen,<sup>5,18,19</sup> and these were assigned by Bovey et al. and also by Satoh et al. to the syndiotactic, heterotactic, and isotactic CH resonances, respectively, from the low field. This assignment is supported by the three-unit model compounds. The chemical shifts of the  $\text{H}_Y$  methine protons of the three stereoisomers, which represent the configurations of the above three CH groups in the polymer, are 5.56  $\tau$  for synd-TCH, 5.76  $\tau$  for hetero-TCH, and 5.87  $\tau$  for iso-TCH, and this order is the same as that in the polymer. This also confirms the assignment of the *meso*  $\text{CH}_2$  resonance appearing at lower field than the racemic  $\text{CH}_2$  one.

### Chain Conformation of the Model Compounds

In the previous papers,<sup>1,15</sup> we discussed the stable chain conformations of the two- and three-unit models of PVC, mainly by means of infrared spectra and measurements of dipole moment. The discussions proved to be consistent with the following ones on NMR spectra.

It may be said that the stable conformations of the model compounds should satisfy the following two conditions: (1) conformation around the C—C bond is staggered; (2) Any of the pairs  $\text{CH}_3 \dots \text{CH}_2$ ,  $\text{CH}_3(\text{or } \text{CH}_2) \dots \text{Cl}$ , and  $\text{Cl} \dots \text{Cl}$  are not close together. The resultant possible conformers are shown in Figure 15.

On the other hand, magnitudes of vicinal couplings depend upon the conformation of the relevant hydrogens. Accordingly, we may study the chain conformations of the model compounds on the basis of the observed

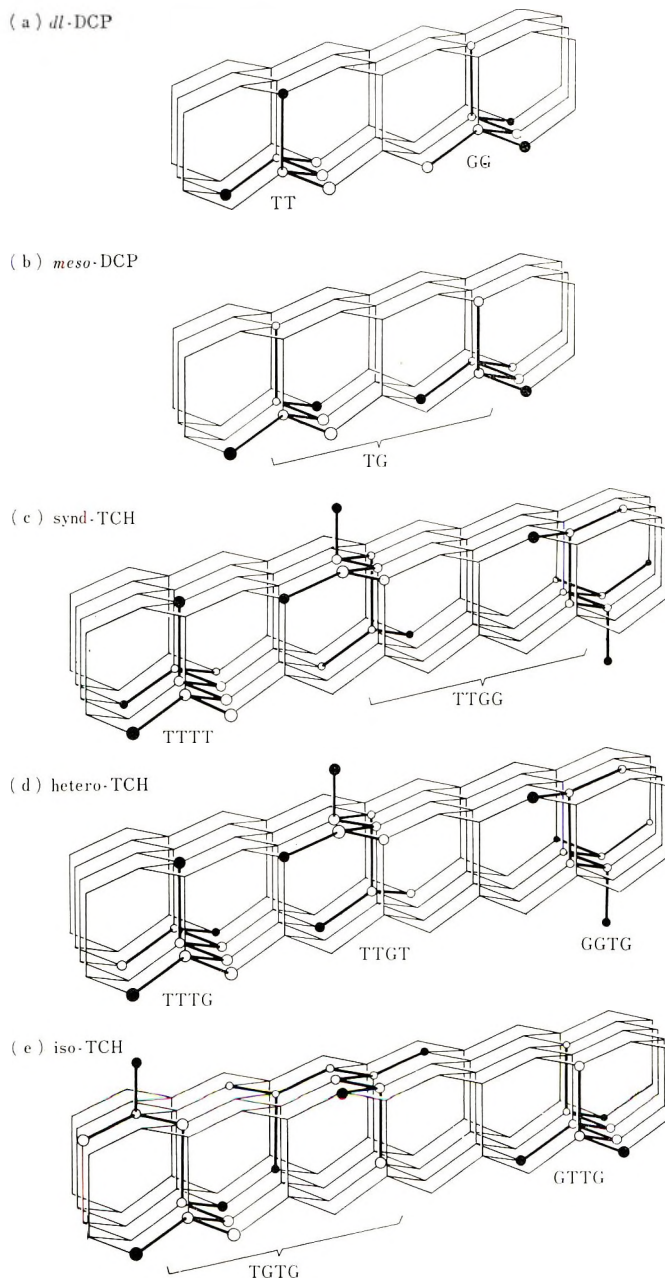


Fig. 15. Rotational isomers of model compounds of poly(vinyl chloride): (○) carbon; (●) Chlorine. Two forms (TTGG and TGTG) are isoenergetic since one is the mirror image of the other.

TABLE III  
Relation between Vicinal Couplings and Concentration of Conformers<sup>a,b,c</sup>

Compound	$J_{AX}$	$J_{AY}$	$ J_{AX} - J_{AY} $	$\frac{ J_{AX} - J_{AY} }{J_{AY}^{obs}}$ , cps
<i>dl</i> -DCP	$(1-p)J_t + J_o$	$pJ_t + (1-p)J_o$	$(1-2p)(J_t - J_o)$	7.0
<i>meso</i> -DCP	$\frac{1}{2}(J_t + J_o)$	$\frac{1}{2}(J_t + J_o)$	0.0	0.0
Synd-TCH	$(1 - \frac{1}{2}p)J_t + \frac{1}{2}pJ_o$	$\frac{1}{2}pJ_t + (1 - \frac{1}{2}p)J_o$	$(1-p)(J_t - J_o)$	8.2
Iso-TCH	$\frac{1}{2}(1+p)J_t + \frac{1}{2}(1-p)J_o$	$\frac{1}{2}(1-p)J_t + \frac{1}{2}(1+p)J_o$	$p(J_t - J_o)$	0.1
Hetero-TCH				
Racemic	$p'J_t + (1-p')J_o$	$(1-p')J_t + p'J_o$	$(1-2p')(J_t - J_o)$	8.3
<i>meso</i>	$(1-p)J_t + pJ_o$	$pJ_t + (1-p)J_o$	$(1-2p)(J_t - J_o)$	2.2

<sup>a</sup>  $J_t = 7-10$  cps and  $J_o = 2-5$  cps.

<sup>b</sup> Designations of protons refer to the structural formulae in Figure 1.

<sup>c</sup>  $p$  is the concentration of the conformers: GG of *dl*-DCP, TTGG of synd-TCH, GTTG' of iso-TCH, and TTGT of hetero-TCH;  $p'$  is the concentration of the conformer GG'TG of hetero-TCH.



coupling constants between the CH<sub>2</sub> and the CH protons. The observed values are those averaged over all the isomeric forms, that is:

$$J_{AX} = \sum_i p^i J_{AX}^i$$

where  $p^i$  is the concentration of the form  $i$  and  $J_{AX}^i$  is the coupling between the two protons, A and X, in the form  $i$ . It would be reasonable to take this average over only the forms shown in Figure 15, since  $p^i$ 's for others may be extremely small. The thus averaged vicinal couplings with respect to one of the CH<sub>2</sub> protons are listed in Table III. We discuss this quantity  $|J_{AX} - J_{AY}|$ , taking into account that  $J_t = 7-10$  and  $J_g = 2-5$  cps, where  $J_t$  and  $J_g$  are the couplings between the two vicinal hydrogens in the *trans* and *gauche* conformation respectively.

From the analysis of the spectra of *dl*-DCP it was obtained that  $|J_{AX} - J_{AY}| = 7.0$  cps,<sup>4,5,9</sup> which means that  $p \cong 0$  or  $p \cong 1$ , i.e., only one of the two forms, TT and GG in Figure 15, is stable. This is consistent with the conclusion from infrared study that only the TT form is predominant for this molecule.<sup>15</sup>

As for *meso*-DCP, it is expected that  $J_{AX} = J_{AY}$ , since the two forms shown in Figure 15 are energetically equivalent. This is just the fact observed.

As for synd-TCH, the observed  $|J_{AX} - J_{AY}|$  is 8.2 cps, and this large difference requires  $p \cong 0$  in Table III, i.e., TTTT is the most stable form, which is the same result as obtained from the infrared spectra and the dipole moment.<sup>1</sup>

From the infrared spectra and the dipole moment, it was concluded that hetero-TCH assumes mainly the TTTG form. The result that this molecule has one stable form is confirmed by the NMR spectra. As for racemic CH<sub>2</sub>,  $|J_{AX} - J_{AY}|_{\text{obs}} = 8.3$  cps, which means that  $p' \cong 0$  or  $p' \cong 1$ , and for *meso* CH<sub>2</sub>,  $|J_{AX} - J_{AY}|_{\text{obs}} = 2.2$  cps which means that  $p$  deviates appreciably from 0.5. In conclusion, hetero-TCH mainly has one form, which is TTTG if  $p' \cong 0$  and  $p < 0.5$ , TTGT if  $p' \cong 0$  and  $p > 0.5$ , or GGTG if  $p' \cong 1$ . As mentioned in the preceding section, it is interesting that in hetero-TCH the values of  $J_{AX}$  and  $J_{AY}$  of the *meso* part are considerably different at room temperature and approach each other at high temperature, whereas they are always equal in *meso*-DCP. The *meso* part of hetero-TCH may not undergo free inversion.

The NMR spectra were particularly useful in the study of the conformation of iso-TCH, since both infrared spectra and dipole moment were not very effective in this case. Table III shows  $p \cong 0$ , i.e., the TGTT form is the predominant form. This does not necessarily mean that iso-TCH exclusively assumes only one form, since some crude approximations were made in the above discussion. But it may be said that the TGTT form, threefold helix, is the most stable form for iso-TCH.

We analyzed the spectra at high temperatures to see the temperature dependence of parameters. It is possible, in principle, to estimate the



energy differences among the conformers in Figure 15 from the temperature dependence of the vicinal coupling constants. However, in order to get significant results to be used for further discussions, both theoretical and experimental improvements would be required.

*Note:* After this work had been completed we received a private communication from B. Schneider and co-workers who had independently studied the stereoisomers of 2,4,6-trichloroheptane. Their work was reported in detail at the International Symposium on Macromolecular Chemistry held in Prague, Czechoslovakia, August-September 1965.

### References

1. T. Shimanouchi, M. Tasumi, and Y. Abe, *Makromol. Chem.*, **86**, 43 (1965).
2. S. Satoh, R. Chûjô, E. Nagai, Y. Abe, M. Tasumi, and T. Shimanouchi, *Repts. Progr. Polymer Phys. Japan*, **8**, 311 (1965).
3. R. Chûjô, S. Satoh, T. Ozeki, and E. Nagai, *Repts. Progr. Polymer Phys. Japan*, **5**, 248 (1962).
4. S. Satoh, R. Chûjô, and E. Nagai, *Repts. Progr. Polymer Phys. Japan*, **7**, 295 (1964).
5. S. Satoh, *J. Polymer Sci. A*, **2**, 5221 (1964).
6. G. V. D. Tiers and F. A. Bovey, *J. Polymer Sci. A*, **1**, 833 (1963).
7. H. G. Clark, *Makromol. Chem.*, **63**, 69 (1963).
8. Y. Fujiwara and S. Fujiwara, *Bull. Chem. Soc. Japan*, **37**, 1010 (1964).
9. D. Doskocilova and B. Schneider, *Collection Czech. Chem. Commun.* **29**, 2290 (1964).
10. D. Doskocilova, *J. Polymer Sci. B*, **2**, 421 (1964).
11. D. Doskocilova and B. Schneider, *J. Polymer Sci. B*, **3**, 213 (1965).
12. D. E. McMahon and W. C. Tincher, *J. Mol. Spectry.*, **15**, 180 (1965).
13. F. A. Bovey, F. P. Hood III, E. W. Anderson, and L. C. Snyder, *J. Chem. Phys.*, **42**, 3900 (1965).
14. T. Shimanouchi and Y. Abe, *Kogyo Kagaku Zasshi*, **68**, 1395 (1965).
15. T. Shimanouchi and M. Tasumi, *Spectrochim. Acta*, **17**, 755 (1961).
16. U. Johnsen, *J. Polymer Sci.*, **54**, S6 (1961).
17. W. C. Tincher, *J. Polymer Sci.*, **62**, S148 (1962).
18. S. Satoh, R. Chûjô, and E. Nagai, *Repts. Progr. Polymer Phys. Japan*, **7**, 301 (1964).
19. F. A. Bovey, E. W. Anderson, D. C. Douglass, and J. A. Mason, *J. Chem. Phys.*, **39**, 1199 (1963).
20. T. Yoshino and J. Komiyama, *J. Polymer Sci. B*, **3**, 311 (1965).
21. F. A. Bovey and G. V. D. Tiers, *Fortschr. Hochpolymer.-Forsch.*, **3**, 139 (1963).

### Résumé

Les spectres NMR de trois stéréoisomères de 2,4,6-trichloroheptane comme substances modèles de chlorure de polyvinyle ont été étudiés. Les spectres ont été observés à 60 et 100 Mc, aussi bien à température de chambre qu'à température élevée. On a exécuté des expériences avec couplage de spin. L'analyse par computer de ces spectres a été effectuée sur une machine IBM 7090. La différence dans les glissements chimiques des protons méthyléniques méso à 60 Mc a été trouvée d'environ 7 cycles/sec. pour le modèle à 3 unités isotactiques, tandis qu'il était de 16 cycles/sec. pour le modèle à 2 unités isotactiques ou le modèle à 3 unités hétérotactiques. Le spectre du chlorure de polyvinyle a été interprété raisonnablement sur la base de ces résultats. Les valeurs observées des constantes de couplage vicinal des substances modèles ont été interprétés comme la moyenne en poids de ceux pour de nombreuses conformations et les conformères stables de ces modèles ont été déterminés.

### Zusammenfassung

Die NMR-Spektren der drei Stereoisomeren von 2,4,6-Trichlorheptan, Modellverbindungen für Poly(vinylchlorid), wurden untersucht. Die Spektren wurden bei 60 und 100 MHz bei Raumtemperatur und höheren Temperaturen gemessen. Ein Spinentkopplungsversuch wurde durchgeführt. Die Spektren wurden mit einem IBM 7090-Computer ausgewertet. Die Unterschiede der chemischen Verschiebung der beiden Mesomethylenprotonen betrug bei 60 MHz für das isotaktische Dreibausteinmodell etwa 7 Hz, während er für das isotaktische Zweibausteinmodell oder für das heterotaktische Dreibausteinmodell 16 Hz betrug. Die Spektren von Poly(vinylchlorid) wurden aufgrund dieser Ergebnisse interpretiert. Die beobachteten Werte für die vicinalen Kopplungskonstanten der Modellverbindungen wurden als gewogenen Mittelwerte der verschiedenen Konformationen interpretiert, und die stabilen Konformationen der Modelle wurden bestimmt.

Received September 3, 1965

Revised October 24, 1965

Prod. No. 4965A

## Electron Paramagnetic Resonance of Ultraviolet-Irradiated Polyolefins\*

H. L. BROWNING, JR., HAZEL D. ACKERMANN, and H. W. PATTON, *Research Laboratories, Tennessee Eastman Company, Division of Eastman Kodak Company, Kingsport, Tennessee*

### Synopsis

If films of polyolefins are ultraviolet-irradiated at liquid nitrogen temperature, alkyl radicals which can be examined by EPR are produced. No EPR spectra are observed from polyolefins irradiated at room temperature in air. Ultraviolet irradiation of polyolefins containing small alkyl side chains generally produces radicals corresponding to the pendant group or methyl radicals if the side chains contain a methyl branch. For some polymers the radical species could not be identified with certainty. Stabilization studies indicate that an optimum concentration of ultraviolet stabilizer is necessary for maximum stabilization of polyolefins. Preliminary results of EPR studies of the ultraviolet irradiation of various polyolefins are given, and some possible radical species are discussed.

### INTRODUCTION

Electron paramagnetic resonance (EPR) has been used extensively to study free radicals in polymers.<sup>1-8</sup> Most of these studies have been concerned with radiation damage produced by ionizing radiation, and relatively little work has been reported on the EPR spectra of polymers exposed to ultraviolet light. Patton and Dilmore<sup>9</sup> have reported EPR studies on ultraviolet-irradiated cellulose esters, and Yoshida and Rånby<sup>10</sup> have reported the presence of methyl radicals in ultraviolet-irradiated polypropylene.

This work is concerned with the EPR spectra of selected polyolefins irradiated with ultraviolet light. For some polymers, the results of ultraviolet photolysis will be contrasted with those of x-irradiation. In addition, some preliminary results on the ultraviolet stabilization of polypropylene will be discussed. Most of the work discussed here is qualitative, but some quantitative work is reported on the ultraviolet stabilization of polypropylene.

### EXPERIMENTAL

#### Apparatus

A Varian Associates V4500 EPR spectrometer equipped with a 100 kc./sec. accessory and a dual cavity was used in this study. Some of the spec-

\* Presented at the 150th National Meeting of the American Chemical Society, Atlantic City, N.J., September 12-17, 1965.

tra were recorded with the Varian precession field scanning unit and others were recorded with the Varian Fieldial. The first-derivative spectra were recorded in the conventional manner. The second-derivative<sup>11</sup> spectra were produced by double modulation at 100 kc./sec. and 200 cps with subsequent phase-sensitive detection at each frequency. The standard Varian liquid nitrogen Dewar vessel was used for measurements at 77°K. Magnetic field measurements were made with the aid of an NMR gaussmeter constructed at the Tennessee Eastman Co. Research Laboratories.

The source of ultraviolet radiation was the Hanovia Sc2537 low-pressure mercury arc for which the output is primarily at a wavelength of 2537 Å.

The x-ray source was the Machlett Laboratories AEG-50 tungsten target tube. The samples were irradiated 15 min. with 50-kvp., 35-ma. x-rays.

### Materials

The polyolefins studied were polyethylene, polypropylene, poly-1-butene, poly-4-methyl-1-pentene, poly-1-dodecene, polystyrene, and poly-1-pentene. These were experimental polyolefins produced at Tennessee Eastman Co. and used in the form of film or injection-molded test specimens. One sample of high-density Tenite polyethylene 3300 with a draft ratio of 6.5 to 1 was used for x-ray investigations. 2,2-Diphenyl-1-picrylhydrazyl was obtained from Eastman Kodak Co. MnO in CaO (1 part MnO/100 parts CaO) was prepared in the Tennessee Eastman Co. Research Laboratories. An aqueous solution of  $Mn(C_2H_3O_2)_2$  and  $Ca(C_2H_3O_2)_2$  was evaporated to dryness and subsequently heated in air at 750°C. for 12 hr.

### Methods

Polyolefin samples, cut into rectangular strips, were placed in 4-mm. o.d. quartz sample tubes. The samples were ultraviolet-irradiated through liquid nitrogen outside the cavity in a quartz Dewar vessel and transferred, still frozen, to the cavity for EPR analysis at 77°K. The duration of irradiation varied from a few minutes to several hours. During the irradiation of some of the polyolefins, a Vycor filter was used to eliminate essentially all the 1849 Å. radiation. Since the spectra of the samples irradiated with and without the filter were identical, the use of the Vycor filter was discontinued.

The samples for x-irradiation were in the form of bundles of strips which had been heat-sealed together. The strips were cut so that the direction of orientation could be aligned with or against the external magnetic field. The samples were x-irradiated in air with one side in contact with Dry Ice and, immediately following irradiation, were stored in liquid nitrogen.

The  $g$  values were measured relative to 2,2-diphenyl-1-picrylhydrazyl.

The first- and second-derivative spectra were recorded on most samples in order to obtain the maximum amount of information about the radical species present.

## RESULTS AND DISCUSSION

## Polyethylene

Ultraviolet-irradiated polyethylene at room temperature in air had no detectable EPR signal. The spectrum of irradiated, unoriented film at 77°K. was a sextet having a  $g$  value of 2.0028 and a spacing of about 30 gauss (Fig. 1). The spectrum was attributed to the  $-\text{CH}_2-\dot{\text{C}}\text{H}-\text{CH}_2-$  radical in which the  $\alpha$ - and  $\beta$ -coupling constants are approximately equal. When the sample was warmed to room temperature, it had no EPR spectrum.

Kashiwabara<sup>6</sup> reported that unoriented polyethylene irradiated with ionizing radiation had a six-line EPR spectrum. Kashiwagi<sup>7</sup> and Salovey and Yager<sup>8</sup> reported that irradiated, oriented polyethylene had a spectrum that depended on the orientation of the molecular axis relative to the external magnetic field. When the magnetic field is parallel to the molecular

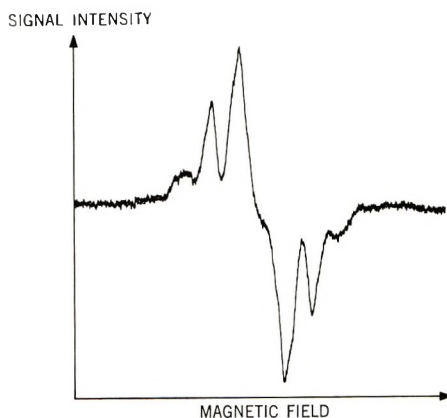


Fig. 1. First-derivative spectrum of ultraviolet-irradiated polyethylene at 77°K.

axis, a sextet with spacings of about 34 gauss is observed, but when the magnetic field is perpendicular to the molecular axis, a ten-line spectrum with spacings of about 14 gauss is produced. They deduced that the alkyl radicals are present primarily in the molecular chains normal to the lamellar surfaces or at least randomly distributed between the "straight portions" and the "folds." We examined a sample of high-density Tenite polyethylene 3300 with a draft ratio of 6.5 to 1 by ultraviolet irradiation at 77°K. and by x-irradiation on Dry Ice. Ultraviolet-irradiated, oriented film had a six-line spectrum with a  $g$  value of 2.0028 and a spacing of about 30 gauss regardless of the orientation in the magnetic field (Fig. 2). In addition to the six-line multiplet, a singlet was observed in the center of the spectrum. The radicals produced decayed slowly at 77°K. and disappeared completely when the sample was warmed to room temperature. The six-line spectrum was attributed to the radical  $-\text{CH}_2-\dot{\text{C}}\text{H}-\text{CH}_2-$  and the singlet was attributed to the peroxy radical formed by diffusion of oxygen into the sample.

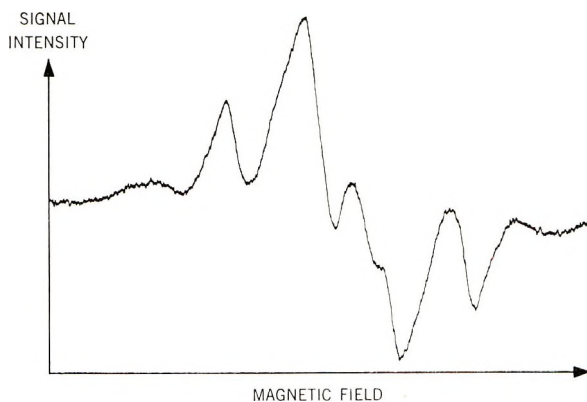


Fig. 2. First-derivative spectrum of ultraviolet-irradiated Tenite polyethylene 3300 at 77°K.

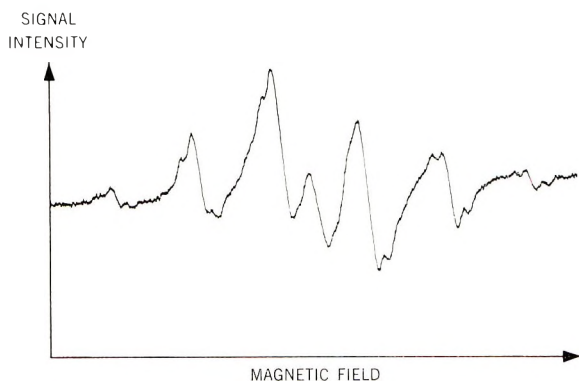


Fig. 3. First-derivative spectrum of x-irradiated Tenite polyethylene 3300 at room temperature aligned parallel to field.

The x-irradiated sample of polyethylene had nearly the same spectrum at room temperature and at liquid nitrogen temperature (Fig. 3), but the room temperature spectrum was more clearly defined. When the sample was aligned with its molecular axis parallel to the external magnetic field, the six-line spectrum was observed (Fig. 3), but when the sample was rotated so that the molecular axis was perpendicular to the external magnetic field, a spectrum of ten lines resulted (Fig. 4). The separations for the lines are approximately 34 gauss for the sextet and approximately 15 gauss for the ten-line spectrum. These results are in good agreement with those of Salovey and Yager.<sup>8</sup>

The lack of preferred orientation of ultraviolet-produced radicals and the ease of decay on warming lead us to suggest the following differences between the effects of x-rays and ultraviolet light. X-rays penetrate the sample essentially uniformly and produce damage randomly. Hence, in a highly crystalline, highly oriented polymer, most radicals will be formed in



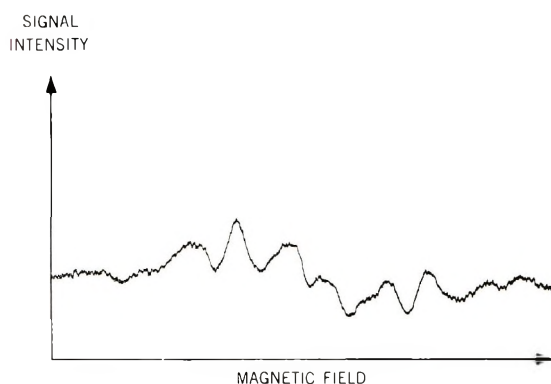


Fig. 4. First-derivative spectrum of x-irradiated Tenite polyethylene 3300 at room temperature aligned perpendicular to field.

well-ordered regions. These radicals will have greatly restricted mobility and good protection from atmospheric components. However, ultraviolet light will tend to be selectively absorbed by impurities and chain imperfections (e.g., olefinic or oxidized segments). Such materials and segments tend to be selectively segregated from the crystallites and are poorly oriented on stretching. These noncrystalline regions or chain folds should be more mobile and more easily penetrated by oxygen.

### Polypropylene

The spectrum of polypropylene consists of a well-resolved four-line multiplet with relative intensities of 1:3:3:1 superimposed over more diffuse components (Figs. 5 and 6). The observed hyperfine splitting of 22.9 gauss and the  $g$  value of 2.0028 agree well with the results of Fessenden and Schuler<sup>12</sup> for methyl radicals in liquid methane and with the results of

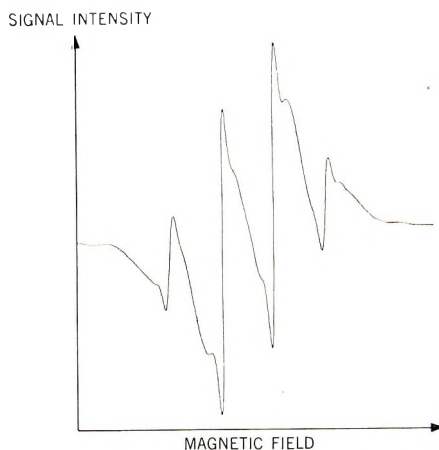


Fig. 5. First-derivative spectrum of ultraviolet-irradiated polypropylene at 77°K.

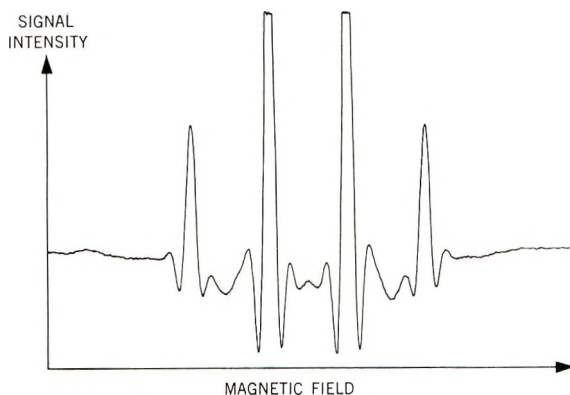
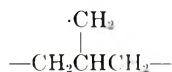


Fig. 6. Second-derivative spectrum of ultraviolet-irradiated polypropylene at 77°K.

Yoshida and Rånby<sup>10</sup> for polypropylene. In the irradiated sample at 77°K., the methyl radicals decay in approximately one week. The remaining radicals have EPR spectra which we believe to be a sextet and a quartet which overlap. The underlying sextet and quartet are broader and more diffuse than the methyl radical quartet. The sextet is attributed to the  $-\text{CH}_2-\dot{\text{C}}\text{H}-\text{CH}_2-$  radical reported by Libby, Ormerod, and Charlesby<sup>5</sup> for polypropylene irradiated with ionizing radiation. The quartet is thought to be due to the radical



which has been reported by Forrestal and Hodgson<sup>3</sup> or to the radical



Since the anisotropic broadening apparently is the same for all four lines, the latter species may be preferable.<sup>13</sup> Both could be present. The decay of the methyl radical spectrum was followed kinetically (Fig. 7). After an initial period of about 1 hr., the decay appeared to follow second-order kinetics.

Several EPR studies on polypropylene irradiated with ionizing radiation have been made but the presence of methyl radicals has not been detected. However, the transient existence of methyl radicals is indicated by the presence of methane in the radiation products.<sup>14</sup> Yoshida and Rånby<sup>10</sup> have observed methyl radicals from ultraviolet irradiation of polypropylene. These workers attributed the difference observed between the spectra of x-irradiated and ultraviolet-irradiated polypropylene to the energy difference between ionizing radiation and ultraviolet radiation. Ionizing radiation imparts excessive energy to the methyl radicals and they are thus lost before the spectrum may be recorded. However, the methyl radicals produced by ultraviolet irradiation receive only slightly more energy than

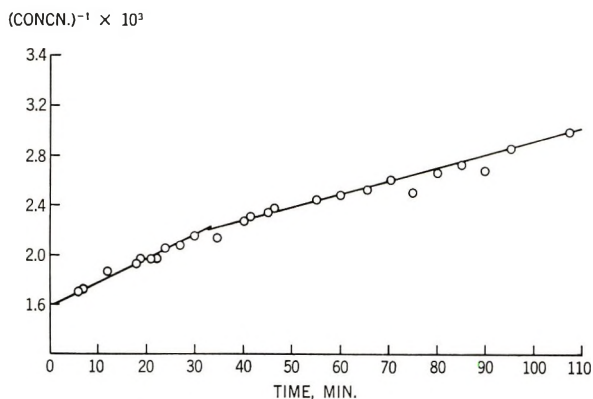


Fig. 7. Decay of methyl radicals of ultraviolet-irradiated polypropylene at 77°K.

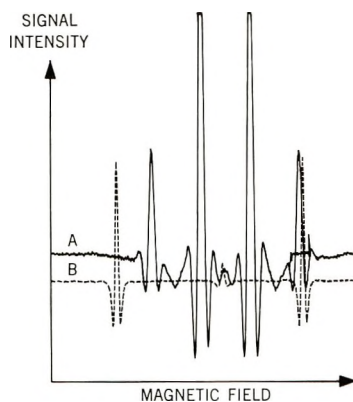


Fig. 8. Second-derivative spectra of (A) ultraviolet-irradiated polypropylene at 77°K.; (B) MnO in CaO at room temperature.

is required to break the bonds. Therefore, the methyl radicals formed by ultraviolet irradiation have longer lifetimes, and their EPR spectrum may be recorded.

The effect of one ultraviolet stabilizer on the methyl radical production in ultraviolet-irradiated polypropylene has been studied. A series of samples containing varying amounts of Santowhite powder [4,4'-butylidenebis(6-*tert*-butyl-*m*-cresol)] was ultraviolet-irradiated at 77°K. The second-derivative spectrum (Fig. 8A) was recorded, and the spectrum of MnO in CaO (Fig. 8B) was superimposed over the methyl radical spectrum. The relative concentrations of methyl radicals were determined by taking the ratio of the peak height of the second component of the methyl radical spectrum to the peak height of the third component of the MnO spectrum. The results indicate that a concentration of 0.1% Santowhite powder (Table I) is the most effective in reducing the formation of methyl radicals by ultraviolet radiation. The proposed mechanism of ultraviolet stabilization is that light is absorbed by the Santowhite powder and disposed of

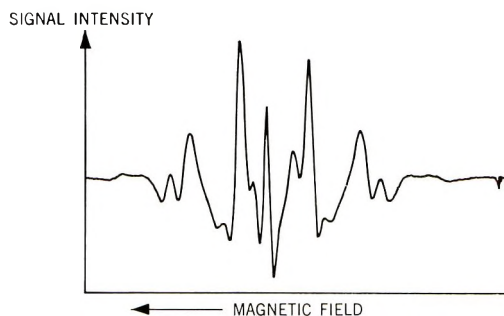


Fig. 9. Second-derivative spectrum of ultraviolet-irradiated poly-1-butene at 77°K.

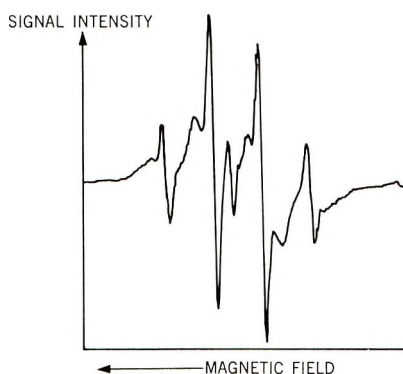


Fig. 10. First-derivative spectrum of ultraviolet-irradiated poly-4-methyl-1-pentene at 77°K.

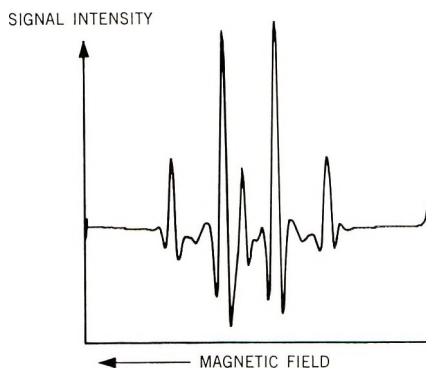


Fig. 11. Second-derivative spectrum of ultraviolet-irradiated poly-4-methyl-1-pentene at 77°K.

as harmless energy either through reemission at longer wavelengths or through vibrational interaction. The low concentrations apparently do not absorb enough of the incident radiation. The high concentrations do absorb the incident light but energy transfer between the stabilizer and the polymer leads to bond cleavage.

TABLE I  
Effect of Santowhite Powder on the Production of Methyl Radicals in Polypropylene

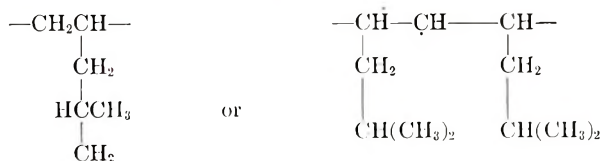
Santowhite powder, %	Relative no. of unpaired spins
3	0.932
1	1.07
0.33	0.573
0.1	0.247
0.033	0.355
0.01	0.807
0	2.83

### Poly-1-butene

Ultraviolet irradiation of poly-1-butene produced an EPR spectrum of twelve lines (Fig. 9). The splitting of approximately 27 G. and the  $g$  value of 2.0026 indicate that this spectrum is due to ethyl radicals. The relative intensities of the lines do not correspond to those reported by Fessenden and Schuler<sup>12</sup> for the ethyl radicals in liquid ethane. However, the underlying spectrum of  $-\text{CH}_2-\dot{\text{C}}\text{H}-\text{CH}_2-$  radicals overlaps the spectrum of the ethyl radicals. Broadening due to anisotropic coupling (not appreciable for the radicals in liquid ethane) also would be expected to influence the relative peak heights for ethyl radicals in a rigid polymer. The central line of the spectrum is due to resonance of the quartz container.

### Poly-4-methyl-1-pentene

The EPR spectrum of ultraviolet-irradiated poly-4-methyl-1-pentene (Figs. 10 and 11) is quite similar to that obtained from polypropylene. A sharp quartet with spacings of 22.5 gauss is superimposed over a broad quartet. The sharp quartet is believed to be due to methyl radicals. The broad quartet could arise from the radicals



or from some combination of both radicals.

### Poly-1-dodecene

The EPR spectrum of ultraviolet-irradiated poly-1-dodecene (Fig. 12) consisted of a six-line pattern similar to that of polyethylene. The spectrum could be due to a radical produced by hydrogen abstraction from the side chain such as  $\sim\text{CH}_2-\dot{\text{C}}\text{H}-\text{CH}_2\sim$  in which the  $\alpha$ - and  $\beta$ -coupling constants are approximately equal. Alternatively, the spectrum could arise from the two radicals produced by cleavage of the side chain. The resulting main chain radical would be similar to the one just postulated.

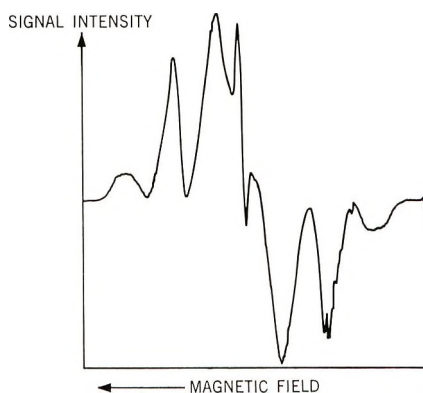


Fig. 12. First-derivative spectrum of ultraviolet-irradiated poly-1-dodecene at 77°K.

The radical from the side chain might be expected to produce a six-line multiplet if the unpaired electron were situated on the terminal carbon.<sup>15</sup>

### Polystyrene

The EPR spectrum of ultraviolet-irradiated polystyrene (Fig. 13) consisted of a single, broad resonance centered about  $g = 2$ . This spectrum could be due to phenyl radicals, but there is no conclusive evidence for or against this speculative assignment.

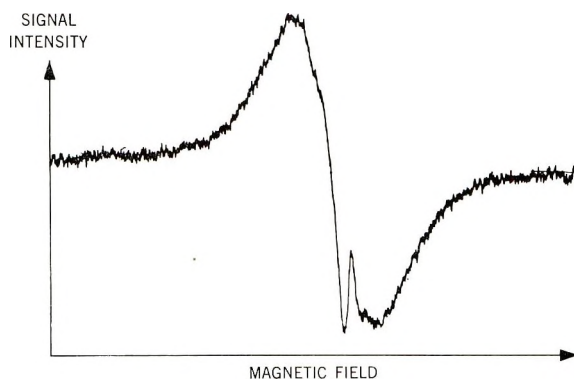


Fig. 13. First-derivative spectrum of ultraviolet-irradiated polystyrene at 77°K.

### Poly-1-pentene

The EPR spectrum of ultraviolet-irradiated poly-1-pentene (Fig. 14), like that of polyethylene, consisted of six asymmetric lines and a single line in the center due to the peroxide radical. It appeared that each line in the sextet was undergoing secondary splitting into two lines; but, because of poor resolution, this could not be verified. The spectrum could arise from the two radicals produced by cleavage of the side chains,  $-\text{CH}_2-\dot{\text{C}}\text{H}-\text{CH}_2-$  and  $\cdot\text{CH}_2\text{CH}_2\text{CH}_3$ . The radicals from the side chains might be expected to produce a six-line multiplet.<sup>15</sup>



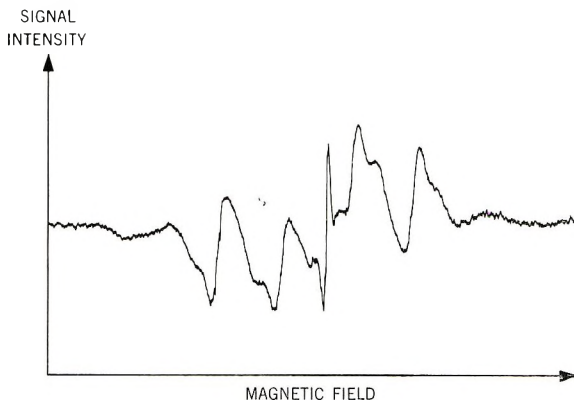


Fig. 14. First-derivative spectrum of ultraviolet-irradiated poly-1-pentene at 77°K.

### CONCLUSION

Ultraviolet irradiation produces free radicals in all the polyolefins studied. These radicals are sufficiently stable at 77°K. for observation of the EPR spectrum but react rapidly at room temperature. The radicals appear to be present only at selected sites in the polymer.

The stabilization studies indicate that the quantity of stabilizer used must be closely controlled for optimum stabilization. For polypropylene the optimum concentration of Santowhite powder is 0.1%.

The presence of methyl radicals in ultraviolet-irradiated polypropylene presents a direct contrast to the x-irradiated polypropylene. It is concluded that the methyl radicals, which are fairly mobile, obtain excessive energy from ionizing radiation and quickly diffuse through the sample and are quenched by interaction with other radicals, by collision with the walls of the container, or by abstracting hydrogen to produce methane. On the other hand, the ultraviolet irradiation imparts only slightly more energy than that required to break the C—C and C—H bonds. Therefore, little excess energy is imparted to the radicals produced by ultraviolet photolysis, and the methyl radicals, while still quite mobile, are not lost to the system.

We are indebted to Dr. R. L. Combs and Dr. Richard L. McConnell for furnishing the samples used in this work and to Mr. C. A. Boye and Mr. J. B. Davis for their aid in the x-irradiation of polypropylene.

### References

1. A. Charlesby and D. K. Thomas, *Proc. Roy. Soc. (London)*, **A269**, 202 (1962).
2. M. Kashiwagi, *J. Polymer Sci. A*, **1**, 189 (1963).
3. L. J. Forrestal and W. G. Hodgson, *J. Polymer Sci. A*, **2**, 1275 (1964).
4. A. Charlesby, D. Libby, and M. G. Ormerod, *Proc. Roy. Soc. (London)*, **A262**, 207 (1961).
5. D. Libby, M. G. Ormerod, and A. Charlesby, *Polymer*, **1**, 212 (1960).
6. H. Kashiwabara, *J. Phys. Soc. Japan*, **16**, 2494 (1961).
7. M. Kashiwagi, *J. Chem. Phys.*, **36**, 575 (1962).
8. R. Salovey and W. A. Yager, *J. Polymer Sci. A*, **2**, 219 (1964).

9. H. W. Patton and H. Dilmore, paper presented at the Southeastern Regional Meeting of the American Chemical Society, Charlotte, N.C., September 14-16, 1963.

10. H. Yoshida and B. Rånby, *J. Polymer Sci. B*, **2**, 1155 (1964).

11. B. Smaller and E. L. Yasatis, *Rev. Sci. Instr.*, **24**, 991 (1953).

12. R. W. Fessenden, and R. H. Schuler, *J. Chem. Phys.*, **39**, 214 (1963).

13. E. L. Cochran, F. J. Adrian, and V. A. Bowers, *J. Chem. Phys.*, **34**, 1161 (1961).

14. M. Dole, *Trans. Am. Nucl. Soc.*, **3**, 356 (1960).

15. P. B. Ayscough, K. J. Ivin, J. M. O'Donnell, and C. Thomson, paper presented at the Fifth International Symposium on Free Radicals, Institute of Physical Chemistry, University of Uppsala, Sweden, July 6-7, 1961.

### Résumé

Lorsque des films de polyoléfine sont irradiés à la lumière ultraviolette, à la température de l'azote liquide, les radicaux alkyles qui sont produits, peuvent être examinés par EPR. On n'observe pas de spectres EPR pour des polyoléfines irradiées à température ordinaire dans l'air. L'irradiation ultraviolette des polyoléfines contenant des chaînes latérales petites produisent généralement des radicaux correspondants au groupe latéral ou au groupe méthyle si les chaînes latérales contiennent une ramification méthylée. Pour certains polymères la nature des radicaux n'a pas pu être identifiée avec certitude. Des études de stabilisation indiquent qu'une concentration optimum de stabilisant ultraviolet est indispensable pour assurer une stabilisation maximum de polyoléfines. Des résultats préliminaires des études EPR de l'irradiation sous lumière ultraviolette de diverses polyoléfines sont indiqués et on soumet à discussion certaines espèces possibles de radicaux formés.

### Zusammenfassung

Bei der UV-Bestrahlung von Polyolefinfilmen bei der Temperatur des flüssigen Stickstoffs werden Radikale gebildet, welche mittels EPR untersucht werden können. Keine EPR-Spektren werden bei der Bestrahlung von Polyolefinen bei Raumtemperatur unter Luft beobachtet. Die UV-Bestrahlung von Polyolefinen mit kleiner Alkylseitenkette erzeugt im allgemeinen Radikale, welche der Seitengruppe entsprechen oder Methylradikale, wenn die Seitenkette eine Methylverzweigung enthält. Bei einigen Polymeren konnte die Radikalspezies nicht mit Sicherheit identifiziert werden. Stabilisierungsuntersuchungen zeigen, dass für eine maximale Stabilisierung von Polyolefinen eine optimale Konzentration eines UV-Stabilisators notwendig ist. Vorläufige Ergebnisse von EPR-Untersuchungen der UV-Bestrahlung verschiedener Polyolefine werden mitgeteilt und einige mögliche Radikalspezies diskutiert.

Received August 4, 1965

Revised October 22, 1965

Prod. No. 4967A

# Polymerization of Aromatic Nuclei. X.

## Polymerization of Benzene to *p*-Polyphenyl Oligomers by Nitrogen Dioxide–Aluminum Chloride

PETER KOVACIC and ROGER J. HOPPER, *Department of Chemistry, Case Institute of Technology, Cleveland, Ohio*

### Synopsis

Benzene was polymerized to *p*-polyphenyl oligomers by nitrogen dioxide–aluminum chloride. Polymer production was favored by  $\text{AlCl}_3:\text{NO}_2$  ratios of at least 2, long reaction times, and higher temperatures. Evidence for the polymer structure was obtained from elemental analyses, oxidative degradation, solubility, molecular weight, functional group tests, low molecular weight products, and infrared and ultraviolet spectra. The chains contained small amounts of chloro, amino, hydroxyl, and carboxyl substituents. Molecular weight data on the benzene-soluble portion (40–71%) revealed an average of 4–6 phenylene units per chain. Under altered conditions nitrobenzene could be obtained as the major product, indicating the sensitivity of the system to changes in reaction variables. With nitrobenzene as oxidant, a similar type of polymer resulted. The theoretical aspects are discussed.

### INTRODUCTION

Prior to recent disclosures from this laboratory, there were few reports dealing with the self-coupling of benzene in the presence of a Lewis acid and oxidant. Of pertinence is the conversion of benzene to biphenyl in low yield on exposure to aluminum chloride.<sup>1</sup> By-products included alkylbenzenes, naphthalene, phenols, and tar.<sup>1–5</sup> On treatment of benzene with nitrobenzene and aluminum chloride, Freund<sup>6</sup> obtained a low yield of *p*-aminobiphenyl together with uncharacterized resin. Schaarschmidt<sup>7</sup> observed the formation of brown resin in the system, benzene–aluminum chloride–nitrogen dioxide, the major product being nitrobenzene.

Several years ago a new polymerization method was disclosed involving use of the aromatic nucleus as the monomer for conversion to homopolymer.<sup>8,9</sup> For example, benzene was smoothly coupled in high yield to *p*-polyphenyl in Lewis acid catalyst–oxidant systems. Aluminum chloride, aluminum bromide, or antimony pentachloride was an effective catalyst<sup>8,9</sup> with cupric chloride, cupric bromide, manganese dioxide, lead dioxide, benzoquinones, or nitrogen oxides as oxidant.<sup>8,9</sup> Ferric chloride<sup>10,11</sup> and molybdenum pentachloride<sup>12</sup> can apparently assume the dual role of catalyst and oxidant.

This transformation is analogous to the Scholl reaction,<sup>13,14</sup> except that in our case the coupling can continue far beyond the dimer stage. Similar

reaction schemes entailing an oxidative cationic mechanism have been proposed for these two cases.<sup>8,13,14</sup> Moreover, evidence for Brønsted acid cocatalysis has been noted in benzene polymerization effected by ferric chloride.<sup>11</sup> By analogy, certain Scholl reactions are inhibited by removal of hydrogen chloride, and conversely, promoted by its addition.<sup>14,15</sup>

The nature of the aromatic monomer is an important factor governing the degree of polymerization in Lewis acid catalyst-oxidant systems. Whereas benzene provided relatively high molecular weight material, oligomers were formed from biphenyl,<sup>16</sup> *p*-terphenyl,<sup>16</sup> mesitylene,<sup>17</sup> *m*- and *p*-xylene,<sup>18,19</sup> and naphthalene.<sup>20</sup>

Molecular weight control in benzene polymerization can be effected by variation in monomer concentration, temperature, and solvent.<sup>21</sup> Of the various solvents studied (chloroaromatics, stannic chloride, titanium tetrachloride, and carbon disulfide), *o*-dichlorobenzene proved to be particularly effective.<sup>21</sup> Kovacic and Oziomek noted evidence for chain termination in benzene-aluminum chloride systems when nitrogen dioxide and dinitrogen trioxide were used as oxidants.<sup>9</sup>

This paper presents a more detailed investigation of benzene polymerization with nitrogen dioxide-aluminum chloride. We were particularly interested in the detailed structure of the product, degree of polymerization, and nature of the termination reaction.

## RESULTS AND DISCUSSION

### Reaction Variables

Several reaction variables ( $\text{AlCl}_3:\text{NO}_2$  ratio, temperature, and time) were investigated relative to their effect on the reaction course, including yield and nature of the polymer. It became apparent that the system was quite sensitive to changes in conditions. On the one hand, the reaction yielded polymer almost exclusively, whereas under other circumstances nitrobenzene was the predominant product.

**$\text{AlCl}_3:\text{NO}_2$  Ratio.** The effect of variation in the  $\text{AlCl}_3:\text{NO}_2$  ratio at 25–35°C. is summarized in Table I. It is evident that large amounts of catalyst are necessary for the production of polymer in good yields. This requirement presumably arises from the presence of substances which can deactivate or destroy the aluminum chloride. Various possibilities come to mind in this connection: (1) complexing with nitrogen dioxide,<sup>7,22</sup> (2) reaction with nitrogen dioxide to form aluminum oxide<sup>23</sup> and aluminum nitrate,<sup>24</sup> (3) complexing with substances which might be produced during the reaction, e.g., nitrosyl chloride, nitryl chloride, other nitrogen oxides, and nitrogen-containing acids, (4) hydrolysis by water which might plausibly be generated *in situ*. A high catalyst requirement was previously observed in the benzene-aluminum chloride-cupric chloride system, apparently due to aluminum chloride deactivation during the reaction course.<sup>9</sup>

Although the yield of nitrobenzene was low in all cases, increased amounts were observed at the lower ratios of  $\text{AlCl}_3:\text{NO}_2$ .

TABLE I  
Effect on Polymer Yield and Properties of Variation of  $\text{AlCl}_3:\text{NO}_2$  Ratio<sup>a</sup>

		Crude		Polymer					Caustic-insoluble fraction					C
$\text{AlCl}_3:\text{NO}_2$ mole	Nitro- benzene, yield, mole	Yield, g.	Color	$R^b$	Sol. in Sol. in caus- tic, %	ben- zene, %	Mol. wt. <sup>c</sup>	C, %	H, %	N, %	Cl, %	O, %	[H + (NH <sub>2</sub> ) + Cl + OH] atomic ratio	
0.15:0.15	0.01	4.8	Dk. red-brown	0.43	6.5	60	556	75.27	4.14	2.79	9.63	8.17 <sup>d</sup>	1.50	
0.30:0.15	<0.01	17	Red-brown	0.51	2.7	40	461	83.64	4.90	1.89	2.67	4.59	1.45	
0.60:0.15	Trace <sup>e</sup>	19	Med. brown	0.64	5.5	42	465	83.49	4.77	1.76	2.74	5.05	1.48	

<sup>a</sup> Temp., 25–35°C.;  $\text{NO}_2$  addition time, 5–6 hr.; total reaction time, 18–21 hr.;  $\text{C}_6\text{H}_6:\text{NO}_2 = 10:1$  (molar).

<sup>b</sup> See Experimental Section.

<sup>c</sup> Benzene-soluble fraction.

<sup>d</sup> By difference.

<sup>e</sup> Detectable by gas chromatography.

TABLE II  
Effect of Temperature on Polymer Yield and Properties<sup>a</sup>

Temp., °C.	Nitro- benzene yield, mole	Crude				Polymer						
		Yield, g.	Color	$\eta^b$	Sol. in caustic, benzene, %	Sol. in benzene, %	Caustic-insoluble fraction					C [H + (NH <sub>2</sub> ) + Cl + (OH)] atomic ratio
							Elemental analysis					
						C, %	H, %	N, %	Cl, %	O, %		
27-34	0.04	9.4	Lt. brown	0.51	4.6	66	78.63	4.57	0.80	7.62	5.04	1.39
Reflux	0.005	15	Dk. brown	0.33	4.3	52	86.09	5.04	1.45	2.29	3.01	1.45

<sup>a</sup> AlCl<sub>3</sub>, 0.30 mole; NO<sub>2</sub>, 0.15 mole; NO<sub>2</sub> addition time, 2 hr.; total reaction time, 3 hr.; C<sub>6</sub>H<sub>6</sub>:NO<sub>2</sub> = 10:1 (molar).

<sup>b</sup> See Experimental Section

<sup>c</sup> Benzene-soluble fraction.



TABLE III  
Effect on Polymer Yield and Properties of Variation in Reaction Time<sup>a</sup>

Time, hr.		Nitro- benzene, yield, mole	Yield, g.	Crude		Sol. in Sol. in caustic, ben- zene, %	Mol. wt. <sup>c</sup>	Elemental analysis					C [H + (NH <sub>2</sub> ) + Cl + (OH)] atomic ratio	
NO <sub>2</sub> add'n.	Total			Color	R <sup>b</sup>			C, %	H, %	N, %	Cl, %	O, %		
0.25 <sup>d</sup>	11-12	0.01	8.8	Dk. red-brown	0.32	18.1	43	453	79.33	4.87	3.34	2.92	7.03	1.41
2	3	0.04	9.4	Lt. brown	0.51	4.6	66	500	78.63	4.57	0.80	7.62	5.04	1.39
6	20-21	<0.01	17	Med. brown	0.51	2.7	40	461	83.64	4.90	1.89	2.67	4.59	1.45
22	22	Trace <sup>e</sup>	14	Med. brown	0.64	5.1	43	479	81.77	4.92	2.10	2.66	8.55 <sup>f</sup>	1.42

<sup>a</sup> Temperature, 25-35°C.; AlCl<sub>3</sub>, 0.30 mole; NO<sub>2</sub>, 0.15 mole; C<sub>6</sub>H<sub>6</sub>:NO<sub>2</sub> = 10:1 (molar).

<sup>b</sup> See Experimental Section.

<sup>c</sup> Benzene-soluble fraction.

<sup>d</sup> NO<sub>2</sub> introduced at 15-20°C.

<sup>e</sup> Detectable by gas chromatography.

<sup>f</sup> By difference.

**Temperature.** There was an appreciable increase in polymer yield when the reaction was carried out at reflux as compared with room temperature (Table II). The production of nitrobenzene bore an inverse relationship to that of polymer.

The procedure could be easily altered so that nitration constituted the major pathway. When the components were mixed at low temperatures (5–15°C.), nitrobenzene was obtained in high yield accompanied by minor amounts of polymer. This technique simulates the nitration methods of Schaarschmidt<sup>7,25</sup> and Titov.<sup>22,25</sup> Nitration of aromatic nuclei also has been accomplished with boron trifluoride complexes of nitrogen dioxide.<sup>25</sup>

**Time.** The influence of alteration in reaction time was determined at 25–35°C. with AlCl<sub>3</sub>:NO<sub>2</sub> ratios of 1 and 2 (Table III). The production of polymer versus nitrobenzene was dependent on both the oxidant addition time and the total reaction time. In general, an extension of these times resulted in higher yields of polymer at the expense of nitrobenzene.

### Polymer Structure

The evidence indicates that the coupled product is a relatively low molecular weight *p*-polyphenyl containing minor amounts of various substituents. Let us first deal with the nature of the substituents present. Elemental analyses (Tables I–III) revealed that the polymer contained, in addition to carbon and hydrogen, small amounts of chlorine (2.3–9.6%), nitrogen (0.8–3.4%), and oxygen (3–7%).

At least some of the nitrogen was present in the form of amino groups, since diazotization, followed by reaction with  $\beta$ -naphthol, imparted a red color to the product. The infrared spectra of the polymers exhibit absorption bands characteristic of amino groups. The basic components possessed low solubility in aqueous acid, as evidenced by extraction of only trace amounts. Analogy can be drawn with the formation of amino-substituted products from Scholl couplings in the presence of nitrobenzene.<sup>6,13,14</sup>

Data are available which shed light on the nature of the oxygen-containing groups. The caustic-soluble portion, a small fraction of the total, gave a positive ferric chloride test and absorption maxima in the infrared region which are characteristic of phenolic compounds. In addition, this extract dissolved to a slight extent (7%) in sodium bicarbonate. Infrared analysis of the soluble material revealed bands attributable to a carboxyl functionality.

Additional clues are provided by the nature of the nonpolymeric products. In addition to nitrobenzene, traces of chlorobenzene, biphenyl, *p*-chlorobiphenyl and *p*-phenylphenol were found in the reaction product. The presence of these substituents, particularly in the dimer fraction, suggests that the same moieties might well be contained in the higher molecular weight material.

Designation of the polymer as a *p*-polyphenyl was based partly on oxidative degradation, and the infrared and ultraviolet spectra. Oxidation with

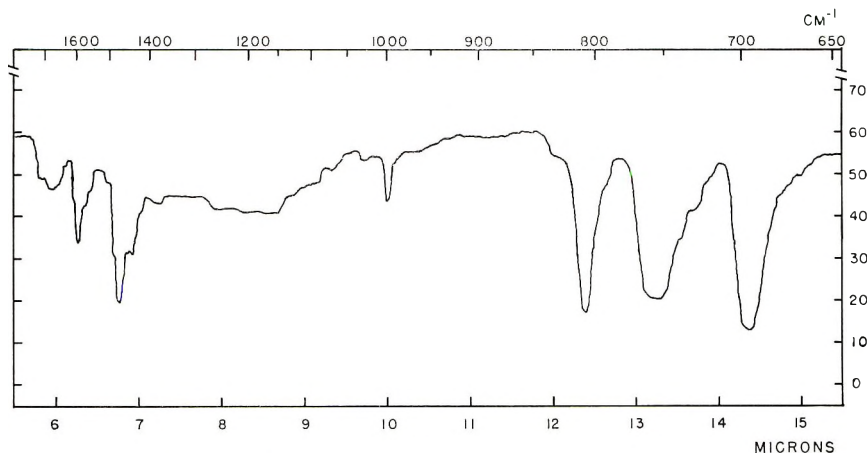


Fig. 1. Infrared spectrum of polymer (entry 2, Table I).

chromic acid yielded a gross mixture of acids from which the low molecular weight components were isolated as the methyl esters. The formation of biphenyl-4,4'-dicarboxylic acid and isomerically pure terephthalic acid indicates that the polymer possesses essentially an all-*para* configuration. This observation is in complete accord with previous findings concerning the nature of polyphenyl prepared in a variety of catalyst-oxidant systems.<sup>8,10,12,21</sup> Benzoic and *p*-chlorobenzoic acids, also observed in previous related studies,<sup>12,21</sup> were derived from endgroup structures.

Infrared investigation revealed a spectrum, typical of a *p*-polyphenyl,<sup>8,10</sup> which exhibited absorption frequencies characteristic of *para* substituents and of mono substitution (770-740 and 705-690  $\text{cm}^{-1}$ ). The ultraviolet reflectance spectrum was in agreement with those previously observed<sup>21</sup> for this type of polymer.

Various means were used to approach the question of molecular weight: solubility, vapor pressure osmometry, and the infrared and ultraviolet spectra. The solubility of *p*-polyphenyls generally decreases with an increasing number of *p*-phenylene units. An important limitation is the rapid decline of solubility in the series. Since the polymers from this investigation possessed rather low molecular weights, the solubility technique proved quite useful. Solubility in benzene at room temperature varied in the range 40-71% (Tables I-III). In general, solubility increased with an increase in chlorine content. This is not surprising since substitution in *p*-polyphenyls is known to favor this property.<sup>21</sup>

Molecular weights of the benzene-soluble fractions were determined by vapor pressure osmometry. The values obtained (450-550) correspond to an average of about four to six rings per chain. Of course, the unfractionated polymer represents a somewhat higher degree of polymerization, since a significant portion comprises insoluble, higher molecular weight material.

Information from the infrared spectra also proved useful for estimation of the degree of polymerization. Infrared spectra of *p*-polyphenyls con-

tain three typical bands in the 1000–650  $\text{cm}^{-1}$  region. The maximum between 840 and 800  $\text{cm}^{-1}$  is characteristic of *para* substitution. Two monosubstitution absorption frequencies at 770–730 and 710–690  $\text{cm}^{-1}$  arise from terminal phenyl units. Two trends have been noted among the lower members as the series is ascended: (1) the *para* band shifts to lower wave numbers:<sup>8,9,23</sup> *p*-terphenyl, 837  $\text{cm}^{-1}$ ; *p*-quaterphenyl, 825  $\text{cm}^{-1}$ ; *p*-quinquephenyl, 818  $\text{cm}^{-1}$ ; *p*-sexiphenyl, 812  $\text{cm}^{-1}$ ; (2) the intensity of the *para* band increases relative to that of the mono bands.<sup>9,21</sup> Since the magnitude of the *para*-band shift decreases sharply with increasing molecular weight, this approach is limited to the lower homologs or to those polymers which differ drastically in molecular weight. The polymers prepared in the presence of nitrogen dioxide exhibited *para*-band positions at 810–806  $\text{cm}^{-1}$  (Fig. 1). Since this band often possessed a rounded shape, it perhaps would be more informative to designate the limits of the tip spread, 812–803  $\text{cm}^{-1}$ . These data are in accord with other lines of evidence concerning molecular weight. Analysis of two fractionated polymers by this method revealed a slight shift to lower frequencies for the benzene-soluble portions. The *para*-band positions for the benzene-insoluble fractions, unfractionated polymers, and benzene-soluble fractions, respectively were: 812–804, 810–805, 814–806  $\text{cm}^{-1}$  (entry 1, Table II) and 809–805, 809–805, 825–815  $\text{cm}^{-1}$  (entry 2, Table II). For the sake of comparison, the spectrum of relatively high molecular weight *p*-polyphenyl from the benzene–aluminum chloride–cupric chloride system has a sharp *para* band at 801–803  $\text{cm}^{-1}$ .<sup>9,21</sup> It should be pointed out that certain *para* substituents, in contrast to the phenyl group, produce *para* bands at lower wave numbers. For example, compare *p*-terphenyl (837  $\text{cm}^{-1}$ ) to a variety of other *p*-substituted ( $\text{CH}_3$ , Cl, and OH) biphenyls, which absorb at about 820–826  $\text{cm}^{-1}$ .<sup>27</sup>

The applicability of the band-intensity method was then investigated. This technique constitutes a type of endgroup analysis. However, there are several potential interferences which should be recognized. Since substituents are known to be present, their location along the backbone and on the terminal phenyl groups would be expected to alter the spectral pattern. Nevertheless, the findings demonstrated that this approach possessed some validity as applied to our products. The ratio (*R* value) of the band intensities was calculated from  $\text{intensity}_{para} : (\text{intensity}_{mono_1} + \text{intensity}_{mono_2})$ . In general, the *R* values remained fairly constant (0.33–0.64) for the various preparations (Tables I, II and III). These figures are in rather good agreement with the corresponding ratios for *p*-quaterphenyl (0.51),<sup>28</sup> *p*-quinquephenyl (0.67),<sup>28</sup> and *p*-sexiphenyl (0.82).<sup>29</sup> In addition, investigation of fractionated polymers revealed a decrease in *R* values in the order: benzene-insoluble fraction > unfractionated polymer > soluble fraction (Fig. 2). Apparently, the small number of substituents present do not give rise to a prohibitive interference. A similar result was previously observed in certain cases in a study of molecular weight control by solvents in benzene polymerization.<sup>21</sup>

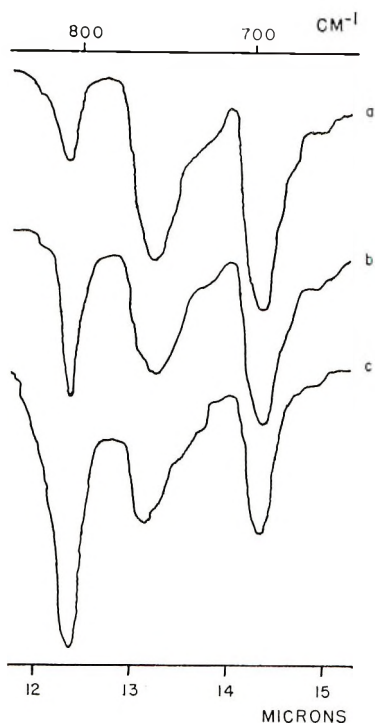


Fig. 2. Infrared spectra of fractionated polymer (entry 1, Table II, crude product): (a) benzene-soluble fraction; (b) reaction product; (c) benzene-insoluble fraction.

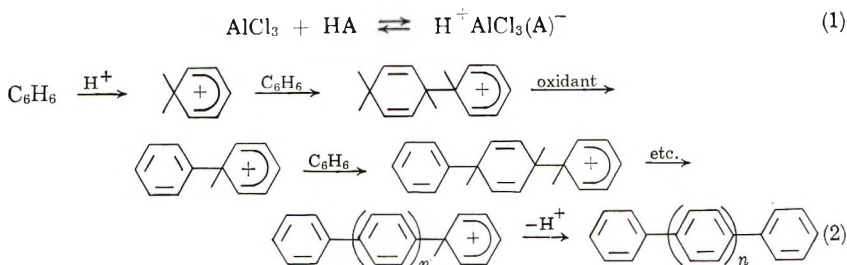
A brief investigation was made of the approach involving ultraviolet analysis. In this spectral region of *p*-polyphenyls,  $\lambda_{\max}$  shifts in decreasing increments to longer wavelengths as the chain length increases. Because of polymer insolubility the spectra were obtained by the reflectance technique. The pertinent  $\lambda_{\max}$  values for various *p*-polyphenyls are indicated: *p*-sexiphenyl,<sup>21</sup> 321  $m\mu$ ; our product (entry 1, Table II), 340  $m\mu$ ; *p*-polyphenyl from cupric chloride-aluminum chloride, 386  $m\mu$ .<sup>21</sup> The observed order is consistent with the other evidence dealing with molecular weight. Some unanswered questions relating to the ultraviolet reflectance method as applied to *p*-polyphenyls are treated elsewhere.<sup>21</sup>

Theoretically, the C/H atomic ratios derived from elemental analyses can provide information concerning molecular weight. The calculated values range from 1.285 for *p*-terphenyl to a limiting value of 1.5 for an infinitely long chain. Unfortunately, with an increasing number of phenylene units, the change in ratio rapidly diminishes to less than the experimental error. For example, a polyphenyl of quite low molecular weight ( $n = 20$ ) possesses a C/H value, 1.46, which is experimentally indistinguishable from the limiting value. In our case, the experimentally determined value takes into account the presence of nuclear substituents (chloro, hydroxyl, and amino groups). The values for the adjusted ratios varied from 1.39 to 1.50 (Tables I-III).



### Nature of the Polymerization

The oxidative cationic mechanism which has been proposed<sup>8</sup> for benzene polymerization in Lewis acid catalyst-oxidant systems is illustrated in eqs. (1) and (2).



Let us consider the nature of the dehydrogenation step in the present case. A brief summary calling attention to certain properties of the oxidant is appropriate to the discussion. Nitrogen dioxide exists in equilibrium with its dimer, with displacement to the monomer form at higher temperatures.<sup>25</sup> The property of paramagnetism is exhibited by the monomer, whereas dinitrogen tetroxide is diamagnetic.<sup>25</sup> Nitrogen dioxide has been shown to oxidize dihydroaromatic structures, presumably by a free-radical mechanism.<sup>30</sup> Its role during polymerization, however, is evidently more complex. The yield data obtained under various conditions suggest that polymer may have been formed at the expense of nitrobenzene. Specifically, nitrobenzene might serve as an oxidant as has been observed for the Scholl reaction.<sup>14,31</sup> To test this hypothesis, an equimolar amount of nitrobenzene (Table IV) was used in place of nitrogen dioxide. The resulting polymer possessed properties quite similar to those of the corresponding products from analogous nitrogen dioxide reactions. However only about half the amount of polymer was formed when nitrobenzene was used. Hence, in the nitrogen dioxide reactions dehydrogenation cannot be due entirely to nitrobenzene formed *in situ*. It should be mentioned that no relatively high molecular weight *p*-polyphenyl was obtained in earlier scouting work with nitrobenzene as oxidant.<sup>9</sup> Since exhaustive solvent extraction was employed in the prior study, any oligomers present would presumably be removed during work-up.

The evidence for phenyl, *p*-chlorophenyl, and *p*-hydroxyphenyl endgroups aids in elucidation of the termination reaction. An unsubstituted phenyl structure might arise by loss of a proton from the propagating chain. Alternatively, according to our working hypothesis, this same structure is formed in the initiation-dehydrogenation step. Another possible termination route entails interaction with chloride, followed by dehydrogenation. The *p*-chlorophenyl endgroup might be generated to some extent in this manner. One should also consider chain stoppage via attack on some species containing nitrogen and oxygen, e.g., nitrogen oxides or a nitrogen-containing acid. This could lead to nitro or nitrite groups. Analogy may be found in the conversion of an alkyl halide to a nitroalkane and alkyl nitrite by reaction with a nitrite salt.<sup>32</sup> Since the polymerization product



TABLE IV  
 Polymerization with Nitrobenzene as Oxidant<sup>a</sup>

Time, hr.		Crude				Sol. in caustic, benzene, %				Elemental analysis				C [H + (NH <sub>2</sub> ) + Cl + OH] atomic ratio
NO <sub>2</sub> add'n	Total	Yield, g.	Color	R <sup>b</sup>	caustic, %	benzene, %	Mol. wt. <sup>c</sup>	C, %	H, %	N, %	Cl, %	O, %		
8	20	8.9	Yellow brown	0.61	1.6	64	469	85.76	5.63	2.08	1.71	3.65	1.31	
6	20	9.0	Yellow brown	—	0.5	71	481	85.87	5.53	3.95	1.94	2.80	1.35	

<sup>a</sup> Temp., 20–30°C.; AlCl<sub>3</sub>, 0.30 mole; C<sub>6</sub>H<sub>5</sub>NO<sub>2</sub>, 0.15 mole; C<sub>6</sub>H<sub>6</sub>:C<sub>6</sub>H<sub>5</sub>NO<sub>2</sub> = 10:1 (molar).

<sup>b</sup> See Experimental Section.

<sup>c</sup> Benzene-soluble fraction.

is subjected to hydrolytic conditions, nitrite would be expected to act as a precursor of *p*-hydroxyl groups. Termination by the nitrite route is not likely in the nitrobenzene system. Here, most of the nitrogen should be present as amino groups. The fact that the nitrogen content relative to oxygen is significantly larger for the benzene–nitrobenzene–aluminum chloride product may, in part, be due to these different modes of termination. The literature<sup>33</sup> contains evidence for retardation by nitro bodies in the cationic polymerization of olefins, presumably due to complexing with the catalyst or growing carbonium ion. Although a careful search was made, no evidence (e.g., in the form of *p*-nitrobenzoic acid or nitroterephthalic acid) for the presence of nitro groups could be detected in the oxidation studies. Reduction of nitro to amino could result from participation in dehydrogenation in a manner similar to the involvement of nitrobenzene in the Scholl reaction.<sup>13,14</sup> Another possible route for introduction of the amino functionality involves nitration of the polymer by nitrogen dioxide followed by reduction via dehydrogenation. It should be noted that the precise location of amino groups in the polymer is not known.

Terminal groups in the product may also arise from attack of the growing carbonium ion on a benzene nucleus bearing a substituent, e.g., hydroxyl, amino, or chloro. In a previous study, chloroaromatics in solvent quantities were effective terminating agents in benzene polymerization.<sup>21</sup> There was some incorporation of the diluent as an endgroup, although to only a minor extent.<sup>21</sup> In our case chlorobenzene would be present in appreciably lower concentration. Participation of aromatic diluents in termination during olefin polymerization has been observed by various investigators.<sup>34</sup>

Direct halogenation of the polymer is deemed a likely occurrence. Nuclear chlorination has been commonly observed in nitrations with aluminum chloride–nitrogen dioxide,<sup>7,23</sup> evidently due to the *in situ* formation of molecular chlorine. Nitryl chloride, known to arise in systems of this type, is relatively unstable and decomposes to nitrogen dioxide and chlorine.<sup>23</sup> Hydrogen chloride which is generated during the polymerization can be oxidized to chlorine and nitrosyl chloride by nitrogen dioxide.<sup>35</sup>

The fact that both nitrogen dioxide and nitrobenzene gave quite similar polymers suggests that the two reaction pathways bear close resemblance. Since the systems are so exceedingly complex, many unanswered questions remain concerning the interactions which are occurring.

Finally, attention should be drawn to the similarities between this polymerization mechanism and the hypotheses advanced for  $\sigma$ -substitution<sup>36,37</sup> and nucleophilic  $\sigma$ -substitution.<sup>38</sup> Hence,  $\sigma$ -polymerization would constitute a simple, meaningful description for the oxidative cationic pathway involving the aromatic nucleus.

## EXPERIMENTAL

### Materials

Benzene, reagent, A.C.S., thiophene-free (Matheson, Coleman and Bell), nitrobenzene, reagent (Matheson, Coleman and Bell), aluminum chloride,

anhydrous, (Fisher Scientific Co. or Baker and Adamson), and nitrogen dioxide (Matheson Co.) were used.

### Analytical Methods

Infrared spectra of low molecular weight materials and oxidation products were taken in cavity cells (carbon disulfide solvent) on a Beckman IR-5 spectrometer. Spectra of polymers, 0.25% in potassium bromide, were obtained on a Beckman IR-8 spectrometer calibrated with polystyrene film. A programmed slit width was used. Gas chromatographic analyses were carried out with an Aerograph A-90-P.

A Beckman DK-2 spectrometer with reflectance attachment was used for the ultraviolet spectra. The samples, from 10 mg. of polymer in 1.0 g. of magnesium oxide, were mixed (usually more than four times) in a Wig-L-Bug amalgamator equipped with a stainless steel capsule, then pressed into a 1-in. disk at 1500–2000 psi for several minutes.

Molecular weight data were obtained, with a Mechrolab 301A vapor pressure osmometer (benzene as solvent at 37°C.). Biphenyl was used for calibration.

### Polymerization of Benzene by Nitrogen Dioxide–Aluminum Chloride

**General Procedure.** Benzene (distilled over sodium) and aluminum chloride were mixed under a dry nitrogen atmosphere in a 250-ml. three-necked flask equipped with a paddle stirrer. Nitrogen dioxide was introduced into the reaction mixture by means of a carrier stream of dry nitrogen. The amount of nitrogen dioxide was initially measured by condensing the gas into a calibrated receiver at 0°C. Variation in addition time was accomplished by controlling the rate of vaporization into the carrier stream.

The mixture in the flask turned dark red upon exposure to nitrogen dioxide. The amount of heat evolved depended upon the rate of introduction. Acidic vapor (hydrogen chloride and nitrogen oxides) was given off during the reaction. After the reaction had proceeded for the desired time, the mixture was stirred with ice–hydrochloric acid and distilled to remove the benzene–water azeotrope. Following exhaustive steam distillation, the steam-distillable organic material was extracted with ether and dried over sodium sulfate. Any nitrobenzene present was distilled under nitrogen at reduced pressure. The crude solid residue from steam distillation was pulverized in a Waring Blendor, triturated with hot 30% hydrochloric acid until the filtrate was colorless, pulverized again, washed with hot deionized water until chloride ion was removed, and then dried. During work-up, care was taken to avoid contamination of the polymer.

Polymers for which elemental composition, benzene solubility, and molecular weight were determined were subjected to a more extensive purification procedure. The polymer was triturated with boiling 30% hydrochloric acid, water, and 30% sodium hydroxide respectively, with blending between steps. The entire sequence was repeated, and the product was washed and blended with hot deionized water until the filtrate was neutral

and free of chloride ion. Drying was accomplished either in air below 100°C. or over phosphorus pentoxide at 75°C. under vacuum.

**Polymer Fractionation by Caustic and Bicarbonate.** The basic extract (see preceding section) was acidified and extracted with ether to recover the caustic-soluble organic material. A sample of this fraction (from entry 5, Table III) was analyzed by gas chromatography (6-ft. column, 20% SF-96 on acid-washed Chromosorb P; 220°C.; 86 ml. He/min.), and the single component (R.T. 10.1 min.) was collected. The infrared spectrum of this material exhibited bands at 1310 and 1185  $\text{cm}^{-1}$ , characteristic of phenolic compounds<sup>39a</sup> (the OH stretching region was not well defined), and a positive ferric chloride test was obtained. The base-soluble extract (0.14 g.) was dissolved in 8 ml. of benzene and extracted with 4 ml. of 5% sodium bicarbonate solution. The aqueous layer was separated, acidified with dilute hydrochloric acid and extracted with ether. The ether layer was separated, dried, and evaporated, leaving a yellow, viscous liquid (0.01 g.), whose infrared spectrum indicated the presence of a carboxylic acid group (broad band at 3200–2850  $\text{cm}^{-1}$ , strong bands at 1700 and 1260  $\text{cm}^{-1}$ ).<sup>39b</sup>

### Low Molecular Weight Products

The steam-distillable material from the polymerization was analyzed by gas chromatography either before or after distillation of nitrobenzene, (5-ft. column, 20% SF-96 on firebrick; 60 ml. He/min.). A manual temperature program was generally used in the range of 100–240°C. during 1 hr. The components were trapped and identified by comparison of their melting points (solid products), infrared spectra, and gas-liquid chromatography (GLC) retention times with those of authentic samples (Table V).

### Nitration of Benzene with Nitrogen Dioxide-Aluminum Chloride

A solution of nitrogen dioxide (0.183 mole) in benzene (22 ml.) was added with stirring during 2 hr. at 10–15°C. to a mixture of benzene (42.6 ml.) and aluminum chloride (26.2 g., 0.197 mole). After an additional hour at 10–15°C, the mixture was stirred with ice-hydrochloric acid and worked up according to the general procedure. The products were polymer (0.5 g.) nitrobenzene (9.2 g., 82% yield based on  $\text{N}_2\text{O}_4$ ).

Aluminum chloride (40 g., 0.30 mole) was added slowly from a solid-

TABLE V  
Low Molecular Weight Products

Product	GLC retention time, min.	M.p., °C.	
		Found <sup>a</sup>	Lit. <sup>b</sup>
Chlorobenzene	11.9	—	—
Nitrobenzene	37.2	—	—
Biphenyl	47.2	69–71	69.2
4-Chlorobiphenyl	54.4	78–80	77
<i>p</i> -Phenylphenol	58.7	169–171	165

<sup>a</sup> Uncorrected.

<sup>b</sup> Data of Weast.<sup>40</sup>



addition funnel to a stirred solution of nitrogen dioxide (0.15 mole) in benzene (133 ml.) during 80 min. at 5–10°C. Benzene (90 ml.) was also added during this time to maintain a fluid mixture. After an additional hour at 5–10°C, the mixture was agitated for 1 hr. with the cooling bath removed. Work-up yielded polymer (about 0.5 g.) and nitrobenzene (7.44 g., 80% yield based on N<sub>2</sub>O<sub>4</sub>).

### Polymerization of Benzene by Nitrobenzene–Aluminum Chloride

The reaction was conducted according to the general procedure, except that nitrobenzene was introduced by means of a dropping funnel. During the course of addition, the mixture turned from green to red-brown after about 1 hr.

### Infrared Analysis of Polymers

The intensity of the *para* band relative to the mono bands was placed on a numerical basis by a modified baseline technique.<sup>41</sup> The baseline optical density  $D$  was obtained by the expression,  $D = \log(I_B/I)$ , where  $I$  and  $I_B$  are the per cent transmittance at the maximum and baseline respectively. The baseline was determined by a tangent to the minima on either side of the absorption band. The relative intensity  $R$ , where  $R = D_{para}/(D_{mono_1} + D_{mono_2})$  was then used as a measure of relative molecular weight.

In addition to the *para* and mono bands, characteristic maxima for *p*-polyphenyl occurred at 1000 and 1475 cm.<sup>-1</sup> (Fig. 1). Other bands were present at 1690–1650 and 2000–1800 cm.<sup>-1</sup>. Absorption in the 1650–1590 cm.<sup>-1</sup> region is assigned to NH deformation in the amino groups.<sup>39c</sup> It is significant that aminopolyphenyl<sup>42</sup> and *p*-aminobiphenyl also absorb strongly in the 1690–1650 cm.<sup>-1</sup> region.

### Polymer Oxidation with Chromic Acid

The polymer, 19 g. (entry 2, Table II, 4x run), was mixed with glacial acetic acid (800 ml.) and water (200 ml.) in a 2-liter three-necked flask equipped with a mechanical stirrer, reflux condenser, and dropping funnel. After slow addition of a solution of chromic anhydride (100 g.) in 40% glacial acetic acid (150 ml.), the mixture was stirred for 8 hr. with occasional warming. Filtration yielded a black solid (13 g.) which was further oxidized under slightly stronger conditions (700 ml. of glacial acetic acid and 20 ml. water). Following 5.5 hr. of intermittent heating, the green, heterogeneous mixture was stirred with hydrochloric acid and filtered. The tan mixture of crude acids (1.4 g.) was esterified with excess diazomethane. That portion of the ester product which was soluble in boiling ether was analyzed in benzene solvent by gas chromatography (20-ft. column, 5% Carbowax 6000–15% silicone grease on 40/60 mesh Chromosorb P). The esters were identified by comparison of retention times and infrared spectra with those of the authentic compounds. The following manual temperature program was used: initial column temperature, 170°C.; after 4 min. the Variac setting of the column oven was increased to 60; when the temperature reached 200°C. (11–12 min.), isothermal operation was main-

TABLE VI  
 Gas Chromatography Data

Compound	GLC retention time, min.	
	Product	Authentic material
Methyl benzoate	13.2	13.1
Methyl <i>p</i> -chlorobenzoate	21.0	21.4
Methyl <i>p</i> -nitrobenzoate	—	41.6
Dimethyl terephthalate <sup>a</sup>	46.4	46.2

<sup>a</sup> M.p. 140–143°C.; lit.,<sup>40</sup> m.p. 141°C.

tained. The flow rate was 110 ml. He/min. The GLC retention times are listed in Table VI. The column was capable of separating dimethyl phthalate, dimethyl terephthalate, and dimethyl isophthalate. There was no evidence for the presence of the phthalate or isophthalate isomers.

A 9-ft. column (20% SF-96 on acid-washed 40/60 mesh Chromosorb P; column temp., 230°C., 20 psi of He) was used for detection of the dimethyl ester of nitroterephthalic acid. The authentic material had a retention time of 11.8 min. No evidence for this component could be found in the crude ester mixture from the oxidation. The ester mixture was then separated on a 6-ft. column (15% silicone rubber on Chromosorb P; column temp., 252°C.; flow rate, 300 ml. He/min.). A peak appeared at a retention time of 7 min. The infrared spectrum of the compound was identical to that of the dimethyl ester of biphenyl-4,4'-dicarboxylic acid, m.p. 214–217°C.; lit.<sup>43</sup> m.p. 212–213°C. The retention time of the authentic material was also 7 min.

### Diazo Coupling Test

Polymer, 5 g. (entry 3, Table I, caustic-insoluble fraction), was mixed with a solution of concentrated sulfuric acid (0.8 ml.) and water (5 ml.). Enough benzene was added to facilitate mixing. After the mixture was cooled to 6–10°C., a solution of sodium nitrite (0.52 g.) in 2.4 ml. of water was added below 10°C. A positive nitrous acid test was obtained (starch-potassium iodide paper) and the mixture was then vigorously stirred for 3 hr. A small amount of the diazonium salt mixture was added to a cold, saturated solution of  $\beta$ -naphthol in 20% sodium hydroxide. After being shaken for several minutes, the suspension acquired a red color. A polymer-benzene-water mixture which was not diazotized exhibited no color change when shaken with the  $\beta$ -naphthol solution. When the diazonium salt mixture was added to 20% sodium hydroxide in the absence of  $\beta$ -naphthol, the polymer also became red, but to a lesser degree.

### Polymer Solubility in Benzene

Polymer (0.600 g.) was added to benzene (15.0 ml.) at room temperature. After the mixture was allowed to stand overnight in a stoppered vial with



occasional shaking, it was filtered under pressure. The filtrate was collected in an ice-cold receiver to minimize evaporation of benzene. An aliquot (3.00 ml.) of the filtrate was placed in a weighed receiver, heated under vacuum overnight on a steam bath to remove the solvent, and then weighed to determine the amount of soluble material.

### Elemental Analysis

The elemental analyses (carbon, hydrogen, nitrogen) were performed by Dr. Weiler and Dr. Strauss, Oxford, England. Average values for duplicate analyses are listed in the tables. Maximum deviations were: C,  $\pm 0.12\%$ ; H,  $\pm 0.14\%$ ; N,  $\pm 0.15\%$ ; Cl,  $\pm 0.10\%$ . Oxygen analyses (single) were by Galbraith Laboratories, Knoxville, Tenn. The above elements totaled 96.7–97.9 wt.-% of the polymers from benzene–nitrogen dioxide–aluminum chloride, and 98.8–100.1 wt.-% of those produced with nitrobenzene oxidant.

We are grateful to the National Science Foundation for support, and to the Dow-Badische Chemical Co. for a Fellowship to R. J. H. during part of 1963.

### References

1. C. Friedel and J. M. Crafts, *Compt. Rend.*, **100**, 692 (1885).
2. A. Homer, *Proc. Camb. Phil. Soc.*, **16**, 65 (1911); *Chem. Abstr.*, **5**, 1399 (1911).
3. E. Wertyporoch and H. Sagel, *Ber.*, **66**, 1306 (1933).
4. V. N. Ipatieff and V. I. Komarewsky, *J. Am. Chem. Soc.*, **56**, 1926 (1934).
5. R. J. Moore and G. Egloff, *Met. Chem. Eng.*, **17**, 61 (1917); *Chem. Abstr.*, **11**, 2665 (1917).
6. M. Freund, *Monatsh.*, **17**, 395 (1896).
7. A. Schaarschmidt, *Ber.*, **57**, 2065 (1924).
8. P. Kovacic and A. Kyriakis, *J. Am. Chem. Soc.*, **85**, 454 (1963).
9. P. Kovacic and J. Oziomek, *J. Org. Chem.*, **29**, 100 (1964).
10. P. Kovacic and F. W. Koch, *J. Org. Chem.*, **28**, 1864 (1963).
11. P. Kovacic, F. W. Koch, and C. E. Stephan, *J. Polymer Sci. A*, **2**, 1193 (1964).
12. P. Kovacic and R. M. Lange, *J. Org. Chem.*, **28**, 968 (1963).
13. C. D. Nenitzescu and A. T. Balaban, *Ber.*, **91**, 2109 (1958).
14. A. T. Balaban and C. D. Nenitzescu, in *Friedel-Crafts and Related Reactions*, G. A. Olah, Ed., Interscience, New York, 1964, Vol. II, Chap. 23.
15. G. Baddeley, *J. Chem. Soc.*, **1950**, 994.
16. P. Kovacic and R. M. Lange, *J. Org. Chem.*, **29**, 2416 (1964).
17. P. Kovacic and C. Wu, *J. Org. Chem.*, **26**, 759 (1961).
18. P. Kovacic and C. Wu, *J. Org. Chem.*, **26**, 762 (1961).
19. A. C. Akkerman-Faber and J. Coops, *Rec. Trav. Chim.*, **80**, 468 (1961).
20. P. Kovacic and F. W. Koch, *J. Org. Chem.*, **30**, 3176 (1965).
21. P. Kovacic and L. C. Hsu, *J. Polymer Sci. A-1*, **4**, 5 (1966).
22. A. I. Titov, *Zh. Obshch. Khim.*, **7**, 591 (1937).
23. S. J. Kuhn and G. A. Olah, *J. Am. Chem. Soc.*, **83**, 4564 (1961).
24. J. D. Archambault, H. H. Sisler, and G. E. Ryschkewitsch, *J. Inorg. Nucl. Chem.*, **17**, 130 (1961).
25. G. A. Olah and S. J. Kuhn, in *Friedel-Crafts and Related Reactions*, G. A. Olah, Ed., Interscience, New York, 1964, Vol. III, Chap. 43.
26. M. Jozefowicz, Ph.D. Thesis, University of Paris, 1963.
27. C. G. Cannon and G. B. B. M. Sutherland, *Spectrochim. Acta*, **4**, 373 (1951).
28. A. Kyriakis, M.S. Thesis, Case Institute of Technology, 1962.
29. R. M. Lange, Ph.D. Thesis, Case Institute of Technology, 1964.
30. A. I. Titov, *Tetrahedron*, **19**, 557 (1963).

31. R. Scholl and C. Seer, *Ber.*, **55**, 330 (1922).
32. L. F. Fieser and M. Fieser, *Advanced Organic Chemistry*, Reinhold, New York, 1961, pp. 128-129.
33. A. R. Mathieson, in *The Chemistry of Cationic Polymerization*, P. H. Plesch, Ed., MacMillan, New York, 1963, p. 246.
34. C. G. Overberger and G. F. Endres, *J. Polymer Sci.*, **16**, 283 (1955).
35. L. Harris and B. M. Siegel, *J. Am. Chem. Soc.*, **63**, 2520 (1941).
36. P. Kovacic and J. A. Levisky, *J. Am. Chem. Soc.*, **88**, 1000 (1966).
37. P. Kovacic, C. T. Goralski, J. J. Hiller, Jr., J. A. Levisky, and R. M. Lange, *J. Am. Chem. Soc.*, **87**, 1262 (1965).
38. P. Kovacic, J. J. Hiller, Jr., J. F. Gormish and J. A. Levisky, *Chem. Commun.*, No. **22**, 580 (1965).
39. L. J. Bellamy, *The Infra-Red Spectra of Complex Molecules*, Wiley, New York, 1960; (a) p. 96; (b) pp. 162-163; (c) p. 249.
40. R. Weast, Ed., *Tables for Identification of Organic Compounds*, 2nd Ed., The Chemical Rubber Co., Cleveland, Ohio, 1964.
41. J. J. Heigl, M. F. Bell, and J. U. White, *Anal. Chem.*, **19**, 293 (1947).
42. P. Kovacic, V. J. Marchionna, F. W. Koch, and J. Oziomek, unpublished work.
43. M. Weiler, *Ber.*, **32**, 1056 (1899).

### Résumé

Le benzène était polymérisé en oligomères *p*-polyphénylés au moyen de dioxyde d'azote et de chlorure d'aluminium. La production de polymères était favorisée par des rapports  $\text{AlCl}_3/\text{NO}_2$  minimum de 2, des durées de réaction prolongées, et des températures élevées. La structure du polymère a été déterminée au départ d'analyses élémentaires, de dégradations oxydantes, de la solubilité, du poids moléculaire, de tests concernant des groupes fonctionnels de produits de bas poids moléculaire, de spectres infra-rouges et ultraviolets. Les chaînes contiennent de faibles quantités de substituants chlorés, aminés, hydroxylés et carboxylés. Les données du poids moléculaire de la partie soluble dans le benzène (40-71%) indiquent une moyenne de 4-6 unités phénylènes par chaîne. Dans des conditions modifiées le nitrobenzène pouvait être obtenu comme produit majeur ce qui indique la sensibilité du système à des variations dans les conditions de réaction. Avec le nitrobenzène comme oxydant, un polymère de type semblable a été obtenu; les aspects théoriques sont discutés.

### Zusammenfassung

Benzol wurde durch Stickstoffdioxid Aluminiumchlorid zu *p*-Polyphenyloligomeren polymerisiert. Die Polymerbildung wurde durch ein  $\text{AlCl}_3:\text{NO}_2$ -Verhältnis von mindestens 2, durch lange Reaktionsdauer und höhere Temperatur begünstigt. Zur Aufklärung der Polymerstruktur wurden Elementaranalyse, oxydativer Abbau, Löslichkeit, Molekulargewicht, Prüfung auf funktionelle Gruppen, niedermolekulare Produkte sowie Infrarot- und Ultraviolettspektren herangezogen. Die Ketten enthielten kleine Mengen an Chlor-, Amino-, Hydroxyl- und Carboxylsubstituenten. Molekulargewichtsdaten für den benzollöslichen Teil (40-71%) zeigten im Mittel 4-6 Phenylenbausteine pro Kette. Unter geänderten Bedingungen konnte Nitrobenzol als Hauptprodukt erhalten werden, was die Empfindlichkeit des Systems gegen Veränderung der Reaktionsvariablen erkennen lässt. Mit Nitrobenzol als Oxydationsmittel wurde ein ähnlicher Polymertyp gebildet. Die theoretischen Gesichtspunkte werden diskutiert.

Received September 27, 1955

Prod. No. 4951A

## Polyamides Having Long Methylene Chain Units

KAZUO SAOTOME and HIROSHI KOMOTO, *Technical Research Laboratory, Asahi Chemical Industry Company, Ltd., Itabashi-ku, Tokyo, Japan*

### Synopsis

Three series of polyamides having long methylene chain units have been prepared from *p*-xylylenediamine and 2,2'-*p*-phenylenebisethylamine with aliphatic dicarboxylic acids of long methylene chain units: aliphatic diamines of long methylene chain units with terephthalic, *p*-benzenediacetic, and *p*-benzenedipropionic acids; and aliphatic diamines with aliphatic dicarboxylic acids, both having long methylene chain units. The effects of the length of the methylene chain units on the melting point, the glass transition temperatures and the densities of these polyamides were investigated. The aromatic polyamides, in which even methylene chains are joined between a phenylene and an amide group generally have higher melting points than the corresponding ones with odd methylene chains. On the plots of the melting points and the densities of the aliphatic series against the amide concentrations, both the melting point and the density extrapolated to the zero amide concentration are found below the values for polymethylene.

### INTRODUCTION

Various kinds of polyamides have been prepared from diamines with dicarboxylic acids since Carothers' original work, and the relationship of the chemical structure of the polymers to their physical properties has been dealt with in many reports. Coffman et al.<sup>1</sup> reported various aliphatic polyamides from diamines of carbon atoms up to C<sub>12</sub> with dicarboxylic acids. Frunze et al.<sup>2</sup> prepared the polyamides of *p*-xylylenediamine with  $\alpha,\omega$ -octadecanedioic and  $\alpha,\omega$ -docosanedioic acids. However, no systematic study of the polyamides containing methylene chains longer than C<sub>10</sub> has been carried out.

In a preceding paper,<sup>3</sup> the synthesis of diamines and dicarboxylic acids with long methylene chains up to C<sub>22</sub> was reported. The present paper deals with the preparation and some properties of the polymer from these diamines and dicarboxylic acids with long methylene chains. The polyamides are classified into the following three series: (1) polyamides from aromatic diamines such as *p*-xylylenediamine and 2,2'-*p*-phenylenebisethylamine with aliphatic dicarboxylic acids having long methylene chains; (2) polyamides from aliphatic diamines having long methylene chains with aromatic dicarboxylic acids such as terephthalic, *p*-benzenediacetic, and *p*-benzenedipropionic acids; (3) polyamides from aliphatic diamines and dicarboxylic acids, both having long methylene chains. The effects of

methylene chain length on the melting points, the glass transition temperatures, and the densities of the polyamides of each series have been investigated.

## EXPERIMENTAL

### Materials

The preparation and the characteristics of long-chain diamines and dicarboxylic acids were described in the preceding paper.<sup>3</sup> Hexamethylenediamine and terephthalic acid were obtained commercially. *p*-Xylylenediamine was prepared from terephthalonitrile by catalytic hydrogenation.<sup>4</sup> 2,2'-*p*-Phenylenebisethylamine was prepared from 1,1'-dichloro-*p*-xylene through the biscyano derivative.<sup>5</sup> *p*-Benzenediacetic acid, m.p. 251–252°C., was prepared from 1,1'-dichloro-*p*-xylene according to the method of Kipping.<sup>6</sup> *p*-Benzenedipropionic acid, m.p. 231°C., was prepared from 1,1'-dichloro-*p*-xylene through the malonic ester synthesis.

### Methods

**Polymer Melting Points.** The melting point was determined by observing solid particles of the polymer between crossed nicol polarizers on an electrically heated hot-stage microscope. The melting point was taken as the temperature at which the last trace of birefringent crystallinity completely disappeared. This is the crystalline melting point of the polymer.

**Glass Transition Temperatures.** The glass transition temperature  $T_g$  was determined on small film strips in an apparatus designed to measure the dynamic modulus of elasticity (for a resonant vibration frequency of 110 cps) as a function of temperature. The point at which the maximum loss modulus ( $E''_{\max}$ ) was observed was taken as  $T_g$ .<sup>7</sup> To check the  $T_g$  values obtained by the above method, dilatometric measurements for several polyamides samples were carried out. The results of the two different methods are in good agreement.

**Densities of Polyamides.** The density was measured at 25°C. in a density gradient tube prepared with toluene and carbon tetrachloride. The polymer particles used in the measurement were prepared after being gradually cooled from the melts and annealed at 180°C. for 1 hr. in atmospheric nitrogen.

**Reduced Viscosities.** The polymers were dissolved in *m*-cresol at temperatures of 60–80°C. for 2 hr. by use of a magnetic stirrer. Solutions of 0.5% concentration at 25°C. were used for viscosity measurement.

**Preparation of Nylon Salts.** Equimolar alcoholic solutions of diamine and dicarboxylic acid at 10% concentration were combined, and the mixture was refluxed for 0.5 hr. After being cooled with ice water, the precipitated salt was filtered off and recrystallized from a water-acetone mixture. The yields of the nylon salts were generally quantitative. In the



cases of terephthalic acid, however, the nylon salts were precipitated from the aqueous solutions by the addition of acetone.

**Polycondensation of Nylon Salts.** A few grams of the nylon salt were sealed in a glass tube under reduced pressure. The glass tube was heated in an oil bath at temperatures of 230–260°C. for 2 hr. The glass tube was opened, and the content was heated at 280–300°C. for 1 hr., and then for an additional 0.5 hr. under reduced pressure of 1 mm. Hg. to complete the reaction. All polymers obtained are white, hornlike crystalline solids.

## RESULTS AND DISCUSSION

In the first series of experiments, the polyamides of *p*-xylylenediamine and 2,2'-*p*-phenylenebisethylamine with  $\alpha,\omega$ -alkanedioic acids having 9–22 carbon atoms were prepared. The results are shown in Tables I and II.

TABLE I  
Polyamides of *p*-Xylylenediamine (PXD) with  
 $\alpha,\omega$ -Alkanedioic Acids,  $\text{HOOC}(\text{CH}_2)_n\text{COOH}$

<i>n</i>	Polymer code	N salt m.p., °C.	Polymer m.p., °C.	$\eta_{sp}/c$	Density, g./cc.	$T_g$ , °C. <sup>a</sup>
7	PXD-9	197	282	1.15	1.152	
8	PXD-10	215	291	1.25	1.152	115
9	PXD-11	192	264	1.40	1.130	110 (107)
10	PXD-12	200	270	1.50	1.129	105 (105)
11	PXD-13	189	247	1.30	1.108	100
12	PXD-14	192	257	1.12	1.110	
13	PXD-15	183	241	1.01	1.090	90
14	PXD-16	190	248	1.07	1.092	
15	PXD-17	184	239	1.05	1.080	
16	PXD-18	189	242	1.21	1.075	75
20	PXD-22	187	225	1.31	1.056	

<sup>a</sup>  $T_g$  values in parentheses denote those determined by the dilatometric method.

The polyamides of  $\alpha,\omega$ -alkylenediamines with such dicarboxylic acids as terephthalic, *p*-benzenediacetic, and *p*-benzenedipropionic acids were prepared in the second series, while, the polyamides of  $\alpha,\omega$ -alkylenediamines with  $\alpha,\omega$ -alkanedioic acids, both of long methylene chains, were obtained in the third series. The data are tabulated in Tables III and IV.

It is noted that two different melting points have been reported for poly-*p*-xylylenesbacamide (PXD-10), one at approximately 270°C.<sup>8</sup> and another at approximately 300°C.<sup>9</sup> Bell et al.<sup>10</sup> recently reported several polyamides of *p*-xylylenediamine and determined the melting points of PXD-10 and PXD-12 as 279–281°C. and 268–272°C., respectively. While the melting point of PXD-12 in the present work is in good agreement with that given in the literature,<sup>10</sup> the melting point of PXD-10 is somewhat different from it. It has been ascertained that although the PXD-10 polymer

TABLE II  
Polyamides of 2,2'-Phenylenedimethylamine (PBE)  
with  $\alpha,\omega$ -Alkanedioic Acids,  $\text{NOOC}(\text{CN}_2)_n\text{COON}$

$n$	Polymer code	N salt, m.p., °C.	Polymer m.p., °C.	$\eta_{sp}/c$	Density, g./cc.	$T_g$ , °C.
7	PBE-9	197	290	1.06	1.140	
8	PBE-10	210	300	1.23	1.139	105
9	PBE-11	202	275	1.25	1.108	96
10	PBE-12	201	280	1.28	1.108	
11	PBE-13	191	262	1.30	1.095	
12	PBE-14	177	267	1.15	1.091	93
13	PBE-15	171	248	1.08	1.075	
14	PBT-16	175	258	1.06	1.077	85
15	PBE-17	170	249	1.12	1.067	
16	PBE-18	175	248	1.15	1.055	75
20	PBE-22	173	230	1.30	1.050	

TABLE III  
Polyamides of  $\alpha,\omega$ -Alkylenediamines,  $\text{H}_2\text{N}(\text{CH}_2)_n\text{NN}_2$ , with Terephthalic (T),  
*p*-Benzenediacetic (BDA) and *p*-Benzenedipropionic Acids (BDP)

Acid	Amine $n$	Polymer code	N salt m.p., °C.	Polymer m.p., °C.	$\eta_{sp}/c$	Density, g./cc.	$T_g$ , °C.
T	12	12-T	253	296	0.85	1.152	
	14	14-T	242	265	0.92	1.115	
	18	18-T	228	255	1.03	1.067	
BDA	6	6-BDA	259	300	1.21	1.182	
	8	8-BDA	225	280	1.15	1.152	110
	10	10-BDA	198	265	1.16	1.130	
	12	12-BDA	191	256	1.21	1.095	
	14	14-BDA	184	235	0.75	1.075	
	18	18-BDA	177	225	1.31	1.036	78
BDP	8	8-BDP	197	289	1.23	1.151	
	10	10-BDP	178	271	1.15	1.120	
	12	12-BDP	174	263	1.30	1.080	85
	14	14-BDP	171	246	0.85	1.067	
	18	18-BDP	169	232	1.05	1.034	65

apparently begins to melt (softening point) at 282–284°C., the crystallite melts sharply at 291°C. In polyamides having melting points higher than 250°C., the crystalline melting point of the polymer is generally observed at a temperature about 10°C. higher than the softening point. The melting points of these polyamides containing benzene rings in the chain are plotted against the cohesion energies per chain unit in Figures 1 and 2. The calculation of the cohesion energy was carried out according to Bunn's method.<sup>11</sup> In the case of terephthalamides, however, the  $-\text{OC}-\text{C}_6\text{H}_4-\text{CO}-$  group was separated into two chain units, 2 CO and phenyl, in accordance with the phenylene groups in *p*-benzenediacetamide and *p*-benzenedipropionamide, neglecting the rigidity due to resonance effects. In



TABLE IV  
Polyamides of  $\alpha,\omega$ -Alkylenediamines with  $\alpha,\omega$ -Alkanedioic Acids

--HN(CH <sub>2</sub> ) <sub>m</sub> - NHCO(CH <sub>2</sub> ) <sub>n</sub> - CO--		Polymer code	N salt m.p., °C.	Polymer m.p., °C.	$\eta_{sp}/c$	Density, g./cc.
m	n					
6	8	6-10	171	225	0.88	1.101
6	10	6-12	166	219	1.04	1.070
6	16	6-18	151	192	0.98	1.040
6	20	6-22	152	180	0.82	1.032
8	8	8-10	168	206	1.15	1.075
8	10	8-12	167	200	1.08	1.062
8	16	8-18	150	179	0.93	1.030
8	20	8-22	151	175	0.85	1.021
10	8	10-10	183	198	0.98	1.063
10	10	10-12	169	192	1.19	1.057
10	16	10-18	150	170	0.80	1.024
10	20	10-22	150	169	0.73	1.010
12	8	12-10	158	192	1.15	1.050
12	10	12-12	178	183	1.20	1.036
12	16	12-18	150	167	1.12	1.016
12	20	12-22	150	164	1.16	1.006
14	8	14-10	149	175	0.83	1.042
14	10	14-12	150	175	0.93	1.027
14	16	14-18	152	158	0.92	1.013
14	20	14-22	149	153	0.84	0.999
18	8	18-10	148	171	0.92	1.024
18	10	18-12	147	170	1.11	1.015
18	16	18-18	148	158	0.99	0.998
18	20	18-22	152	146	0.87	0.990

the case of aromatic diamine or dicarboxylic acid, the plots of melting point versus cohesion energies are separated into two lines according to odd or even numbers of the carbon atoms in the aliphatic component. The melting points of the polyamides of 2,2'-*p*-phenylenebisethylamine are generally higher than those of *p*-xylylenediamine in both the cases of odd and even numbers in the corresponding aliphatic dicarboxylic acids. Similar relations are observed between the polyamides of terephthalic and *p*-benzenedicarboxylic acids and those of *p*-benzenedipropionic and *p*-benzenedicarboxylic acids. These tendencies are summarized as follows: in the aromatic polyamides of these five types, the melting point of the polymer which has a methylene chain with even numbers of carbon atoms between the phenylene and the amide groups is generally higher than that of the corresponding one which has a methylene chain with an odd number of carbon atoms. The densities of these five polyamides which are isomers of each other when the methylene numbers are equal in the repeating chain units are plotted against the methylene numbers in a repeating chain unit in Figures 3 and 4. Parallel relationships are observed between the melting points and the densities against the methylene numbers in a repeating chain unit. The

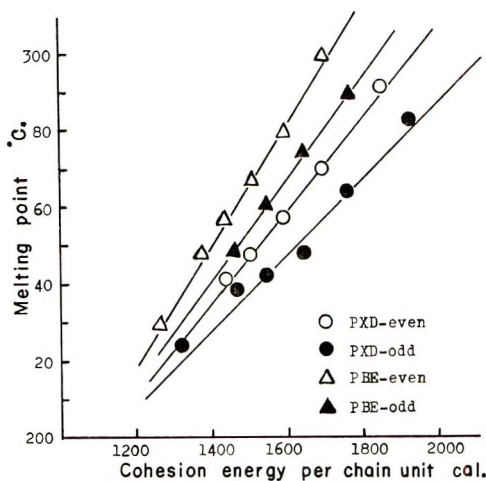


Fig. 1. Melting points vs. cohesion energies per chain unit.

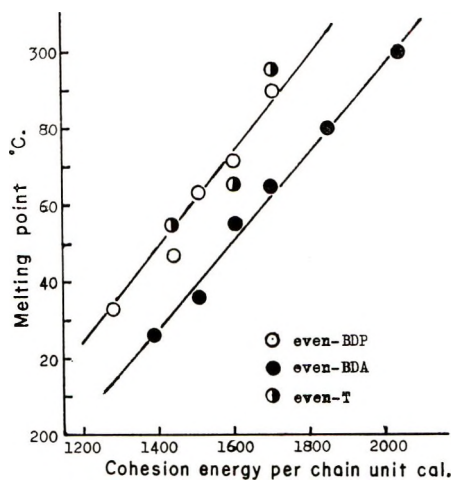


Fig. 2. Melting points vs. cohesion energies per chain unit.

densities of the polyterephthalamides agree with those of the corresponding poly-*p*-benzenedipropionamides. On the other hand, the densities of poly-*p*-benzenediacetamides lie below those of poly-*p*-benzenedipropionamides. The depressions, both of the melting point and of the density, for poly-*p*-benzenediacetamides, seen in Figures 2 and 4, may be attributed to the odd-numbered methylene chain joined directly to the benzene ring. The fact that no practical differences in the melting points and the densities are observed between the polyterephthalamides and their isomeric poly-*p*-benzenedipropionamides is considered to indicate the absence of the conjugation of the carbonyl group with the benzene ring in polyterephthalamides. Perhaps, the conjugation between the carbonyl and the benzene ring is interfered with by the intermolecular hydrogen bond with the amide

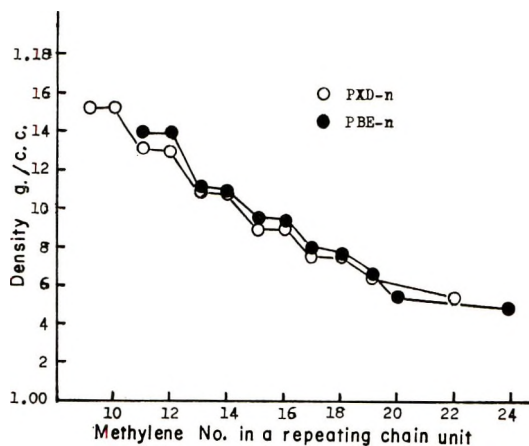


Fig. 3. Densities vs. methylene number in a repeating chain unit.

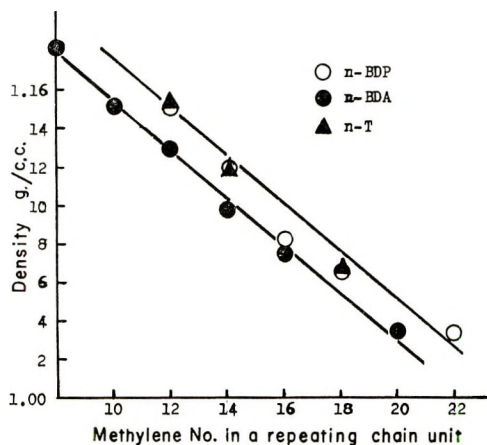


Fig. 4. Densities vs. methylene number in a repeating chain unit.

groups. This is quite different from poly(ethylene terephthalate), in which the resonance between the carbonyl and the benzene ring causes its melting point to increase anomalously.<sup>11</sup>

The linear relationship between the glass transition temperatures and the methylene numbers in a repeating chain unit for these aromatic polyamides is plotted in Figure 5. The effect of the benzene ring on the glass transition temperature is conspicuous, since the glass transition temperatures of most aliphatic polyamides are between 40 and 50°C., irrespective of their methylene chain length. The glass transition temperatures of some aliphatic polyamides were obtained as follows; 50°C. (6-12), 50°C. (18-18), 52°C. (nylon 7<sup>12</sup>), and 48°C. (nylon 9<sup>12</sup>).

The melting points and the densities of the aliphatic polyamides containing long methylene chains are plotted against the amide group numbers per 100 chain atoms in Figures 6 and 7. The extrapolation of the linear

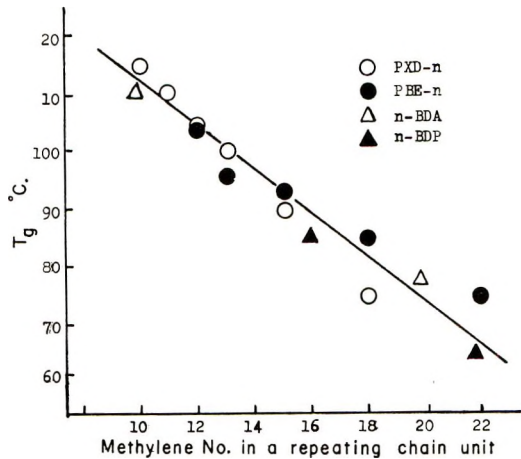


Fig. 5. Glass transition temperatures vs. methylene number in a repeating chain unit.

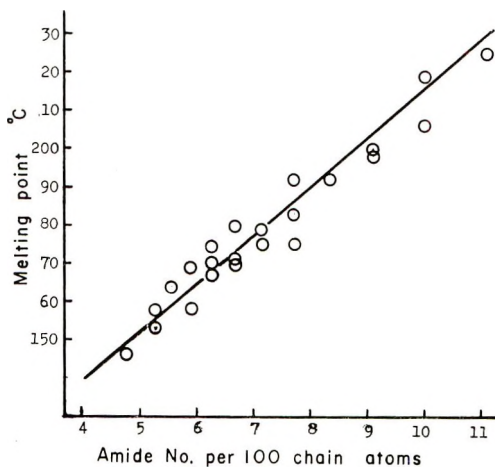


Fig. 6. Melting points of aliphatic polyamides vs. amide number per 100 chain atoms.

relation of the melting points at zero amide number affords the value of 90°C. This well agrees with Bunn's result,<sup>11</sup> which was obtained from the relation between the melting points and the cohesion energies of aliphatic polyamides extrapolated to the point corresponding to polymethylene. On the other hand, Izard<sup>9</sup> described an equation representing the melting point of long straight-chain aliphatic polyamides with  $n$  methylene groups per repeating chain unit as;

$$T = \frac{\Delta H}{\Delta S} = \frac{2300 + 220n}{0.645(n + 4)}$$

for  $n \rightarrow \infty$ ,  $T = 66^\circ\text{C}$ . He estimated that there exists a minimum melting point at about the polyamide 20-20, the melting point of which should be

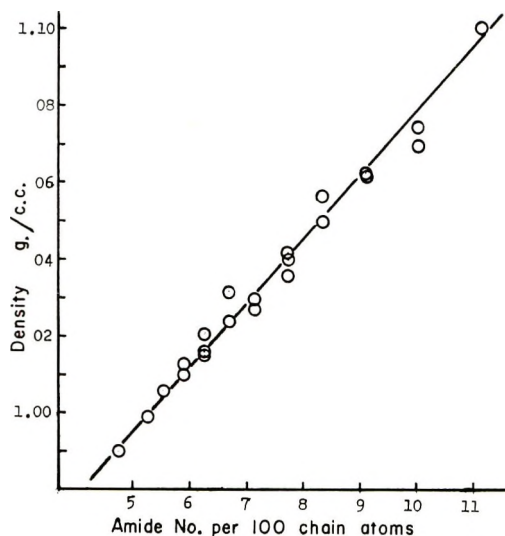


Fig. 7. Densities of aliphatic polyamides vs. amide number per 100 chain atoms.

calculated from the above equation as  $120^{\circ}\text{C}$ . The melting point of 18-22, which corresponds to 20-20 is obtained as  $146^{\circ}\text{C}$ ., while, the melting point of polymethylene prepared from diazomethane is reported as  $136.5^{\circ}\text{C}$ .<sup>13</sup> The linear relationship of the melting points and the fact that the melting point of 18-22 is only  $10^{\circ}\text{C}$ . higher than that of polymethylene suggest that the melting points of the polyamides of lower amide concentrations are lower than that of polymethylene. Obviously, the minimum melting point should appear at the point which corresponds to a lower amide concentration than that of 18-22 (or 20-20). A similar linear relationship is also found between the densities and the amide concentrations. The density at zero amide concentration is given as  $0.91\text{ g./cc}$ . On the other hand, the density of polymethylene is reported as  $0.988\text{ g./cc}$ .,<sup>14</sup> while the density of polymethylene is calculated to be  $1.006\text{ g./cc}$ . from the x-ray analysis.<sup>15</sup> The extrapolated density is much less than that of polymethylene, even considering that the crystallinity of polymethylene is somewhat higher than that of polyamides having very long polymethylene linkages. The crystallinity of the annealed samples of 18-22 was ascertained by x-ray examination to be very large, and a tendency for increasing crystallinity with decreasing amide concentration was also observed.

Two different explanations have been discussed for the depression of the melting points of polyamides with very low amide concentrations below that of polymethylene. Izard<sup>9</sup> connected this depression with Flory's treatment<sup>16</sup> of the lowering of the melting point by copolymerization. Bunn<sup>11</sup> contradicted the application of the Flory's treatment to these crystalline homopolymers by pointing out the differences between a copolymer with a random succession of chain units and a homopolymer in which different chain units are arranged into crystals and suggested that

the depression of the melting point is due to the introduction of easily rotating bonds; the CO—NH bonds appear to have some double-bond character, and so any additional ease of rotation should be in the adjacent CO—CH<sub>2</sub> and NH—CH<sub>2</sub> bonds. However, there is no consideration of density in either of these arguments. In the polyamides in which long methylene chains are sparsely interspersed with amide groups, the contribution of the methylene chains toward the cohesion energy which binds the chain molecules together is estimated to become so great that it dominates the total heat content of fusion. Since the melting point is expressed by  $T = \Delta H/\Delta S$ , the introduction of easily rotating bonds obviously enlarges the entropy of fusion to depress the melting point. However, if the intermolecular spacing between the polymethylene chains which occupy the dominant portion in the polyamide crystals is not affected by the insertion of the amide groups, the contribution due to the increase of the entropy of fusion must decrease with the decrease of the amide concentration and no minimum melting point should be observed. The facts that the densities of the polyamides with very small amide concentrations are much lower than that of polymethylene and a minimum density is estimated to exist as well as a minimum melting point indicate the effect of the amide groups of increasing the intermolecular spacing between the polymethylene chains. The amide group itself has obviously a greater cohesion energy and a larger density than the methylene group. In the polyamides with compositions close to polymethylene, the increase of the intermolecular spacings should become the dominant effects both on the melting point and on the density. Although the contribution of the increase of the entropy of fusion by the introduction of the easily rotating bonds can not be neglected, the increase in the intermolecular spacings which causes an enormous decrease of the heat content of fusion is considered to be the main reason for the depression both of the melting points and of the densities to minimum points below those of polymethylene.

### References

1. D. D. Coffman, C. J. Berchet, W. R. Peterson, and E. W. Spanagel, *J. Polymer Sci.*, **2**, 306 (1947).
2. T. M. Frunze, V. V. Korshak, and E. A. Krasnyanskaya, *Vysokomol. Soedin.*, **1**, 495 (1959).
3. K. Saotome, H. Komoto, and T. Yamazaki, *Bull. Chem. Soc. Japan*, **39**, 485 (1966).
4. L. Kh. Freidlin et al., *Izv. Akad. Nauk SSSR, Otd. Khim. Nauk*, **1961**, 1713.
5. P. Ruggli, B. B. Bussemaker, W. Müller, and A. Staub, *Helv. Chim. Acta*, **18**, 1388 (1935).
6. J. S. Kipping, *Ber.*, **21**, 42 (1888).
7. K. H. Illers and H. Breuer, *J. Colloid Sci.*, **18**, 1 (1963).
8. T. M. Frunze and V. V. Korshak, *Vysokomol. Soedin.*, **1**, 287 (1959).
9. E. F. Izard, *J. Polymer Sci.*, **8**, 503 (1952).
10. A. Bell, J. G. Smith, and C. J. Kibler, *J. Polymer Sci.*, **A**, **3**, 19 (1965).
11. C. W. Bunn, *J. Polymer Sci.*, **16**, 323 (1955).
12. H. Komoto and K. Saotome, *Kobunshi Kagaku*, **22**, 337 (1965).



13. L. Mandelkern, M. Hellman, D. W. Brown, D. E. Roberts, and F. A. Quinn, *J. Am. Chem. Soc.*, **75**, 4093 (1953).
14. R. R. Richards, *J. Appl. Chem.*, **1**, 370 (1951).
15. C. W. Bunn, *Trans. Faraday Soc.*, **35**, 482 (1939).
16. P. J. Flory, *J. Chem. Phys.*, **17**, 223 (1949).

### Résumé

Trois séries de polyamides ayant des chaînes méthyléniques longues ont été préparées au départ de *p*-xylylènediamine et de 2,2'-*p*-phénylène-bis-éthylamine avec des acides aliphatiques dicarboxylés à unités méthyléniques longues; de même au départ de diamines aliphatiques à chaînes méthyléniques longues avec les acides téréphthaliqes, *p*-benzènediacétiques et *p*-benzènedipropioniques; au départ de diamines aliphatiques, avec des acides dicarboxyliques aliphatiques ayant tous deux de longues chaînes méthyléniques. Les effets de la longueur des chaînes méthyléniques sur le point de fusion, la température de transition vitreuse et les densités de ces polyamides ont été étudiés. Les polyamides aromatiques, dans lesquels les chaînes à nombre pair d'unités méthyléniques sont réunies par un groupe phénylène et un groupe amide, ont en général un point de fusion plus élevé que les polyamides correspondants avec un nombre de méthylène impair. En portant en diagramme les points de fusion et les densités de la série aliphatique en regard de la concentration en amides, les points de fusion et les densités extrapolées à concentration en amide nulle correspondent dans les deux cas à une valeur inférieure aux valeurs du polyméthylène.

### Zusammenfassung

Drei Polyamidreihen mit langen Methylenkettenbausteinen wurden aus *p*-Xylylen-diamin und 2,2'-*p*-Phenylen-bis-äthylamin mit aliphatischen Dicarbonsäuren mit langen Methylenketten, aus aliphatischen Diaminen mit langen Äthylenketten mit Terephthal-, *p*-Benzoldiessig- und *p*-Benzoldipropionsäure, aus aliphatischen Diaminen mit aliphatischen Dicarbonsäuren, beide mit langen Methylenketten, dargestellt. Der Einfluss der Länge der Methylenketten auf den Schmelzpunkt, die Glasumwandlungstemperatur und die Dichte dieser Polyamide wurde untersucht. Die aromatischen Polyamide, bei welchen sich geradzahlige Methylenketten zwischen einer Phenylen- und einer Amidgruppe befinden, besitzen im allgemeinen höhere Schmelzpunkte als die entsprechenden Polyamide mit ungeradzahligen Methylenketten. Bei der Auftragung der Schmelzpunkte und der Dichten der aliphatischen Reihen gegen die Amidkonzentration liegt der auf die Amidkonzentration 0 extrapolierte Schmelzpunkt und die extrapolierte Dichte unterhalb der Werte für Polymethylen.

Received August 30, 1965

Revised October 20, 1965

Prod. No. 4959A

## Isomorphism in Copolyamides of Long Repeating Chain Units Containing Oxa- and Thia-Alkylene Linkages

KAZUO SAOTOME and HIROSHI KOMOTO, *Technical Research Laboratory, Asahi Chemical Industry Company, Ltd., Itabashi-ku, Tokyo, Japan*

### Synopsis

Various copolyamides of long repeating chain units were prepared from hexamethylenediamine (HMDA) and *p*-xylylenediamine (PXDA) with aliphatic dicarboxylic acids of three structural types:  $\alpha,\omega$ -alkanedioic,  $\alpha,\omega$ -oxaalkanedioic, and  $\alpha,\omega$ -thiaalkanedioic acids. Both binary and ternary combinations of these dicarboxylic acids having the same number of chain atoms with the diamine afforded highly crystalline copolyamides. In all cases of these copolymers, the plots of the melting points versus the compositions are expressed by linear relations, even in the ternary systems. For example, the melting points of the copolyamides of HMDA with 6-oxaundecanedioic and 6-thiaundecanedioic acids are practically unchanged in all ranges of composition. The same relation is also observed in the corresponding copolyamides of PXDA. The relation between the densities and the composition is plotted with good linearity in every case. From x-ray examination, the lattice spacings of each copolyamide are ascertained to be unchanged by the composition. These results reveal that methylene, ether, and thioether linkages are in the relation of isomorphous replacements for each other in these copolyamide systems. Moreover, the linear relationship between the melting point and the composition is explained by assuming that the entropy of fusion in these copolyamides changes linearly according to the change of the composition.

### INTRODUCTION

Since Edgar and Hill<sup>1</sup> first observed a linear relationship between melting points and composition in copolyamides of hexamethylenediamine with adipic and terephthalic acids, this relationship has been accepted as a criterion for isomorphous replacement. Cramer and Beaman<sup>2</sup> found a better linearity of melting points versus composition in the copolyamides of heptamethylenediamine and bis-3-aminopropyl ether with dicarboxylic acids. Isomorphous replacement between benzene ring and a four-methylene sequence was also investigated by Yu and Evans.<sup>3,4</sup> Levine and Temin<sup>5</sup> observed that there is good linearity of melting points versus composition in the copolyamides of  $\epsilon$ -caprolactam with *p*-aminomethylcyclohexylcarboxylic acid. Recently, Tranter<sup>6</sup> pointed out from the x-ray examination of the copolyamides of hexamethylenediamine with several dicarboxylic acids that the shape of the melting point versus composition

curve is not a reliable criterion for isomorphous replacement. In preceding papers,<sup>7,8</sup> the preparation of polyamides having long alkylene and long oxaalkylene chain units has been reported. In addition to these, the polyamides from several  $\omega,\omega'$ -thiodialkanoic acids have been prepared. This paper deals with isomorphous replacement in copolyamides of long repeating chain units containing oxa- and thia-alkylene linkages.

## EXPERIMENTAL

### Methods

The melting point was determined by observing solid particles of the polymer between crossed nicol polarizers on an electrically heated hot-stage microscope. The melting point was taken as the temperature at which the last trace of birefringent crystallinity completely disappeared. This is the crystalline melting point of the polymer.

Glass transition temperatures, reduced viscosities, and densities were determined according to the same methods as described in the preceding papers.<sup>7,8</sup> A mixture of each nylon salt was polymerized in the same manner as described previously for the preparation of homogeneous polyamides. Prior to the copolymerization experiments, several polyamides from  $\omega,\omega'$ -thiodialkanoic acids were prepared.

### Polyamides from $\omega,\omega'$ -Thiodialkanoic Acids

$\omega,\omega'$ -Thiodialkanoic acids having the formula  $S[(CH_2)_nCOOH]_2$ , where  $n = 4, 5,$  and  $6$ , were prepared by the reaction of  $\omega$ -chloroalkanoic acids with sodium sulfide.<sup>9</sup> The nylon salts of hexamethylenediamine (HMDA) and *p*-xylylenediamine (PXDA) with these  $\omega,\omega'$ -thiodialkanoic acids were precipitated from ethanol solution and were polymerized. The characteristics of these are shown in Table I.

TABLE I  
Polyamides from  $\omega,\omega'$ -Thiodialkanoic Acids  $S[(CH_2)_nCOOH]_2$

Diamine	Dicarboxylic acid $n$	Polymer code	N salt m.p., °C.	Polymer m.p., °C.	$\eta_{sp}/c$
HMDA	4	6-5S5	164	185	0.78
PXDA	4	PXD-5S5	184	242	0.80
PXDA	5	PXD-6S6	178	236	0.73
PXDA	6	PXD-7S7	175	228	0.85

## RESULTS

### Copolyamides of Binary Systems

In order to investigate isomorphous replacement of methylene, ether, and thioether linkages, various copolymers of several different compositions

were prepared in binary systems, each containing two different acid residues: alkylene/oxaalkylene, alkylene/thiaalkylene, or oxaalkylene/thiaalkylene groups. The melting points and the reduced viscosities are listed in Tables II–IV. In the notation used the polyamide is X-Y, X representing diamine and Y representing dicarboxylic acid. PXD denotes *p*-xylylenediamine and simple numerals denote aliphatic diamine or dicarboxylic acid, while *mOn* and *mSn* show oxa- and thiaalkanedioic acids of the following formulas:  $\text{HOOC}(\text{CH}_2)_{m-1}\text{O}(\text{CH}_2)_{n-1}\text{COOH}$  and  $\text{HOOC}(\text{CH}_2)_{m-1}\text{S}(\text{CH}_2)_{n-1}\text{COOH}$ .

TABLE II  
Copolyamides Containing Ether Linkages

Copolyamide	Composition, mole-%	Copolyamide, m.p., °C.	$\eta_{sp}/c$
PXD-9	100	282	1.15
PXD-9/PXD-404	75/25	276	0.86
“	50/50	261	0.73
“	25/75	250	0.78
PXD-404	100	243	0.72
PXD-11	100	264	1.36
PXD-11/PXD-505	75/25	258	0.86
“	50/50	254	0.91
“	25/75	249	0.88
PXD-505	100	243	1.35
PXD-13	100	247	1.30
PXD-13/PXD-606	75/25	243	1.00
“	50/50	237	0.98
“	25/75	235	0.97
PXD-606	100	234	0.88
PXD-13/PXD-705	75/25	243	0.83
“	50/50	220	0.84
“	25/75	213	0.85
PXD-705	100	207	0.93
PXD-15	100	241	1.01
PXD-15/PXD-905	75/25	232	0.92
“	50/50	223	0.88
“	25/75	216	0.88
PXD-905	100	217	0.75
6-11	100	206	1.37
6-11/6-505	75-25	195	1.30
“	50/50	192	1.21
“	25/75	184	1.05
6-505	100	180	1.00

The relations between the melting points and the compositions of the copolyamides which contain two different acid residues of the same number of chain atoms are plotted in Figures 1–4. Linear relations between the densities and the compositions are also obtained in the following copolyamides; PXD-11/PXD-505, PXD-11/PXD-5S5, and PXD-505/PXD-5S5, (Fig. 5).

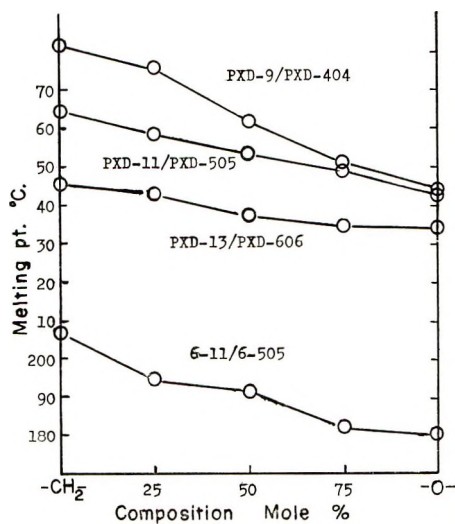


Fig. 1. Melting points vs. composition in copolyamides having symmetric oxaalkylene groups.

TABLE III  
Copolyamides Containing Thioether Linkages

Copolyamide	Composition, mole-%	Copolyamide m.p., °C.	$\eta_{sp}/c$
PXD-11/PXD-5S5	75/25	260	0.82
"	50/50	253	0.81
"	25/75	245	0.83
PXD-13/PXD-6S6	75/25	245	0.92
"	50/50	241	0.85
"	25/75	239	0.75
PXD-15/PXD-7S7	75/25	240	0.95
"	50/50	235	0.98
"	25/75	228	0.80
6-11/6-5S5	75/25	186	0.78
"	50/50	192	0.69
"	25/75	183	0.79

The glass transition temperatures of the copolyamides of PXD-11/PXD-505 are plotted against the concentration of the ether linkages in Figure 6. The glass transition temperature is depressed significantly by the introduction of ether linkages, and the degree of depression is practically unchanged in the composition range where the mole fraction of oxaalkanedioic acid is more than half.

### Copolyamides of Ternary Systems

Since very good linear relationships between the melting points and the compositions were observed in these copolyamides of binary systems, co-

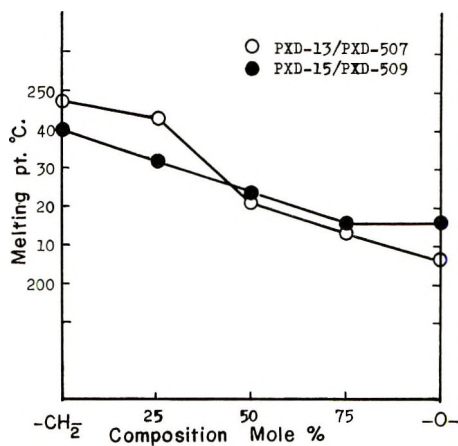


Fig. 2. Melting points vs. composition in copolyamides having unsymmetric oxaalkylene groups.

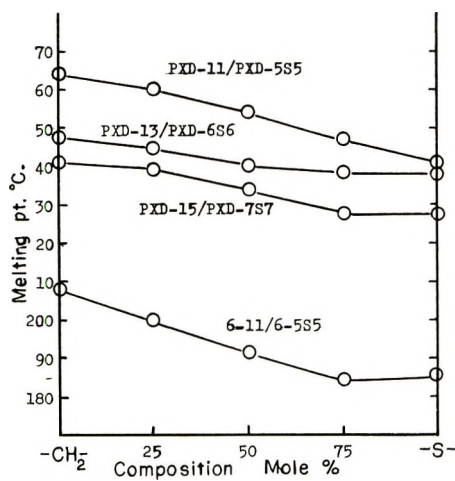


Fig. 3. Melting points vs. composition in copolyamides having thiaalkylene groups.

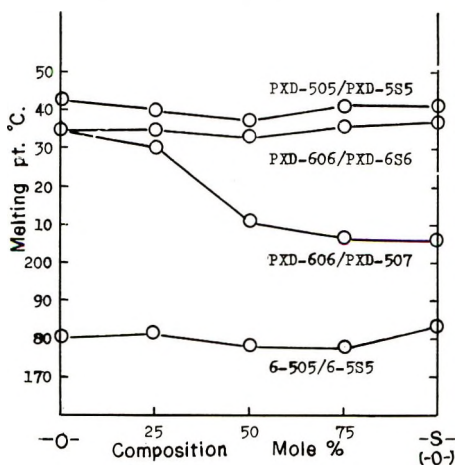


Fig. 4. Melting points vs. composition in copolyamides having both ether and thioether linkages and two different ether linkages.



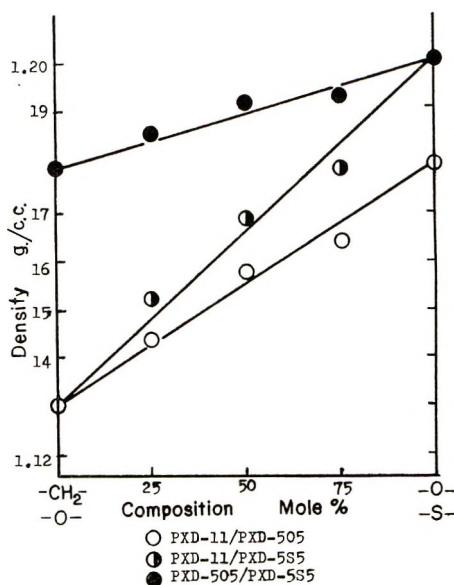


Fig. 5. Densities vs. composition in binary copolyamides.

TABLE IV  
Copolyamides Containing Both Ether and Thioether Linkages or Containing Two Different Ether Linkages

Copolyamide	Composition, mole-%	Copolyamide m.p., °C.	$\eta_{sp}/c$
PXD-505/PXD-5S5	75/25	243	0.89
"	50/50	238	0.78
"	25/75	242	0.90
PXD-606/PXD-6S6	75/25	234	0.85
"	50/50	232	0.78
"	25/75	234	0.83
6-505/6-6S6	75/25	182	0.92
"	50/50	178	0.86
"	25/75	179	0.83
PXD-606/PXD-705	75/25	231	0.99
"	50/50	210	0.81
"	25/75	205	0.75

polyamides of ternary systems were also investigated. Two copolyamides, PXD-11/PXD-505/PXD-5S5 and PXD-13/PXD-507/PXD-606, were selected for this study. A 1/1 or 3/1 molar mixture of the nylon salts PXD-505/PXD-5S5 or PXD-507/PXD-606 was combined with different amounts of the nylon salts PXD-11 or PXD-13 and then each mixture was converted into the copolyamide of ternary components. Results are shown in Table V.

The melting points of these ternary copolyamides are plotted against their compositions in Figures 7 and 8, while the relation between the densities

TABLE V  
Copolyamides of Ternary Systems

Copolyamide	Composition, mole-%	Copolyamide m.p., °C.	$\eta_{sp}/c$
PXD-11/PXD-505(1), PXD-5S5(1)	75/25	260	0.91
"	50/50	249	0.85
"	25/75	238	0.80
PXD-11/PXD-505(3), PXD-5S5(1)	75/25	262	0.85
"	50/50	249	0.79
"	25/75	244	0.86
PXD-13/PXD-507(1), PXD-606(1)	75/25	241	0.89
"	50/50	225	0.84
"	25/75	215	0.90
PXD-13/PXD-507(3), PXD-606(1)	75/25	241	0.91
"	50/50	227	0.85
"	25/75	210	0.87

and the compositions of the copolyamides PXD-11/PXD-505/PXD-5S5 is shown in Figure 9.

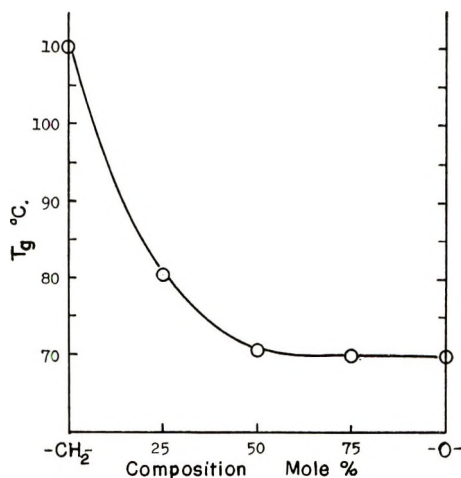


Fig. 6. Glass transition temperatures vs. composition in copolyamides PXD-11/PXD-505.

### X-Ray Examination of Copolyamides

From the bulk polymer samples, pieces about 1 mm. thick were cut and photographed with Ni-filtered  $\text{CuK}\alpha$  radiation. The lattice spacings were calculated from the diameters of the Debye-Scherrer rings. The lattice spacings of several copolyamides of different compositions from *p*-

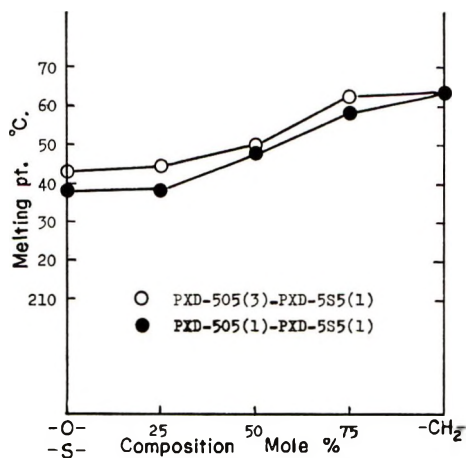


Fig. 7. Melting points vs. composition in the ternary copolyamides PXD-11/PXD-505/PXD-5S5.

xylylenediamine and dicarboxylic acids of 11 chain atoms involving ether or thioether linkages are shown in Table VI.

TABLE VI  
Lattice Spacings of Copolyamides

Copolyamide	Composition, mole-%	Lattice spacings, Å.							
		3.9	4.1	4.4	4.5	5.0	5.1	5.5	9.0
PXD-11/PXD-505	100/0	3.9	—	4.5	5.1	—	9.0	18.0	
	75/25	3.8	4.1	4.5	5.1	—	8.9	18.0	
	50/50	3.7	4.1	4.4	5.1	—	8.8	18.0	
	25/75	3.8	4.2	4.5	5.0	5.5	8.8	18.0	
	0/100	3.7	4.2	4.5	—	5.5	8.9	17.6	
PXD-11/PXD-5S5	100/0	3.9	—	4.5	5.1	—	9.0	18.0	
	75/25	3.8	4.1	4.4	5.0	5.6	9.1	17.5	
	50/50	3.8	4.0	4.5	5.0	5.5	9.1	17.6	
	25/75	3.7	4.1	4.5	5.0	5.5	9.0	17.9	
	0/100	3.6	4.0	4.6	4.9	5.4	—	18.0	
PXD-505/PXD-5S5	100/0	3.7	4.2	4.5	—	5.5	8.9	17.6	
	75/25	3.7	4.1	4.4	5.0	5.5	8.7	17.6	
	50/50	3.7	4.0	4.4	5.0	5.5	8.7	17.5	
	25/75	3.7	4.0	4.5	5.0	5.5	8.8	17.6	
	0/100	3.6	4.0	4.6	4.9	5.4	—	18.0	
PXD-11/PXD-505/PXD-5S5	25/50/25	3.6	4.1	4.3	5.0	5.5	8.5	17.4	

## DISCUSSION

The similarity in the length of a repeating chain unit has been deemed the most important requisite for the occurrence of isomorphous replacement in the crystal lattice or the interchange of different repeating units within the crystal lattice without reduction in crystallinity.

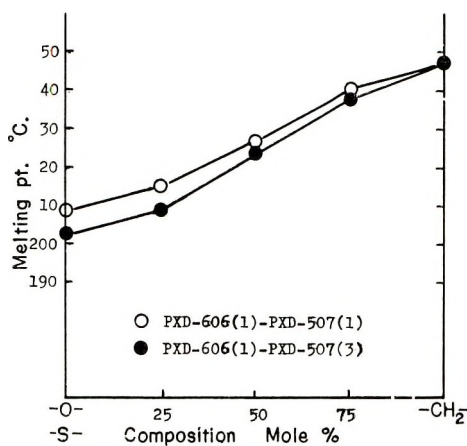


Fig. 8. Melting points vs. composition in the ternary copolyamides PXD-13/PXD-606/PXD-507.

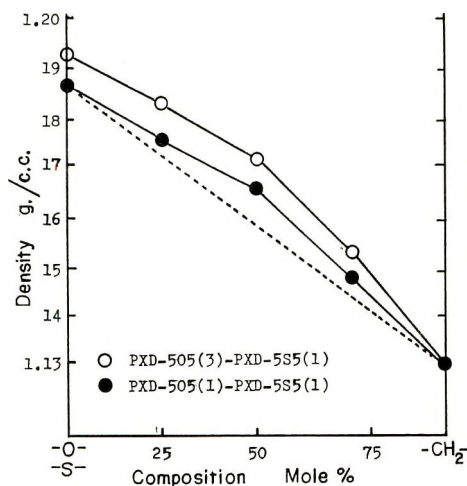


Fig. 9. Densities vs. composition in the ternary copolyamides PXD-11/PXD-505/PXD-5S5.

The copolyamides investigated in this work have the following repeating chain units:  $6-mYn$  represents  $-\text{HN}(\text{CH}_2)_6\text{NHCO}(\text{CH}_2)_m-\text{Y}-(\text{CH}_2)_n-\text{CO}-$  and  $\text{PXD}-mYn$ , represents  $-\text{HNCH}_2-\text{C}_6\text{H}_4-\text{C}_2\text{NHCO}-(\text{CH}_2)_m-\text{Y}-(\text{CH}_2)_n\text{CO}-$ . In  $Y$  we take the  $\text{C}-\text{C}-\text{C}$  angle as  $110^\circ$  and the length of the bond as 1.53 Å.; the  $\text{C}-\text{O}-\text{C}$  angle (in diethyl ether) is  $108^\circ$  and the bond length is 1.43 Å.; the  $\text{C}-\text{S}-\text{C}$  bond is taken as 1.82 Å.<sup>10</sup>

Tranter<sup>6</sup> investigated the isomorphous relationship in copolyamides containing  $p$ -phenylene linkages. In a series of binary copolymers based on homopolymers prepared from hexamethylenediamine and several dicarboxylic acids containing  $p$ -phenylene linkage such as  $p$ -phenylenedi-

propionic (3P3), 3-(*p*-carboxymethyl)phenylbutyric (2P4), 2-(*p*-carboxymethoxy)-phenylpropionic (3PO2), hydroquinonediacetic (2OPO2), and terephthalic acids, he found that only the 6-3P3/6-3PO2 system showed a linear relationship between the softening points and the compositions. From x-ray examination and infrared and density measurements, he pointed out that the form of the softening point versus composition curve is not a reliable criterion for isomorphous replacement, and it seems likely that this conclusion applies equally to the melting point versus composition curve. There is no evidence in the criterion that a linear melting point versus composition relationship indicates isomorphous replacement in copolymers. Isomorphism in copolyamides should be decided from the following observations; no practical difference is observed in the x-ray diagrams between the copolymer and the homopolymers and no large depression of crystallinity is observed in the copolymer.

In the preceding paper,<sup>8</sup> we pointed out from the comparison of the densities of the aliphatic polyamides having very long methylene chains with that of polymethylene that polyamide molecules are more loosely packed than polymethylene molecules in the crystal lattice. Therefore, it may be considered that there is enough space remaining in the polyamide crystal lattice for different repeating chain units with similar dimensions to interchange isomorphously. As shown in Table VI, the differences in lattice spacings among the homopolymers PXD-11, PXD-505, and PXD-5S5 are very small irrespective of the fact that the C—S bond length is longer by 0.4 Å. than that for C—O. Perhaps, the lengths of the repeating chain units of PXD-11, PXD-505, and PXD-5S5 are equalized through the arrangement of the bond angles in long sequences of atoms in these copolyamides. No practical differences in the lattice spacings within the repeating units so that isomorphous replacement is accomplished are actually found among these copolyamides with different compositions, even in the case of the ternary components. A good linear relationship is observed between the densities and the compositions in every binary copolyamide. In the case of the ternary copolyamides PXD-11/PXD-505/PXD-5S5, however, the densities at about 50% composition of PXD-11 are somewhat larger than those of the linear relation. The possible explanation for this is as follows: the chain molecules of the ternary copolyamide at those compositions may increase their flexibility and can be packed more compactly as a whole than those estimated from the linear relationship. From these experimental results, isomorphous replacement in these binary and ternary copolyamides can be ascertained. For all copolyamide systems investigated in this work, the relations between the melting points and the compositions show a good linearity. No minimum melting point can be found in any case. It is surprising that the melting points are practically unchanged in the whole range of composition in such copolyamides as PXD-505/PXD-5S5, PXD-606/PXD-6S6, and 6-505/6-5S5. Moreover, in the copolyamides of ternary systems, both PXD-11/PXD-505/PXD-5S5 and PXD-13/PXD-606/PXD-507, the lin-

ear relations of the melting points versus the compositions are followed as well as in the cases of binary systems.

Polymer melting points are generally expressed by:

$$T_m = \Delta H / \Delta S$$

where  $\Delta H$  is the heat of fusion and  $\Delta S$  is the entropy of fusion.

The value of the heat of fusion is related to the value of the cohesion energy. The cohesion energies of the replacing groups are as follows:  $-\text{CH}_2-$ , 680 cal./mole;  $-\text{O}-$ , 1000 cal./mole;  $-\text{S}-$ , 2200 cal./mole. These differences are small enough to be neglected for the whole repeating chain unit. At least,  $\Delta H$  may be estimated as a linear function against the polymer compositions. Taking the values in the case of the methylene linkage as the standard,  $\Delta H$  and  $\Delta S$  can be expressed as:

$$\begin{aligned}\Delta H &= (\Delta H)_C + (\Delta^2 H)y, \\ \Delta S &= (\Delta S)_C + (\Delta^2 S)y\end{aligned}$$

where  $y$  represents the mole fraction of the ether or the thioether linkages as the replacing groups.

Since  $(\Delta^2 S)y$  is considered to be small compared with  $(\Delta S)_C$ , and if  $(\Delta^2 S)y$  can be expressed by  $ky$ , proportional to the composition,  $T_m$  is written as:

$$T_m = \frac{\Delta H}{(\Delta S)_C} \cdot \frac{1}{1 + k'y} \cong \frac{\Delta H}{(\Delta S)_C} (1 - k'y)$$

where  $k' = k/(\Delta S)_C$ .

This relation expresses a straight line which passes through both melting points of the homopolymers and corresponds well with the experimental results. As a matter of fact, there is no substantial evidence that the entropy of fusion is expressed as a linear relation with the copolyamide compositions. However, it may be concluded from the above explanation that the entropy of fusion in these copolyamides increases steadily as the mole fraction of the hetero-atom linkages such as ether and thioether groups increases.

The authors are indebted to Dr. K. Katayama and Dr. T. Amano of the Textile Research Laboratory, who made the x-ray studies of these copolyamides.

### References

1. O. B. Edgar and R. Hill, *J. Polymer Sci.*, **8**, 1 (1952).
2. F. B. Cramer and R. G. Beaman, *J. Polymer Sci.*, **11**, 237 (1956).
3. A. J. Yu and R. D. Evans, *J. Am. Chem. Soc.*, **81**, 5361 (1959).
4. A. J. Yu and R. D. Evans, *J. Polymer Sci.*, **42**, 249 (1960).
5. M. Levine and S. C. Temin, *J. Polymer Sci.*, **49**, 241 (1961).
6. T. C. Tranter, *J. Polymer Sci. A*, **2**, 4289 (1964).
7. K. Saotome and K. Sato, *J. Polymer Sci. A-1*, **4**, 1303 (1966).
8. K. Saotome and H. Komoto, *J. Polymer Sci. A-1*, **4**, 1463 (1966).
9. A. N. Nesmeyanov, L. I. Zakharkin, and R. Kh. Freidlina, *Izv. Akad. Nauk SSSR, Otd. Khim. Nauk*, **1954**, 253.
10. R. B. Corey and L. Pauling, *Proc. Roy. Soc. (London)*, **B141**, 10 (1953).



### Résumé

Divers copolyamides contenant des unités de chaînes longues et périodiques ont été préparés au départ d'hexaméthylènediamine (HMDA) et de para-xylylènediamine (PXDA) avec des acides dicarboxyliques aliphatiques de 3 caractéristiques structurales; les acides  $\alpha,\omega$ -alkanedioiques,  $\alpha,\omega$ -oxaalkanedioiques, et  $\alpha,\omega$ -thiaalkanedioiques. Les combinaisons binaires et ternaires de ces acides dicarboxyliques ayant un même nombre de atomes de carbones avec la diamine fournissent des copolyamides hautement cristallins. Dans tous les cas de ces copolymères, les diagrammes des points de fusion en fonction de la composition correspondent à une relation linéaire, même dans le cas de systèmes ternaires. Par exemples, les points de fusion des copolyamides de HMDA avec le 6-oxaundécanedioique et du 6-thia-undécanedioique sont pratiquement inchangés dans tout le domaine de composition. La même relation est également observée dans les copolyamides correspondants du PXDA. La relation entre les densités et la composition correspondent à un diagramme linéaire dans tous les cas. À l'examen aux rayons-X, la périodicité de réseau de chaque copolyamide, est inchangée par la composition. Ces résultats démontrent que les liens méthylènes éthers et thioéthers sont en relation de substitution isomorphe l'un pour l'autre dans ce système copolyamide. En outre, la relation linéaire entre le point de fusion et la composition est expliquée en admettant que l'entropie de fusion de ces copolyamides varie linéairement conformément à la variation de composition.

### Zusammenfassung

Verschiedene Copolyamide mit langkettigen Bausteinen wurden aus Hexamethylen-diamin (HMDA) und *p*-Xylylendiamin (PXDA) mit aliphatischen Dicarbonsäuren von drei verschiedenen Strukturtypen, nämlich  $\alpha,\omega$ -Alkandicarbonsäure,  $\alpha,\omega$ -Oxaalkandicarbonsäure und  $\alpha,\omega$ -Thiaalkandicarbonsäure dargestellt. Binäre und ternäre Kombinationen dieser Dicarbonsäuren mit der gleichen Anzahl von Kettenatomen wie das Diamin lieferten hochkristalline Copolyamide. Bei allen diesen Copolymeren liefert die Auftragung der Schmelzpunkte gegen die Zusammensetzung sogar im Falle der ternären Systeme geradlinige Beziehungen. Es bleiben z.B. die Schmelzpunkte der Copolyamide von HMDA mit 6-Oxaundecandicarbonsäure und 6-Thiaundecandicarbonsäure praktisch im ganzen Zusammensetzungsbereich unverändert. Die gleiche Beziehung wird auch bei den gleichen Copolyamiden von PXDA beobachtet. Die Beziehung zwischen den Dichten und der Zusammensetzung zeigt in jedem Fall eine gute Linearität. Durch Röntgenuntersuchungen wird gezeigt, dass die Gitterabstände eines jeden Copolyamids nicht von der Zusammensetzung abhängen. Methylen-, Äther- und Thioätherbindungen können sich in diesen Copolyamidsystemen isomorph vertreten. Schliesslich wird die lineare Beziehung zwischen Schmelzpunkt und Zusammensetzung durch die Annahme erklärt, dass die Schmelzentropie bei diesen Copolyamiden linear von der Zusammensetzungsänderung abhängt.

Received August 30, 1965

Revised October 20, 1965

Prod No. 4960A

## Structure and Physical Properties of Glow Discharge Polymers. I. Polymers from Hydrocarbons

K. JESCH, J. E. BLOOR, and P. L. KRONICK, *Chemistry Division, The Franklin Institute Research Laboratories, Philadelphia, Pennsylvania*

### Synopsis

The polymers deposited from the vapors of pentane, ethylene, butadiene, benzene, styrene, and naphthalene subjected to glow discharge have been analyzed by infrared absorption techniques. The reaction products show unsaturation, hydrogenation, and branching in the polymer chains. Aromaticity is present only in polymers from aromatic monomers.

### INTRODUCTION

The formation of organic polymers by means of the glow discharge process of applying an electric field to the vapor of an organic molecule at low pressure, has been known for many years.<sup>1</sup> However, it is only recently<sup>2-4</sup> that attention has been given to the possible use of this process in producing useful surface coatings. Although there have been some investigations<sup>1,5</sup> into the nature of ions and radicals produced in the primary processes of the glow discharge, and in the volatile products,<sup>6,7</sup> very little attention has been given to the structure of the polymers, which are reported to have unusual electrical properties.<sup>8-10</sup>

We present here the results of an infrared spectroscopic investigation of the structure of a number of polymers produced by this technique as part of a general investigation into the relationship between structure and properties of thin polymer films.

### EXPERIMENTAL

Organic vapors were subjected to glow discharge in a glass chamber provided with heated walls, a vapor inlet, a thermometer, a pressure gauge, and two 1 in.  $\times$  3 in. parallel-plate electrodes 0.5 in. apart. The chamber was connected to a high-vacuum system evacuated to  $10^{-5}$  torr, and transferred to the vapor source by a turn of a stopcock. After 600 cm.<sup>3</sup> of vapor at 1 torr was admitted, the chamber was closed off, and the discharge was allowed to proceed at 250 v. ac, 10-20 ma. 20 kc./sec., the negative glow regions just covering the electrodes, which were aluminized Mylar film.

Infrared spectra were obtained by means of a Wilks Model 9 single-beam frustrated multiple internal reflection (FMIR) attachment with a KRS-5

reflector plate, transmitting from 300 to 4000  $\text{cm}^{-1}$ , and a Perkin-Elmer spectrophotometer, Model 521. The polymer layers were 0.5–5  $\mu$  thick, deposited on the aluminum side of the metallized plastic films. The metal layer prevented the infrared absorption of the Mylar from interfering.

## RESULTS AND DISCUSSION

The appearance of the films suggested an unusual polymer structure. All showed an unresolved distribution of absorption bands from the near ultraviolet into the violet spectral regions, suggesting a mixture of materials with extended conjugation or free valences. They adhered tightly to their aluminum substrates and showed no swelling in a variety of polar and nonpolar solvents. Solvents would introduce local strains resulting in rolling, peeling, and cracking of the thicker films from the electrodes.

The experiments were carried out with the primary objective of determining whether the glow-discharge polymers from different types of monomers actually differ among themselves in structure and secondly whether they were similar to polymers produced by more conventional polymerization methods. We investigated the structures of the polymers from (a) a typical saturated hydrocarbon, pentane, (b) a typical olefinic hydrocarbon containing one double bond, ethylene, (c) a conjugated olefin, butadiene, and (d) typical aromatic compounds, benzene and naphthalene. We also have compared the structures of glow-discharge polymers produced from ethylene, butadiene, and styrene with the structures of commercial samples of polyethylene, polybutadiene, and polystyrene.

### Pentane

The glow-discharge polymer produced from pentane was found to be identical with that produced from ethylene, showing that during the polymerization process considerable unsaturation was introduced into the saturated hydrocarbon either by hydrogen abstraction, by active radicals, or by direct C—H bond breaking. The absence of any band in the 720–750  $\text{cm}^{-1}$  expected for a long-chain aliphatic hydrocarbon shows that branches are formed along the length of every pentane molecule.

### Ethylene

The FMIR spectra of the glow-discharge polymer produced from ethylene is quite different from that of commercial polyethylene (Fig. 1). Unlike the latter, the glow-discharge polymer possessed considerable unsaturation.<sup>11–13</sup> A band at 960  $\text{cm}^{-1}$  is assigned to a  $\text{RCH}=\text{CHR}$  vibration, while a band at 890  $\text{cm}^{-1}$  could be due to either the out-of-plane deformation of a  $\text{RCH}=\text{CHR}'$  grouping or to the rocking vibration of a methyl group in a chain of three or four carbon atoms.<sup>13</sup> In the 720–750  $\text{cm}^{-1}$  region, which is characteristic of linear methylene chains of greater than four methylene groups,<sup>11</sup> there are no bands. At 1370  $\text{cm}^{-1}$  there is a band characteristic of a deformation of the  $\text{CH}_3$  group. The absence of any sign

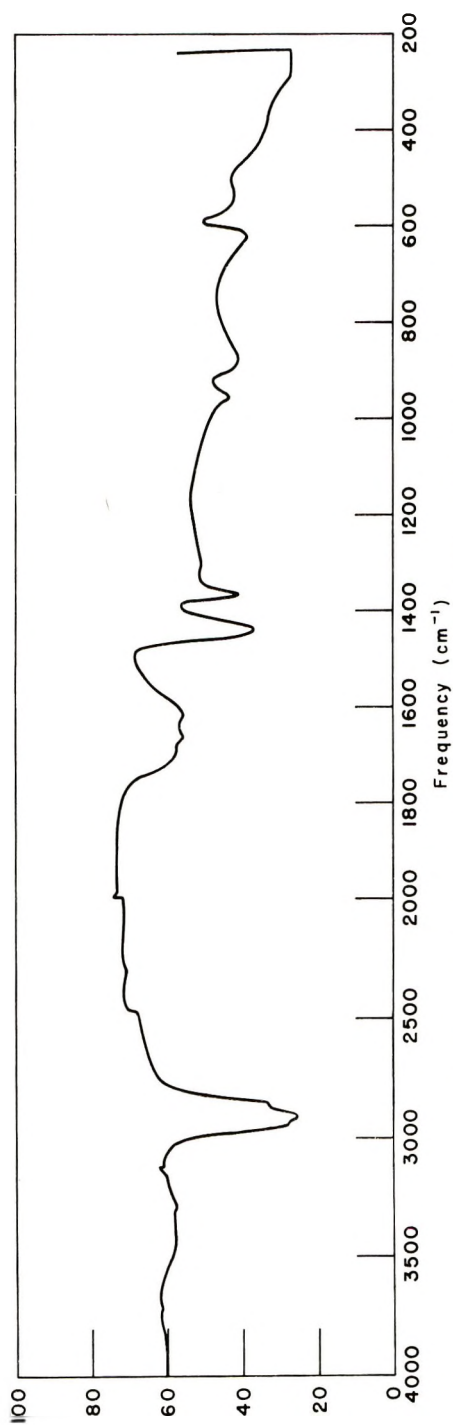


Fig. 1. Infrared spectrum of polymer produced in ethylene glow discharge.

of splitting in this band shows that there are no secondary or tertiary methyl groups.<sup>11,12</sup> At 1450  $\text{cm.}^{-1}$  is a band characteristic of the  $\text{CH}_2$  symmetric scissors vibration.

These results imply that the glow-discharge polymer from ethylene formed at low voltage contains vinylene groups joined by chains of one to three methylene groups with methyl groups on the ends of the chains. The insolubility and brittleness of the polymer indicate that it is highly cross-linked.

On allowing the polymer film to be exposed to air for 24 hr. the growth of a broad carbonyl band in the 1700–1720  $\text{cm.}^{-1}$  region was observed. This aging process was characteristic of all glow-discharge polymers produced from hydrocarbons. Some observations on the glow-discharge polymer from benzene suggest that free radicals trapped in the polymer are reacting with oxygen and water during the aging.

### Butadiene

The glow-discharge polymer produced from butadiene was similar to that produced from ethylene but with two extra bands. In the ethylene glow-discharge polymer the double-bond stretch was too weak to be observed, but in our butadiene glow-discharge polymer it was clearly seen at 1640  $\text{cm.}^{-1}$ . An extra band at 845  $\text{cm.}^{-1}$  due to the  $\text{RR}'\text{C}=\text{CHR}''$  group was also observed, indicating that, unlike in the ethylene glow-discharge polymer some of the crosslinking occurred on olefinic carbon atoms. On standing in air the carbonyl band appeared, but there was no weakening of the 1640  $\text{cm.}^{-1}$   $\text{C}=\text{C}$  stretching frequency, showing that aging to completion did not involve loss of unsaturation.

### Benzene

The FMIR spectra of glow-discharge polymer for benzene showed clearly the presence of aliphatic methylene (2925, 2850  $\text{cm.}^{-1}$ ), methyl (2950, 2875  $\text{cm.}^{-1}$ ), and aromatic  $\text{C}-\text{H}$  (3010  $\text{cm.}^{-1}$ ) groups. The presence of the methylene groups was confirmed by another band at 1445  $\text{cm.}^{-1}$  (methylene skeleton vibration); the presence of the methyl group, by a weak band at 1370  $\text{cm.}^{-1}$ . The presence of the aromatic ring was further confirmed by the presence of the characteristic vibrations at 1595 and 1495  $\text{cm.}^{-1}$ . In the 600–900  $\text{cm.}^{-1}$  region we confirmed the presence of two strong previously reported<sup>2</sup> bands at 745 and 690  $\text{cm.}^{-1}$ . These we assign to  $\text{CH}$  ( $\gamma$ ) and to a ring vibration ( $\delta$ ) respectively. The presence of these two vibrations and no others in this region clearly demonstrates that the benzene ring in the glow-discharge polymer is monosubstituted.

The presence of olefinic double bonds in the benzene glow-discharge polymer is shown by the presence of two bands at 835 and 960  $\text{cm.}^{-1}$ . Similar bands are present in the butadiene glow discharge polymer, and our interpretation is that they are due to vibrations of the  $\text{R}_1\text{R}_2\text{C}=\text{CR}_3\text{R}_4$  grouping. A band at 870  $\text{cm.}^{-1}$  could be due to either an olefinic grouping or a short methylene chain.<sup>13</sup>

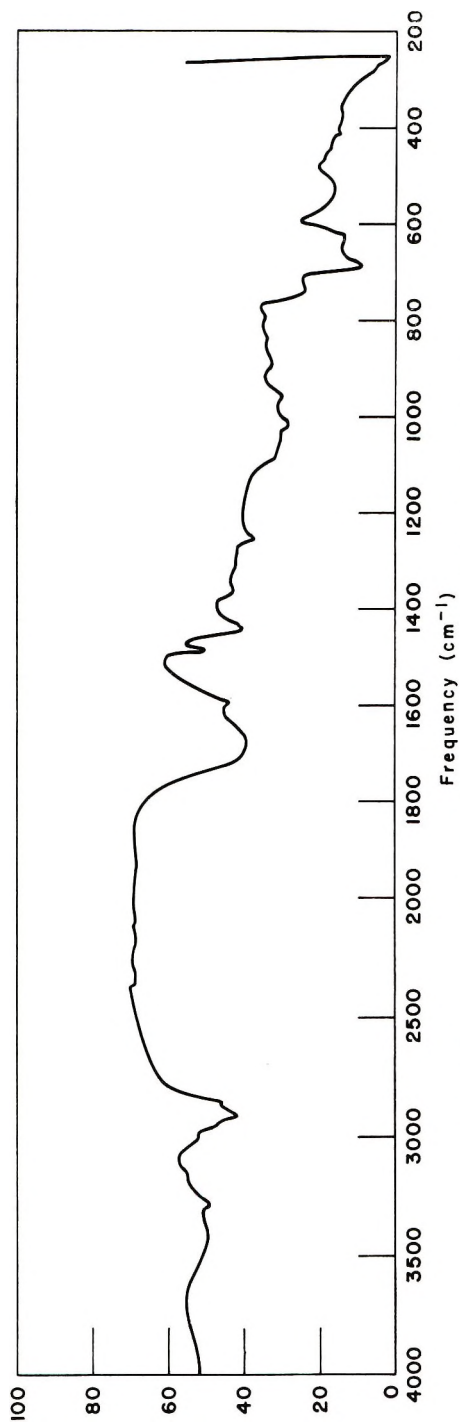


Fig. 2. Infrared spectrum of aged polymer produced in benzene glow discharge.



A novel feature that we have observed in the glow-discharge polymer from benzene, not present in the glow-discharge polymers from aliphatic compounds, is the presence of weak bands at 3300, 2200, and 2100  $\text{cm.}^{-1}$ . All these bands correlate with triple bonds.<sup>11</sup> The second and third of these frequencies are due to the  $\text{RC}\equiv\text{CR}$  and a  $\text{R}\equiv\text{CH}$  triple bond vibration, and the first one is due to an acetylenic  $\text{C}-\text{H}$  stretching frequency. We also observed a weak band at 1940  $\text{cm.}^{-1}$  which could be either one of the ring vibrational overtones or possibly due to the presence of cumulative double bonds ( $\text{C}=\text{C}=\text{C}$ ).

Changes were noted in the film after standing in air for 12 hr. The background absorption in the 1400–600  $\text{cm.}^{-1}$  region increased considerably, submerging the individual absorption bands in this region (Fig. 2). This loss of fine structure with increase in background absorption is typical of the behavior of many glow-discharge polymers on standing and is probably due to crosslinking brought about by combination of free valences on neighboring chains.

Simultaneously with the above changes, very large bands in the hydroxyl stretching region (3300–3600  $\text{cm.}^{-1}$ ) and in the carbonyl absorption region at 1700–1720  $\text{cm.}^{-1}$  appeared. The carbonyl band was also a feature of a fresh film prepared from moist benzene vapor but not from a dry benzene-oxygen mixture. A polymer film prepared by electron bombardment of silicone oil has been reported to age at a similar rate as evidenced by a gradual increase in dielectric constant.<sup>14</sup> The increase was suppressed when the film was stored in dry air or in vacuum. The change in dielectric constant could have been due to the appearance of carbonyl and hydroxyl groups. Evidently, the reactive sites in these polymer films incorporate water vapor or perhaps oxygen in the presence of water to yield a considerable number of polar groups in the final structure. Further study on the aging process is being made by using electron spin resonance techniques. We observe strong paramagnetism in these films, as have others.<sup>15</sup>

### Styrene

The fresh glow-discharge polymer from styrene was very similar to conventional polystyrene except for the presence of a few weak additional bands (Fig. 3) appearing at 3290, 2200, 2100, 2950, 2880, 1370, 1250, and 1290  $\text{cm.}^{-1}$ . The first three of these may be ascribed to the presence of the  $-\text{C}=\text{H}$  and  $-\text{C}=\text{CR}$  groupings, while the bands at 2950, 2880, and 1370  $\text{cm.}^{-1}$  may be assigned to vibrations of the methyl groups. The bands at 1250 and 1290  $\text{cm.}^{-1}$  are harder to assign, and it is only possible to speculate that they are due to the presence of ether linkages produced by the presence of minute traces of oxygen in the apparatus. They were however not observed in glow-discharge polymers produced from other hydrocarbons.

The fairly strong band at 1370  $\text{cm.}^{-1}$  is a characteristic difference between our glow-discharge polymer and conventional polystyrene. In the latter a weak band in this region appears and has been ascribed to a methylene group vibration.<sup>16</sup> It has also been established that an asymmetric

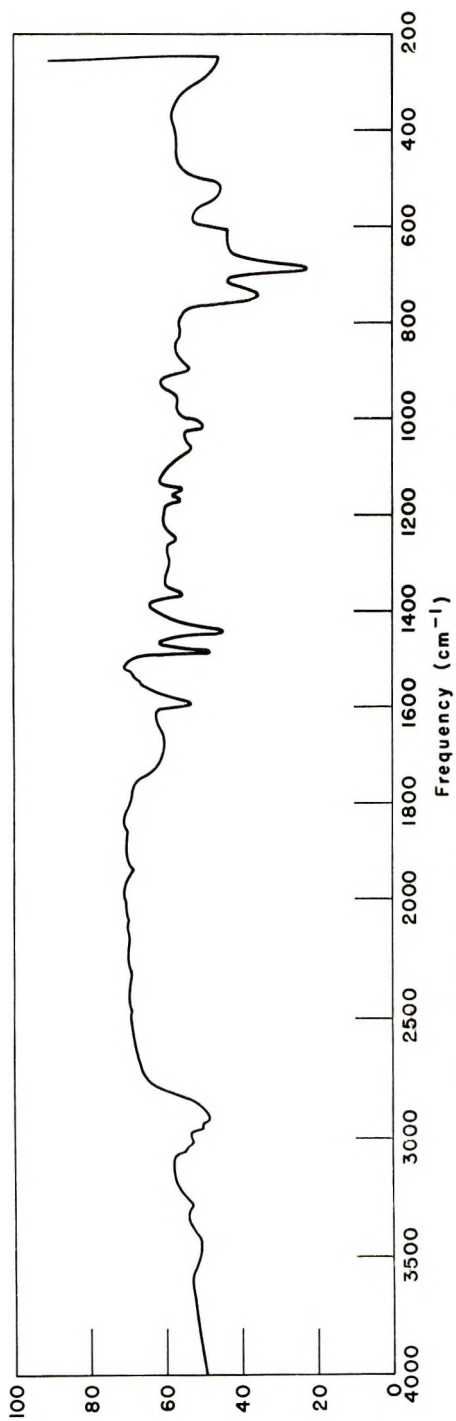


Fig. 3. Infrared spectrum of polymer produced in styrene glow discharge.

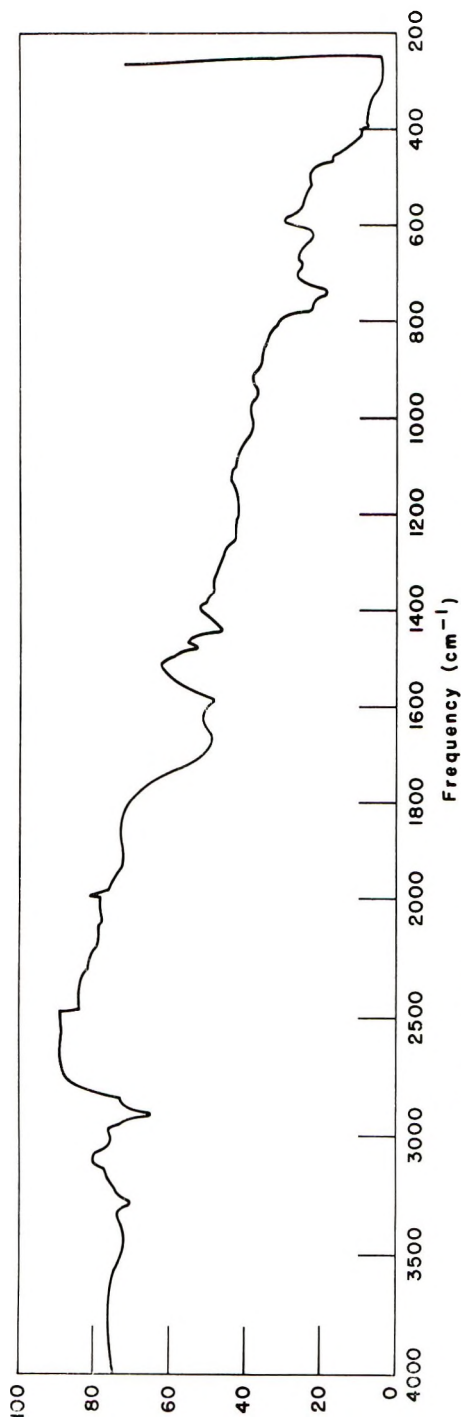


Fig. 4. Infrared spectrum of polymer produced in naphthalene glow discharge.

scissors vibration of a methyl group also occurs in this region.<sup>16,17</sup> Because of its intensity and the extra evidence of bands at 2950 and at 2880  $\text{cm.}^{-1}$  we prefer assigning this band in our glow-discharge polymers to the methyl group, which is apparently not present in conventional polystyrene. The absence of splitting of this band in our glow-discharge polymer of styrene is evidence for the absence of carbon atoms containing more than one methyl group.

On standing overnight the glow-discharge styrene polymer showed the usual appearance of carbonyl absorption in 1700–1720  $\text{cm.}^{-1}$  region and the loss in fine structure in the lower frequency region, giving a spectrum similar to those reported for polystyrene which has been exposed to ultra-violet light,<sup>19</sup> the changes in the case of the glow-discharge polymer being more pronounced.

### Naphthalene

By heating the glow-discharge cell to 60°C. sufficient vapor pressure of naphthalene was obtained to give a glow discharge when a potential of 300 v. was applied. The resulting polymer gave a somewhat different FMIR spectrum (Fig. 4) than benzene or polystyrene. It contained three bands characteristic of the presence of triple bonds (3290, 2100, and 2200  $\text{cm.}^{-1}$ ). The strong band at 1590  $\text{cm.}^{-1}$  shows conclusively the presence of an aromatic structure. A band at 1370  $\text{cm.}^{-1}$  previously assigned to a vibration of a methyl group is much weaker than in the glow-discharge polymer from styrene. Other bands at 1020, 950, 740, and 690  $\text{cm.}^{-1}$  are similar to those observed in the styrene glow-discharge polymer but are considerably broader. There is an extra band at 777  $\text{cm.}^{-1}$  not found in the other glow-discharge polymers. The presence of three bands, at 690, 745, and 777  $\text{cm.}^{-1}$ , could be construed as indicating either the presence of a 1,2,3- or 1,2,4-trisubstituted naphthalene ring, but the spectra are insufficiently detailed to decide between these possible assignments.

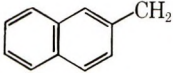
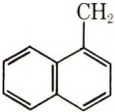
### CONCLUSIONS

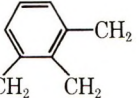
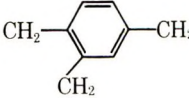
Prominent features found in glow-discharge hydrocarbon polymers are summarized in Table I.

Subjected to energetic electron bombardment in a glow discharge, hydrocarbon vapors produce cations which are collected on the cathode to form dense, crosslinked polymer films retaining few features of the original reactant. Whether the vapor is aromatic, olefinic conjugated or unconjugated, or fully saturated, the solid product is a dense, highly branched, and crosslinked polymer containing much identifiable unsaturation in the form of both olefinic bonds and free valences. These features may be responsible for the photoconductive properties of the films.<sup>10</sup> While aromaticity is not produced in the reaction, it is preserved in the products formed from aromatic reagents. As examples, *n*-pentane, ethylene, and butadiene yield similar polymers, with some small but reproducible variation due to the

TABLE I  
Structures in Glow-Discharge Polymers from Hydrocarbons

Starting vapor	Functional groups in polymers
Pentane	Branches at each pentane molecule, methyl chain ends, ( $-\text{CH}=\text{CH}-$ )
Ethylene	( $-\text{CH}_2-\text{CH}_2-\text{CH}_2-$ ), methyl chain ends, ( $-\text{CH}=\text{CH}-$ ), crosslinks at saturated carbons
Butadiene	( $-\text{CH}_2-\text{CH}_2-\text{CH}_2-$ ), ( $-\text{CH}=\text{CH}-$ ), methyl chain ends, and crosslinks at saturated and unsaturated carbons
Benzene	( $-\text{CH}_2-\text{CH}_2-\text{CH}_2-$ ), ( $-\text{CH}=\text{CH}-$ ), ( $-\text{C}\equiv\text{C}-$ ) or ( $-\text{C}=\text{C}=\text{C}-$ ), methyl chain ends, and phenyl side-groups
Styrene	Same as benzene, ( $\text{C}_6\text{H}_5$ )- $\text{CH}_2-$
Naphthalene	( $-\text{CH}_2-\text{CH}_2-\text{CH}_2-$ ), ( $-\text{CH}=\text{CH}-$ ), ( $-\text{C}\equiv\text{C}-$ ) or ( $-\text{C}=\text{C}=\text{C}$ ), methyl chain ends,

and  or 

or  or 

monomer structures. Benzene, styrene, and naphthalene produce polymers containing the features of the nonaromatic condensates, plus acetylene groups and the aromatic function of each starting material.

Freshly prepared, the polymers show a high reactivity to atmospheric vapor, reacting with water vapor to form carbonyl and hydroxyl groups and also perhaps undergoing internal crosslinking reactions. That these reactions do not drastically reduce the number of unsaturated valences actually observed (by ESR) may be taken as an indication of the rigidity of the polymer matrix, in which the molecular movements required for chemical rearrangements are restricted.

### References

1. E. G. Linder and A. P. Davis, *J. Phys. Chem.*, **35**, 3649 (1931).
2. R. M. Brick and J. R. Knox, *Mod. Packaging*, 123 (January 1965).
3. J. Goodman, *J. Polymer Sci.*, **44**, 351 (1960).
4. J. Harrick, *Ann. N. Y. Acad. Sci.*, **101**, 928 (1963).
5. H. Schuler and M. Stockburger, *Spectrochim. Acta*, **15**, 981 (1959).
6. A. Streitwieser, Jr. and H. R. Ward, *J. Am. Chem. Soc.*, **84**, 1065 (1962); *ibid.*, **85**, 539 (1963).
7. A. Brockes and H. König, *Z. Physik*, **152**, 75 (1958).
8. A. Bradley, *Insulation*, **10**, 31 (1964).
9. N. B. Bashara and C. T. Doty, *J. Appl. Phys.*, **35**, 3498 (1964).
10. A. Bradley, *Trans. Faraday Soc.*, **61**, 773 (1965).

11. L. J. Bellamy, *The Infra-red Spectra of Complex Molecules*, Methuen, London, 2nd Ed., 1958.
12. H. A. Szymanski, *Interpreted Infrared Spectra*, Vol. 1, Plenum Press, New York, 1964.
13. R. Zbinden, *Infrared Spectroscopy of High Polymers*, Academic Press, New York, 1964.
14. H. T. Mann, *J. Appl. Phys.*, **35**, 2173 (1964).
15. R. Mangiaracina and S. Mrozowski, *Proc. 5th Carbon Conf.*, **2**, 89 (1963).
16. S. Krimm, *Fortsch. Hochpolymer.-Forsch.*, **2**, 51 (1960).
17. J. K. Brown, N. Sheppard, and D. M. Simpson, *Discussions Faraday Soc.*, **9**, 261 (1950).
18. L. H. Cross, R. B. Richards, and H. A. Willis, *Discussions Faraday Soc.*, **9**, 235 (1950).
19. B. G. Achhammer, M. J. Reiney and F. W. Reinhart, *J. Res. Natl. Bur. Std.*, **47**, 116 (1951).

### Résumé

Les polymères déposés au départ de vapeurs de pentane, d'éthylène, de butadiène, de benzène et de styrène et de naphthalène soumis à une décharge ont été analysés par des techniques d'absorption infra-rouge. Les produits de réaction montrent une insaturation, une ramification dans les chaînes polymériques, de même qu'une hydrogénation. Un caractère aromatique est uniquement présent dans les polymères obtenus au départ de monomères aromatiques.

### Zusammenfassung

Die Polymeren, welche sich aus Pentan-, Äthylen-, Butadien-, Benzol-, Styrol- und Naphthalindämpfen unter der Einwirkung einer Glimmentladung abschieden, wurden mittels Infrarotabsorption analysiert. Die Reaktionsprodukte zeigten ungesättigte Gruppen, Hydrierung und Verzweigung in der Polymerkette. Aromatischen Charakter besitzen nur Polymeren aus aromatischen Monomeren.

Received September 21, 1965

Revised October 26, 1965

Prod. No. 4962A



## Anionic Oligomerization of Methacrylonitrile

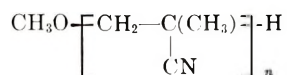
BEN-AMI FEIT,\* ERI HELLER, and ALBERT ZILKHA,  
*Department of Organic Chemistry, The Hebrew University, Jerusalem,  
Israel*

### Synopsis

The anionic oligomerization of methacrylonitrile by alcoholic solutions of sodium alkoxide in dimethyl sulfoxide, methanol and ethanol was studied. The  $\overline{DP}$  of the oligomers was directly proportional to the monomer concentration and inversely proportional to the alcohol concentration, in accordance with the equation  $\overline{DP} = K[\text{MAN}]/[\text{ROH}]$ ,  $K$  being equal to  $K_p/K_{tr}$ . The value of  $K$  in DMSO (with sodium methoxide-methanol) was  $2.9 \pm 0.2$ , in methanol was  $1.5 \pm 0.1$ , and in ethanol (with sodium ethoxide as initiator) was  $1.9 \pm 0.1$ . The physical properties of the oligomers are given.

### INTRODUCTION

In the anionic homogeneous polymerization of methacrylonitrile (MAN) in dimethylformamide (DMF) with methanolic solutions of sodium and potassium methoxides as initiators,<sup>1</sup> the degree of polymerization was given by the equation,  $\overline{DP} = K [\text{MAN}]/[\text{CH}_3\text{OH}]$ . The  $K$  values were low ( $\sim 2$ ) and consequently it was possible to obtain low liquid oligomers of the type



where  $n = 2-5$ . It was the purpose of the present work to extend this study, and to investigate the anionic oligomerization of methacrylonitrile in other aprotic solvents as well as in alcohols.

The methoxide-initiated anionic polymerization of methyl methacrylate was reported.<sup>2</sup>

### RESULTS

Oligomers having methoxy or ethoxy endgroups were prepared by methoxide or ethoxide initiation, respectively. The boiling points and the indices of refraction of both types of oligomers were about the same, being uninfluenced by the alkoxy moiety (Table I).

\* Present address: Chemistry Institute, University Tel-Aviv, Israel.

TABLE I  
Oligomers of Methacrylonitrile

$n$	B.p., °C./mm. Hg		$n_D$	B.p., °C./mm. Hg		$n_D$	OC <sub>2</sub> H <sub>5</sub> , %		C, %		H, %		N, %	
	113/2 142/10	175-180/2 238-245/2		1.438 1.464 1.478	115/2 145/10		177-182/2 238-245/2	1.439 1.465 1.480	Calcd.	Found	Calcd.	Found	Calcd.	Found
	$\text{CH}_3\text{O}-\left(\text{CH}_2-\overset{\text{CH}_3}{\underset{\text{CN}}{\text{C}}}-\text{H}\right)_n$ $\text{C}_2\text{H}_5\text{O}-\left(\text{CH}_2-\overset{\text{CH}_3}{\underset{\text{CN}}{\text{C}}}-\text{H}\right)_n$													
2 <sup>b</sup>							25.1	25.3	66.6	66.0	8.9	8.9	15.6	15.3
3							18.3	18.1	68.0	67.4	8.5	8.5	17.0	17.1
4							14.4	14.1	—	—	—	—	17.8	17.4

<sup>a</sup> Reported in ref. 1.

<sup>b</sup>  $\beta$ -Ethoxyisobutyronitrile, b.p. 39-40°C./2 mm., 56°C./10 mm., 62°C./14 mm., 68°C./18 mm.

### Oligomerization in Dimethyl Sulfoxide (DMSO)

The dependence of  $\overline{DP}$  on the  $[\text{MAN}]/[\text{CH}_3\text{OH}]$  ratio in this solvent was investigated at 25°C. with constant concentrations of monomer (2.98 mole/l.) and sodium methoxide (0.097 mole/l.). The initiator was added as a methanolic solution. The oligomerization started after an induction period, as was noticed by the appearance of a yellow color, which varied between a few seconds to several minutes, depending on the ratio ( $[\text{MAN}]/[\text{ROH}]$ ); lower ratios led to longer induction periods.

The oligomerizations were carried out to full conversion. The degree of polymerization was proportional to the  $[\text{MAN}]/[\text{CH}_3\text{OH}]$  ratios. The values of  $K$ , defined by the equation  $\overline{DP} = K[\text{MAN}]/[\text{CH}_3\text{OH}]$ , were approximately constant ( $K \sim 3$ ) for the various  $[\text{MAN}]/[\text{CH}_3\text{OH}]$  ratios used. (Table II).

Oligomerization in DMSO with a methanolic solution of sodium hydroxide resulted in formation of  $\text{CH}_3\text{O} + \text{CH}_2\text{C}(\text{CN})(\text{CH}_3) +_n\text{H}$  type oligomers and not of  $\text{HO} + \text{CH}_2\text{C}(\text{CN})(\text{CH}_3) +_n\text{H}$  type oligomers.  $K$  values were about the same as those obtained with the methoxide initiator.

An appreciable yield of oligomers was also obtained under similar experimental conditions on using for initiation an aqueous solution of potassium hydroxide. The oligomers obtained were very high-boiling. Only a small part of the oligomer mixture distilled out in the range 100–130°C./1 mm. Hg, the rest being nondistillable and viscous. The nature and physical properties of these oligomers were not investigated.

### Oligomerization in Methanol and Ethanol

While the oligomerization of MAN in the aprotic solvents, dimethyl sulfoxide or dimethylformamide, was carried out successfully at room tem-

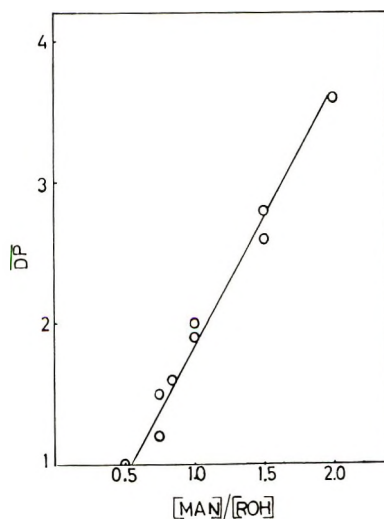


Fig. 1. Dependence of the degree of polymerization on the ratio  $[\text{MAN}]/[\text{C}_2\text{H}_5\text{OH}]$ . ( $K = 1.85$ ).

TABLE II  
Oligomerization of Methacrylonitrile in DMSO by Sodium Methoxide<sup>a</sup>

Expt. no.	$\frac{[\text{MAN}]}{[\text{CH}_3\text{OH}]}$	Yield, % <sup>b</sup>	Yield of oligomers, % <sup>c</sup>				$\bar{DP}^d$	$K$
			$n = 1$	$n = 2$	$n = 3$	$n = 4$		
M9	1.2	99	10	15	10	40	3.5	2.9
M12	1.2	100	9	20	31	35	3.0	2.5
M5	1.0	96	35	20	10	—	2.8	2.8
M10	1.0	93	12	38	30	—	2.8	2.8
M6	0.85	95	25	25	10	—	3.0	3.5
M7	0.75	95	22	35	8	—	2.5	3.3
M8	0.60	80	25	50	5	—	1.7	2.8
							$\bar{K} = 2.9 \pm 0.2$	

<sup>a</sup> Experimental conditions: sodium methoxide (0.097 mole/l.) was added to a solution of monomer (2.98 mole/l.) and methanol in DMSO. The total volume of the reaction mixture was 100 ml., and the temperature of reaction was  $25 \pm 2^\circ\text{C}$ .

<sup>b</sup> Per cent of reacted MAN as determined by titration.<sup>1</sup>

<sup>c</sup> Based on the fraction isolated by distillation from the oligomerization mixture. The percentage is out of the total mixture.

<sup>d</sup> Based on the methoxyl content of the oligomerization mixture.

TABLE III  
Oligomerization of Methacrylonitrile in Alcohols

Expt. no.	[MAN] [ROH]	Yield, % <sup>a</sup>	Yield of oligomers, %				$\bar{DP}$	$K$
			$n = 1$	$n = 2$	$n = 3$	$n = 4$		
Series A <sup>b</sup>								
P1	2.0	95	9	17	10	22	3.6	1.8
P10	2.0	90	20	26	16	34	2.5	1.3
P11	1.5	70	30	35	14	—	2.1	1.4
P6	1.33	89	50	20	10	—	1.8	1.4
P5	1.0	87	70	15	15	—	1.5	1.5
P12	1.0	72	70	15	15	—	1.4	1.4
								$\bar{K} = 1.5 \pm 0.1$
Series B <sup>c</sup>								
R6	2.0	92	7	17	25	32	3.6	1.8
R7	2.0	90	10	14	24	17	3.6	1.8
R2	1.5	81	25	28	17	17	2.6	1.8
R8	1.5	80	13	25	17	—	2.8	1.9
R1	1.0	83	38	27	7	9	2.0	2.0
R3	1.0	100	36	28	15	—	1.9	1.9
R4	0.84	90	57	31	—	—	1.6	1.9
R5	0.75	87	71	23	—	—	1.5	2.0
R10	0.75	78	90	—	—	—	1.2	1.6
R11	0.50	83	97	—	—	—	1.0	2.0
								$\bar{K} = 1.9 \pm 0.1$

<sup>a</sup> Determined by titration.

<sup>b</sup> Oligomerization in methanol. Sodium methoxide 0.007 mole, monomer 0.358 mole.

<sup>c</sup> Oligomerization in ethanol. Sodium ethoxide 0.011 mole, monomer 0.358 mole.

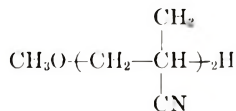
perature with methanol and ethanol as solvents reflux temperatures were essential for the oligomerization. The derived sodium alkoxides were used as initiators.

The dependence of the degree of oligomerization on the  $[\text{MAN}]/[\text{ROH}]$  ( $\text{R} = \text{CH}_3, \text{C}_2\text{H}_5$ ) ratios was investigated using constant amounts of initiator and monomer. The average degree of oligomerization which was calculated from alkoxy endgroup analysis, was directly proportional to the  $[\text{MAN}]/[\text{ROH}]$  ratio (Figure 1) (Table III). The value of  $K$  in the case of methanol was smaller than in the case of ethanol, 1.5 and 1.9, respectively.

Some oligomerization experiments were carried out with the use of benzyltrimethylammonium methoxide-methanol as initiator. The results were similar to those obtained with sodium methoxide.

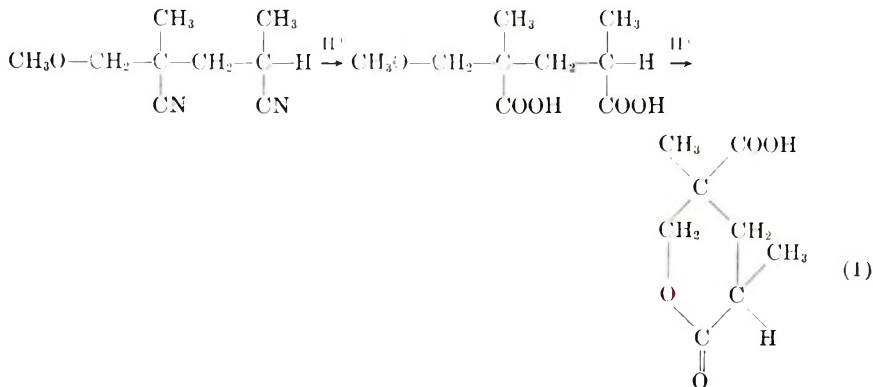
### Hydrolysis of the Oligomers

The dimer



was heated under reflux with hydrochloric acid for several hours. From the reaction mixture a product was isolated, m.p.  $110^\circ\text{C}$ ., which from its physical properties and IR spectrum was identical with that of 2-methyl-4-carboxy-4'-methyl valerolactone, obtained by hydrolysis of the respective oligomer of methyl-methacrylate.<sup>2</sup>

The hydrolysis thus proceeded by the path shown in eq. (1).

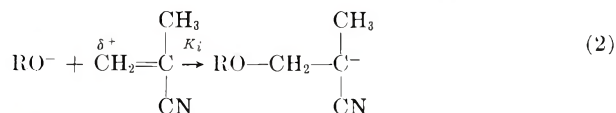


### DISCUSSION

Elementary analyses, hydrolyses experiments, and infrared spectra indicated that the general structure of the oligomers isolated was  $\text{RO}-[\text{CH}_2-\text{C}(\text{CN})(\text{CH}_3)]_n\text{H}$ , with  $\text{R} = \text{CH}_3, \text{C}_2\text{H}_5$ ,  $n = 1-4$ , which obviously was the result of a direct nucleophilic attack of the alkoxide anion on the

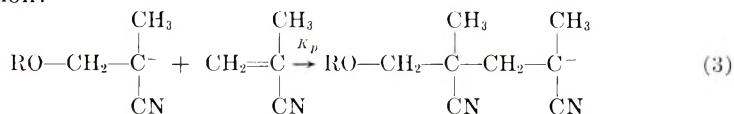


acidic double bond of the monomer in the initiation step, as shown in eq. (2)

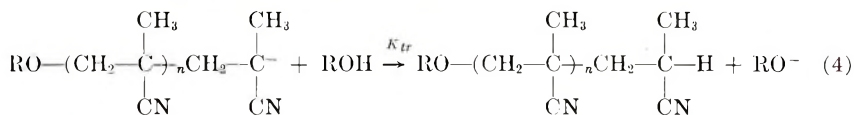


Since  $\overline{\text{DP}}$  is given by  $\overline{\text{DP}} = R_p/R_t$ , where  $R_p$  and  $R_t$  are the rate constants of the propagation and termination steps, respectively, the linear dependence of  $\overline{\text{DP}}$  on the ratio  $[\text{MAN}]/[\text{ROH}]$  (Tables II and III, Fig. 1) should be the result of the propagation and termination steps shown in eqs. (3) and (4), respectively.

Propagation:



Termination by transfer to the alcohol:



Based on this proposed mechanism, the constant  $K$  calculated was actually the ratio of the propagation and transfer to alcohol rate constants,  $K = K_p/K_{tr}$ .

The formation of significant amounts of  $\beta$ -alkoxyisobutyronitrile, is due to protonation of  $\text{RO}-\text{CH}_2-\overset{\text{CH}_3}{\underset{\text{CN}}{\text{C}}}^--(\text{CH}_3)-\text{CN}$  formed in the initiation step. The basicity of the carbanion in this compound is different from that of the growing end of oligomers having  $\overline{\text{DP}} \geq 2$  due to the inductive withdrawing effect of the alkoxy group, and consequently the transfer constant to the alcohol will be different from that of the transfer constants of the higher oligomers. However the constancy of the  $K$  values found in DMSO, in methanol, and in ethanol (Tables II and III and Fig. 1) indicates that the overall change caused in the average value of the transfer rate constant was not very significant.

It is interesting to add in this connection that in the previously studied oligomerization of MAN by  $\text{CH}_3\text{O}^--\text{CH}_3\text{OH}$ , the constant  $K$  ( $\overline{\text{DP}} = K [\text{M}]/[\text{ROH}]$ ) found in the polymerization region ( $[\text{MAN}]/[\text{CH}_3\text{OH}] = 5-50$ ) was the same ( $K = 2-2.2$ ) as that found in the oligomerization region in the presence of larger concentrations of methanol ( $[\text{MAN}]/[\text{CH}_3\text{OH}] = 1-2$ ).

In the case of acrylonitrile, it was shown in the study of the kinetics of the cyanoethylation of alcohols<sup>3,4</sup> that the rate-determining step was that of the nucleophilic addition of the alkoxide anion to the double bond, which was followed by a fast protonation by the alcohol. Indeed, the rate differences between propagation and transfer to alcohol in the case of AN are so great that under the same conditions as those used in the oligomeriza-

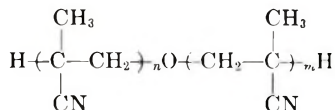
tion of MAN, practically no oligomers of AN could be obtained, and only  $\beta$ -alkoxypropionitrile or polymers were obtained.<sup>5</sup>

Different values of  $K$  were found for the oligomerization of MAN by methanolic sodium methoxide in various solvent systems:  $K(\text{DMSO}) = 2.9 \pm 0.2$ ;  $K(\text{DMF})^1 = 2.0\text{--}2.2$ ;  $K(\text{CH}_3\text{OH}) = 1.5 \pm 0.1$ . These differences are due to changes in the ratio of  $K_p/K_{tr}$ . Increasing  $K_p$  more than  $K_{tr}$  will lead to an increase in  $K$ . The relatively lower value of  $K$  in methanol might be due, besides, to the higher temperature of the oligomerization, to the low nucleophilic reactivity of the methanol-solvated propagating carbanions, (hence smaller  $K_p$ ) as compared to the relatively high reactivity of the nonsolvated (or less solvated) carbanions in mixed methanol aprotic solvents,<sup>6-8</sup> such as DMF or DMSO. The higher value of  $K$  in DMSO as compared to its value in DMF might be due to the greater solvation and dielectric constant of DMSO. The strong interaction between DMSO and hydroxylic materials<sup>9</sup> might have reduced the concentration and availability of "free" alcohol for solvation of carbanions and for termination by transfer to alcohol, leading to higher values of  $K$ .

The higher  $K$  value for the oligomerization in ethanol ( $1.9 \pm 0.1$ ) as compared to methanol may be due to the lower acidity of ethanol which would cause both a reduced solvation of nucleophiles and a lower extent of transfer reaction to alcohol (smaller  $K_{tr}$ ).

The optimal preparative reaction conditions were different for each solvent system. On using  $[\text{MAN}]/[\text{ROH}] \leq 1$ , within the range investigated, the mixture of oligomers obtained consisted essentially of  $\beta$ -alkoxyisobutyronitrile,  $n = 1$ , on carrying out the oligomerization in the pure alcohol (Table III), while the yield of this product was relatively low (20-25%) in a mixed alcohol-protic solvent (Table II).

The fact that on using alcoholic potassium hydroxide, the oligomers contained the methoxyl endgroup is due to the presence of the equilibrium:  $\text{KOH} + \text{CH}_3\text{OH} \rightleftharpoons \text{CH}_3\text{OK} + \text{H}_2\text{O}$ . Such an equilibrium was shown by Caldin and Long<sup>10</sup> to be almost completely in favor of the formation of the alkoxide, which served in the present case as the initiator of the oligomerization. In the cyanoethylation of water,<sup>11</sup> it was found that  $\beta,\beta$ -dicyanoethyl ether,  $\text{NCCH}_2\text{CH}_2\text{OCH}_2\text{CH}_2\text{CN}$ , was formed, so that it is possible that the oligomers obtained in the oligomerization in the presence of water have the structure:



## EXPERIMENTAL

### Materials

The purification of materials and isolation of the oligomers was carried out as previously described.<sup>1</sup> Dimethyl sulfoxide was purified in the same manner as DMF.<sup>1</sup>

### Oligomerization of MAN in DMSO by a Methanolic Solution of Sodium Hydroxide

A methanolic solution of sodium hydroxide (10 ml., 2.4*N*) was added to a solution of MAN (25 ml.) and methanol (10 ml.) in DMSO (55 ml.). The molar ratio of methacrylonitrile to methanol was 0.6. The reaction was carried out at room temperature for several hours. The yield of the mixture of oligomers was 16.5 g. The average degree of polymerization was 1.7, corresponding to  $K = 2.8$ . On fractionation *in vacuo* the following fractions were obtained:  $\beta$ -methoxyisobutyronitrile, 50%; dimer, 35%; trimer, 10%; and higher nondistillable oligomers, 5%.

### Oligomerization of MAN in DMSO by Aqueous Potassium Hydroxide

The general procedure for the oligomerization in DMSO was followed. An aqueous solution of potassium hydroxide (10.8 ml. 3.02*N*) was added to a solution of methacrylonitrile (25 ml.) in DMSO (64.2 ml.). The molar ratio of methacrylonitrile to water was 0.5. The yield of the mixture of oligomers isolated was 15 g. On fractionation, 7.5 g. of the mixture distilled at 95–100°C./0.5 mm. Hg, 1.5 g. at 130°C./0.5 mm. Hg, and 6 g. of higher oily oligomers remained as nondistillable residue.

### Oligomerization of Methacrylonitrile in Methanol and Ethanol

The oligomerization was carried in a three-necked flask fitted with a self-sealing rubber cap through which the reagents were added with syringes, and a condenser fitted with a calcium chloride tube. The whole system was flushed with argon before introducing reagents, and the reaction was carried out under argon. The reaction was carried out for several hours at reflux temperature. An aliquot portion was removed and titrated for unreacted methacrylonitrile by the dodecyl mercaptan method.<sup>1</sup> The oligomers were isolated as described before.<sup>1</sup>

### Oligomerization in Methanol by N-Benzyltrimethylammonium Methoxide

Trimethylbenzyl ammonium methoxide in methanol (4.4 ml. 2.05*N*) was added to methacrylonitrile (30 ml.) and methanol (6.4 ml.),  $[\text{MAN}]/[\text{CH}_3\text{-OH}] = 1.33$ . The reaction mixture was heated for a short time at 60°C. and then was left overnight at room temperature. The yield of the mixture of oligomers was 19g. Fractionation of the mixture gave  $\beta$ -methoxyisobutyronitrile (32%), dimer (40%), trimer (13%), and higher oligomers (15%).  $\overline{\text{DP}}$  from methoxyl determination was 2.2, and  $K$  was 1.6.

### Hydrolysis and Lactonization of the Dimer of Methacrylonitrile

The dimer,  $\text{CH}_3\text{O-CH}_2\text{-C}(\text{CN})(\text{CH}_3)\text{-CH}_2\text{CH}(\text{CN})\text{CH}_3$ , (10 g.) was heated with concentrated hydrochloric acid (80 ml.) under reflux for 8 hr. The reaction mixture was cooled and the precipitated  $\text{NH}_4\text{Cl}$  (5.5 g., 86%) filtered off. The filtrate was concentrated *in vacuo* and extracted with

benzene. The benzene was dried over anhydrous magnesium sulfate, filtered and distilled. The solid residue was recrystallized from acetone to give a product, m.p. 110°C. Its infrared spectrum showed absorption bands at (5.8  $\mu$ , 9.7  $\mu$ ) ( $\delta$ -lactone), while the nitrile absorption band at 4.5  $\mu$  disappeared. This product was identical with that obtained in the acidic hydrolysis of the analogous methyl methacrylate dimer;<sup>3</sup> molecular weight 172, found 170 (by titration with sodium methoxide).

### References

1. B. A. Feit, J. Wallach, and A. Zilkha, *J. Polymer Sci. A*, **2**, 4743 (1964).
2. Th. Volker, A. Neumann, and U. Baumann, *Makromol. Chem.*, **63**, 182 (1963).
3. B. A. Feit and A. Zilkha, *J. Org. Chem.*, **28**, 406 (1963).
4. M. Wronski and J. Bogdanski, *Zeszyty Nauk Univ. Lotz, Ser. II*, **14**, 153 (1963).
5. Y. Barzilai, B. A. Feit, and A. Zilkha, unpublished results.
6. B. A. Feit, J. Simreich, and A. Zilkha, *J. Org. Chem.*, **28**, 3245 (1964).
7. A. J. Parker, *Quart. Rev. (London)*, **16**, 163 (1962).
8. D. J. Cram, B. Rickborn, C. A. Kingsbury, and P. Haberfield, *J. Am. Chem. Soc.* **83**, 3678 (1961).
9. E. Tommila and M. A. Murto, *Acad. Chem. Scand.*, **17**, 1947 (1963).
10. E. F. Caldin and G. Long, *J. Chem. Soc.*, **1954**, 3737.
11. H. A. Bruson, in *Organic Reactions*, Vol. 5, R. Adams, Ed., Wiley, New York, 1949, p. 89.

### Résumé

L'oligomérisation anionique du méthacrylonitrile dans des solutions alcooliques d'alkoxyde de sodium dans le diméthylsulfoxyde, le méthanol et l'éthanol a été étudiée. Le degré de polymérisation des oligomères était directement proportionnel à la concentration en monomère, inversement proportionnel à la concentration en alcool, ceci en accord avec l'équation  $\overline{DP} = K[\text{MAN}]/[\text{ROH}]$ , où  $K$  est égal au rapport  $K_p/K_t$ . La valeur de  $K$  dans le diméthylsulfoxyde (en utilisant le méthoxyde de sodium dans le méthanol) était de  $2.9 \pm 0.2$ , dans le méthanol  $1.5 \pm 0.1$ , et dans l'éthanol (utilisant l'éthoxyde de sodium comme initiateur)  $1.9 \pm 0.1$ . Les propriétés physiques des oligomères sont indiquées.

### Zusammenfassung

Die anionische Oligomerisation von Methacrylnitril durch alkoholische Natriumalkoxydlösungen in Dimethylsulfoxyde, Methanol und Athanol wurden untersucht.  $\overline{DP}$  der Oligomeren war der Monomerkonzentration direkt und der Alkoholkonzentration umgekehrt proportional, in Übereinstimmung mit der Gleichung  $\overline{DP} = K[\text{MAN}]/[\text{ROH}]$ , wo  $K = K_p/K_t$  ist. Der Wert von  $K$  betrug in DMSO (mit Natriummethoxyd/Methanol)  $2,9 \pm 0,2$ , in Methanol  $1,5 \pm 0,1$  und in Athynol (mit Natriumäthoxyd als Starter)  $1,9 \pm 0,1$ . Die physikalischen Eigenschaften der Oligomeren werden beschrieben.

Received September 27, 1965

Prod. No. 4968A

## Chemistry of Polybutadiene-Iron Carbonyl Systems

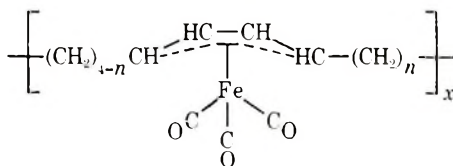
M. BERGER and T. A. MANUEL, *Central Basic Research Laboratory, Esso Research and Engineering Company, Linden, New Jersey*

### Synopsis

The treatment of polybutadienes with iron carbonyls results in formation of polymers containing tricarbonyl(conjugated diene)iron units  $[C_8H_{12}Fe(CO)_3]$  and also results in geometrical isomerization of free double bonds. Heating of the iron carbonyl-containing polymers gives ferromagnetic products with enhanced thermal stability. The incorporation of iron carbonyl groups into the polymer is favored by basic solvents and high temperatures, the geometrical isomerization by acidic solvents and low temperatures. Steric factors are powerful in determining the rate of isomerization.

### Introduction

We have prepared polybutadiene-iron carbonyl complexes, which constitute examples of that class of organometallic polymers having a hydrocarbon backbone bonded to metal-containing groups. The products of the reaction between polybutadiene and iron carbonyls are effectively copolymers of uncomplexed polybutadiene  $(C_4H_6)_n$  and tricarbonyl(diene)-iron units  $[C_8H_{12}Fe(CO)_3]$  of the type known for many nonpolymeric unsaturated hydrocarbons.<sup>1</sup> We believe that the initially isolated double bonds in the polymer become conjugated under the reaction conditions so that the complexed portion of the product may be depicted by I,



I

where  $n = 0-4$ .

Those double bonds not involved in formation of the complex I are found to have undergone geometrical isomerization; it is probable that some of them have migrated as well. Since the reactions leading to formation of the iron carbonyl complex and to isomerization of free double bonds must be closely related, it is not possible to separate the two phenomena completely, although with proper selection of reaction conditions one or the other may be maximized.



### Experimental

In a typical experiment a solution of 3.5 g. [65 mmole of  $(C_4H_6)_n$ ] of *Cis*-4 polybutadiene (Phillips Petroleum Co.) in 315 ml. of benzene was mixed with 8.0 g. (16 mmole) of  $Fe_3(CO)_{12}$  and 35 ml. of 1,2-dimethoxyethane. This mixture was refluxed under nitrogen for 3 $\frac{1}{2}$  hr., cooled, and added dropwise to a stirred mixture of 1 l. of 95% ethanol with 50 ml. of concentrated hydrochloric acid, giving a clear yellow solution and a rubbery yellow product. Infrared analysis of a portion of the product by a method based on that of Hampton<sup>2</sup> showed the distribution of free double bonds remaining to be 78% *cis*-1,4, 18% *trans*-1,4, and 4% vinyl; the portion of the product composed of  $[C_8H_{12}Fe(CO)_3]$  units was deduced to be 38% by weight. Combustion analysis for iron indicated the presence of 36% by weight of  $[C_8H_{12}Fe(CO)_3]$  units, corresponding to 20% by weight of  $Fe(CO)_3$  units. The infrared spectrum also exhibited the pair of carbonyl stretching frequencies in the region of 2000  $cm^{-1}$  characteristic of tricarbonyl(conjugated diene)iron complexes.<sup>1</sup> Figure 1 shows the typical infrared spectrum of a complexed polybutadiene.

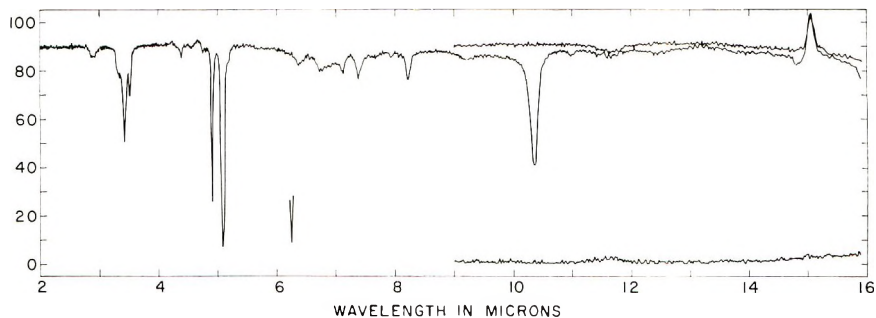


Fig. 1. Infrared spectrum of polybutadiene-iron carbonyl complex. Initial polymer: *Trans*-4 polybutadiene; product: 22 wt.-%  $[Fe(CO)_3]$ ; 61% uncomplexed polybutadiene-79% *trans* isomer.  $CS_2$  solution; concentration 5.0 g./l.

In another typical experiment a solution of 3.5 g. (65 mmole) of *Cis*-4 polybutadiene (Phillips Petroleum Co.) in 320 ml. of benzene was mixed with 3.0 g. (6 mmole) of  $Fe_3(CO)_{12}$  and 40 ml. of glacial acetic acid. The mixture was stirred under nitrogen in a bath at 22–23°C. Aliquots of 50 ml. were withdrawn and dropped into a stirred mixture of 500 ml. of acetone with 10 ml. of concentrated HCl. The white polymer was analyzed by an infrared method based on that of Hampton.<sup>2</sup>

### Iron Carbonyl Complexes

The complexing reaction may be carried out in a variety of hydrocarbon solvents, with either pentacarbonyliron or dodecacarbonyltriiron as the reagent; xylene in the former case and benzene in the latter are especially favorable. When a hydrocarbon alone is used as the solvent, the ap-



TABLE I  
 Iron Carbonyl Complexes of Polydienes

Initial polymer	Iron carbonyl	Concentration		Molar ratio Fe/monomer	Solvent	Time, hr.	Temp., °C.	Fe(CO) <sub>5</sub> in product, wt.-%	% double bonds complexed
		g./100 ml. solvent	Polymer						
Cis-4 polybutadiene <sup>a</sup>	Fe(CO) <sub>5</sub>	14.6	3.0	1.3	1% Dioxane-xylene	48	135	37	46
Trans-4 polybutadiene <sup>a</sup>	Fe <sub>2</sub> (CO) <sub>12</sub>	2.3	1.0	0.7	10% Ethanol-benzene	2	80	23	23
Styrene-butadiene copolymer (25:75)	Fe <sub>2</sub> (CO) <sub>12</sub>	2.5	1.0	0.8	Benzene	20	80	8	9
Polybutadiene (81% 1,2)	Fe <sub>2</sub> (CO) <sub>12</sub>	2.0	1.0	0.6	10% 1,2-Dimethoxyethane-benzene	2.5	80	16	15
Natural rubber	Fe(CO) <sub>5</sub>	7.7	0.9	3.0	8% Dioxane-xylene	5	125	17	20
Buton 150 resin <sup>b</sup>	Fe(CO) <sub>5</sub>	18.2	3.0	1.7	2.5% Dioxane-xylene	48	135	21	21

<sup>a</sup> Phillips Petroleum Company.<sup>b</sup> Enjay Chemical Company, Polybutadiene, mol. wt. 2300.

pearance and rheology of the recovered polymer indicate the occurrence of substantial molecular weight breakdown. The breakdown may be largely avoided by the use of a few per cent of a polar, nonacidic solvent component, such as an alcohol, ketone, or ether.

In the presence of such basic solvents the reaction assumes a dark red or brown color typical of carbonylferrate anions. Precipitation of the polymer in the presence of a mineral or organic acid gives a product largely free of inorganic impurities. Almost any polymer containing appreciable amounts of olefinic unsaturation will undergo the complex-forming reaction. Table I indicates some of the variety of substrates and conditions employed. By the use of very large excesses of iron carbonyl up to 80% of the double bonds present have been utilized in complex formation.

The high molecular weight iron carbonyl-containing polymers are yellow to orange in color, depending upon the degree of complexing reached. Their solubilities resemble those of the starting polymers, and they are rubbery in appearance and feel. They may be handled in air, but upon prolonged standing oxidation occurs, producing a brownish surface and insolubility. Attempts to cleave the iron carbonyl groups from the polymer in solution by basic reagents such as pyridine or triphenylphosphine have been partially successful, but the recovered polymers are heavily crosslinked or of very low molecular weight. Crosslinking also occurs when the rubbery materials are heated briefly in a conventional press at about 200°C., even in the absence of additional curing agents. If vulcanization is carried out at higher temperatures or for a longer time, the carbon monoxide is lost and the vulcanizate is ferromagnetic, containing iron or  $\text{Fe}_3\text{O}_4$ , depending upon the access of air to the sample.

Thermogravimetric analysis of an iron carbonyl-containing polybutadiene carried out in a nitrogen atmosphere at a heating rate of 5°C./min. reveals a characteristic pattern, which further verifies the composition of the polymers. The weight lost in the region of 180–260°C. corresponds to the loss of three carbonyl groups per iron atom shown present by other analyses. The additional weight lost in the region of 350–450°C. corresponds to the loss of "uncomplexed" polybutadiene; this inflection occurs where it does under the same conditions with the starting material. The amount of residue then approximates the amount of  $[\text{C}_8\text{H}_{12}\text{Fe}]$  in the polymer. This residue, a brittle, black, magnetic material shown by x-ray analysis to contain elemental iron, diminishes only slightly up to 1000°C.; isothermal experiments reveal that the main change at higher temperatures is dehydrogenation, together with some loss of hydrocarbon. Clearly, the highly reactive iron present during the pyrolysis causes extensive crosslinking of polymer associated with it.

### Geometrical Isomerization

Isomerization of polybutadienes has been accomplished by other processes<sup>3-7</sup> and the iron carbonyl-catalyzed isomerization of low molecular weight mono- and diolefins has been extensively studied<sup>8-13</sup> Table II

TABLE II  
Reactions between Iron Carbonyls and Cis-4 Polybutadiene

Run	Solvent	Iron carbonyl	Concn., g/100 ml.		Molar ratio Fe/monomer	Time, hr.	Temp., °C.	Fe(CO) <sub>5</sub> wt.-%	Uncomplexed isomer distribution		
			Fe(CO) <sub>5</sub>	Cis-4					cis-1,4, %	trans-1,4, %	1,2, %
1	Benzene	Fe <sub>3</sub> (CO) <sub>12</sub>	2.0	1.0	0.64	1 1/3	78	9.1	71	24	4
2	5% Acetone-benzene	Fe <sub>3</sub> (CO) <sub>12</sub>	2.0	1.0	0.64	1 1/3	73	16.8	81	13	5
3	5% Acetic acid-benzene	Fe <sub>3</sub> (CO) <sub>12</sub>	2.0	1.0	0.64	1 1/3	75	6.6	24	71	4
4	7% Acetic acid-benzene	Fe <sub>3</sub> (CO) <sub>12</sub>	0.86	1.0	0.28	2	72	4.3	19	76	4
5	7% Acetic acid-cyclohexane	Fe <sub>3</sub> (CO) <sub>12</sub>	0.86	1.0	0.28	2	74	<5	27	68	5
6	7% Acetic acid-heptane	Fe <sub>3</sub> (CO) <sub>12</sub>	0.86	1.0	0.28	2	75	<5	87	8	5
7	3% Acetic acid-benzene	Fe(CO) <sub>5</sub>	2.7	2.1	0.34	6	80	<5	31	64	4
8	5% 1,2-Dimethoxy-ethane-benzene	Fe <sub>3</sub> (CO) <sub>12</sub>	2.0	1.0	0.64	1 1/3	77	10.2	56	38	5
9	7% 1,2-Dimethoxy-ethane-benzene	Fe <sub>3</sub> (CO) <sub>12</sub>	0.86	1.0	0.28	168	25	<1	26	69	4
10	7% Acetic acid-benzene	Fe <sub>3</sub> (CO) <sub>12</sub>	0.86	1.0	0.28	93	23	<1	20	75	4

indicates reaction conditions under which polybutadienes undergo predominant geometrical isomerization rather than complex formation; notable factors are low temperatures and the presence of an acidic component in the solvent. The apparent equilibrium in this process lies at 77% *trans*.<sup>7</sup>

Considerable differences in the rate of geometrical isomerization have been observed for polymers of different structure. That Trans-4 polybutadiene (Phillips Petroleum Co.) is converted to the equilibrium mixture much more slowly than high *cis* content polybutadienes is consistent with the lower reactivity of *trans* double bonds in monoolefin isomerizations.<sup>9</sup> More intriguing is the difference in isomerization rate for two high *cis*-content polybutadienes: Cis-4 (Phillips Petroleum Co., 92% *cis*-1,4; 4% *trans*-1,4; 4% 1,2; viscosity-average molecular weight, 246,000) and Ameripol CB (Goodrich-Gulf Chemical Co.; 94% *cis*-1,4; 4% *trans*-1,4; 2% 1,2; viscosity-average molecular weight, 180,000). Table III shows that at 77° the Ameripol CB was isomerized rather more slowly than the Cis-4. Over longer times at room temperature the Ameripol CB, though reacting less rapidly than the Cis-4, did yield the equilibrium *cis-trans* product.

TABLE III  
Isomerization of Two High *cis*-Content Polybutadienes at 77°C.  
(7% Acetic Acid-Benzene; 1.0 g./ml. Polybutadiene; 0.86 g./ml. Fe<sub>3</sub>(CO)<sub>12</sub>)

Polymer	% <i>trans</i> -1,4 at various times					
	30 min.	40 min.	50 min.	60 min.	90 min.	120 min.
Cis-4	12	58	64	66	71	76
Ameripol CB	10	13	24	29	37	39

The presence of tricarbonyl(iron) groups retards geometrical isomerization. A solution of Cis-4 (1.0 g./ml. in 10% 1,2-dimethoxyethane-benzene) was treated with 0.74 equivalent of Fe<sub>3</sub>(CO)<sub>12</sub> at 80°C. for 2.5 hr. The complexed polymer was recovered, redissolved, and treated again at the same concentration and temperature with 0.74 equivalent of Fe<sub>3</sub>(CO)<sub>12</sub> for 2.5 hr., but in a 10% acetic acid-benzene solution. A second portion of Cis-4 was subjected to the identical sets of conditions, but in the reverse order—those favoring isomerization preceding those favoring complexing. The four products are compared in Table IV. The extent of isomerization,

TABLE IV  
Consecutive Fe<sub>3</sub>(CO)<sub>12</sub>-Cis-4 Polybutadiene Reactions

Sample	Conditions	Fe-	<i>trans</i> ,	Conditions	Fe-	<i>trans</i> ,
		(CO) <sub>3</sub> ,			(CO) <sub>3</sub> ,	
		%	%		%	%
A	Complexing	19.8	13	Isomerization	25	32
B	Isomerization	11.7	74	Complexing	28	71

but not of complex formation, depended markedly upon the sequence of reactions. We believe this may be ascribed to steric interference by the bulky  $[\text{Fe}(\text{CO})_3]$  group with subsequent reaction.

The polybutadiene isomerization is effectively inhibited by the presence of a monoolefin in the reaction mixture. An equimolar mixture of Cis-4 polybutadiene and (82% *cis*) 2-hexene was treated with  $\text{Fe}_3(\text{CO})_{12}$  at 72°C. in a benzene-acetic acid mixture. After 2 hr., 10% of the 2-hexene was changed and the polybutadiene contained only 10% of *trans*-1,4 units. Under the same conditions Cis-4 alone yielded a 70% *trans* product in 1 hr., and 2-hexene alone was isomerized to the extent of 10% in three hours. The monoolefin seems to react with the active iron carbonyl species more rapidly than does the polybutadiene. However, the more extensive isomerization of the polymer by itself shows that it utilizes each contact more efficiently. Furthermore, although in simple monoolefins terminal double bonds react more readily with iron carbonyls than do internal double bonds,<sup>9</sup> the reverse is true with the unsaturated polymers. Under conditions which gave the *cis-trans* equilibrium product from Cis-4, a polybutadiene with 81% 1,2 units was converted to a product with its infrared spectrum still showing 75% of the unsaturation as vinyl groups.

There is no need to propose a mechanism for the polymer isomerization differing significantly in principle from that believed to occur in the case of monoolefins and simple nonconjugated dienes.<sup>8-13</sup> However, our results indicate a greater importance of structural factors in the case of the polydienes. With monoolefins, both geometrical and positional isomerization are believed to occur within an olefin-iron carbonyl complex and not in a stepwise fashion with free olefin at each stage.<sup>9,11,13</sup> Our data for polybutadienes suggest that isomerization proceeds with an iron carbonyl group moving down the chain and isomerizing several bonds, once the initial complex is formed. A concerted mechanism may be involved with a single iron atom bonded at least temporarily to two double bonds. The reason for the specific solvent effect of acetic acid is not clear; acetic acid retards and bases promote the isomerization of monoolefins.<sup>9</sup>

## References

1. R. Pettit and G. F. Emerson, in *Advances in Organometallic Chemistry*, F. G. A. Stone and R. West, Eds., Vol. I, Academic Press, New York, 1964, p. 1.
2. R. H. Hampton, *Anal. Chem.*, **21**, 923 (1949).
3. M. A. Golub, *J. Polymer Sci.*, **25**, 373 (1957).
4. M. A. Golub, *J. Am. Chem. Soc.*, **80**, 1794 (1958).
5. M. A. Golub, *J. Am. Chem. Soc.*, **81**, 54 (1959).
6. W. A. Bishop, *J. Polymer Sci.*, **55**, 827 (1961).
7. M. Berger and D. J. Buckley, *J. Polymer Sci. A*, **1**, 2945 (1963).
8. R. Pettit and J. E. Arnet, *J. Am. Chem. Soc.*, **83**, 2954 (1961).
9. T. A. Manuel, *J. Org. Chem.*, **27**, 3941 (1962).
10. F. Asinger and O. Berg, *Ber.*, **88**, 445 (1955).
11. M. D. Carr, V. V. Kane, and M. C. Whiting, *Proc. Chem. Soc.*, **1964**, 408.
12. F. Asinger, B. Fell, and K. Schrage, *Ber.*, **98**, 372 (1965).
13. F. Asinger, B. Fell, and K. Schrage, *Ber.*, **98**, 381 (1965).

### Résumé

Le traitement des polybutadiènes avec les fer-carbonyles ont comme conséquence la formation de polymères contenant des unités fer-tricarbonyles diène conjugué de formule  $[C_8H_{12}Fe(CO)_3]$  et il en résulte une isomérisation géométrique de doubles soudures libres. Par chauffage des polymères contenant du fer-carbonyle, on obtient des produits ferromagnétiques avec une stabilité thermique améliorée. L'incorporation de fer-carbonyle au sein du polymère est favorisée par des solvants basiques et des températures élevées; l'isomérisation géométrique est favorisée par des solvants acides et par de basses températures. Les facteurs stériques sont importants dans la détermination de la vitesse d'isomérisation.

### Zusammenfassung

Die Behandlung von Polybutadien mit Eisencarbonylen führt zur Bildung von Polymeren mit Tricarbonyl- (konjugiertes Dien) Eisenbausteinen  $[C_8H_{12}Fe(CO)_3]$  sowie zur geometrischen Isomerisierung der freien Doppelbindungen. Erhitzen der Polymeren mit Eisencarbonylgruppen liefert ferromagnetische Produkte mit erhöhter thermischer Stabilität. Der Einbau von Eisencarbonylgruppen in das Polymere wird durch basische Lösungsmittel und hohe Temperatur begünstigt, die geometrische Isomerisierung durch saure Lösungsmittel und niedrige Temperatur. Sterische Faktoren haben grosse Bedeutung für die Bestimmung der Isomerisierungsgeschwindigkeit.

Received August 20, 1965

Revised October 28, 1965

Prod. No. 4970A



## Initiation and Propagation in $\gamma$ -Radiation-Induced Polymerization of Ethylene\*

SUEO MACHI, MIYUKI HAGIWARA, MASAO GOTODA, and  
TSUTOMU KAGIYA, *Japan Atomic Energy Research Institute,  
Takasaki Radiation Chemistry Research Establishment, GUNNAN-mura  
Gumma, Japan*

### Synopsis

The initiation and propagation reaction in  $\gamma$ -ray-induced polymerization of ethylene was studied by the two-stage irradiation method, i.e., a first stage in which initiation and propagation occur at a high dose rate, and a second stage where only the growth of polymer radical occurs. The rate of initiation is calculated from the amount of polymerized monomer and the degree of polymerization as the rate of increase in the number of polymer chains. The initiation rate is shown to be proportional to the ethylene density in the reactor and dose rate.  $G_R$  of radical formation is found to be about 1.6 at 30°C. at a dose rate of  $2.5 \times 10^4$  rad/hr. and is almost independent of ethylene density but decreases slightly with increasing irradiation dose rate. The lifetime of the growing polymer chain radical is shown to be long at normal temperature. The absolute propagation rate is proportional to the square of ethylene fugacity and depends on dose rate to some extent. For chain growth, irradiation of low dose rate is necessary. The apparent activation energy for the propagation reaction is  $-9$  kcal./mole.

### INTRODUCTION

In the previous papers,<sup>1-3</sup> we indicated that the polymerization rate and polymer molecular weight increase continuously with reaction time and that the lifetime of the growing chain radical is long in the bulk polymerization of ethylene induced by  $\gamma$ -radiation at normal temperature. From the kinetics of overall polymerization<sup>3</sup> it was concluded that the chain termination and transfer reaction are almost absent, and the initiation and propagation, therefore, are the main elementary reactions at normal temperature.

The purpose of this paper, a sequel to the previous paper,<sup>2</sup> is to show the effects of ethylene pressure, dose rate, and reaction temperature on the initiation and propagation reaction and to discuss the polymerization mechanism from the point of kinetics.

### EXPERIMENTAL

The reaction vessel, ethylene monomer (free from CO and H<sub>2</sub>S, containing 3 ppm O<sub>2</sub>) irradiation facilities, and experimental procedure are the

\* Presented at the 6th Japan Conference on Radioisotopes, Tokyo, Japan, November 16-19, 1964.

same as described in the previous paper.<sup>1,3</sup> However, in the experiment by which the rate of propagation was determined, the polymerization was carried out in two different stages. The first irradiation was carried out at a dose rate of  $2.5 \times 10^4$  rad/hr. at  $30^\circ\text{C}$ .; this was followed by a second irradiation at an extremely low dose rate under various conditions. By this method the propagation reaction is almost separated in the second stage from the initiation.

The ethylene pressure remained essentially constant during polymerization because of the low conversion of ethylene to polyethylene. The temperature was maintained constant in the course of reaction within  $\pm 1^\circ\text{C}$ . In order to change the radiation intensity, the distance between the reactor and the  $^{60}\text{Co}$  source was varied. Interruption of irradiation between the two stages was about 20 min.

## RESULTS AND DISCUSSION

### Initiation Rate

Since ethylene polymerization by  $\gamma$ -rays at normal temperature is free from chain transfer and termination as described before, the increase in number of polymer molecules is due solely to the initiation reaction. The rate of initiation, therefore, is equal to the rate of increase in the number of polymer chains, which is calculated from the ratio of the amount of polymerized monomer to the number-average degree of polymerization, namely:

$$R_i = dN_p/dt \quad (1)$$

$$R_i = d(M_p/\overline{DP}_n)/dt \quad (2)$$

where  $R_i$  represents the rate of initiation,  $N_p$  is the number of moles of polymer chains per unit volume,  $M_p$  is the amount of polymerized monomer in unit volume,  $\overline{DP}_n$  is the number-average degree of polymerization, and  $t$  is irradiation time or reaction time. Since chain termination is absent, the number of polymer chains should also be the number of polymer radicals.

The experimental results and calculated data are summarized in Tables I and II.

The initiation step of radiation polymerization is brought about by an absorption of radiation energy, which results in various secondary processes finally leading to the production of free radicals. The reaction scheme and rate of initiation are expressed as follows for the bulk polymerization:



$$R_i = k_i \rho_M I \quad (4)$$

where, M is monomer,  $\text{R}\cdot$  is the radical leading to polymer molecule,  $k_i$  is the initiation rate constant,  $\rho_M$  is monomer density in the reactor, and  $I$  is dose rate.

TABLE I  
 Effect of Ethylene Density on Initiation Rate<sup>a</sup>

Ethylene		Irradiation time, hr.	Polymerized monomer, mole/l.	Degree of polymerization $\overline{DP}_n \times 10^{-3}$	No. of moles of polymer chain $\times 10^{-5}$ mole/l.	Initiation rate $R_i \times 10^6$ , mole/l.-hr.	
Pressure, kg./cm. <sup>2</sup>	Density, mole/l.					$R_i$	$(R_i)_{\text{mean}}$
40	2.1	18.0	0.008	0.36	2.22	0.112	0.112
60	4.2	18.0	0.040	0.50	8.00	0.445	0.445
70	7.2	15.0	0.149	0.75	19.9	1.24	1.45
70	7.2	20.7	0.189	0.57	33.1	1.52	
70	7.2	44.6	1.100	1.54	71.4	1.60	
120	11.4	7.0	0.279	2.75	10.1	1.45	1.45
152	13.4	2.5	0.111	3.14	3.53	1.40	1.40
200	14.4	0.7	0.029	2.11	1.37	1.94	1.56
200	14.4	1.2	0.043	2.36	1.82	1.51	
200	14.4	2.5	0.179	5.87	3.04	1.22	
295	15.4	0.7	0.057	4.76	1.20	1.72	1.62
295	15.4	1.0	0.097	6.23	1.55	1.55	
295	15.4	1.7	0.254	9.48	2.68	1.58	
400	16.4	0.26	0.011	2.50	0.44	1.65	2.06
400	16.4	0.53	0.050	5.15	0.97	1.83	
400	16.4	1.00	0.265	9.52	2.70	2.70	

<sup>a</sup> Reaction conditions: temperature, 30°C.; dose rate,  $2.5 \times 10^4$  rad/hr.; reactor volume, 100 cc.

 TABLE II  
 Effect of Dose Rate on Initiation Rate<sup>a</sup>

Ethylene		Dose rate $\times 10^{-4}$ , rad/hr.	Irradiation time, hr.	Polymerized monomer, mole/l.	Degree of polymerization, $\overline{DP}_n \times 10^{-3}$	Initiation rate $R_i \times 10^6$ , mole/l.-hr.	$R_i/\rho_M \times 10^6$ , hr. <sup>-1</sup>
Density, mole/l.	Pressure, kg./cm. <sup>2</sup>						
14.4	200	0.50	5.0	0.204	9.30	0.44	0.31
		0.77	4.0	0.193	9.10	0.53	0.37
		1.3	5.0	0.385	8.75	0.89	0.62
		2.5	2.5	0.178	4.53	1.57	1.09
		5.6	1.0	0.089	2.36	3.78	2.63
		12	1.0	0.129	2.07	6.21	4.32
		21	1.0	0.196	1.96	10.0	6.95
		43	1.0	0.323	1.57	20.7	14.4
		16.4	450	0.012	7.0	0.081	18.6
0.030	4.0			0.047	13.3	0.088	0.054
0.072	4.0			0.134	18.9	0.187	0.11
0.19	4.1			0.197	15.5	0.31	0.19
0.73	2.0			0.248	15.2	0.82	0.50
2.5	0.5			0.05	5.1	1.84	1.12

<sup>a</sup> Reaction conditions: temperature, 30°C.; reactor volume, 100 cc.

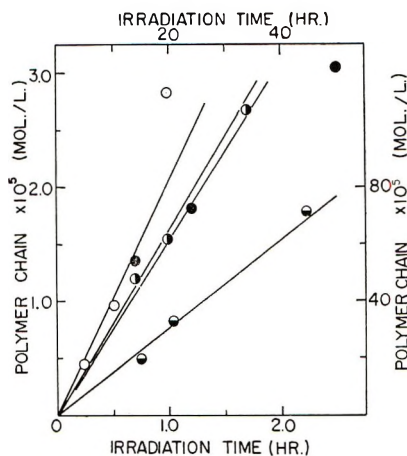


Fig. 1. Number of polymer chains vs. irradiation time at various ethylene pressures: (◐) 70 kg./cm.<sup>2</sup>, (●) 200 kg./cm.<sup>2</sup>; (●) 300 kg./cm.<sup>2</sup>; (○) 400 kg./cm.<sup>2</sup>. Dose rate,  $2.5 \times 10^4$  rad/hr.; temperature 30°C.

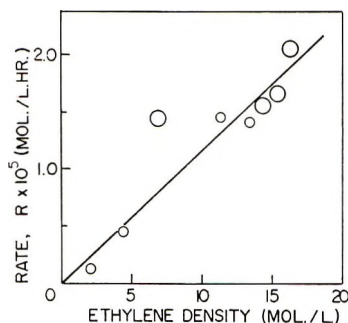


Fig. 2. Ethylene density vs. initiation rate at 30°C.,  $2.5 \times 10^4$  rad/hr. Large circles show mean value of the data at different reaction times.

By substituting eq. (4) into eq. (1) and integrating,  $N_p$  at time  $t$  is given by:

$$N_p = k_i \rho_M I t \quad (5)$$

This means that the number of polymer chains is proportional to the monomer density, dose rate, and irradiation time.

From the experimental data, the number of moles of polymer chains per unit volume is plotted against the irradiation time in Figure 1. An almost linear relation was found between them, for 70, 200, 300, and 400 kg./cm.<sup>2</sup>.\* The slope of the line equals  $k_i \rho_M I$ . The rate of initiation is also shown to be independent of time unless monomer concentration changes.

\* The data for the pressure of 150 kg./cm.<sup>2</sup> does not give so good a linear relation between number of polymer chains and time as the other data. Scattering to this extent, however, may be permissible, and the linear relation is proved by a majority of data.

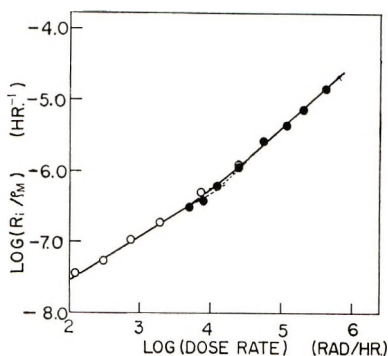


Fig. 3. Logarithmic plots of  $R_i/\rho_M$  vs. dose rate: (●) 200 kg./cm.<sup>2</sup>; (○) 400 kg./cm.<sup>2</sup>. Reaction temperature, 30°C.

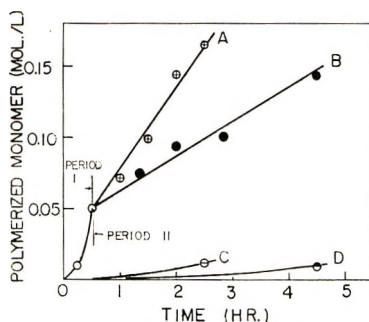


Fig. 4. Amount of polymerized monomer vs. irradiation time: (○)  $2.5 \times 10^4$  rad/hr., 400 kg./cm.<sup>2</sup>, 30°C.; (⊕) 300 rad/hr., 395 kg./cm.<sup>2</sup>, 30°C.; (●) 300 rad/hr., 200 kg./cm.<sup>2</sup>, 30°C.; (⊖) 300 rad/hr., 400 kg./cm.<sup>2</sup>, 30°C.; (⊗) 300 rad/hr., 200 kg./cm.<sup>2</sup>, 30°C.

The effect of pressure and concentration of ethylene on the initiation rate was investigated at pressures of 40–400 kg./cm.<sup>2</sup> at 30°C.; results are shown in Table I. Since ethylene at high pressure is not an ideal gas, pressure is not proportional to density. Figure 2 shows that the initiation rate is almost proportional to the monomer density or concentration in spite of the deviation of the data for only 70 kg./cm.<sup>2</sup>\* Equation (4) is, therefore, shown to coincide with the facts.

Further, the effect of irradiation intensity was studied over the wide range of 120–430,000 rad/hr., and the results are summarized in Table II. The dependence of the initiation rate on dose rate is shown in Figure 3, from which it is seen that dose rate exponent increases slightly with dose rate, i.e., from 120 to 7000 rad/hr. the exponent is ca. 0.7, and from 2500 to 430,000 it is ca. 0.9. The reason for this change in the exponent is not

\* Since the linearity of the number of polymer chains versus time is assumed,  $R_i$  may be determined from just one experiment at any irradiation time for one pressure, for instance, 40, 60, 120, and 150 kg./cm.<sup>2</sup>. These values are plotted in Figure 2 though they can not be shown in Figure 1. The linearity of Figure 2 then seems to be certain in spite of the deviation of data for 70 kg./cm.<sup>2</sup>.

clear. The dose rate dependence, especially in the range of higher intensity, however, almost coincides with eq. (4).

These kinetical data are seen to confirm the assumption that the radiation initiation in ethylene bulk polymerization is brought about by the absorption of radiation energy in the ethylene molecule, resulting the production of free radicals by a monomolecular reaction.

The  $G$  value of radical formation ( $G_R$ ) is also calculated from the initiation rate. There is a simple relation between  $G_R$  and initiation rate:

$$G_R = R_i/\rho_M I \quad (6)$$

If the dose rate exponent is unity as expected from the above scheme,  $G_R$  is independent of dose rate and ethylene density. However, since there is a small deviation of the experimental exponent from unity,  $G_R$  decreases with increasing dose rate to some extent. At a dose rate of 25,000 rad/hr. under a pressure of 40–400 kg./cm.<sup>2</sup> and at 30°C.,  $G_R$  is obtained as 1.6 free radicals/100 e.v. absorbed in ethylene. This value is of comparable order of magnitude as the  $G_R$  of 4.4 estimated by Hayward<sup>4</sup> for ethylene polymerization at low pressure and is of reasonable order of magnitude on comparison with the  $G_R$  values of 1.5–3.9 for isobutylene<sup>5</sup> and 2.7–3.1 for hexadecene.<sup>6</sup>

### Existence of Long-Lived Polymer Chain Radical

We have assumed the lifetime of the polymer radical to be long at normal temperature from the overall polymerization kinetics.<sup>3</sup> In this section we present further evidence for this assumption which is obtained by means of the irradiation of two stages.

The experimental results are given in Table III. Figure 4 shows a plot of polymerized monomer against irradiation time. In period I ethylene was irradiated at a dose rate of  $2.5 \times 10^4$  rad/hr. at 30°C., and this was followed by a irradiation at a low dose rate, 300 rad/hr., in period II. It should be noted that the polymer increase in period II is quite considerable. When the entire polymerization was carried out at the same low dose rate as was used in period II (Figs. 4C and 4D), the amount of polymer formed was much less than that formed in period II after the initial high dose rate irradiation (Figs. 4A and 4B). It is, therefore, apparent that the polymerization in period II is markedly affected by the reaction in period I. This fact does not result from inhibition by impurities because the amount of oxygen in the ethylene is very small (3 ppm), and, further, no induction period was observed.<sup>1,3</sup> It may be due to the fact that the polymer radical introduced in period I survives, and the polymer chain growth can occur at a low dose rate.

On the other hand, the degree of polymerization of polymer formed increases with reaction time in both periods I and II. The relation between degree of polymerization and the amount of polymerized monomer is shown in Figure 5, where a small correction for the amount of polymerized monomer and degree of polymerization in period II was made to eliminate the



TABLE III  
Results of Two-Stage Irradiation Systems<sup>a</sup>

Conditions in period II			Time of second irradiation, hr.	Overall polymerized monomer $M_p$ mole/l.	$\overline{DP}_n$ of final polymer $\times 10^{-3}$	$(M_p)_{corr.}$ mole/l. <sup>b</sup>	$(DP_n)_{corr.}$ $\times 10^{-3}$ b
Temp., °C.	Dose rate, rad/hr.	Pressure, kg./cm. <sup>2</sup>					
30	300	395	0.5	0.072	7.04	0.071	7.45
			1.0	0.099	9.12	0.096	9.98
			1.5	0.144	10.2	0.138	11.3
30	300	200	2.0	0.165	11.4	0.154	12.8
			0.84	0.075	5.83	0.074	6.20
			1.50	0.094	6.40	0.092	7.01
92	300	400	2.3	0.101	6.98	0.097	7.90
			4.0	0.143	8.22	0.133	9.76
			1.8	0.083	5.15	0.077	7.2
			3.5	0.112	6.43	0.110	11.8
			5.0	0.148	5.86	0.132	12.8

<sup>a</sup> Reaction conditions in the first stage (period I): temperature, 30°C.; dose rate,  $2.5 \times 10^4$  rad/hr.; ethylene pressure, 400 kg./cm.<sup>2</sup>; time, 0.5 hr. reactor  $p$  volume, 100 cc.; in period I 0.005 mole ethylene is polymerized and  $\overline{DP}_n$  is 5150.

<sup>b</sup>  $M_p$  and  $DP_n$  were corrected by eliminating the effect of small amount of polymer formed at a dose rate of 300 rad/hr. (shown in Figs. 4C and 4D) as follows:

$$(\overline{DP}_n)_{corr.} = (\overline{DP}_n - \overline{DP}_{nII})N_{PI}/N_{PII}$$

where,  $\overline{DP}_n$  represents observed  $DP$  of final polymer,  $\overline{DP}_{nII}$ ,  $DP$  of polymer formed by the initiation with 300 rad/hr. in period II,  $N_{PI}$ , number of moles-polymer formed in period I,  $N_{PII}$ , number of moles of polymer formed by the initiation with 300 rad/hr. in period II.

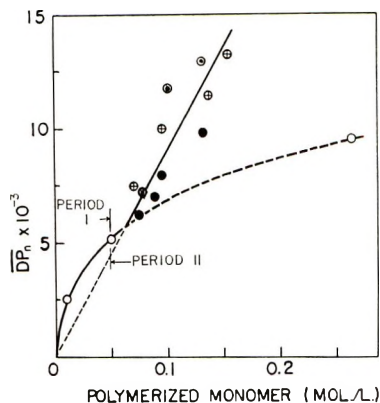


Fig. 5. Degree of polymerization vs. amount of polymerized monomer: (○)  $2.5 \times 10^4$  rad/hr., 400 kg./cm.<sup>2</sup>, 30°C.; (⊕) 300 rad/hr., 395 kg./cm.<sup>2</sup>, 30°C.; (●) 300 rad/hr., 200 kg./cm.<sup>2</sup>, 30°C.; (⊙) 300 rad/hr., 400 kg./cm.<sup>2</sup>, 92°C.

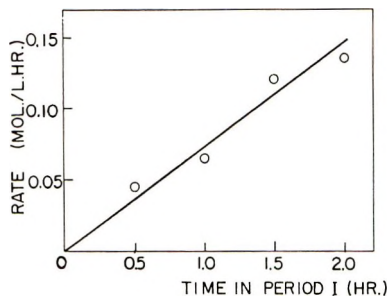


Fig. 6. Overall propagation rate vs. irradiation time in period I. Period I: 30°C.,  $2.5 \times 10^4$  rad/hr., 400 kg./cm.<sup>2</sup>; period II: 30°C., 300 rad/hr., 350 kg./cm.<sup>2</sup>.

effect of the small amount of polymer formed at a dose rate of 300 rad/hr. (shown in Figs. 4C and 4D). In the polymerization at high dose rate,  $2.5 \times 10^4$  rad/hr., a convex curve is obtained, while in period II subsequent to period I, a straight line is obtained.

Since the ratio of polymerized monomer to degree of polymerization ( $M_p/DP_n$ ) equals the number of moles of polymer chains or radicals, it can be seen that the number of polymer chains increases in period I, but remains constant in period II. In other words, both initiation and propagation reactions occur in period I with a high dose rate, while in period II, at a low dose rate, only the propagation reaction occurs, and the initiation reaction is eliminated. These facts may indicate that the polymer radical introduced in period I survives and the polymer chain growth can occur at a low dose rate in period II.

Table IV and Figure 6 show other experimental results which are consistent with the above assumption. A linear relation between the overall propagation rate, i.e., monomer consumption per unit time, in period II and irradiation time in period I is given in Figure 6. According to the as-

sumption, the overall propagation rate in period II is proportional to the number of polymer radicals per unit volume, which increases with total irradiation dose in period I.

However, since no polymer increase in period I is observed without irradiation in this period, post-polymerization does not take place. From this fact, it is presumed that the excitation of either monomer or polymer chain is necessary for the propagation reaction.\*

TABLE IV  
Effect of Irradiation Dose in Period I on Overall Propagation Rate in Period II

Period I <sup>a</sup>		Period II <sup>b</sup>		
Irradiation time, hr.	Total dose $\times 10^{-4}$ , rad	Time, hr.	Monomer consumed for propagation, mole/l.	Overall propagation rate, mole/l.-hr.
0.5	1.3	1.5	0.067	0.045
1.0	2.5	2.0	0.129	0.065
1.5	3.8	2.0	0.241	0.121
2.0	5.0	2.0	0.272	0.136

<sup>a</sup> Reaction conditions: temperature 30°C.; pressure, 400 kg./cm.<sup>2</sup>; dose rate,  $2.5 \times 10^4$  rad/hr.

<sup>b</sup> Reaction conditions: temperature 30°C.; pressure, 350 kg./cm.<sup>2</sup>; dose rate, 300 rad/hr.

The effect of irradiation temperature in period I on the polymer increase in period II is shown in Table V. When the polymerization in period I is carried out at 100°C., the polymer increase in period II is shown to be small and nearly equal to that of the entire polymerization at a low dose rate (300 rad/hr.). This fact suggests the polymer chain radical does not survive at as high a temperature as 100°C.

\* The nature of the growing active chain end and its change in dark is certainly interesting and important. We are going to undertake an investigation of the nature of this chain end by using ESR. Indirect evidence for the radical mechanism of this polymerization is the similarity of polyethylene structure to that of the free-radical polymer obtained with a radical initiator, namely, both  $\gamma$ -ray-polymerized and free-radical-polymerized polyethylenes have almost only vinylidene unsaturation, while polyethylene produced by an ionic polymerization like the Marlex process and Ziegler process has terminal vinyl and internal *trans* unsaturation.<sup>7</sup> In addition, the formation of short-chain branching in  $\gamma$ -ray-initiated polymerization is very similar to that in free-radical polymerization in the frequency of branching formation and its excess activation energy on propagation reaction.<sup>8,9</sup> Recently, Ohmishi et al.<sup>10</sup> reported that electron-irradiated solid ethylene showed a 12-line ESR spectrum due to ethyl radical, and the spectrum gradually decayed even at  $-196^\circ\text{C}$ . and disappeared; the 5-line spectrum remaining was rather stable, and was converted to the 12-line spectrum upon ultraviolet irradiation. The discovery of ethyl radical from ethylene and the transformation of the radical on irradiation and dark interests us in connection with ethylene polymerization.

TABLE V  
Effect of Irradiation Temperature in Period I on the Amount of  
Polymerized Monomer in Period II

Period I <sup>a</sup>			Period II <sup>b</sup>		
Temp., °C.	Time, hr.	Polymerized monomer, mole/l.	Temp., °C.	Time, hr.	Polymerized monomer, mole/l.
30	0.5	0.05	30	4.0	0.009
30	0.5		30	4.0	0.125 <sup>c</sup>
100	1.0	0.06			
100	1.0		30	4.0	0.063 <sup>c</sup>

<sup>a</sup> Reaction conditions: dose rate,  $2.5 \times 10^4$  rad/hr.; pressure, 400 kg./cm.<sup>2</sup>.

<sup>b</sup> Reaction conditions: dose rate, 300 rad/hr.; pressure, 150 kg./cm.<sup>2</sup>.

<sup>c</sup> Overall polymerized monomer in period I continued to period II.

### Propagation Rate

The propagation reaction was almost separated from the initiation reaction by carrying out the irradiation in two stages as mentioned above. The two-stage method is useful for the study of the propagation reaction. The experimental results are shown in Tables VI–VIII and Figures 7–9 which show the variation of the absolute propagation rate, i.e., monomer consumption per growing polymer radical per unit time, with pressure, temperature, and dose rate.

The propagation rate under high pressure should be represented by a function of fugacity of monomer. Figure 7 indicates that the absolute propagation rate is proportional to the second power of ethylene fugacity. This is also consistent with the overall polymerization kinetics.<sup>3</sup> The high fugacity exponent of the absolute propagation rate may indicate that ethyl-

TABLE VI  
Effect of Ethylene Fugacity on Absolute Propagation Rate<sup>a</sup>

Ethylene		Overall propagation rate, mole/l.-hr.	Absolute propagation rate $\times 10^{-3}$ , mole C <sub>2</sub> H <sub>4</sub> / mole radical-hr.
Pressure, kg./cm. <sup>2</sup>	Fugacity, kg./cm. <sup>2</sup>		
51	35.7	0.003	0.31
100	52.0	0.008	0.83
150	60.5	0.017	1.75
200	70.0	0.022	2.28
250	80.0	0.029	3.00
300	91.0	0.033	3.40
350	103	0.045	4.64
400	115	0.049	5.05

<sup>a</sup> Reaction conditions: temperature, 30°C.; dose rate, 300 rad/hr.; moles of polymer chain radicals,  $9.7 \times 10^{-6}$  mole/l.

TABLE VII  
 Effect of Dose Rate on Absolute Propagation Rate<sup>a</sup>

Dose rate $\times 10^{-4}$ , rad/hr.	Overall propagation rate, mole/l.-hr.	Absolute propa- gation rate $\times 10^{-3}$ , mole C <sub>2</sub> H <sub>4</sub> / mole radical-hr.
0.012	0.028	2.86
0.030	0.049	5.05
0.072	0.062	6.39
0.19	0.081	8.35
0.73	0.150	15.5

<sup>a</sup> Reaction conditions: temperature, 30°C.; pressure, 395 kg./cm.<sup>2</sup>; moles of polymer chain radicals,  $9.7 \times 10^{-6}$  mole/l.

 TABLE VIII  
 Effect of Temperature on Absolute Propagation Rate<sup>a</sup>

Temper- ature, °C.	Ethylene fugacity, kg./cm. <sup>2</sup>	Overall propagation rate, mole/l.-hr.	Absolute propagation rate $R_p \times 10^{-3}$ , mole C <sub>2</sub> H <sub>4</sub> / mole radical-hr.	$R_p/(\text{fugacity})^2$
30	115	0.049	5.05	0.382
45	136	0.512	5.28	0.285
60	157	0.037	3.82	0.155
75	178	0.024	2.48	0.078
92	199	0.015	1.55	0.039

<sup>a</sup> Reaction conditions: pressure, 395 kg./cm.<sup>2</sup>; dose rate, 300 rad/hr.; moles of polymer chain radicals,  $9.7 \times 10^{-6}$  mole/l.

ene reacts with a growing radical in the dimer form, whose concentration is proportional to the square of ethylene fugacity. The negative apparent activation energy of  $-9$  kcal./mole for the propagation reaction obtained

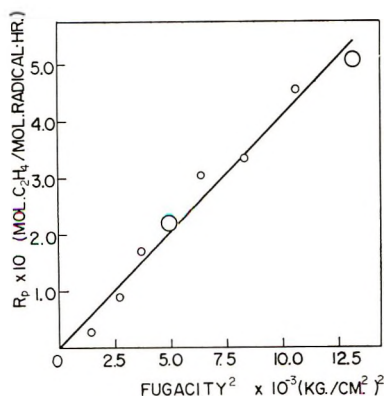


Fig. 7. Absolute propagation rate vs. square of ethylene fugacity at 30°C., 300 rad/hr.; large circle is mean value of the data at different reaction times.

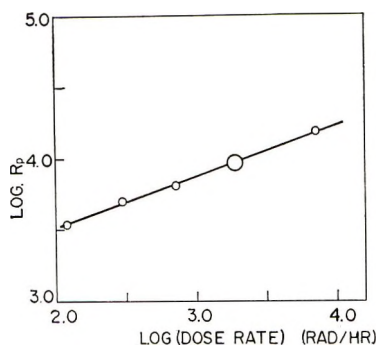


Fig. 8. Logarithmic plots of absolute propagation rate vs. irradiation dose rate at 30°C.; 395 kg./cm.<sup>2</sup>

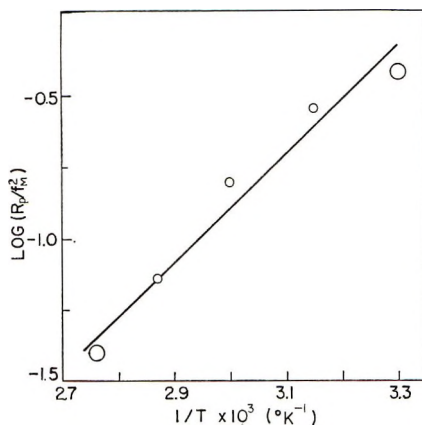


Fig. 9. Effect of temperature on propagation reaction at 300 rad/hr.

from Figure 9 may be mainly attributed to exothermic heat of formation of ethylene dimer. In Figure 8 the absolute propagation rate is shown to increase with dose rate to some extent. A dose rate exponent of 0.3 is given over the range of 120–7300 rad/hr. Both this small effect of dose rate and the fact that the chain growth does not occur without irradiation, may indicate the excitation of either monomer or polymer radical is necessary.

### References

1. S. Machi, M. Hagiwara, M. Gotoda, and T. Kagiya, *J. Polymer Sci. B*, **2**, 765 (1964).
2. S. Machi, M. Hagiwara, M. Gotoda, and T. Kagiya, *J. Polymer Sci. A*, **3**, 2931 (1965).
3. S. Machi, M. Hagiwara, M. Gotoda, and T. Kagiya, paper presented at 17th Meeting of the Japan Chemical Society, Tokyo, Apr. 2, 1964; *Bull. Chem. Soc. Japan*, in press.
4. J. C. Hayward, Dissertation, Yale Univ., 1955; NYO-3313; J. C. Hayward and R. H. Bretton, *Chem. Eng. Progr. Symp. Ser.*, **50**, No. 13, 73 (1954).



5. F. S. Dainton, *J. Polymer Sci.*, **34**, 241 (1959).
6. R. A. Back, E. A. Cherniak, E. Collinson, W. Cooper, F. S. Dainton, G. M. Meaburn, N. Miller, W. H. Stafford, G. A. Swan, P. S. Timmons, D. C. Walker, and D. Wright, *Proc. 2nd Intern. Conf. Peaceful Uses Atomic Energy, Geneva*, **1958**, **29**, 115 (1958).
7. S. Machi et al., *J. Appl. Polymer Sci.*, **9**, 2537 (1965).
8. S. Machi et al., *J. Polymer Sci. A-1*, **4**, 283 (1966).
9. S. Machi et al., *J. Polymer Sci. B*, **3**, 709 (1965).
10. Ohnishi et al., *Ann. Rept. JARRP*, **5**, 215 (1963-1964).

### Résumé

Les réactions d'initiation et de propagation de polymérisations induites par rayons- $\gamma$  de l'éthylène ont été étudiées par la méthode d'irradiation en 2 étapes, à savoir une première étape au cours de laquelle l'initiation et la propagation se passent sous une vitesse de dose élevée et d'une seconde étape où uniquement la croissance du radical polymérique se passe. La vitesse d'initiation est calculée au départ de la quantité de monomère polymérisé et du degré de polymérisation en fonction de la vitesse d'accroissement du nombre de chaînes de molécules polymérisées. La vitesse d'initiation est proportionnelle à la densité de l'éthylène dans la réaction et à la vitesse de dose.  $G_R$  de formation du radical est environ égale à 1.6 à 30°C pour une vitesse dose de  $2.5 \times 10^4$  rad/hr., et est pratiquement indépendante de la densité en éthylène et décroît faiblement avec une vitesse de dose d'irradiation décroissante. La durée de vie du radical polymérique en croissance est longue à température normale. On montre que la vitesse de propagation absolue est proportionnelle au carré de la fugacité de l'éthylène et dépend de la vitesse de dose pour une certaine mesure. Pour la croissance de chaîne, l'irradiation à vitesse de dose faible est indispensable. Une énergie d'activation apparente de la réaction de propagation de  $-9$  Kcal/mole a été obtenue.

### Zusammenfassung

Start- und Wachstumsreaktion bei der  $\gamma$ -strahleninduzierten Äthylenpolymerisation wurde nach der Zwei-Stufen-Bestrahlungsmethode untersucht. In der ersten Stufe findet Start und Wachstum bei einer hohen Dosisleistung statt und in der zweiten Stufe tritt nur das Wachstum der Polymerradikale auf. Die Startgeschwindigkeit wird aus der Menge des polymerisierten Monomeren und dem Polymerisationsgrad als Geschwindigkeit der Zunahme der Anzahl der Polymerketten berechnet. Die Startgeschwindigkeit ist der Dichte des Äthylens in einem Reaktor und der Dosisleistung proportional.  $G_R$  für die Radikalbildung betrug bei 30°C und einer Dosisleistung von  $2,5 \cdot 10^4$  rad/hr etwa 1,6 und ist von der Äthylen-dichte fast unabhängig, nimmt aber mit steigender Bestrahlungsdosisleistung schwach ab. Das wachsende Polymerkettenradikal hat bei normaler Temperatur eine lange Lebensdauer. Es zeigt sich, dass die absolute Wachstumsgeschwindigkeit dem Quadrat der Fugazität des Äthylens proportional ist und in einem gewissen Ausmass von der Dosisleistung abhängt. Für das Kettenwachstum ist eine Bestrahlung mit niedriger Dosisleistung notwendig. Die scheinbare Aktivierungsenergie der Wachstumsreaktion wird zu  $-9$  kcal/Mol erhalten.

Received August 9, 1965

Revised October 25, 1965

Prod. No. 4971A

## Aromatic Polyesterimides

D. F. LONCRINI, *Insulating Materials Department, General Electric Company, Schenectady, New York*

### Synopsis

Several novel arylene bis(trimellitate) dianhydrides have been prepared by: the acidolysis reaction of trimellitic anhydride (TMA) with aromatic diacetoxy compounds and the reaction of trimellitic anhydride monoacid chloride with diphenols. These novel aromatic bisesteranhydrides were reacted with aromatic diamines in polar solvents to give high molecular weight polyamic acid solutions. Heat converted these soluble precursors to insoluble aromatic polyesterimides having good physical and thermal properties. The mechanism of the acidolysis reaction between an aromatic acid and an aromatic acetoxy compound is briefly discussed.

### INTRODUCTION

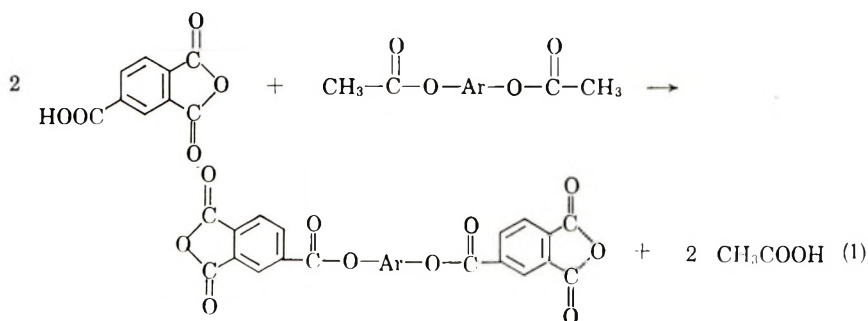
In the synthesis of aromatic polyesters<sup>1</sup> involving the acetate-exchange approach, we have observed that acid interchange proceeds readily with most aromatic polycarboxylic acids but does not occur with acids having the carboxy groups in the *ortho* position. With acids such as *o*-phthalic, pyromellitic, 2,3-naphthalenedicarboxylic, etc., ring closure to the corresponding anhydrides occurs prior to the acid interchange and at this point reaction stops. In view of these findings, the use of trimellitic anhydride (TMA) offered a unique opportunity to prepare novel dianhydride monomers which could subsequently be converted to imide polymers.<sup>2</sup> The present paper is concerned with the preparation and properties of a series of linear polymers having good heat stability in which the aromatic rings are linked together by both ester and imide groups.

### RESULTS AND DISCUSSION

#### Preparation of the Bisesteranhydrides

The reaction of two moles of TMA with one mole of an aromatic diacetoxy compound proceeds according to the eq. (1) (see following page). The reaction proceeds smoothly in the melt but the use of a solvent gives a cleaner product. Aroclor, a chlorinated biphenyl (Monsanto Chemical Company), was found to be an effective reaction medium, with reaction commencing around 270°C. The theoretical amount of acetic acid was collected by gradually raising the temperature to 320°C. over a 90-min period. In most cases the product precipitated on cooling to room tem-

perature. This was filtered, washed, and finally recrystallized from an appropriate solvent. The yields were generally high.



I

A second method of preparation, not fully explored, involved the reaction of the monoacid chloride of TMA with an aromatic dihydroxy compound in the presence of an HCl acceptor such as pyridine.

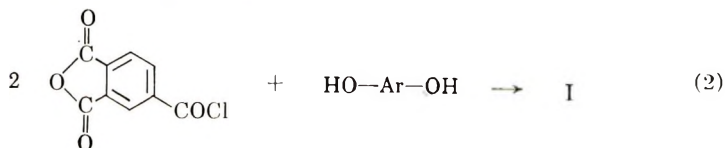

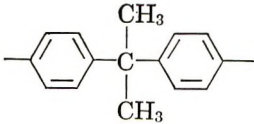
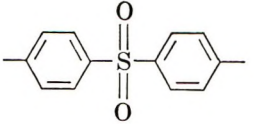
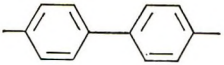
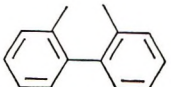


TABLE I  
Physical Properties and Analysis of Bisesteranhydride Monomers (I)

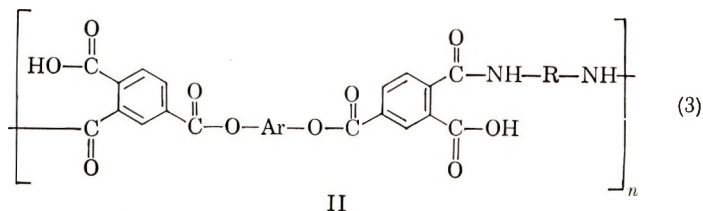
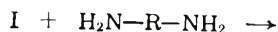
Anhydride	Ar	M.p., °C.	Yield, %	Carbon, %		Hydrogen, %	
				Calcd.	Found	Calcd.	Found
I		274	89	62.89	62.84	2.20	2.03
II		192	94	68.75	67.96	3.50	4.10
III		256	89	60.20	59.24	2.36	2.44
IV		298-301	64	67.42	66.89	2.64	2.66
V		156	70	67.42	67.29	2.64	2.97

This method was used to some advantage in preparing the more soluble bisphenol A derivative.

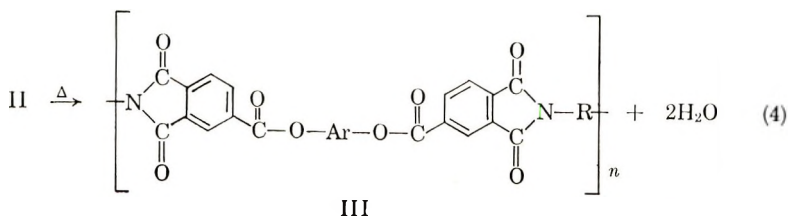
The novel bisester anhydrides are listed in Table I.

### Polymer Preparation

The reaction of these bisesteranhydrides with a diprimary diamine proceeds first to the polyamic acid (II),



which, when heated, is converted to the cyclic imide III with the elimination of water.




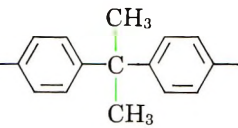
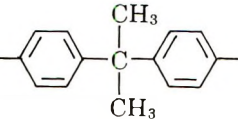
The resulting polymer has alternating ester, ester, imide, imide linkages.

No problems were encountered in the preparation of the polyamic acids. In general, equimolar amounts of the dianhydride and the diamine were mixed together and to this was added the appropriate amount of solvent. Stirring the solution for 1 hr. under a nitrogen atmosphere was usually sufficient to ensure complete reaction. The order of mixing the reagents was studied briefly. There was no apparent difference, whether the amine was added to the anhydride-solvent slurry or the anhydride added to the amine solution. In all cases, the inherent viscosities were approximately the same. This is in direct contrast to the observations made by Bowers and Frost,<sup>4</sup> who found that the molecular weights of poly(pyromellitic acids) were dependent upon the order of mixing of the reagents.

The polymers shown in Table II were all prepared in *N*-methyl-2-pyrrolidone as the solvent. Other solvents, such as *N,N*-dimethylformamide, *N,N*-dimethylacetamide, dimethylsulfoxide, and *m*-cresol, were equally as effective for the preparation of the polymers.

Tough, clear, and flexible films could be prepared simply by spreading the viscous solutions on a glass or tin panel and heating for 1 hr. at 100°C., an additional hour at 200°C., and finally for 1-2 hr. at 240°C. Any attempts to remove the initial solvent too quickly usually resulted in a badly blistered

TABLE II  
 Properties of Polyesterimides

Film	Anhydride Ar =	Diamine	Inherent viscosity <sup>a</sup>	Properties of cured films <sup>b</sup>	Polymer melt tempera- ture, °C.
1		<i>p</i> -Phenylenediamine	2.80	Flexible	>500
2	"	<i>m</i> -Phenylenediamine	1.35	Flexible	"
3	"	3,3'-Dimethoxy-4,4'-diamino diphenyl	1.04	Flexible	"
4	"	Benzidine	3.00	Flexible	"
5	"	4,4'-Diaminodiphenyl ether	1.00	Flexible	"
6	"	4,4'-Diaminodiphenyl methane	0.81	Flexible	"
7	"	4,4'-Diaminodiphenyl sulfone	0.45	Brittle	"
8	"	3,5-Diaminobenzoic acid	0.62	Flexible	"
9	"	50% 4,4'-Diaminodiphenyl ether-50% benzidine	0.78	Flexible	"
10	"	Durenediamine	0.46	Brittle	"
11		4,4'-Diaminodiphenyl ether	0.35	Flexible	390
12		Benzidine	0.41	Flexible	>500

(continued)

and brittle film. Toughness and flexibility were usually improved by heating the film to a higher temperature for a short period of time.

The tensile properties of the films are tabulated in Table III.

The tensile strengths were found to be in good agreement with the values expected for polymers of this type. The tensile moduli, on the other hand, were surprisingly high. In most cases these values were greater than the modulus reported for H-Film.<sup>4</sup>

### Thermal Stability of Aromatic Polyesterimides

The thermal stabilities of the polymers were measured by heating in an air circulating oven at increasing temperatures of 260, 280, and 300°C. for 100 hr. at each temperature. The weight losses of the polymer films after each period of heating are recorded in Table IV. Films 2 and 5 were still flexible to a fingernail crease after the above thermal treatment.

The low weight loss of film 5 prompted us to compare the thermal stability of this polyesterimide with those of other known systems. These results are shown in Table V. Both the amide-imide and ester polymers em-

TABLE II (continued)

Film	Anhydride Ar =	Diamine	Inherent viscosity <sup>a</sup>	Properties of cured films <sup>b</sup>	Polymer melt temperature, °C.
13		<i>p</i> -Phenylenediamine	1.03	Flexible	>500
14		4,4'-Diaminodiphenyl ether	0.34	Flexible	235
15		<i>p</i> -Phenylenediamine	0.31	Brittle	>500
16		<i>m</i> -Phenylenediamine	0.31	Brittle <sup>c</sup>	"
17		4,4'-Diaminodiphenyl ether	0.53	Brittle <sup>c</sup>	"
18		4,4'-Diaminodiphenyl methane	0.45	Brittle <sup>c</sup>	"
19		(Polyamic acids of this material were insoluble)			

<sup>a</sup> Inherent viscosities at 0.5% concentration in *N*-methyl-2-pyrrolidone.

<sup>b</sup> The film was judged to be flexible if it would take a full 180° bend without cracking.

<sup>c</sup> These films were flexible when heat-cured to 150°C. but became brittle when heated to 200°C.

brittled rapidly at the 300°C. point, while the ester-imide and imide polymers were still flexible to a fingernail crease after the 100-hr. treatment at 325°C. These latter two polymers embrittled after the 350°C. treatment but still retained some degree of toughness as evidenced by their ability to take a 1/8-in. mandrel bend. The polyesterimides, especially those prepared from *p*-phenylenebis(trimellitate)dianhydride (Structure I where Ar=*p*-phenylene), are indeed thermally stable systems.

### Mechanism of the Acidolysis Reaction

It is somewhat surprising that the mechanism of acidolysis reactions involving phenols has been given little attention. Their counterparts, on



TABLE III  
 Tensile Properties of Polyesterimide Films

Anhy- dride (Table I)	Amine	Cure condi- tions <sup>a</sup>	Tensile strength		Tensile modulus		Elongation,	
			× 10 <sup>3</sup> , psi		× 10 <sup>3</sup> , psi		%	
			Room temp.	200°C.	Room temp.	200°C.	Room temp.	200°C.
I	<i>p</i> -Phenylenediamine	A	22.3	11.3	—	—	5	16
I	<i>m</i> -Phenylenediamine	A	12.7	4.4	—	—	5	40
I	4,4'-Diaminodiphenyl ether	A	13.1	3.2	—	—	5	50
	ML <sup>b</sup>	A	13.7	6.8	—	—	11	20
I	<i>m</i> -Phenylenediamine	B	14.8	7.5	542	276	7	20
I	<i>m</i> -Phenylenediamine	C	15.8	6.5	454	255	9	15
I	<i>p</i> -Phenylenediamine	C	16.8	11.3	1310	549	3	3
I	4,4'-Diaminodiphenyl ether	C	15.0	6.3	440	193	14	23
I	50% 4,4'-Diamino- phenyl ether- 50% benzidine	C	22.7	9.9	790	354	6	11
	ML <sup>b</sup>	C	14.8	9.7	468	172	28	45
I	4,4'-Diaminodi- phenylmethane	D	14.5	6.1	544	191	6	21
II	4,4'-Diaminodi- phenyl ether	D	9.9	6.3	360	152	4	7
II	Benzidine	D	13.4	6.2	471	208	6	10

<sup>a</sup> A = 1 hr. at 100°C. + 1 hr. at 200°C.; B = 1/2 hr. at 100°C. + 1/2 hr. at 200°C. + 1 hr. at 260°C.; C = 1 hr. at 100°C. + 1/2 hr. at 200°C. + 1 hr. at 240°C.; D = 1 hr. at 100°C. + 1/2 hr. at 200°C. + 4 hr. at 225°C.

<sup>b</sup> ML obtained from du Pont is a polyamic acid reaction product of pyromellitic dianhydride and 4,4'-diaminodiphenyl ether.

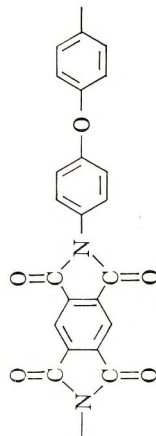
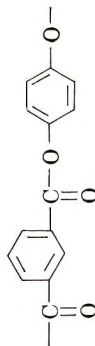
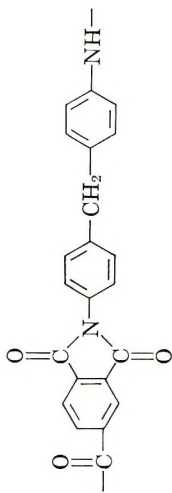
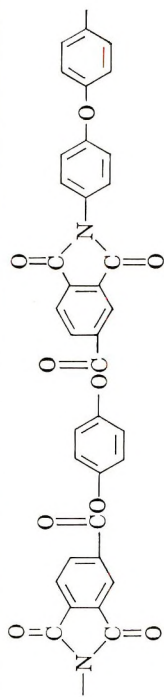
 TABLE IV  
 Weight Loss of Polymers Heated at Various Temperatures in Air

Film	Anhy- dride <sup>a</sup>	Diamine	Wt. loss during 100 hr. of heating, wt.-%			Total wt. loss, wt.-%
			260°C.	280°C.	300°C.	
5	I	4,4'-Diaminodiphenyl ether	1.20	1.38	3.42	6.00
2	I	<i>m</i> -Phenylenediamine	1.86	0.62	3.56	6.04
11	II	4,4'-Diaminodiphenyl ether	7.46	11.20	15.80	34.40
12	II	Benzidine	8.60	5.36	12.00	25.96
14	V	4,4'-Diaminodiphenyl ether	9.25	7.77	8.54	25.56

<sup>a</sup> Refer to Table I.

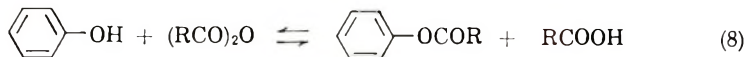
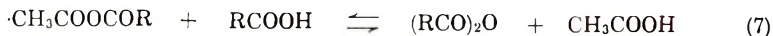
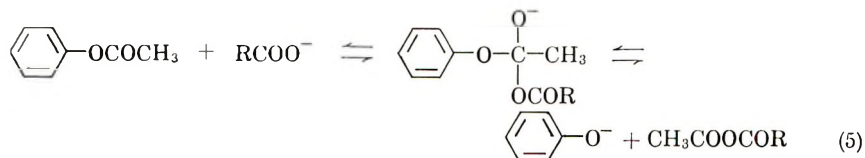
TABLE V. Weight Loss of Polymers Heated at Various Temperatures in Air

Type	Wt. loss during 100 hr. of heating, wt.-%				Total wt. loss, wt.-%
	260°C.	280°C.	300°C.	325°C.	
Ester imide <sup>a</sup>	1.20	1.38	3.42	7.95	29.0
Amide imide <sup>b</sup>	6.17	1.58	6.49	10.92	71.8
Ester	3.90	1.39	10.44	22.92	60.4
Imide <sup>c</sup>	1.16	0.07	1.38	2.40	12.0

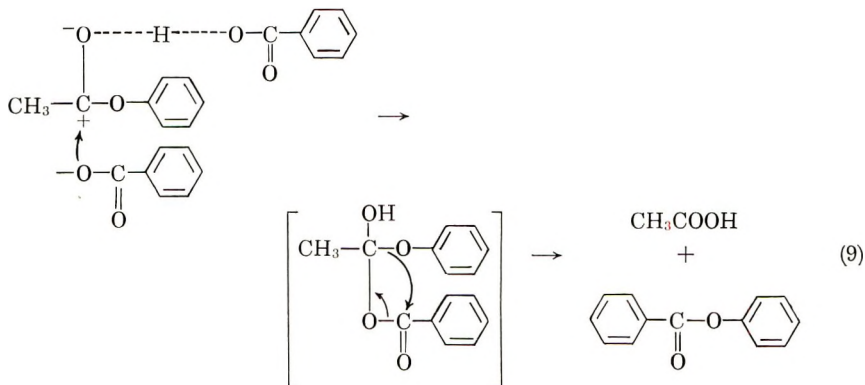


<sup>a</sup> This paper; <sup>b</sup> Amoco Chemical Co. AI-10; <sup>c</sup> du Pont's H film.

the other hand (esterification, hydrolysis, and alcoholysis) have been quite thoroughly investigated. Temin,<sup>5</sup> in an attempt to clarify the mechanism of this reaction which was catalyzed with magnesium ion, postulated the formation of a mixed anhydride as an intermediate which subsequently undergoes interchange with the original acid to liberate the more volatile acid. The new anhydride which is formed then reacts with the phenol to give the ester and the original acid. Temin's postulation is shown in eqs. (5)-(8).



The fact that the anhydride ring of TMA did not react under the conditions of our uncatalyzed exchange reaction suggests that a different mechanism must be in operation here. In support of this, no reaction was found to occur when phenol was refluxed with phthalic, benzoic, or trimellitic anhydride. The mechanism of the acidolysis reaction then may conceivably employ initial hydrogen bonding of the carbonyl oxygen of the ester to increase the electrophilic character of the carbonyl. Nucleophilic attack by the carboxylate anion on the electrophilic center of the ester yields an intermediate which can undergo intramolecular acylation through a four-membered ring transition state. This is shown schematically in eq. (9)



The driving force for the formation of the products is due, in this case, to the liberation of the more volatile acid. This mechanism is further sub-

stantiated by the fact that the rate of acid exchange is increased with solvents of higher dielectric constant. More polar solvents would favor the formation of the initial ions leading to the above intermediate.

A similar mechanism has been reported for the acidolysis reaction of substituted benzoic acids with *N*-methylacetanilide to yield the corresponding *N*-methylbenzanilides and acetic acid.<sup>6</sup>

## EXPERIMENTAL

### Bisesteranhydrides

The general procedures used for the syntheses of the bisester anhydrides are given below for the preparation of *p*-phenylenebis(trimellitate) dianhydride (acidolysis reaction) and for the synthesis of 2,2-bis(*p*-trimellitoxypheyl)propane dianhydride (acid chloride method).

**Preparation of *p*-Phenylenebis(trimellitate) Dianhydride.** A mixture of 192 g. (1.0 mole) of TMA, 97 g. (0.5 mole) of *p*-phenylene diacetate and 500 ml. of Aroclor #1242 was heated with stirring to 300°C. A total of 60 g. (100% of theory) of acetic acid was collected over a 3-hr. period. The mixture was cooled to 80°C., and the slurry was diluted with 2 liters of *n*-heptane. The tan powdery precipitate was filtered, washed three times with diethyl ether, and dried *in vacuo*. A total of 200 g. of crude product melting between 255 and 260°C. was collected. This corresponded to a yield of 89% of theory. Neutral equivalent after hydrolysis was 121 (theory of 123).

The crude product was dissolved in boiling acetic anhydride, treated with activated charcoal, and filtered. On cooling, fine white needles of *p*-phenylenebis(trimellitate) dianhydride melting sharply at 274°C. (uncorrected) was obtained. The yield at this point was 196 g. or 82.3% of theory.

ANAL. Calcd. for C<sub>24</sub>H<sub>10</sub>O<sub>10</sub>: C, 62.89%; H, 2.20%. Found: C, 62.84%; H, 2.03%.

A cleaner product results if acetone is used to wash the precipitate in place of the diethyl ether.

**Preparation of 2,2-Bis(*p*-Trimellitoxypheyl)propane Dianhydride.** Into a 3-liter three-necked flask fitted with a mechanical stirrer, a reflux condenser protected with a drying tube, and a powder addition funnel was added 421 g. (2.0 mole) of TMA monoacid chloride, 225 g. of dry pyridine, and 1300 g. of dry benzene. Bisphenol A, 228 g. (1.0 mole), was added to the mixture portionwise over a period of 30 min. The mixture was stirred under reflux for 1 hr. and finally allowed to cool to room temperature. The pyridine hydrochloride was removed by filtration and the product was precipitated by adding the filtrate to several volumes of dry hexane. The product was washed several times with dry hexane and finally dried in a vacuum oven at 130°C. A 94% yield of product was obtained having a melting range between 165 and 170°C.

The crude product was dissolved in 400 g. of boiling acetic anhydride, cooled to 70°C., diluted with 1 liter of benzene and the mixture refluxed for 1 hr. The pure dianhydride was precipitated with several volumes of dry hexane, filtered, and dried in a vacuum oven at 150°C. Pure 2,2-bis(*p*-trimellitoxypheyl)propane dianhydride melts sharply at 192°C. after three treatments.

ANAL. Calcd. for  $C_{33}H_{20}O_{10}$ : C, 68.75%; H, 3.50%. Found: C, 67.96%; H, 4.10%.

### Polymerization

The most convenient method found for the polymerization step was as follows:

To an equivalent mixture of the diamine and the dianhydride was added in one portion enough organic solvent to make a 10–20% solids concentration. The slurry was stirred vigorously under a nitrogen atmosphere; external cooling was necessary to maintain the reaction temperature below 25°C. Within a few minutes, the mixture became homogeneous and the viscosity of the solution increased rapidly. Stirring was continued for a period of 1 hr. to ensure complete reaction. At this point the viscous polyamic acid polyester solution was ready for further use.

**Precipitation of the Polyamic Acid Polyester for Viscosity Determinations.** The polymer solutions were precipitated with methyl alcohol in a Waring Blender followed by two methyl alcohol washes. The filtered polymers were dried in a vacuum desiccator at room temperature for a period of 8–10 hr. The viscosity measurements were taken in an Ostwald type viscometer with *N*-methyl-2-pyrrolidone as the solvent. The inherent viscosities were calculated on a 0.5% concentration.

**Preparation of the Polyesterimide Films.** The viscous polyamide acid solutions obtained from the reaction were filtered, deaerated, and cast onto glass panels with a doctor knife having a 15–20 mil opening. The panels were dried for 1 hr. at 100°C. in an air circulating oven followed by an additional hour at 200°C. The films were stripped from the glass panels and retaped onto the panels again with Mylar tape. (Failure to do this resulted in films adhering so tightly to the glass that they could not be stripped off.) The panels were then put into a 240°C. oven for 1 hr. or into a 225°C. oven for 4 hr. to complete the imidization reaction.

The author gratefully acknowledges the help of Dr. N. Johnston and Mr. R. Hughes in some of the polymer preparations, and the continued encouragement of Dr. J. Witzel and Dr. J. Elliot.

### References

1. A. Conix, *Ind. Eng. Chem.*, **51**, 147 (1959).
2. C. E. Sroog, A. L. Endrey, S. V. Abramo, C. E. Berr, W. M. Edwards, and K. L. Olivier, *J. Polymer Sci. A*, **3**, 1375 (1965).
3. G. M. Bowers and L. W. Frost, *J. Polymer Sci. A*, **1**, 3135 (1963).
4. L. E. Amborski, *Ind. Eng. Chem., Prod. Res. Develop.*, **2**, No. 3, 189 (1963).

5. S. C. Temin, *J. Org. Chem.*, **26**, 2518 (1961).
6. R. N. Ring, J. G. Shareskin, and D. Davidson *J. Org. Chem.*, **27**, 2428 (1962).

### Résumé

De nombreux nouveaux dianhydrides arylène-bis-trimellitiques ont été préparés par réaction d'acidolyse d'anhydride trimellitique (TMA) avec des dérivés aromatiques diacétoxylés et la réaction du monochlorure acide de l'anhydride trimellitique avec des diphénoles. Ces nouveaux bis-ester-anhydrides aromatiques ont été mis en réaction avec des diamines aromatiques dans des polaires solvants et fournissent des solutions d'acide polyamique de poids moléculaire élevé. Par la chaleur ces précurseurs solubles sont transformés en polyester-imides aromatiques insolubles présentant des propriétés physiques et thermiques de bonne qualité. Le mécanisme de la réaction d'acidolyse entre l'acide aromatique et un dérivé aromatique acétoxylé est soumis à brève discussion.

### Zusammenfassung

Einige neue Arylen-bis(trimellitit)dianhydride wurden durch die Acidolyse-reaktion von Trimellitsäureanhydrid (TMA) mit aromatischen Diacetoxyverbindungen und durch die Reaktion von Trimellitsäureanhydridmonosäure-chlorid mit Diphenolen dargestellt. Diese neuen aromatischen Bisesteranhydride wurden in polaren Lösungsmitteln mit aromatischen Diaminen unter Bildung von hochmolekularen Polyamidsäurelösungen zur Reaktion gebracht. Durch Hitzeeinwirkung wurden diese löslichen Vorstufen in unlösliche aromatische Polyesterimide mit guten physikalischen und thermischen Eigenschaften umgewandelt. Der Mechanismus der Acidolysreaktion zwischen einer aromatischen Säure und einer aromatischen Acetoxyverbindung wird kurz diskutiert.

Received September 13, 1965

Revised October 18, 1965

Prod. No. 4973A



## Oxygen Diffusion Limitation In Autoxidation of Polypropylene

C. R. BOSS and J. C. W. CHIEN, *Hercules Research Center,  
Wilmington, Delaware*

### Synopsis

The induction period for the autoxidation of polypropylene increases with increasing sample thickness (from 1 to 75 mils) and with decreasing oxygen pressure. The rate of oxidation shows the opposite dependences. In contrast, neither the rate nor the induction period in well stirred oxidations of squalane is oxygen pressure-dependent. It is concluded that autoxidation of polypropylene is controlled by diffusion of oxygen into the sample.

### INTRODUCTION

The branched-chain autoxidation of polyolefin is characterized by an induction period during which hydroperoxides are produced.<sup>1</sup> The decomposition of these hydroperoxides is commonly recognized as the process responsible for the ensuing rapid oxidation. However, the nature of the process which produces hydroperoxides during the induction period is not yet understood. This process may be reactions between metallic and hydroperoxide impurities,<sup>2</sup> or it may be reactions between molecular oxygen and the substrate.<sup>3-5</sup> Dudorov<sup>5</sup> reported that the length of the induction period in polypropylene oxidation varied linearly with  $\log (p_{O_2})^{1/2}$ . Based upon this observation he proposed an initiation reaction,



However, Dudorov did not consider the possibility that the observed dependence of  $t_{ind}$  upon oxygen pressure is a manifestation of diffusion limitation.

Reliable kinetic measurements on liquid-phase autoxidations are difficult, because of the problem of maintaining oxygen saturation in the liquid phase.<sup>6</sup> In our laboratory, it is found that autoxidation of squalane between 85 and 150°C. is oxygen concentration-dependent at atmospheric pressure unless the liquid is stirred vigorously. It is the purpose of this paper to show that autoxidation of polypropylene is limited by oxygen diffusion even for very small particle size samples.

## EXPERIMENTAL

### Materials

Two types of polypropylene were used in this study: commercial Pro-fax resin (Hercules Powder Company) and an experimental sample. The latter was polymerized, purified, and dried on a vacuum line and stored under nitrogen at 0°C. The two polymers oxidize with the same induction periods and rates. The oxidation characteristics of these polymers with added antioxidants are also similar in every respect.

Squalane, purchased from Eastman Organic Chemicals, was stirred repeatedly with concentrated sulfuric acid, the colored acid being replaced each time by fresh acid and then neutralized, washed, dried, and fractionally distilled.

### Oxygen Absorption

The absorption cell is fabricated from a short section of 50-mm. tubing with a cylindrical dish (10 mm. deep, 40 mm. in diameter) attached to its interior wall. The bottom of the dish is a flat circular disk. Polypropylene, 0.1 g., is placed in this dish. The absorption cell is connected through O-ring joints to a molecular-sieve holder. The holder is constructed from a 22-mm., coarsely sintered, glass disk filled with about 1 g. of activated Linde Type 5A sieve. The absorption cell and the holder were placed in an oven and connected via another O-ring joint to a thermostatted 10-ml. gas buret and one arm of a U-tube equipped with an electrode containing mercury. A known pressure was trapped in the other arm. Absorption of oxygen raised the mercury level, and thereby activated a motor which simultaneously raised a mercury leveling bulb and drove a 10-ohm potentiometer. A strip-chart recorder recorded the position of the mercury leveling bulb.

To study the autoxidation of squalane or a solution of polypropylene, we used a cell made from 20-mm. tubing containing a magnetic stirring bar. The cell was immersed in a constant-temperature bath and connected via a condenser to oxygen absorption equipment similar to that described above. For sample volume greater than 0.5 ml., the magnetic stirring was inadequate as the specific oxidation rate increased with decreasing sample volume; this rate was constant for a sample volume smaller than 0.5 ml. The results given in Table I were obtained on 0.25 ml. of squalane.

## RESULTS

### Effect of Oxygen Pressure on Autoxidation of Squalane

The results of autoxidation of squalane at 125°C. and oxygen pressures of 100–1476 mm. are summarized in Table I. There were no significant variations in either the induction period or the rate of oxidation with oxygen pressure.

TABLE I  
 Autoxidation of Squalane at Different Oxygen Pressures at 125°C.

Oxygen pressure, mm.	Induction period, min.	Steady-state rate of oxidation, ml.(S.T.P.)/min.-g.
100.7	654	0.81
134.6	679	0.86
314.8	604	0.79
758	639	0.82
1476	588	0.81

**Effect of Oxygen Pressure on Autoxidation of Polypropylene**

Table II gives the results of autoxidation of polypropylene flakes. The effect of increasing oxygen pressure is to lower the induction period and to increase the rate of oxidation.

TABLE II  
 Autoxidation of Polypropylene at Different Oxygen Pressures at 110°C.

Average particle size, $\mu$	Oxygen pressure, mm.	Induction period, min.	Steady-state rate of oxidation, ml.(S.T.P.)/min.-g.
35	80	719	0.06
35	147	706	0.08
35	366	418	0.19
35	751	254	0.36
35	1153	366	0.48
35	158 (air)	787	0.09
200	750	260	0.28

Nearly identical results were obtained when either air or oxygen was used at comparable oxygen partial pressure.

TABLE III  
 Effect of Sample Thickness on Polypropylene Oxidation at 150°C.

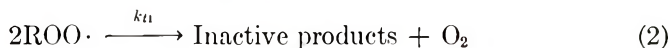
Sample thickness, mil	Induction period, min.	Rate of oxidation ml.(S.T.P.)/min.-g.
75	1422	0.21
40	1550	0.55
25	1390	0.65
15	1121	0.57
10	605	1.21
8	342	1.50
5	459	2.00
3	618	1.83
2	390	1.79

### Effect of Sample Thickness on Autoxidation of Polypropylene

As the thickness of polypropylene sample increases, the rate of oxidation steadily decreases (Table III). On the other hand, the increase of sample thickness up to about 15 mil increases induction period. Thicker samples all have the same induction period. Similar behavior has also been noted by Russell and Pascale.<sup>7</sup>

### DISCUSSION

At relatively high oxygen concentration and when oxygen saturation is maintained in the liquid, the major chain-carrying species is the ROO· radicals, and chain termination is almost exclusively via reaction (2).

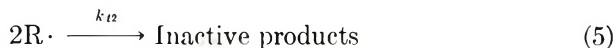


The rate of oxidation has the simple form\* of

$$-d[\text{O}_2]/dt = k_2[\text{RH}] (R_i/2k_{t1})^{1/2} + R_i/2 \quad (3)$$

where  $k_2$  is the rate constant of propagation, and  $R_i$  is the rate of initiation. The rate of oxidation is independent of the oxygen pressure. The results in Table I showed that autoxidation of squalane is not limited by oxygen diffusion when the liquid is vigorously stirred.

When oxygen saturation in a system cannot be maintained (such as in solid samples), other termination reactions become significant.



Of the two reactions, (5) is probably less important because oxidation is not autocatalytic in this region. The rate of oxidation may be expressed as:<sup>8</sup>

$$\frac{dC}{dt} = \frac{k_1k_2 [\text{RH}]CR_i^{1/2}}{(k_1k_2k_{t12}C[\text{RH}] + 2k_1^2k_{t1}C^2 + 2k_2^2k_{t2}[\text{RH}]^2)^{1/2}} \quad (6)$$

where  $C$  is the oxygen concentration and  $k$ , is the rate constant for the reaction between  $\text{R}\cdot$  and  $\text{O}_2$ .

If in addition, the system is not agitated, then the local concentrations of oxygen and of radicals and the rate of oxidation are functions of distance from the surface and of the sample thickness. To solve this diffusion problem, let us consider a volume element of unit cross section between  $x$  and  $x + dx$ ; the changes in oxygen concentration over a period of time  $dt$  are:

$$\text{Diffusing in:} \quad -D \frac{\partial C}{\partial x} dt$$

\* Oxygen liberated in reaction (2) is assumed to be small when the chain length is long.

$$\text{Diffusing out:} \quad D \left( \frac{\partial C}{\partial x} + \frac{\partial^2 C}{\partial x^2} dx \right) dt$$

$$\text{Reacting:} \quad -kCdt dx$$

Where  $D$  is the diffusion coefficient, and the rate of oxidation is first order with respect to oxygen concentration  $C$ , i.e.,  $k = k_1 [\text{R}\cdot]$ . The net increase in concentration is  $[D(\partial^2 C/\partial x^2) - kC]dt dx$ .

This increase may be equated to  $dCdx$  to give

$$\partial C/\partial t = D(\partial^2 C/\partial x^2) - kC \quad (7)$$

Let the boundary conditions be:

$$\begin{aligned} C &= C_0, & x &= 0, & t &> 0 \\ C &= 0, & x &> 0, & t &= 0 \\ C &= 0, & x &= \infty, & t &> 0 \end{aligned}$$

then the solution to eq. (7) is given<sup>9</sup> as

$$\begin{aligned} \frac{C}{C_0} &= \frac{1}{2} \exp \left\{ -x \sqrt{\frac{k}{D}} \right\} \operatorname{erfc} \left( \frac{x}{2\sqrt{tD}} - \sqrt{kt} \right) + \frac{1}{2} \exp \left\{ x \sqrt{\frac{k}{D}} \right\} \\ &\quad \times \operatorname{erfc} \left( \frac{x}{2\sqrt{tD}} + \sqrt{kt} \right) \quad (8) \end{aligned}$$

On differentiating with respect to  $x$  and evaluating at the surface ( $x = 0$ ), eq. (8) becomes,

$$(\partial C/\partial x)_{x=0} = -C_0 \sqrt{k/D} [\operatorname{erf} \sqrt{kt} + (e^{-kt}/\sqrt{\pi kt})] \quad (9)$$

The rate of oxidation per unit volume of sample is,

$$\text{Rate of oxidation} = -(D/l)(\partial C/\partial x)_{x=0} \quad (10)$$

where  $l$  is the thickness of the sample. Substituting eq. (9) into eq. (10) gives

$$\text{Rate of oxidation} = \frac{C_0}{l} \sqrt{kD} [\operatorname{erf} \sqrt{kt} + (e^{-kt}/\sqrt{\pi kt})] \quad (11)$$

Both  $k$  and  $t$  are large positive quantities, therefore,  $\operatorname{erf} \sqrt{kt} \sim 1$  and  $e^{-kt} \sim 0$ . The approximate expression for eq. (11) is

$$\text{Rate of oxidation} \approx (C_0/l) \sqrt{kD} \quad (12)$$

For a given temperature, the rate of oxidation is directly proportional to the oxygen concentration. The results given in Table II obey this relationship (Fig. 1). Equation (12) also requires an inverse linear relationship between the rate of oxidation and the film thickness. Figure 2 shows that the results of Table III obey this relationship for samples thicker than 5 mil. For very thin samples the rate of oxidation appears to be independent of thickness. That oxidation of these thin samples is also oxygen diffusion-limited is established by the dependence of induction period upon

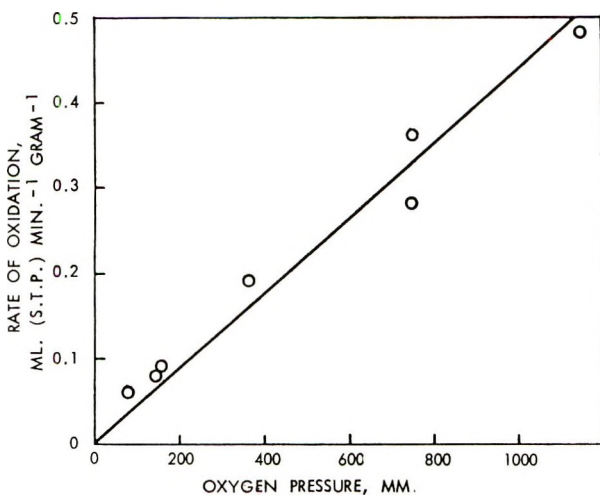


Fig. 1. Variation of steady-state rate of polypropylene oxidation at 110°C. with oxygen pressure.

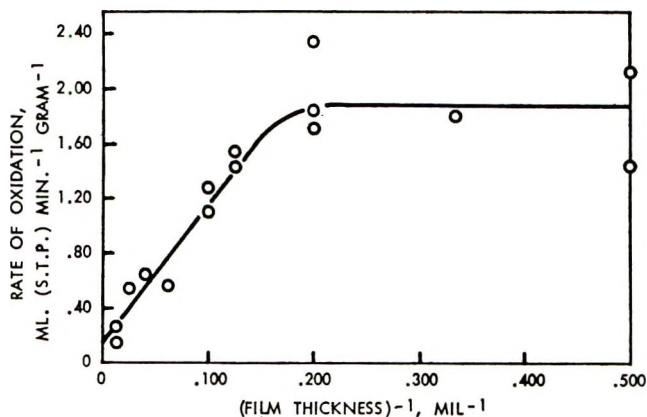


Fig. 2. Variation of steady-state rate of polypropylene oxidation at 150°C. with sample thickness.

oxygen pressure at these thicknesses (*vide infra*). One of the possible explanations for the observed deviation at small thickness is based upon the observation<sup>10</sup> that volatile oxidation products promote further oxidation. These products are more readily volatilized from the thin specimen than the thick ones, resulting in slower oxidation for the former. Furthermore, it is very difficult to press thin films to uniform thickness over a large surface area. This nonuniformity is probably responsible for the poor reproducibility in both the rates of oxidation and the induction period for thin films.

The total amount of oxygen absorbed per unit area in time  $t$  is

$$[O_2] = C_0\sqrt{D/k} [(kt + 1/2) \operatorname{erf} \sqrt{kt} + \sqrt{kt/\pi} e^{-kt}] \quad (13)$$



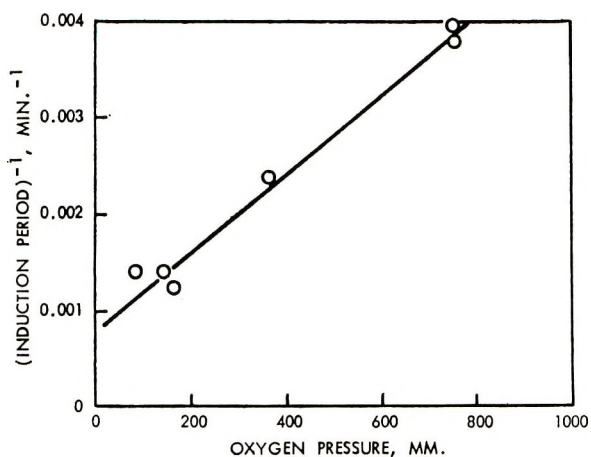


Fig. 3. Variation of induction period of polypropylene oxidation at 110°C. with oxygen pressure.

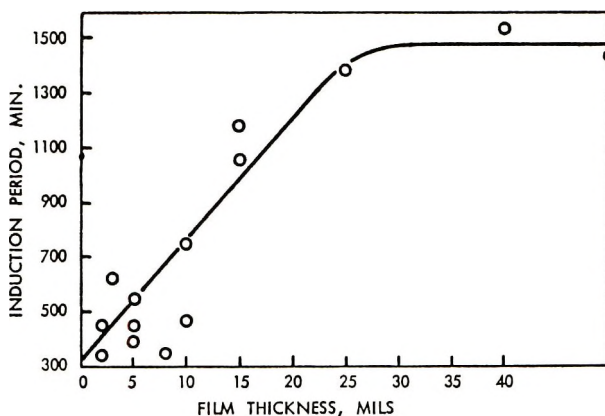


Fig. 4. Variation of induction period of polypropylene oxidation at 150°C. with sample thickness.

It has been found<sup>5,11</sup> that nearly all of the oxygen initially consumed is converted to hydroperoxide. If the induction period is defined<sup>12</sup> as the time required to accumulate a critical concentration of hydroperoxides,  $[\text{ROOH}]_c$ , then

$$[\text{ROOH}]_c = (C_0/l) \sqrt{D/k} \left[ \left( kt_{\text{ind}} + \frac{1}{2} \right) \text{erf} \sqrt{kt_{\text{ind}}} + \sqrt{kt_{\text{ind}}/\pi} e^{-kt_{\text{ind}}} \right] \quad (14)$$

Again, for sufficiently large values of  $kt_{\text{ind}}$ , one obtains

$$t_{\text{ind}} = \frac{[\text{ROOH}]_c l}{C_0 \sqrt{kD}} - \frac{l}{2k} \quad (15)$$

If  $[\text{ROOH}]_c$  is a function of temperature alone, then  $t_{\text{ind}}$  is inversely proportional to oxygen concentration. Figure 3 shows this relationship for the results in Table II. Furthermore, eq. (15) also requires that  $t_{\text{ind}}$  is linearly related to the sample thickness. The results in Table III, plotted in Figure 4, show large scattering for samples with thickness 10 mil or less. This scattering is attributed to nonuniformity of sample thickness. It is reasonable to expect that the thinnest portion of the specimen determines the induction period.

The induction period for samples with thickness greater than 25 mil is apparently independent of thickness. This result indicates that initially, oxidation is limited to the first 25 mil of the specimen.

The results and discussion presented here show fairly conclusively that polypropylene oxidation under most experimental conditions are diffusion-limited at any given temperature as evidenced by the dependence of the rate of oxidation and induction period upon oxygen pressure and sample thickness. It is important to note that these oxidations are also kinetically controlled. Both the  $[\text{ROOH}]_c$  and  $k(=k_1[\text{R}\cdot])$  are functions of the steady-state radical concentrations. A complete description of the kinetics of polypropylene oxidation must include both considerations.

### References

1. K. U. Ingold, *Chem. Revs.*, **61**, 563 (1961).
2. N. Uri, in *Autoxidation and Antioxidants*, W. O. Lundberg, Ed., Interscience, New York, 1961, pp. 55-104.
3. N. T. Notley, *Trans. Faraday Soc.*, **58**, 66 (1962); *ibid.*, **60**, 88 (1964).
4. E. T. Denisov, *Kinetika i Kataliz*, **4**, 508 (1963).
5. V. V. Dudorov, *Kinetika i Kataliz*, **4**, 214 (1963).
6. L. Bateman, *Quart Rev.*, **8**, 147 (1954).
7. C. A. Russell and J. V. Pascale, *J. Appl. Polymer Sci.*, **7**, 959 (1963).
8. C. Walling, *Free Radicals in Solution*, Wiley, New York, 1957, pp. 397-466.
9. J. Crank, *The Mathematics of Diffusion*, Clarendon Press, Oxford, 1957, p. 130.
10. Blumberg, M., C. R. Boss, and J. C. W. Chien, *J. Appl. Polymer Sci.*, **9**, 3837 (1965).
11. C. R. Boss, unpublished results.
12. A. V. Tobolsky, D. J. Metz, and R. B. Mesrobian, *J. Am. Chem. Soc.*, **72**, 1942 (1950).

### Résumé

La période d'induction de l'autooxydation du polypropylène croît avec un accroissement de l'épaisseur de l'échantillon (de 1 à 75 mils) et avec une diminution de pression d'oxygène. La vitesse d'oxydation montrait des dépendances en direction opposée. Par contre ni la vitesse ni la période d'induction de l'oxydation du squalate ne dépendent de la pression d'oxygène. On en conclut que l'autooxydation du polypropylène est contrôlée par la diffusion de l'oxygène au sein de l'échantillon.

### Zusammenfassung

Die Induktionsperiode bei der Autoxydation von Polypropylen nimmt mit steigender Probendicke (von 1 bis 75 Mils) und mit abnehmendem Sauerstoffdruck zu. Die Oxydationsgeschwindigkeit zeigt die entgegengesetzte Abhängigkeit. Im Gegensatz dazu ist

weder die Geschwindigkeit noch die Induktionsperiode bei der Oxydation von Squalan bei guter Rührung vom Sauerstoffdruck abhängig. Man kommt zu dem Schluss, dass die Autoxydation von Polypropylen durch die Diffusion von Sauerstoff in der Probe kontrolliert wird.

Received June 7, 1965

Revised November 5, 1965

Prod. No. 4975A



NCA's of  $\gamma$ -benzyl glutamate and of alanine were investigated by Okamura et al.<sup>2</sup> in somewhat more detail. Their most striking result was the finding that the NCA of the racemic  $\gamma$ -benzyl glutamate polymerized more rapidly than the NCA derivative of the optically active material.

In the present study we attempted to clarify a number of questions raised by this interesting reaction. Since the nature of the initiating process in the solid-state polymerization of a NCA is obscure, it seemed of interest to determine the effect of a variation of the aqueous vapor pressure of the atmosphere on the kinetic pattern and the chain length of the polymeric product. The conformation and the ordering of the polymer were characterized by infrared spectroscopy and x-ray diffraction. Finally, it seemed essential to explore in more detail the difference in the behavior of optically active and racemic monomer samples. If the racemic monomer has a different crystal structure, rather than being made up of a mixture of crystallites of the L and D isomers, then a D-L pair of monomer molecules must constitute the repeat unit. It would be conceivable, under those conditions, that the ordering of the monomer molecules in the crystalline phase favors a polymer chain growth with a regular alternation of D and L residues. Such copolypeptides do not appear to have been made previously, and their production in the solid state would constitute an interesting application of the restraints imposed by the crystalline order for the preparation of novel polymers. However, the results obtained in the present investigation give no indication of the formation of such regularly alternating copolypeptides.

## EXPERIMENTAL

### Monomer Preparation

The NCA of  $\gamma$ -benzyl L-glutamate (BG),  $\gamma$ -methyl L-glutamate (MG) and the corresponding derivatives of DL-glutamic acid esters were prepared as described by Hanby.<sup>3</sup> For the preparation of the NCA of  $\epsilon$ -carbobenzoxy-L-lysine (CL) and the corresponding racemic compound, the method of Bergman et al.<sup>4</sup> was used. The monomers were precipitated several times from dry ethyl acetate solution by the addition of dry hexane. Their melting points are listed in Table I.

All NCA's were prepared with careful exclusion of water vapor to avoid polymer formation. They were stored at  $-30^{\circ}\text{C}$ . over phosphorus pentoxide.

TABLE I  
Melting Points of *N*-Carboxy Amino Acid Anhydrides

	Melting point, $^{\circ}\text{C}$ .	
	L form	DL form
$\gamma$ -Benzyl glutamate NCA	96	70
<i>N</i> -Methyl glutamate NCA	98	115 <sup>a</sup>
$\epsilon$ -Carbobenzoxylysine NCA	97	105

<sup>a</sup> Decomposes rapidly at its melting point.

### Polymerization Kinetics

Monomer samples ranging from 5 mg. to 50 mg. were placed in a tube which was carefully evacuated. It was then filled either with dry nitrogen (passed through columns of activated alumina, calcium chloride and phosphorus pentoxide), with nitrogen saturated with water vapor at 25°C., or with nitrogen half-saturated with water vapor at 25°C. (by passage through a sulfuric acid-water mixture containing 43.8 wt.-%  $\text{H}_2\text{SO}_4$ ). These conditions correspond to an aqueous vapor pressure  $p_{\text{H}_2\text{O}}$  of 0, 13, and 26 mm. Hg, respectively. The container with the monomer sample was then immersed into a thermostated bath and connected to a manometer. The progress of the polymerization was followed by the volume of the evolved carbon dioxide at constant pressure. The total  $\text{CO}_2$  measured when the reaction had run to completion was generally within 3% of the calculated value.

### X-Ray Diffraction

Powder diffraction photographs were taken by using Ni-filtered  $\text{CuK}\alpha$  radiation and a cylindrical camera with a diameter of 114.6 mm.

### Infrared Spectra

Infrared spectra were recorded on a Perkin-Elmer Model 21 infrared spectrophotometer, generally with 300–400 mg. potassium bromide disks containing 1% of the sample to be investigated. In the case of the L-lysine polymers, the samples were investigated in a Nujol mul.

## RESULTS

### Nature of the Racemic Monomer

The melting points listed in Table I show that in the case of two of the NCA's investigated, the racemic material melts higher than the optically active isomer. This shows clearly that the racemate cannot consist of a mixture of D and L crystals but must represent a different crystal structure. In the third case, i.e., that of  $\gamma$ -benzyl glutamate, the racemic sample has a somewhat lower melting point, but the difference of only 26°C. makes it rather unlikely, that it would be the eutectic of the D and L isomers. The x-ray data, represented schematically in Figure 1, fully substantiate the conclusion that the racemic NCA represents a phase different from that of the optically active compound in all three systems under investigation. Similar conclusions were reached from a comparison of the infrared spectra of the optically active and racemic monomers.

### Polymerization Kinetics

It is well known that solid-state reactions are frequently characterized by a slow initial nucleation process, which is followed by a much faster reaction at the interface of the reactant and the reaction product.<sup>5</sup> This pattern



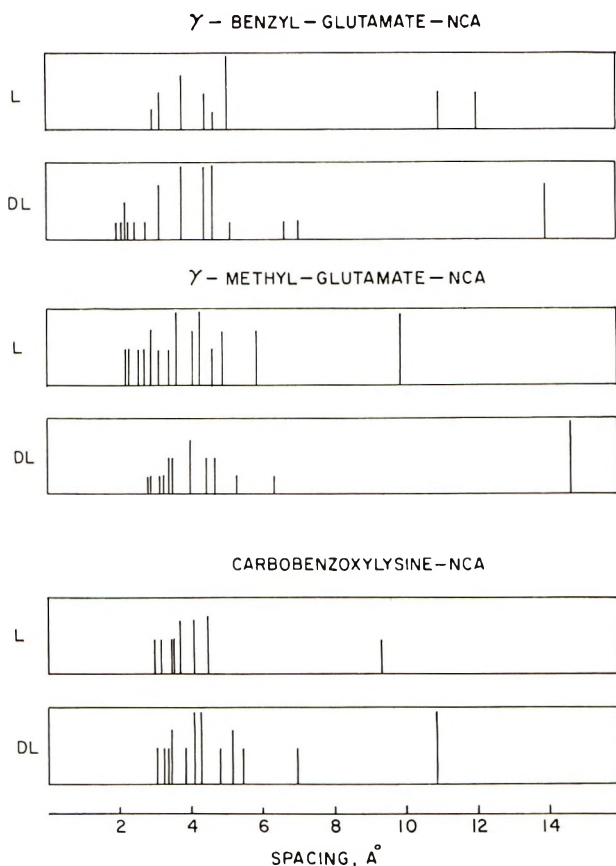


Fig. 1. X-ray diffraction spectra of the L and the DL forms of *N*-carboxy anhydrides.

was found to be characteristic of most of the processes studied in the present investigation. It was then convenient to characterize the kinetic pattern by two parameters, i.e., the maximum reaction velocity  $v_{\max}$  (given as the fractional conversion per minute) and an induction period  $t_i$  (minutes) obtained as the intercept on the time axis of a slope drawn at the steepest point of the conversion-time curve. The results, represented in this manner, are listed in Table II. The following features of the data may be noted. (a) With the NCA of  $\gamma$ -benzyl L-glutamate, the maximum reaction velocity is quite insensitive to the water vapor in the atmosphere. The induction period tends to be reduced as the aqueous vapor pressure is increased, but the effect is relatively small. The kinetic curves obtained at 60°C. are shown in Figure 2. With the NCA of  $\gamma$ -methyl L-glutamate, neither  $v_{\max}$  nor  $t_i$  is altered significantly by the introduction of water vapor. The NCA of  $\epsilon$ -carbobenzoxy-L-lysine differs from the other two L-monomers in that no induction period is observed and the polymerization velocity attains its maximum value as soon as the reaction temperature is reached. Water vapor accelerated the reaction considerably at 70°C., although no

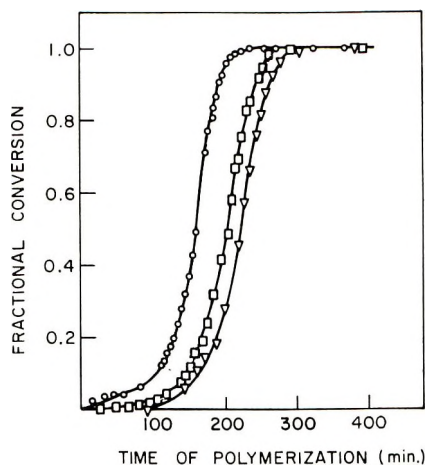


Fig. 2. Thermal polymerization of the *N*-carboxy anhydride of  $\gamma$ -benzyl *L*-glutamate at 70°C. at various ambient aqueous vapor pressures: ( $\nabla$ ) 0 mm. Hg; ( $\square$ ) 13 mm. Hg; ( $\circ$ ) 26 mm. Hg.

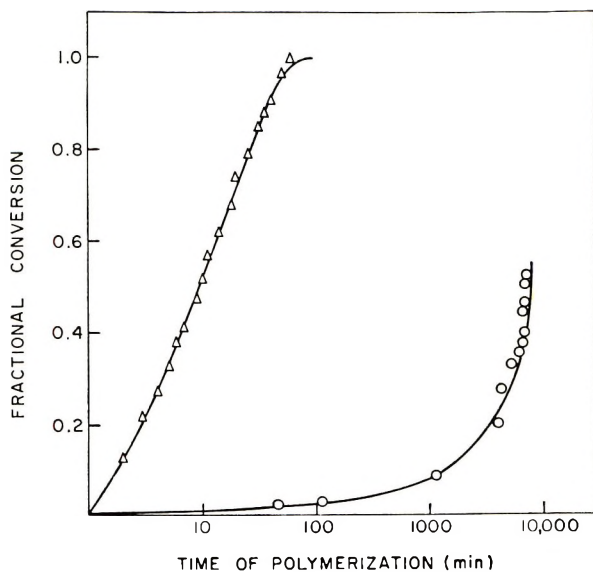


Fig. 3. Thermal polymerization of the *N*-carboxy anhydrides of ( $\Delta$ )  $\gamma$ -methyl-*L*-glutamate and ( $\circ$ )  $\gamma$ -methyl-DL-glutamate at 80°C. and an ambient aqueous vapor pressure of 13 mm. Hg.

significant effect was produced at 80°C. (b) The observation of Okamura et al.,<sup>2</sup> who found the NCA of the racemic  $\gamma$ -benzyl glutamate to react more rapidly than the optically active monomer, was confirmed for the reaction in the presence of aqueous vapor. However, when water vapor was carefully excluded, the racemic monomer had a longer induction period and a lower maximum reaction velocity. (c) The racemic NCA derivatives of

MG and CL were found to be very unreactive. The difference between the behavior of the L and the DL monomer is illustrated in Figure 3 on the NCA of MG. With the NCA of CL at 80°C. and with  $p_{\text{H}_2\text{O}} = 13$  mm. Hg, 20% of the optically active monomer was polymerized in 2 min., while the racemic monomer required 4000 min. to attain the same conversion.

TABLE II  
Maximum Reaction Velocities and Induction Periods in NCA Polymerizations

NCA	$p_{\text{H}_2\text{O}}$ , mm. Hg	50°C.		60°C.		70°C.		80°C.	
		$10^3v_{\text{max}}$ , min. <sup>-1</sup>	$t_i$ , min.	$10^3v_{\text{max}}$ , min. <sup>-1</sup>	$t_i$ , min.	$10^3v_{\text{max}}$ , min. <sup>-1</sup>	$t_i$ , min.	$10^3v_{\text{max}}$ , min. <sup>-1</sup>	$t_i$ , min.
L-BG	0			2.0	760	11.7	185		
"	13			2.0	680	11.7	160		
"	26			1.8	460	15.2	130		
DL-BG	0	0.30	2500	1.5	2220				
"	13	0.28	1600	2.4	550				
"	26	0.30	1050	10.5	320				
L-MG	0			5.6	515	13.7	298		
"	13			7.1	490	13.3	270		
"	26			6.8	475	13.3	252		
DL-MG	26			Very slow <sup>a</sup>					
L-CL	0					1.5	0	72	0
"	13					3.5	0	75	0
"	26			0.6	0	6.4	0	67	0
DL-CL	13							Very slow <sup>b</sup>	

<sup>a</sup> See Fig. 3.

<sup>b</sup> See text.

### Characterization of the Polypeptides

Intrinsic viscosities  $[\eta]$  of polypeptides obtained from the three L-monomers and from the racemic NCA of BG were determined in dichloroacetic acid at 25°C. In the case of the other two racemic monomers, conversion to polymer was too low for evaluation of the reaction product. The results are listed in Table III. In all cases, the intrinsic viscosities decreased when the polypeptide was prepared in the presence of water vapor. Using the relation between  $[\eta]$  and weight-average molecular weights found by Doty et al.,<sup>6</sup> the degrees of polymerization of the poly( $\gamma$ -benzyl L-glutamate) produced at 60°C. under anhydrous conditions and in the presence of 26 mm. Hg of water vapor are 180 and 150, while the corresponding values for the polypeptide obtained from the racemic monomer are 118 and 30, respectively.\*

\* When the NCA's of the L-isomers of lysine, benzyl glutamate, and methyl glutamate were polymerized in the melt (18 hr. at 120°C.), the resulting polypeptides had significantly lower intrinsic viscosities (0.09, 0.09, and 0.12) than those obtained in the solid-state reaction.

TABLE III  
Intrinsic Viscosities of Polypeptides

$p_{H_2O}$ , mm. Hg.	$[\eta]$ , dl./g.			
	Poly(L-CL) (70°C.)	Poly(L-MG) (60°C.)	Poly(L-BG) (60°C.)	Poly(DL-BG) (60°C.)
0	0.15	0.22	0.31	0.10
13			0.28	0.07
26	0.10	0.19	0.28	0.07

The infrared spectra of the polypeptides were used to evaluate the relative proportions of the polymer in the  $\alpha$ -helical form (absorbing at  $1655\text{ cm.}^{-1}$ ) and the extended  $\beta$ -form, absorbing at  $1630\text{ cm.}^{-1}$ .<sup>7</sup> Typical examples of the appearance of this spectral region for the various polypeptides studied are shown in Figure 4. Poly( $\gamma$ -benzyl L-glutamate) exists mostly in the  $\alpha$ -form, and the content of  $\beta$ -structures is almost independent of the presence of water vapor during the polymerization process. With poly( $\gamma$ -methyl L-glutamate) the  $\alpha$  and  $\beta$  peaks are about equal, and the aqueous vapor pressure is again without influence on the appearance of the spectra. In the case of the racemic poly( $\gamma$ -benzyl glutamate), the content of  $\beta$ -

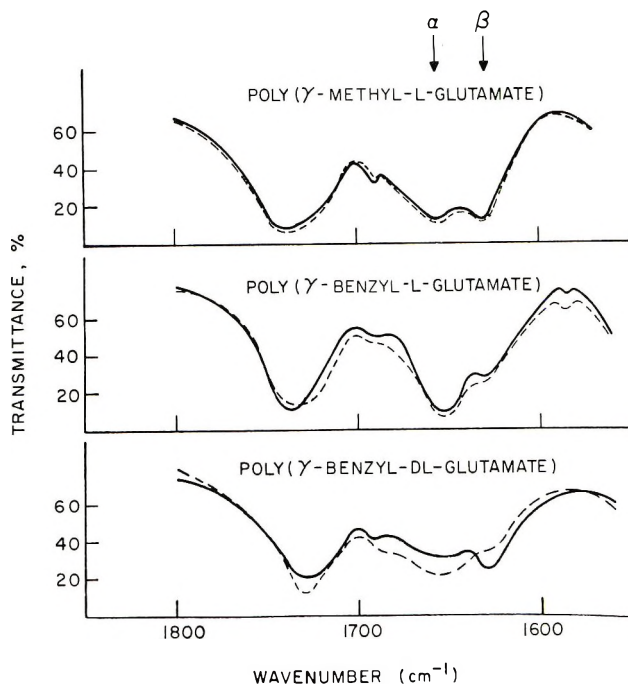


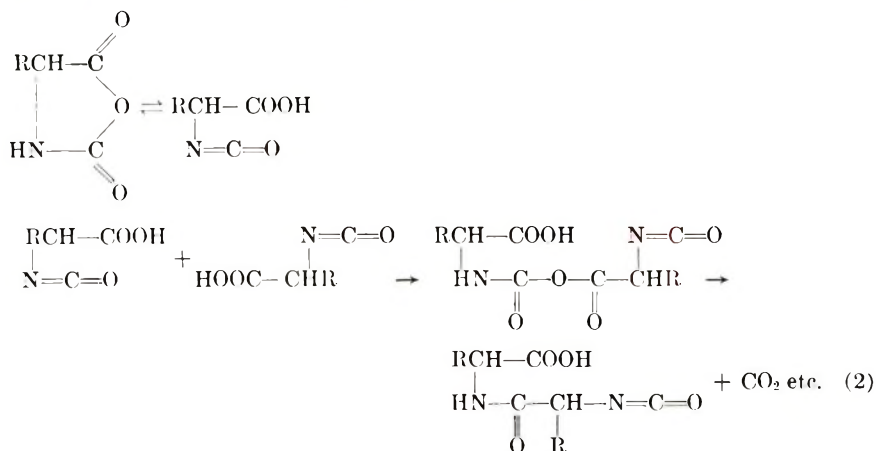
Fig. 4. Infrared spectra of polypeptides prepared by solid-state polymerization (---) in the absence of water vapor and (—) at an aqueous vapor pressure of 26 mm. Hg. The locations of the absorption peaks characteristic of the  $\alpha$  and  $\beta$  polypeptides are indicated at the top of the figure.

structures depends strongly on the aqueous vapor pressure of the atmosphere in which the polymerization was carried out.

The x-ray diffraction photographs showed only diffuse halos with all of the polypeptides.

## DISCUSSION

The nature of the initiation process involved in the thermal polymerization of pure *N*-carboxy- $\alpha$ -amino acid anhydrides has never been clearly established. Szwarc<sup>8</sup> has suggested the mechanism



Our kinetic data show that under most conditions the presence of water vapor has only a relatively small effect on the polymerization rate of a crystalline NCA and reduces only slightly the chain length of the polymer produced. It must be concluded that most of the polymerization proceeds by a mechanism which does not involve initiation by water vapor, possibly by the route proposed by Szwarc.

The racemic NCA was found to be relatively reactive in the case of the BG derivative, where its melting point is lower than that of the optically active compound, while the high-melting racemic NCA derivatives of MG and CL were found to be remarkably inert. The question then arises whether the relative reactivities of the optically active and the racemic monomers merely reflect their relative melting points. The solid-state polymerization of a NCA may be compared to solid-state polymerizations of other cyclic monomers, such as trioxane and trithiane. It is then pertinent to note that trioxane polymerizes in the solid state only within a 40°C. range below its melting point, under conditions which permit conformational transitions of the ring compound in the crystal.<sup>9</sup> In the case of trithiane, polymerization of irradiated crystals also proceeds at a reasonable rate only on heating to within 35°C. of the melting point, while no polymerization is detected 65°C. below the melting point.<sup>10</sup> Since carbon dioxide is eliminated in the NCA polymerization, the reaction can also be

likened to solid-state polycondensations. Such reactions have also been found to be limited to a relatively narrow temperature range below the melting point.<sup>11-13</sup> Nevertheless, there are clearly factors other than proximity to the melting point which affect polymerizability. We may note that the three optically active NCA derivatives which we have studied have almost identical melting points; yet the CL derivative behaves quite differently from the other two in exhibiting no induction period but a relatively low value for the maximum reaction velocity at 70°C. The extremely large difference in the reaction velocity of the L and DL  $\epsilon$ -carboxybenzoyllysine NCA (a ratio of 2000 in the times required for 20% conversion at 80°C. under an aqueous vapor pressure of 13 mm. Hg) can also not be accounted for by the mere 8°C. difference in the melting points of the two compounds. It seems clear that the reactivity of the solid monomers depends to a considerable degree on the characteristics of their crystal structure.

None of the solid-state NCA polymerizations led to oriented growth of the polypeptides, similar to the oriented chain growth observed in the solid-state polymerization of trioxane<sup>14-16</sup> and trithiane<sup>10</sup> and the solid-state polycondensation of  $\epsilon$ -aminocaproic acid.<sup>13</sup> Since diffuse x-ray diffraction photographs were obtained from polypeptides with infrared spectra characteristic of the  $\alpha$ -helical form, it must be assumed that the restraint inherent in the solid-state reaction prevents, in these cases, the growth of crystallites in these intrinsically crystallizable polymers. The high content of the  $\alpha$ -form in the polypeptide obtained from  $\gamma$ -benzyl DL-glutamate NCA excludes the possibility of a regular alternation of D and L monomer units in the polypeptide chain. The reaction product is also unlikely to be a mixture of D and L homopolymers, since such mixtures are known to form highly insoluble complexes<sup>17</sup> and the racemic polymer obtained in this study was more soluble (in a mixture of 10% dichloroacetic acid and 90% trifluoroethanol) than the polypeptide containing L residues only. The data are consistent with the assumption that  $\gamma$ -benzyl DL-glutamate NCA polymerizes in the solid state to a poly peptide with fairly long blocks of L and D units.

We are glad to acknowledge the financial support of this research by the National Science Foundation (grant GP-1711). One of us (G. K.) should also like to express his indebtedness for a Ford Foundation Fellowship which enabled him to participate in this research.

### References

1. E. Miller, U. Fankuchen, and H. Mark, *J. Appl. Phys.*, **20**, 531 (1949).
2. S. Okamura, K. Hayashi, and T. Natori, *Ann. Rept. Japan. Assoc. Radiation Res. Polymers*, **3**, 161 (1961).
3. W. E. Hanby, *J. Chem. Soc.*, **1950**, 3239.
4. M. Bergmann, L. Zervas, and W. F. Ross, *J. Biol. Chem.*, **111**, 245 (1935).
5. W. E. Garner, in *Chemistry of the Solid State*, W. E. Garner, Ed., Butterworths, London, 1955, Chaps. 8 and 9.
6. P. Doty, J. H. Bradbury, and A. M. Holtzer, *J. Am. Chem. Soc.*, **78**, 947 (1957).



7. E. R. Blout and A. Asadourian, *J. Am. Chem. Soc.*, **78**, 955 (1956).
8. M. Szwarc, *Fortschr. Hochpolymer Forsch.*, **4**, 1 (1965).
9. A. Komaki and T. Matsumoto, *J. Polymer Sci. B*, **1**, 671 (1963).
10. J. B. Lando and V. Stannett, *J. Polymer Sci. A*, **3**, 2369 (1965).
11. A. V. Volokhina and G. I. Kudryavtsev, *Dokl. Akad. Nauk SSSR*, **127**, 1221 (1959).
12. A. V. Volokhina, G. I. Kudryavtsev, S. M. Skuratov, and A. K. Bonetskaya, *J. Polymer Sci.*, **35**, 289 (1961).
13. N. Morosoff, D. Lim, and H. Morawetz, *J. Am. Chem. Soc.*, **86**, 3167 (1964).
14. H. W. Kohlschütter and L. Sprenger, *Z. Physik Chem.*, **B16**, 284 (1932).
15. S. Okamura, K. Hayashi, and Y. Kitanishi, *J. Polymer Sci.*, **58**, 927 (1962).
16. G. Carazzolo, S. Lighissa, and M. Mammi, *Makromol. Chem.*, **60**, 171 (1963).
17. T. Yoshida, S. Sakurai, T. Okuda, and Y. Takagi, *J. Am. Chem. Soc.*, **84**, 3590 (1962).

### Résumé

Les cinétiques de polymérisation à l'état solide de *N*-carboxyanhydride (NCA) et de  $\gamma$ -glutamate de benzyle *L*- et racémique, de glutamate de méthyle (MG) et de  $\epsilon$ -carbobenzoxylisine (CL) ont été étudiées en fonction de la température et de la pression de vapeur d'eau. La réaction des formes *L* de BG et MG était caractérisée par une période d'induction tandis que les dérivés CL atteignent un maximum de vitesse de polymérisation dès le démarrage de la réaction. La vapeur d'eau n'exerce qu'un effet mineur en ce qui concerne l'accélération de la réaction et la réduction de longueur de chaînes des polypeptides formés. Les monomères racémiques présentent des structures cristallines différentes de ceux des isomères *L* et les dérivés racémiques de MG et CL polymérisent beaucoup plus lentement. Tous les polymères donnent des réseaux de diffraction aux rayons-X diffus. Les spectres infra-rouges des polypeptides *L* montraient qu'ils avaient principalement une forme en hélice  $\alpha$ . Le polymère dérivé du NCA du BG racémique a une teneur en matériel hélicoïdal qui suggère une structure polypeptidique à blocs importants de résidus *D* et *L*.

### Zusammenfassung

Die Kinetik der Polymerisation von *N*-Carbonsäureanhydriden (NCA) der *L*-unracemischen Form von  $\gamma$ -Benzylglutamat (BG),  $\gamma$ -Methylglutamat (MG) und  $\epsilon$ -Carbobenzoxylisin (CL) im festen Zustand wurde in Abhängigkeit von Temperatur und Wasserdampfdruck untersucht. Die Reaktion der *L*-Form von BG und MG war durch eine Induktionsperiode charakterisiert, während das CL-Derivat die maximale Polymerisationsgeschwindigkeit am Polymerisationsbeginn erreichte. Wasserdampf besass nur einen geringen Einfluss in bezug auf Reaktionsbeschleunigung und Herabsetzung der Kettenlänge der gebildeten Polypeptide. Die racemischen Monomeren besaßen von den *L*-Isomeren verschiedene Kristallstruktur und die racemischen MG- und CL-Derivate polymerisierten viel langsamer. Alle Polymeren lieferten diffuse Röntgenbeugungsdiagramme. Infrarotspektren der *L*-Polypeptide zeigten, dass sie sich grösstenteils in der  $\alpha$ -Helixform befanden. Das vom racemischen BG-NCA-abgeleitete Polymere hatte einen Gehalt an  $\alpha$ -Helixmaterial, welcher seinen Aufbau aus Polypeptiden mit langen Blöcken aus *D*- und *L*-Resten erkennen liess.

Received October 28, 1965

Revised November 5, 1965

Prod. No. 4976A

## Interactions of Inorganic Salts with Poly(ethylene Oxide)

R. D. LUNDBERG, F. E. BAILEY, and R. W. CALLARD,  
*Research and Development Department, Union Carbide Corporation,  
Chemicals Division, South Charleston, West Virginia*

### Synopsis

Evidence is presented for the interaction of metal salts such as potassium iodide with polyethers such as poly(ethylene oxide). This interaction is sufficiently marked that the incorporation of 10-30% of the salt in the bulk polymer markedly reduces crystallinity while retaining compatibility. Examination of electroviscous effects in methanol demonstrates that the salt-polymer adduct behaves as a typical polyelectrolyte at low salt concentrations, while the polymer in absence of salt is essentially insoluble in methanol at room temperature. Measurements of the equilibrium between salt and polymer along with a study of various molecular weight polymers strongly suggest that one salt molecule associates with about nine ethylene oxide units. It is proposed that the association is due to an ion-dipole interaction, and the anion is tentatively postulated as the species directly associating with the polymer. The association of other metal salts and other polymers are interpreted in this light. The significance of these results in interpreting salt-in phenomena is also discussed.

### INTRODUCTION

Previous studies have shown that poly(ethylene oxide) interacts strongly with polymeric acids such as poly(acrylic acid) through a network of hydrogen bonds to form an insoluble gel.<sup>1</sup> Studies of this system have revealed that an interaction also exists between poly(ethylene oxide) and poly(sodium acrylate) which has been attributed to an ion-dipole interaction.<sup>2</sup> This paper is concerned with a more detailed examination of the phenomenon of ion binding presumed to arise from these ion-dipole interactions. The interaction of ionic species with neutral polymers had received relatively little attention until the recent elegant work of Molyneux and Frank with polyvinylpyrrolidone.<sup>3</sup> Their studies have shown that aromatic species such as benzene and sodium benzoate associate rather markedly through what has been called the hydrophobic bond.<sup>3,4</sup> In the case of sodium benzoate and other salts of organic acids, viscosity effects are observed similar to those experienced with polyelectrolytes.

In the present study, interest has been focused primarily on poly(ethylene oxide) and its interactions with inorganic salts. One unusual example of salt-poly(ethylene oxide) interaction has been reported recently wherein mercuric chloride formed an insoluble, infusible complex which appeared

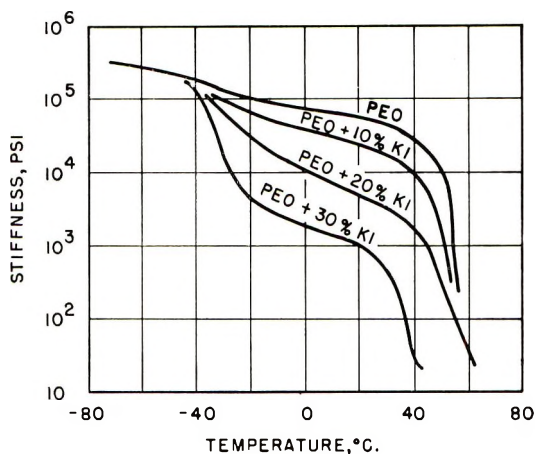


Fig. 1. Stiffness modulus-temperature relations for various poly(ethylene oxide)-potassium iodide compositions.

highly crystalline.<sup>5</sup> Other materials, such as urea and thiourea, have also been shown to form highly crystalline complexes with poly(ethylene oxide).<sup>8</sup> Our studies have indicated that simple salts such as potassium iodide can also associate with poly(ethylene oxide); however, in this case association occurs with disruption of crystalline order originally present in poly(ethylene oxide). In Figure 1, it is seen from stiffness modulus-temperature determinations that high molecular weight poly(ethylene oxide) has a crystalline melting point at about 60°C. and a glass transition at about -55°C. If, however, potassium iodide is milled into the polymer, remarkably compatible compositions result at quite high salt contents. As is evident from Figure 1, the introduction of increasing amounts of potassium iodide progressively lowers the polymer crystalline melting point and finally produces an elastomeric composition at room temperature at about 30-40% KI. We have interpreted these compatible salt-polymer compositions as resulting from an association of potassium iodide with poly(ethylene oxide). The purpose of this study has been to explore the nature of this association in solution.

## EXPERIMENTAL

Viscosity determinations were made with a Ubbelohde-type viscometer, size No. 1. In the preparation of solutions, salt plus solvent solutions were first made up, then added to the required weight of polymer and agitated at room temperature for periods up to 16 hr.

Commercial samples of poly(ethylene oxide) made by Union Carbide Corporation were used in this study. The lower molecular weight members (up to 30,000) bear the trade-mark Carbowax, poly(ethylene glycols), and the higher molecular weight members are trademarked as Polyox water-

soluble resins. For the work on poly(propylene oxide), an experimental sample prepared in the Union Carbide laboratories was used.

Ordinary distilled water and AAA grade anhydrous methanol were employed as liquids, and the salts used were pure commercial materials of the reagent grade.

Dialysis techniques were similar to those used by Molyneux and Frank.<sup>3</sup> Poly(ethylene oxide) in methanol-potassium iodide solution was placed inside a semipermeable membrane (cellulose sausage casing marketed by Food Products Division of Union Carbide Corporation) and was slowly agitated. After about 48 hr., equilibrium was essentially achieved with the result that a substantial amount of potassium iodide was found to have migrated inside the membrane to associate with polymer. By measurement of the concentration differences of potassium iodide through titration of iodide anion, the bound salt concentration was calculated after correction for the Donnan membrane effect.

The bulk interaction of KI and poly(ethylene oxide) as represented in Figure 1 was examined by milling on a two-roll mill at about 80°C. potassium iodide and polymer. Periods of 10–15 min. were normally sufficient to achieve good dispersion.

## RESULTS AND DISCUSSION

### Poly(ethylene Oxide) and Potassium Iodide Complexes

In view of this apparent interaction of potassium iodide in the bulk phase, attempts have been made to study this interaction in solution. Previous publications have discussed the salting-out effects of salts on poly(ethylene oxide) from aqueous solution,<sup>6</sup> but very little published literature is available on attractive forces between inorganic salts and neutral polymers. Since the addition of potassium iodide to aqueous solutions of poly(ethylene oxide) had essentially no effect on reduced viscosity, this result was interpreted as indicating no interaction. Viscosity studies, therefore, were conducted with nonaqueous solvents. As an example, anhydrous methanol is substantially a nonsolvent for high molecular weight poly(ethylene oxide) at room temperature. The addition of very small amounts of certain metal halides, however, converts the salt-methanol system into an excellent solvent for this polymer. While salting-in phenomena are not unusual for most polymer systems, usually quite high salt concentrations are required. These concentrations in polar solvents range from 10 to 50 wt.-% salt, for example, in the dissolution of polyacrylonitrile in aqueous sodium cyanide, lithium bromide, or zinc chloride.<sup>7</sup> In contrast, the addition of as little as 0.5% of potassium iodide renders methanol an excellent solvent for poly(ethylene oxide).

The dilute solution viscosity of poly(ethylene oxide) in methanolic solutions containing varying amounts of potassium iodide is represented in Figure 2. The intrinsic viscosity of this particular polymer sample in aqueous solution is about 3.0. With decreasing potassium iodide concen-



tration, the reduced viscosity of the polymer in methanolic solution increases markedly. Clearly, however, a maximum in reduced viscosity must exist since below 0.02M potassium iodide, the polymer becomes partially insoluble in anhydrous methanol. Indications of similar behavior in anhydrous acetone have also been observed, as shown in Figure 2. It is important to note several distinctions in this apparent electroviscous phenomenon from those salt effects observed for poly(ethylene oxide) reported in aqueous solution. First, the reduced viscosity of the polymer system in methanolic solution increases as a nonsolvent is approached in contrast to the behavior expected on the basis of current polymer solution theories.<sup>9</sup> Second, the reduced viscosity of poly(ethylene oxide) at low salt

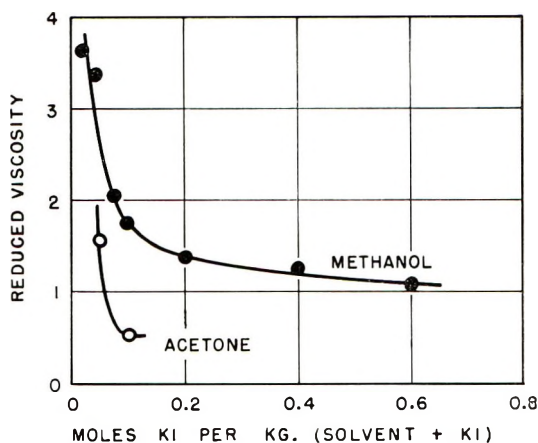
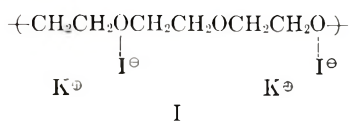


Fig. 2. Reduced viscosity of solutions of poly(ethylene oxide) at polymer concentrations of 1% in various potassium iodide concentrations.

concentrations is actually higher in methanol than that observed in water, indicating that the methanolic salt solution is a better solvent than water. Third, the similarity of the curves in Figure 2 to polyelectrolyte behavior is quite apparent. The viscosity increases in the case of potassium iodide-poly(ethylene oxide) are interpreted in terms of the polymer molecules becoming polyelectrolytes by ion-binding in certain nonaqueous, semipolar solutions.

The polyelectrolyte formed is envisaged as resulting from the association of either potassium or iodide ions with the poly(ethylene oxide) through an ion-dipole interaction. Although there is no definitive evidence at this time, we have tentatively assigned the primary associating species as the iodide anion for reasons to be discussed later. The complexed species can be represented formally as structure I:



Thus, at higher potassium iodide concentrations, a fraction of the iodide anions is assumed to be associated with the polyether, while a substantial amount exists in solution to shield the associated species. At lower salt concentrations, fewer ions are available for shielding, and the associated ions cause the polymer coil to expand due to bound ionic repulsions. Thus, a typical polyelectrolyte effect is observed wherein the same shielding phenomenon occurs.

In order to obtain a more quantitative estimate of the interaction of potassium iodide with poly(ethylene oxide) in methanol, equilibrium dialysis techniques similar to those of Molyneux and Frank<sup>3</sup> were employed. Then, on taking  $x$  as the moles per liter of salt migrated, and  $y$  as that bound to the polymer while  $C_1$  and  $C_2$  are the respective concentrations of salt outside and inside the dialysis membrane, eq. (1) can be used to allow for the Donnan membrane effect:

$$(C_1 - x)(C_1 - x) = (C_2 + x)(C_2 + x - y) \quad (1)$$

Equation (1) may be solved for  $y$ , the concentration of bound anion, or more accurately, the concentration of combined sites. This model makes an implicit assumption that each association would be independent of other intrachain associations, an assumption which neglects ionic repulsions of neighboring associations. Based on this assumption, an equilibrium constant can be calculated from eqs. (2) and (3).



$$K_{\text{eq}} = [\text{Complex}]/[\text{PEO}][\text{I}^{\ominus}] \quad (3)$$

Use of a semipermeable membrane containing poly(ethylene oxide) suspended in a methanolic solution of potassium iodide readily allowed the migration of the salt into the polymer-containing side of the membrane. It was necessary in these experiments to use salt solutions on both sides of the membrane in order to dissolve the polymer. We have assumed in this treatment that activity coefficients are unity and that salt activities on both sides of the membrane are the same. The use of eq. 1 to obtain the amount of combined sites requires that equal volumes of solvent are present on both sides of the membrane. All dialysis experiments in this study were conducted with volumes of 80 ml. outside and 40 ml. inside the membrane with identical initial salt concentrations on both sides. Equation (1) can therefore be expressed in this special case as:

$$(C_1 - x)(C_1 - x) = (C_1 + 2x - y)(C_1 + 2x)$$

In Table I representative equilibrium constants obtained for the association for potassium iodide with poly(ethylene oxide) (PEO) in methanol are shown as a function of potassium iodide concentration.

The apparent equilibrium constant, calculated directly from dialysis data as treated above, decreases at higher salt concentrations, as shown in Figure 3. This reduction in the constant is interpreted as due to electro-



TABLE I  
Establishment of Equilibrium Constants for PEO-KI System at  
25°C., [PEO] = 0.57 Base Molal, (KI Concentration Measured Outside)

Initial KI, mole/1000 g.	Final KI, mole/1000 g.	$K_{eq}$
0.050	0.039	4.3
0.100	0.083	2.9
0.250	0.230	1.0
0.50	0.478	0.52

static repulsion; that is, the tendency for a neighboring association of an iodide ion to occur is reduced by the existing bound ion. It is readily apparent from the data in Table I that the calculated equilibrium constants for this association vary with the KI/poly(ethylene oxide) ratio, and the differences in iodide concentrations are fairly small, especially at high salt concentrations. Nevertheless, it is apparent that equilibrium exists, and the equilibrium constant may be significant in dilute potassium iodide solutions. Based on viscosity data to be presented in a later section, it will be apparent that these equilibrium constants are not a true measure of the association if the molar ratio of ethylene oxide units to KI units is less than 9 or 10. Below these values, the coulombic repulsions are especially pronounced. Experimental limitations have, however, restricted our measurements to a lower limit of about 0.05*M* potassium iodide solutions.

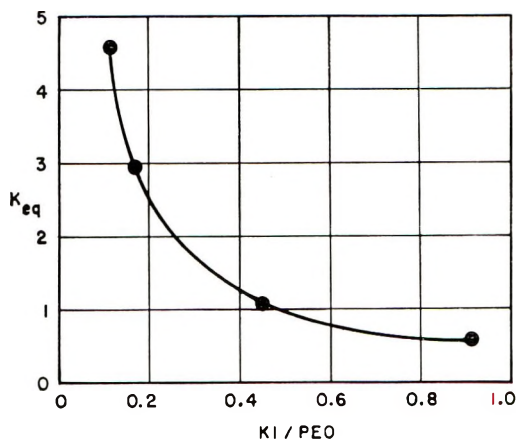


Fig. 3. Equilibrium constant determined as a function of the molar ratio of potassium iodide/ethylene oxide units determined at 25°C. in methanol.

#### Interaction of Poly(ethylene Oxide) with Other Salts in Methanol

The interaction of other potassium halides with poly(ethylene oxide) in methanol as represented by changes in reduced viscosity as a function of salt concentration is illustrated in Figure 4. While this particular sample

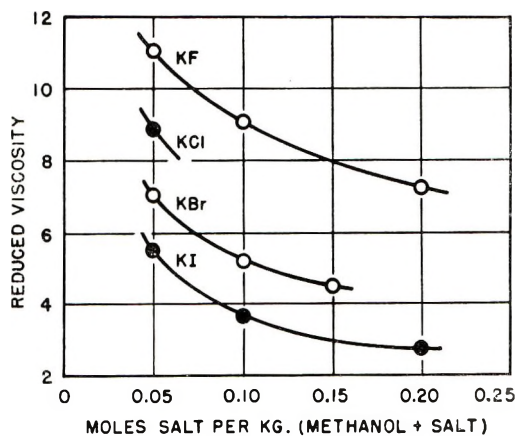


Fig. 4. Reduced viscosities of poly(ethylene oxide) determined at 30°C. at various potassium halide concentrations in methanol. Solubility limitations preclude measurements of some points.

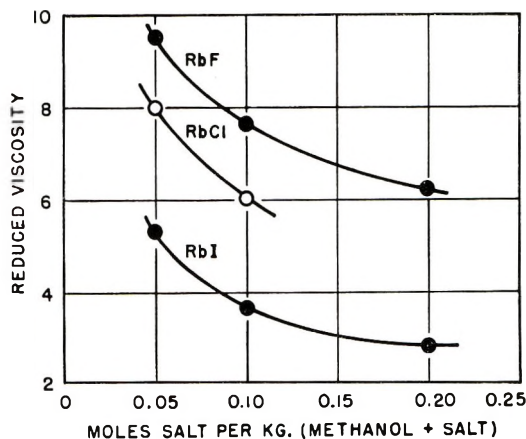


Fig. 5. Reduced viscosities of poly(ethylene oxide) at different rubidium halide concentrations in methanol at 30°C.

of poly(ethylene oxide) has a reduced viscosity in water of 4.9 at the same concentration (1 g./100 cc. of solvent), it is readily apparent that dilute potassium halide solutions all possess reduced viscosities considerably above this value. Furthermore, a progressive increase in reduced viscosity is observed for the halide series  $KI < KBr < KCl < KF$ . Similar behavior is observed for the rubidium halides under identical conditions, as seen in Figure 5. Similar studies have been conducted on the sodium and ammonium fluorides; however, the magnitude of the electroviscous effects is less pronounced in these cases. The interesting case of lithium halides was not studied, because the chloride and bromide were not effective in dissolving the poly(ethylene oxide) in methanol. Briefly, these results suggest that in addition to the simple equilibrium of salt with polymer, there is the

additional complication of salt dissociation in methanol, and this latter effect may have a pronounced influence on both the actual ion binding and the shielding of the repulsive charges which generate the electroviscous effects observed. Thus, the actual nature and magnitude of this ion binding in this case is quite specific to the type of salt and the particular polymer involved. It is important to note that on the basis of these observations, it is not clear whether the cation or anion actually participates in the primary ion binding. Actual ion size in these observations apparently has little effect on the magnitude of the viscosity level since the larger anions actually correspond to the lower viscosity values. Other salts which display strong associating tendencies with poly(ethylene oxide) are the potassium and ammonium thiocyanates.

### Influence of Polymer Molecular Weight

Because these polymer-salt systems essentially behave as polyelectrolytes in methanol with widely separated electric charges, it would be anticipated that, at a particular polymer molecular weight, the onset of polyelectrolyte character would be observed. In Figure 6 the reduced viscosities of poly(ethylene oxide) of different molecular weights are examined both in pure methanol and 0.05*M* KF. Although very high molecular weight polymers of ethylene oxide are not soluble in methanol, the lower polymers, up to 30,000 in molecular weight, are soluble. It is apparent that in dilute KF (0.05*M*) the reduced viscosities observed at 2% polymer concentration are lower than in pure methanol up to a polymer molecular weight of 6000 when the situation is reversed. Similar behavior is observed for potassium iodide solutions. Thus, on this basis, it appears that in the molecular weight range of 4000–6000 the onset of polyelectrolyte behavior is observed.

That this change is observed in this molecular weight range is further substantiated by an examination of the reduced viscosity curves as a

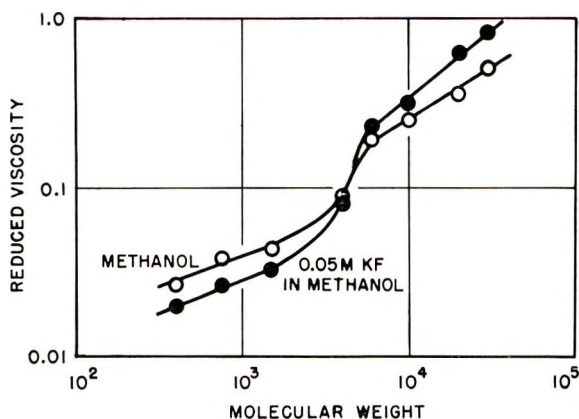


Fig. 6. Reduced viscosities of poly(ethylene oxide) obtained at 2.0% polymer concentration for varying molecular weight polymers in methanol and 0.05*M* KF in methanol at 30°C.

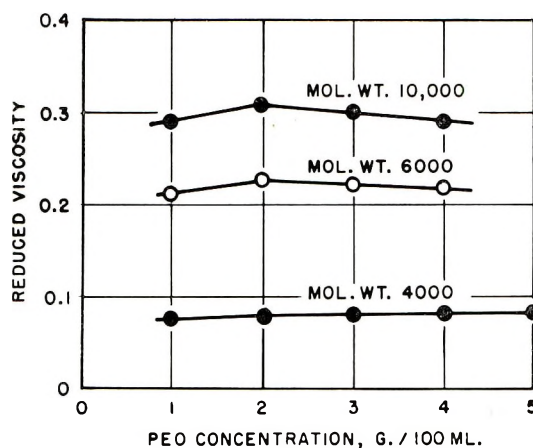


Fig. 7. Reduced viscosities obtained in 0.05M KF-methanol solutions at various polymer concentrations for different molecular weight poly(ethylene glycols) at 30°C.

function of polyether concentration with different polymer molecular weights in dilute KF solution (Figs. 7 and 8). Interestingly, there is a maximum which first appears with molecular weight of 6000 in the vicinity of 2% polyether concentration. No evidence is found for deviation from linearity at polyether molecular weights below 4000. In a greatly expanded scale of Figure 7, it is apparent that very slight deviation is observed at molecular weight of 4000 and it becomes significantly more pronounced at 6000. This behavior is especially apparent in Figure 8, where Carbowax 30,000 is examined in the presence of 0.05M KF. It is apparent that for all these higher molecular weight polymers maximum reduced viscosity is observed at 2% polyether concentration, holding KF at 0.05M. In the absence of salt, the specific viscosity versus concentration curves for all these samples exhibit the expected linear behavior. The explanation for this unusual viscosity behavior can be rationalized quite simply as arising from coulombic repulsion of associated ionic species. Thus, at high salt to polymer ratios, it is apparent that there will be substantial shielding of these charges by free salt molecules and thus lower viscosity values will result. However, as the salt concentration is lowered (or the polymer concentration is increased), the amount of free salt molecules will decrease due to the availability of more potential binding sites. (The apparent equilibrium constant, therefore, will decrease as the salt concentration is increased, as observed in Table I.) Therefore, it would be expected that, if the association were sufficiently strong, at some specific salt/polymer ratio the maximum association of salt and polymer should be observed with minimum shielding of repulsive coulombic forces. This condition should lead to a maximum when the reduced viscosity is examined as a function of polymer concentration. Naturally, the salt-to-polymer concentration at this point is a measure of the number of sites available for ion binding, and if it is assumed that all the salt is associated at this point [2% poly(ethylene

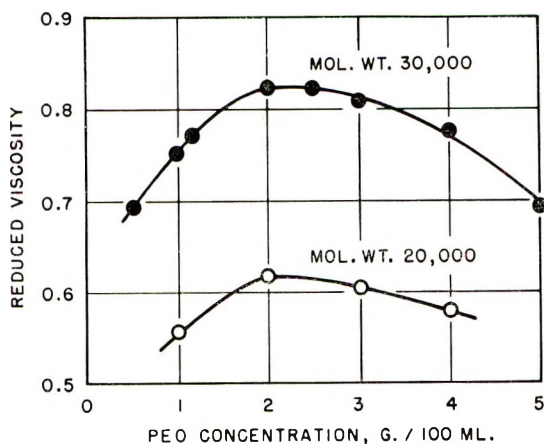


Fig. 8. Reduced viscosities obtained in 0.05M KF-methanol solutions at varying polymer concentrations for high molecular weight poly(ethylene glycols) at 30°C.

oxide) and 0.05M potassium fluoride], it is apparent that 1 potassium fluoride associates per 9 ethylene oxide repeating units. This figure is quite close to the figure of 10 repeating units of vinylpyrrolidone found to be associated with each molecule of aromatic cosolute by Molyneux and Frank.<sup>3</sup> In the latter case, the association phenomena were examined in aqueous solutions whereas here we are considering only methanolic solutions.

The change in viscosity behavior observed in the molecular weight range of 4000–6000 can be rationalized as arising from a change in conformation of the polymer chain over this molecular weight range. Other studies<sup>10,11</sup> have indicated that in this molecular weight region deviations are observed from the Mark-Houwink relation  $[\eta] = KM^a$  for a number of polymer systems. In particular, poly(ethylene oxide)<sup>12</sup> has been observed to display marked viscosity deviations near a molecular weight of 5000. These deviations are rationalized on the basis that below a molecular weight of 5000 the polymer molecules are not large enough to behave as random coils. The viscosity data of the present study are consistent with the concept that a minimum molecular weight of 6000 is required for an expanded conformation of the polymer coil of poly(ethylene oxide) to exist in dilute KF solution. Thus, it is at this molecular weight level that polyelectrolyte behavior is first observed.

### Interaction of Other Polyethers with Metal Halides

The interaction of poly(propylene oxide) with salts in methanol has been studied briefly. Here, the picture is not complicated by polymer insolubility in anhydrous methanol. In Figure 9 the intrinsic viscosity of a sample of poly(propylene oxide) is shown as a function of potassium iodide concentration in methanol. Again, definite evidence of complex formation



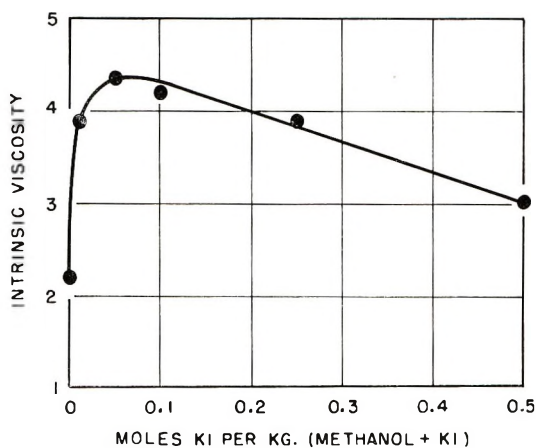


Fig. 9. Intrinsic viscosities obtained for poly(propylene oxide) in methanol-potassium iodide solutions at different KI concentrations at 30°C.

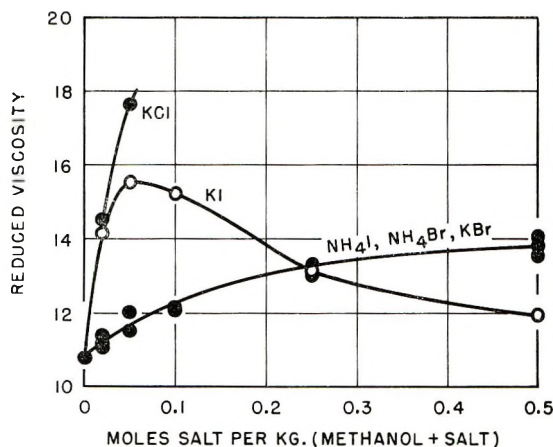


Fig. 10. Reduced viscosities obtained for 1% poly(propylene oxide) solutions in methanol at varying salt concentrations.

is evident. In Figure 10 the change in reduced viscosity of several different salts in methanol is shown at a polymer concentration of 1% for poly(propylene oxide). That there is a significant interaction is evident; however, the character of the curves for these different salt systems may be complicated by their degree of dissociation in methanol.

### Salt-Polymer Associations in Aqueous Solutions

Although the evidence presented for salt-polymer associations in methanol demonstrates a substantial interaction, little evidence has been found for similar interactions in aqueous solutions with poly(ethylene oxide). Indeed, earlier studies demonstrated that most salts tend to decrease the viscosity of aqueous solutions of poly(ethylene oxide).<sup>6</sup> At moderately



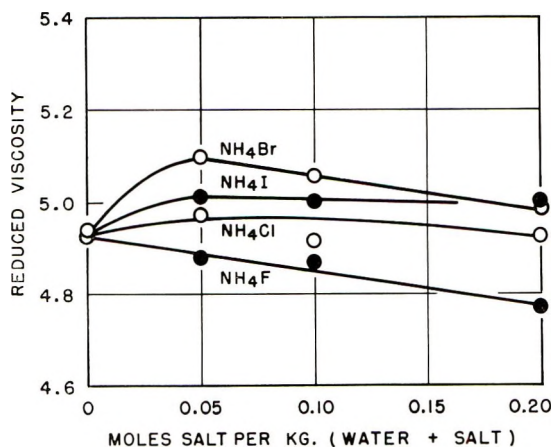


Fig. 11. Reduced viscosities for 1% poly(ethylene oxide) solutions in water at varying salt concentrations.

high salt concentrations, the phenomenon of salting out of poly(ethylene oxide) is observed, indicating that the salt solution here is a poorer solvent than pure water. The difference in behavior for aqueous and methanol solutions is tentatively interpreted as arising from the competitive associations of solvent with polymer and polymer with the salt. In aqueous solution, both of these factors combine to minimize the salt-polymer association.

In several cases, however, viscosity behavior indicative of substantial association between polymers and selected salts has been observed in aqueous solution. The viscosity behavior of poly(ethylene oxide) as a function of salt concentration for ammonium halides is represented in Figure 11. Although the observed maxima are not pronounced, they are apparent for the bromide and iodide species.

Similar but more pronounced maxima in the viscosity curves are observed for the tetraalkylammonium halides in the presence of aqueous solutions of poly(ethylene oxide), as shown in Figure 12.

These results can be interpreted as arising from a weak association of the salt and a consequent viscosity increase arising more from the added bulk of the salt-polymer adduct than from a polyelectrolyte effect. Apparently, the larger alkyl groups are more effective in increasing the reduced viscosity of a given halide series. Similarly, the effect on viscosity of anion size is  $I > Br > Cl$ , in contrast to the behavior in methanol.

Examples of other polymers found in the course of this study to exhibit viscosity behavior in aqueous salt solution characteristic of association phenomena are the homopolymers of acrylamide, methacrylamide, and *N*-methyl-*N*-vinylacetamide. A small but similar interaction between polyvinylpyrrolidone and sodium thiocyanate was observed in aqueous solution by Molyneux and Frank.<sup>3</sup> However, none of these systems have displayed in aqueous solution the pronounced viscosity changes observed

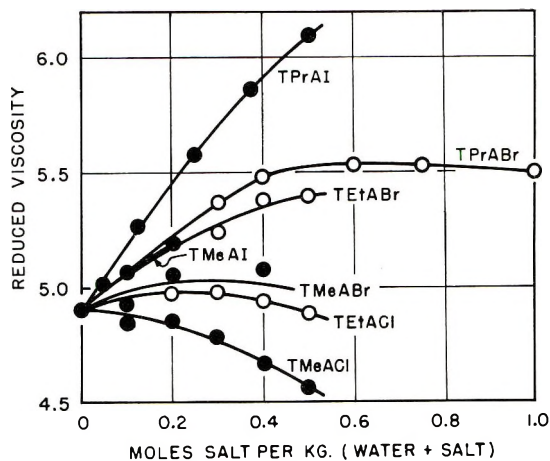


Fig. 12. Reduced viscosities of 1% poly(ethylene oxide) solutions at varying quaternary ammonium halide concentrations: TPrAI = tetrapropylammonium iodide; TEtABr = tetraethylammonium bromide; TMeAI = tetramethylammonium iodide.

for poly(ethylene oxide) in methanol. Presumably, competitive solvation effects play an important role in determining the degree of association and consequent viscosity behavior.

## CONCLUSIONS

The results of this study strongly suggest that selected salts exhibit interaction with polyethers, especially poly(ethylene oxide). This association is more pronounced in nonaqueous solvents, but also occurs in the bulk polymer phase and can result in a marked change of polymer properties. The exact mechanism of this association is unknown but is believed to arise from an ion-dipole interaction.

Currently, there is no direct evidence to indicate whether the cation or anion is directly associated with the polyether. Earlier studies<sup>2</sup> demonstrated that poly(ethylene oxide) and poly(sodium acrylate) interacted to result in a lightly cross-linked product which was attributed to the association of the polymeric anion. Those results, however, are not inconsistent with association of the cation. In a study of the effects of various salts on aqueous solution of poly(ethylene oxide), Bailey and Callard<sup>6</sup> observed that the anion has a more pronounced effect in salting-out phenomena than the cation. Evidence for the absence of binding of cations with polyvinylpyrrolidone has been presented previously.<sup>3</sup> In view of these results, it appears reasonable that in the present study the anion is actually bound with the polyether. In any event, more detailed discussion of the exact mechanism of ion binding is outside the scope of this investigation.

This association study is similar in certain respects to the well known interaction of triiodide anion with polyvinylpyrrolidone.<sup>3</sup> This association has been attributed to the polarizability of the anion. The marked asso-

ciation of potassium fluoride and similar salts which are not readily polarized suggests that the interactions of the present study are significantly different. Efforts to study the interaction between poly(ethylene oxide) and the triiodide anion in methanol, however, were unsuccessful because an insoluble adduct was formed.

Despite our lack of knowledge concerning the exact nature of associated species, it is quite apparent that these weak interactions do contribute to anomalous solution and bulk polymer behavior. Thus, in addition to hydrogen bonding, and the so-called "hydrophobic bond," this additional association described here as an ion-dipole interaction must also be considered as contributing significantly to polymer solution properties.

It is also apparent that the results of this study are closely related to the phenomenon of salting in polymers. It is quite likely that at the higher salt concentrations normally observed in such phenomena, these ion-dipole associations occur with the consequent formation of polyelectrolytes although, under these conditions, charge repulsion along the polymer chain must be minimal due to the shielding character of unassociated salt.

The assistance of Mr. M. E. Casto in performing some of the preliminary experiments in this study and the helpful discussions of Dr. F. J. Welch and Dr. J. A. Faucher in the course of this work are greatly appreciated.

### References

1. K. L. Smith, A. E. Winslow, and D. E. Petersen, *Ind. Eng. Chem.*, **51**, 1361 (1959).
2. F. E. Bailey, R. D. Lundberg, and R. W. Callard, *J. Polymer Sci. A*, **2**, 845 (1964).
3. P. Molyneux and H. P. Frank, *J. Am. Chem. Soc.*, **83**, 3169 (1961); *ibid.*, **83**, 3175 (1961).
4. W. Kauzmann, *Advan. Protein Chem.*, **14**, 1 (1959).
5. A. A. Blumberg, S. S. Pollack, and C. A. J. Hoeve, *J. Polymer Sci. A*, **2**, 2499 (1964).
6. F. E. Bailey and R. W. Callard, *J. Appl. Polymer Sci.*, **1**, 56 (1959).
7. C. E. Schildknecht, *Vinyl and Related Polymers*, Wiley, New York, 1953, p. 270.
8. F. E. Bailey, Jr. and H. G. France, *J. Polymer Sci.*, **49**, 397 (1961).
9. P. J. Flory, *Principles of Polymer Chemistry*, Cornell Univ. Press, Ithaca, N. Y., 1953, p. 600.
10. G. V. Schulz and H. Marzolph, *Makromol. Chem.*, **13**, 120 (1954).
11. P. Doty, J. C. Mitchell, and A. E. Woodward, *J. Am. Chem. Soc.*, **79**, 3958 (1957).
12. J. A. Faucher and R. W. Callard, unpublished results.

### Résumé

On démontre l'existence d'une interaction des sels métalliques tel que l'iodure de potassium avec des polyéthères tel que l'oxyde de polyéthylène. Cette interaction est suffisamment marquée pour que l'incorporation du 10 à 30% de sel dans le polymère en masse réduise de façon appréciable la cristallinité tout en maintenant la compatibilité. L'examen des effets électrovisqueux dans le méthanol démontre que le produit d'addition des sels-polymère se comporte comme un polyelectrolyte typique à basse concentration en sels, tandis que le polymère en absence de sels est essentiellement insoluble dans le méth-

anol à température de chambre. Des mesures d'équilibre entre le sel et le polymère en même temps qu'une étude des polymères de différents poids moléculaires suggèrent qu'une molécule de sel s'associe avec environ 9 unités d'oxyde d'éthylène. On propose que l'association est due à une interaction ion-dipole et que l'anion serait l'espèce directement associée avec le polymère. Les associations d'autres sels métalliques et d'autres polymères sont interprétées sur cette base. La signification de ces résultats pour l'interprétation des phénomènes de sel est également soumise à discussion.

### Zusammenfassung

Polypropylen wurde mit Salpetersäure zur Entfernung seiner amorphen Komponente oxydiert. Gleichzeitig mit dem Gewichtsverlust trat eine Zunahme der Kristallinität, eine Abnahme des Molekulargewichts, ein Abfall des Schmelzpunkts und eine Änderung der sichtbaren Struktur auf. Die kristalline Komponente, die aus einem ursprünglich isotherm kristallisierten Polymeren übrig blieb, bestand aus gestrennten Sphärolithen. Diese Sphärolithe konnten in Lamellen aufgebrochen werden, welche ähnliche Elektronenbeugungsdiagramme lieferten, wie sie bei verschiedenen, aus Lösung gewachsenen Einkristallen auftreten. Im Gegensatz zum hohen Molekulargewicht der nichtoxydierten Stammsubstanz bestanden die Lamellen, welche die saure Behandlung überlebten, aus kurzen Ketten, deren Länge von der Kristallisationstemperatur der Stammsubstanz abhing. Wenn, wie die Beugungsuntersuchungen erkennen lassen, diese kurzen Moleküle in Reihen und Gleich angeordnet sind, dann sollte die Höhe der Lamellen der Höhe der Moleküle entsprechen. Die Höhe der Lamellen konnte nicht genau genug gemessen werden, um eine exakte Korrelation aufzustellen, die aus Viskositätsdaten berechnete Änderung der mittleren Kettenlänge entsprach aber zumindest näherungsweise der Höhe der visuell beobachteten Lamellen.

Received August 27, 1965

Revised November 1, 1965

Prod. No. 4977A

## Polymerization of Butene-2 with Isomerization to Butene-1

TAKAYUKI OTSU, AKIHIKO SHIMIZU, and MINORU IMOTO,  
*Faculty of Engineering, Osaka City University, Sugimotocho,  
Sumiyoshi-ku, Osaka, Japan*

### Synopsis

An attempt has been made to prepare a high molecular weight isotactic polybutene-1 from *cis*- or *trans*-butene-2. Polymerization of butene-2 did not occur due to the steric effect of the substituents. In the presence of  $\text{TiCl}_3\text{-Al}(\text{C}_2\text{H}_5)_3$  catalyst, however, both butene-2 monomers were found to polymerize at a slower rate than butene-1 and to give polymers consisting of the repeating unit of butene-1. From the gas chromatographic determination of the isomer distribution of the butenes recovered after the polymerization, it was found that the butenes isomerized, in the presence of the catalyst system containing  $\text{TiCl}_3$ , to approach the thermodynamic equilibrium mixture of butene-1, *cis*-butene-2, and *trans*-butene-2. It was also found that the rates of polymerization of butene-2 for the catalyst systems used were proportional to the isomerization rates. These results show that butene-2 isomerizes first to butene-1 which has less steric hindrance and then polymerizes as butene-1, through ordinary vinyl polymerization by a coordinated anionic mechanism. This type of polymerization was observed in some other linear  $\beta$ -olefins such as *n*-pentene-2 and *n*-hexene-2.

### INTRODUCTION

It is accepted that butene-1 and isobutene can readily be polymerized by the presence of Ziegler-Natta catalyst and cationic catalyst, respectively. However, *cis*- and *trans*-butene-2 do not give high molecular weight homopolymers with any catalyst, because of the steric effect of the 1,2-dimethyl substituents.<sup>1</sup> Recently, Friedlander has reported that butene-2 homopolymerizes to give a relatively low molecular weight polymer in the presence of montmorillonite<sup>2</sup> and of the ternary catalyst system  $\text{TiCl}_4\text{-Al}(\text{C}_2\text{H}_5)_3$ -activated clay.<sup>3</sup>

In a study comparing the effect of the substituents on the polymerization of the four butene isomers by various catalyst systems, we found that *cis*- and *trans*-butene-2 can be easily polymerized in the presence of  $\text{TiCl}_3\text{-Al}(\text{C}_2\text{H}_5)_3$  catalyst to give a high molecular weight polybutene-1.<sup>4</sup> Nearly the same observations were reported by Iwamoto and Yuguchi,<sup>5</sup> and by Symcox<sup>6</sup> at almost the same time. The radical and ionic polymerizations of the four butene isomers has been reported in detail.<sup>7</sup> The present paper describes the results of coordinated anionic polymerization of butene-2 by a mechanism involving accompanying isomerization to butene-1 in the pres-



ence of the Ziegler-Natta catalyst. Butene-1 and isobutene are used as comparison.

Recently, Kennedy et al.<sup>8</sup> and Ketley et al.<sup>9</sup> reported the isomerization polymerization of some branched  $\alpha$ -olefins by a cationic catalyst. In this case, the migration of a growing cation which is accompanied by a hydride shift to give a more stable carbonium ion was postulated to occur in the propagation reaction. However, the present case is related to anionic polymerization of some  $\beta$ -olefins in which a growing anion was found to be not isomerized to give a more stable carbanion. Butene-2 is sterically hindered but can isomerize in the presence of some transition metal compounds to butene-1, which has less steric hindrance and readily polymerizes by coordinated anionic mechanism.

## EXPERIMENTAL

### Materials

Butene-1, isobutene, and *cis*- or *trans*-butene-2 (Matheson Co.) were dried over calcium hydride, followed by fractional distillation. Their purities determined by gas chromatography, in which an acetonyl acetone column was used in a stream of hydrogen (30 ml./min.) at 0°C., were 97.9, 99.3, 99.2, and 99.4%, respectively. Other  $\beta$ -olefins were used after purification by the usual method.

Diethylaluminum chloride (Texas Alkyls), triethylaluminum, ethylaluminum dichloride (Ethyl Corp.), titanium trichloride (Stauffer Chem. Co.), and lithium aluminum hydride (Metal Hydride Inc.) were used without further purification. Titanium tetrachloride, stannic chloride, and pyridine were purified by distillation.

*n*-Heptane was purified by washing thoroughly with concentrated sulfuric acid, followed by drying over metallic sodium, and then distilled. Other solvents and precipitants were used after purification by the conventional method.

### Polymerization Procedure

In a hard glass tube provided with a rubber stopper, the catalyst was charged through a syringe near the connection to the vacuum system. The required amount of solvent and titanium trichloride was added, and this tube was connected to a vacuum system. After degassing the required amount of alkylaluminum solution was charged through a syringe in a dry nitrogen atmosphere. After the mixture was aged for an hour at room temperature (about 27°C.), the butene monomer was charged by distillation. The system was then sealed.

Polymerizations were carried out with shaking in a thermostat maintained at a constant temperature for a given time. After polymerization the tube was opened, and the unreacted butene monomer was collected and its composition analyzed by gas chromatography. The contents of the



tube were then poured into a large amount of isopropyl alcohol containing concentrated hydrochloric acid to precipitate the polymer. The resulting polymer was then purified by reprecipitating it from hot *n*-heptane solution into isopropyl alcohol. The per cent conversion was then calculated from the weight of the dry polymer obtained.

The composition of the unreacted butene-2 monomers after their polymerization was determined by gas chromatography performed under conditions similar to those mentioned above.

### Characterization of the Polymers

The structure of the resulting polymers was checked by infrared spectra of their films which were made from hot *n*-heptane solution. The isotacticity of the resulting polymer was determined from the weight of hot diethyl ether-insoluble polymer. The intrinsic viscosity of the polymer was also determined by viscosity measurements of dilute Tetralin solutions at 135°C. with an Ubbelohde viscometer.

## RESULTS

### Polymerization and Isomerization of Butenes by $\text{TiCl}_3\text{-Al}(\text{C}_2\text{H}_5)_3$ Catalysts

The results of polymerization of butenes by  $\text{TiCl}_3\text{-Al}(\text{C}_2\text{H}_5)_3$  catalyst are shown in Table I, in which the results of the isomer distribution in the unreacted butenes recovered after their polymerizations are also indicated. From Table I, it is obvious that butene-1 and butene-2 can polymerize in the presence of this catalyst system with Al/Ti molar ratios above 2 to give high molecular weight polymers. However, butene-1 polymerizes faster than *cis*- and *trans*-butene-2, which gives only a trace of the polymer at 60°C.

As the Al/Ti molar ratios in this catalyst system decrease from 2 to 0.5, the rate of polymerization of butene-1 and butene-2 decreases, but that of isobutene increases. These results can be understood from an increased cationic character of the catalyst systems as the Al/Ti molar ratio decreases.

The isomerizations of isobutene and butene-1 which were deduced from the results of composition analyses of the recovered butenes are not observed during the polymerizations under the present conditions. As described later, however, the isomerization of butene-1 to butene-2 is also observed in the presence of  $(\text{C}_2\text{H}_5)_3\text{Al-Ti}(\text{OC}_4\text{H}_9)_4$  or  $\text{TiCl}_3$  (see Table III or V). The isomerization of butene-2 to butene-1 or to the other butene-2 is observed in the cases in which polymerization is performed and the rate of isomerization is found to increase as both polymerization temperature and the Al/Ti molar ratio increase. It is also clear that the rate of polymerization of butene-2 parallels its isomerization rate.

As indicated in the previous paper,<sup>4</sup> the polymers obtained from isobutene and butene-1 are found to show absorption bands due to the re-

TABLE I. Results of Polymerization and Isomerization of Butenes by  $(C_2H_5)_2Al-TiCl_3$  Catalyst in *n*-Heptane<sup>a</sup>

Butene	Al/Ti Temp., ratio	Time, °C.	Conver- sion, hr.	Conver- sion, %	Et <sub>2</sub> O-insoluble polymer		Isomer distribution in butenes recovered after polymerization <sup>c</sup>				
					Wt.-%	$[\eta]^b$	Iso- butene, %	Butene-1, %	<i>trans</i> - Butene, %	<i>cis</i> - Butene, %	
Isobutene	2	60	12	0.5	—	—	—	100.0	0.0	0.0	0.0
	0.5	60	12	1.5	—	—	—	100.0	0.0	0.0	0.0
Butene-1	2	60	0.83	73.1	70.9	(0.87) <sup>d</sup>	—	0.0	100.0	0.0	0.0
	0.5	60	0.5	0.1	—	—	—	0.0	100.0	0.0	0.0
	3	80	0.1	29.4	70.8	—	—	0.0	99.8	0.1	0.1
<i>trans</i> -Butene-2	2	80	0.1	60.0	73.6	2.10	—	0.0	99.8	0.1	0.1
	2	60	12	1.0	74.9	(0.47) <sup>d</sup>	—	0.0	2.1	97.9	0.0
	1	60	12	1.2	—	—	—	0.0	0.5	99.5	0.0
	0.5	60	12	1.4	—	—	—	0.0	0.4	99.6	0.0
	3	80	28	18.4	61.5	—	—	0.0	2.9	65.0	32.1
	2	80	3	1.7	—	—	—	0.0	0.9	91.1	8.0
<i>cis</i> -Butene-2	2	80	28	17.5	66.5	1.19	—	0.0	3.1	65.7	31.2
	2	60	12	4.5	78.9	(0.50) <sup>d</sup>	—	0.0	2.6	27.1	70.3
	1	60	12	0.8	—	—	—	0.0	0.7	6.9	92.4
	0.5	60	12	0	—	—	—	0.0	0.4	0.0	99.6
	3	80	28	19.0	68.3	—	—	0.0	4.0	63.2	32.8
	2	80	0.5	0	—	—	—	0.0	1.1	3.1	95.8
Mixture of butene-1 and <i>cis</i> -butene-2	2	80	28	18.0	74.9	1.28	—	0.0	3.5	55.6	40.9
	2	80	28	54.0 <sup>e</sup>	—	—	—	0.0	4.1	64.4	31.5
	2	80	28	41.1 <sup>f</sup>	—	—	—	0.0	1.4	72.4	26.2

<sup>a</sup> [Butene] = 5.93–6.08 mole/l., [TiCl<sub>3</sub>] = 5.0 × 10<sup>-2</sup> mole/l. Catalyst was used after aging at 27°C. for 1 hr.; <sup>b</sup> Determined in dilute Tetralin solution of the polymer at 135°C.; <sup>c</sup> Corrected values (wt.-%) in the recovered butenes determined by gas chromatography; <sup>d</sup> Determined on the unfractionated polymers obtained by the pre-ence of [TiCl<sub>3</sub>] = 10<sup>-1</sup> mole/l.; <sup>e</sup> [Butene-1]/[*cis*-butene] in initial monomer mixture is 49.2/50.8; <sup>f</sup> [Butene-1]/[*cis*-butene] in initial monomer mixture is 31.1/68.9.

spective recurring butene units. However, the spectra of the polymers from butene-2 showed no absorption band at  $1125\text{ cm.}^{-1}$  due to the butene-2 unit. These polymers are also found to consist of the identical structure as polybutene-1, from the result of x-ray diffraction spectra, as shown in the previous paper.<sup>4</sup> The polymers are found to contain some fraction insoluble in hot diethyl ether which melts at  $126\text{--}128^\circ\text{C.}$  ( $125\text{--}131^\circ\text{C.}$  for isotactic polybutene-1).<sup>10</sup> The percentage of these fractions was nearly equal. Accordingly, it is obvious that *cis*- and *trans*-butene-2 isomerize first to butene-1, which is less stable but has less steric hindrance than butene-2, and then polymerize to give a high molecular weight polybutene-1.

Table I also shows the results obtained with a mixture of butene-1 and *cis*-butene-2. In this case, the polymerization and isomerization were observed and the resulting polymers were found from their infrared spectra to be butene-1 homopolymers, but not copolymers.

#### Polymerization and Isomerization of Butenes by $(\text{C}_2\text{H}_5)_{3-x}\text{AlCl}_x\text{-TiCl}_3$ Catalyst

The results of the polymerization of butenes by the catalyst systems ( $\text{Al/Ti} = 2$  in molar ratio) consisting of  $\text{TiCl}_3$  and various organoaluminum compounds are shown in Table II. From Table II, the polymerizability of the butene monomers in the presence of these catalysts was observed to depend on the kind of organoaluminum component used. For example, the order of polymerizability of these butenes are as follows: for  $x = 0$  in Al component, butene-1  $\gg$  butene-2  $\gg$  isobutene; for  $x = 1$  in Al component, butene-1  $\gg$  isobutene  $>$  butene-2; for  $x = 2$  in Al component, isobutene  $\gg$  butene-1  $>$  butene-2.

These orders can be understood if it is assumed that the cationic character of the catalyst systems increases as the value of  $x$  in the organoaluminum component increases. In a previous paper, the same order of polymerizability of the butene isomers by a catalyst with  $x = 2$  in the Al component was observed in cationic polymerizations by boron trifluoride diethyl etherate.<sup>7</sup>

The polymers resulting from isobutene are colorless, viscous material and are shown by their infrared spectra to be identical with polyisobutene obtained with ordinary cationic catalyst.<sup>7</sup> All the polymers obtained with the other butenes consisted of polybutene-1.

#### Polymerization and Isomerization of Butenes by Other Catalysts

The results of polymerization and isomerization of butene-1 and *trans*-butene-2 in the presence of various systems of organoaluminum compounds and transition metal compounds are shown in Table III. On comparing Tables I and III, the isomer distribution in the recovered butenes after reacting both butenes with  $(\text{C}_2\text{H}_5)_3\text{Al-TiCl}_3$  or  $(\text{C}_2\text{H}_5)_3\text{Al-Ti}(\text{OC}_4\text{H}_9)_4$  catalyst for 28 hr. at  $80^\circ\text{C.}$  is found to approach an equilibrium mixture consisting of butene-1, *cis*-butene-2, and *trans*-butene-2 (see Table VI).

TABLE II  
Results of Polymerization and Isomerization of Butenes by  $(C_2H_5)_2AlCl_x-TiCl_3$  Catalysts (Al/Ti = 2) in *n*-Heptanes

Butene	<i>x</i> in catalyst system	Temp., °C.	Time, hr.	Conversion, %	Isomer distribution in butenes recovered after polymerization			
					Isobutene, %	Butene-1, %	<i>trans</i> -Butene-2, %	<i>cis</i> -Butene-2, %
Isobutene	2	60	0.33	73.3	100.0	0.0	0.0	0.0
	1	60	12	14.3	100.0	0.0	0.0	0.0
	0	60	12	0.5	100.0	0.0	0.0	0.0
Butene-1	2	60	12	3.4	0.0	98.7	0.0	1.8
	1	60	0.83	15.0	0.0	100.0	0.0	0.0
	0	60	0.83	73.1	0.0	100.0	0.0	0.0
<i>trans</i> -Butene-2	2	80	0.1	60.0	0.0	99.8	0.1	0.1
	2	60	12	~0	0.0	0.4	98.1	1.5
	1	60	12	~0	0.0	0.8	99.2	0.0
	0	60	12	1.0	0.0	2.1	97.9	0.0
	2	80	28	0	0.0	0.5	99.5	0.0
	1	80	28	0.05	0.0	0.8	99.2	0.0
<i>cis</i> -Butene-2	0	80	28	17.5	0.0	3.1	65.7	31.2
	2	60	12	~0	0.0	0.5	0.0	99.5
	1	60	12	~0	0.0	0.0	0.0	100.0
	0	60	12	4.5	0.0	2.6	27.1	70.3
	2	80	28	0.03	0.0	0.6	0.0	99.4
	1	80	28	0.05	0.0	0.8	0.0	99.2
0	80	28	18.0	0.0	3.5	55.6	40.9	

\* Experimental conditions are the same as those indicated in Table I.

TABLE III  
Results of Polymerization and Isomerization of Butenes by Organoaluminum and Transition Metal Compounds in *n*-Heptane at 80°C.,  
[Butene] = 6.00 mole/l.

Butene	Catalyst <sup>a</sup>	Al/Ti or Al/V molar ratio	Time, hr.	Conversion, %	Isomer distribution in butenes recovered after polymerization			
					Butene-1, %	<i>trans</i> - Butene-2, %	<i>cis</i> - Butene-2, %	
Butene-1	(C <sub>2</sub> H <sub>5</sub> ) <sub>2</sub> Al- VCl <sub>3</sub>	2	17	3.4	98.0	1.9	0.1	
	(C <sub>2</sub> H <sub>5</sub> ) <sub>2</sub> Al- Ti(OC <sub>2</sub> H <sub>5</sub> ) <sub>4</sub>	3	28	3.9	3.1	72.8	24.1	
Butene-1 <sup>b</sup>	(C <sub>2</sub> H <sub>5</sub> ) <sub>2</sub> AlCl- Ti(OC <sub>2</sub> H <sub>5</sub> ) <sub>4</sub> <sup>c</sup>	3	28	0	99.0	0.0	0.1	
	(C <sub>2</sub> H <sub>5</sub> ) <sub>2</sub> Al- VCl <sub>3</sub>	2	28	0	0.0	95.5	4.5	
<i>trans</i> - Butene-2	(C <sub>2</sub> H <sub>5</sub> ) <sub>2</sub> Al- Ti(OC <sub>2</sub> H <sub>5</sub> ) <sub>4</sub>	3	28	0.1	2.1	77.8	20.1	
	(C <sub>2</sub> H <sub>5</sub> ) <sub>2</sub> AlCl- Ti(OC <sub>2</sub> H <sub>5</sub> ) <sub>4</sub> <sup>d</sup>	3	28	0	0.1	99.5	0.4	

<sup>a</sup> [VCl<sub>3</sub>] = [Ti(OC<sub>2</sub>H<sub>5</sub>)<sub>4</sub>] = 50 mmole/l.

<sup>b</sup> [Butene] = 4.47, [*trans*-butene] = 4.51 mole/l.

<sup>c</sup> [Ti(OC<sub>2</sub>H<sub>5</sub>)<sub>4</sub>] = 37.5 mmole/l.

<sup>d</sup> [Ti(OC<sub>2</sub>H<sub>5</sub>)<sub>4</sub>] = 36.1 mmole/l.

TABLE IV  
Results of Isomerization and Polymerization of Butenes by Ternary Catalyst Systems Containing  $\text{TiCl}_3$  and  $\text{Al}(\text{C}_2\text{H}_5)_3^a$

Butene	Third catalyst compounds (TC)	TC/Ti molar ratio	Method of addition of $\text{TiCl}_3$	Temp., °C.	Time, hr.	Conversion %	Isomer distribution in butenes recovered after polymerization (%)		
							Butene-1, %	<i>trans</i> -Butene-2, %	<i>cis</i> -Butene-2, %
Butene-1	Pyridine	0	—	60	0.083	73.1	100.0	0.0	0.0
		1	A	60	0.03	43.7	98.8	0.0	0.2
		0	—	80	0.1	60.0	99.8	0.1	0.1
<i>trans</i> -Butene-2	Pyridine	1	B	80	7	0.4	99.9	0.0	0.1
		0	—	60	12	1.0	2.1	97.9	0.0
		1	A	60	6	0.5	0.6	99.4	0.0
<i>cis</i> -Butene-2	Pyridine	0	—	80	28	17.5	3.1	65.7	31.2
		1	B	80	28	~0	0.5	99.5	0.0
		0	—	60	12	4.5	2.6	27.1	70.3
<i>cis</i> -Butene-2	Pyridine	1	A	60	6	0.2	0.5	0.0	99.5
		0	—	80	28	18.0	3.5	55.6	40.9
		1	B	80	28	~0	0.3	0.8	98.9
Tetrahydrofuran	Pyridine	1	B	80	28	9.7	3.0	44.0	53.0
		0.5	B	80	28	~0	0.3	1.9	97.8
		$\text{H}_2\text{O}$	B	80	28	17.1	3.6	59.7	36.7
		$\sim 0.05$	B	80	28	10.6	4.3	51.1	44.6
		1	B	80	28	14.5	3.7	57.8	38.5

<sup>a</sup>  $\text{Al}/\text{Ti} = 2$ ;  $[\text{Butene}] = 5.93\text{--}6.08$  mole/l.,  $[\text{TiCl}_3] = 5.0 \times 10^{-2}$  mole/l. in heptane.

<sup>b</sup> Method A:  $\text{TiCl}_3$  was added to a mixture of  $\text{Al}(\text{C}_2\text{H}_5)_3$  and third compound; method B: third compound was added to the Natta catalyst aged for 1 hr. at 27°C.

<sup>c</sup> 20 ml. of hydrogen gas was introduced into the polymerization (ca. 30 ml.) under 750 mm. Hg at 27°C.



TABLE V. Results of Isomerization of Butenes with Various Catalysts in *n*-Heptane at 80°C., [Butene] = 5.67–6.00 mole/l.

Butene	Catalyst	Catalyst concn. $\times 10^2$ , mole/l.	Time, hr.	Isomer distribution in butenes after the reaction			
				Isobutene, %	Butene-1, %	<i>trans</i> -Butene-2, %	<i>cis</i> -Butene-2, %
Isobutene Butene-1	—	—	28	100.0	0.0	0.0	0.0
	—	—	28	0.0	100.0	0.0	0.0
	(C <sub>2</sub> H <sub>5</sub> ) <sub>3</sub> Al	8.3	28	0.0	99.9	0.0	0.1
	(C <sub>2</sub> H <sub>5</sub> ) <sub>2</sub> AlCl	8.3	28	0.0	99.9	0.0	0.1
	(C <sub>2</sub> H <sub>5</sub> )AlCl <sub>2</sub>	8.3	28	0.0	93.5	3.8	2.7
	SnCl <sub>4</sub>	5.0	28	0.0	99.8	0.0	0.2
	TiCl <sub>3</sub>	12.3	28	0.0	73.8	11.6	14.6
	TiCl <sub>3</sub>	12.3	100	0.0	22.3	51.0	26.7
	TiCl <sub>3</sub>	12.3	158	0.0	4.1	63.1	32.8
	VCl <sub>3</sub>	10.0	100	0.0	99.8	0.0	0.2
	—	—	28	0.0	0.0	100.0	0.0
	TiCl <sub>3</sub>	12.5	28	0.0	1.2	95.2	3.6
TiCl <sub>3</sub>	12.5	100	0.0	3.0	86.1	10.9	
TiCl <sub>3</sub>	12.5	158	0.0	3.5	81.4	15.1	
VCl <sub>3</sub>	10.0	100	0.0	0.0	99.9	0.1	
<i>cis</i> -Butene-2	—	—	28	0.0	0.0	0.9	99.1
	(C <sub>2</sub> H <sub>5</sub> ) <sub>3</sub> Al	11.1	28	0.0	0.0	0.9	99.1
	(C <sub>2</sub> H <sub>5</sub> ) <sub>2</sub> AlCl	8.3	28	0.0	0.0	0.0	100.0
	(C <sub>2</sub> H <sub>5</sub> )AlCl <sub>2</sub>	8.3	28	0.0	0.0	0.0	100.0
	SnCl <sub>4</sub>	5.0	28	0.0	0.0	0.0	100.0
	TiCl <sub>3</sub>	45.3	28	0.0	0.0	0.0	100.0
	LiAlH <sub>4</sub>	11.7	28	0.0	0.0	0.0	100.0
	TiCl <sub>3</sub> + H <sub>2</sub> O <sup>a</sup>	5.0	28	0.0	4.0	9.4	86.6
	TiCl <sub>3</sub>	20.2	28	0.0	3.5	15.0	81.5
	TiCl <sub>3</sub>	20.2	100	0.0	3.6	48.5	47.9
	TiCl <sub>3</sub>	20.2	158	0.0	3.8	60.9	35.3

<sup>a</sup> H<sub>2</sub>O/Ti = 0.05 in molar ratio.

This result indicates that the presence of  $\text{TiCl}_3$  and  $(\text{C}_2\text{H}_5)_3\text{Al}$ , unlike the case of  $\text{Ti}(\text{OC}_4\text{H}_9)_4$  and  $(\text{C}_2\text{H}_5)_3\text{Al}$ , causes the polymerization of butene-1 to proceed much faster than its isomerization to butene-2, and hence no butene-2 is detected in the recovered butenes after reacting for a rather short time, as shown in Table I.

The  $(\text{C}_2\text{H}_5)_2\text{AlCl-Ti}(\text{OC}_4\text{H}_9)_4$  catalyst system, which shows a greater cationic character than the  $(\text{C}_2\text{H}_5)_3\text{Al-Ti}(\text{OC}_4\text{H}_9)_4$  catalyst, is ineffective for either polymerization and isomerization of butene-1 or butene-2.

### Polymerization and Isomerization of Butenes by Ternary Catalyst Systems

The effect of a third component in the  $(\text{C}_2\text{H}_5)_3\text{Al-TiCl}_3$  catalyst ( $\text{Al/Ti} = 2$ ) on the polymerization and isomerization of butenes was investigated, and the results are shown in Table IV. The results show that pyridine inhibited the polymerization and the isomerization of butene-1 and butene-2, with the exception of butene-1 at  $60^\circ\text{C}$ ., in which the polymerization is rather accelerated. Although pyridine has been considered to neutralize the acidic site of the  $(\text{C}_2\text{H}_5)_3\text{Al-TiCl}_3$  catalyst it was obvious that the ternary catalyst containing pyridine shows a negative effect on the isomerization from butene-2 to butene-1.

TABLE VI  
Isomerization and Polymerization of *trans*-Butene-2 in the Presence of  
 $\text{Al}(\text{C}_2\text{H}_5)_3\text{-TiCl}_3(\text{Al/Ti} = 2)$  at  $80^\circ\text{C}$ .<sup>a</sup>

Time, hr.	Conversion, %	Isomer distribution		
		Butene-1, %	<i>cis</i> - Butene-2, %	<i>trans</i> - Butene-2, %
0	0	0.0	0.4	99.6
0.08	0	0.6	0.8	98.6
0.17	0	0.9	0.8	98.3
0.5	~0	0.7	0.9	98.4
1.0	~0	0.6	1.1	98.3
3.0	1.7	0.9	8.0	91.1
5.0	3.1	1.5	9.9	88.6
10.0	2.8	2.1	13.7	84.2
28.0	17.5	3.1	31.2	65.7
		(5.1) <sup>b</sup>	(22.5) <sup>b</sup>	(72.4) <sup>b</sup>

<sup>a</sup>  $[\text{TiCl}_3] = 0.05$ ,  $[\text{Butene}] = 6.0$  mole/l. in *n*-Heptane.

<sup>b</sup> Equilibrated concentration calculated from free energies of formation of the respective butene isomers.

No isomerization of butene-2 or butene-1 was observed in the presence of stannic chloride. On the other hand, the presence of tetrahydrofuran, lithium aluminum hydride, hydrogen gas, and a trace of water as the third component does not affect these isomerizations of butene-2. However, the polymerization rates are somewhat decreased.

### Isomerization of Butenes

The results of isomerization of butenes in the presence of various compounds are shown in Table V. From this table, it is clear that none of the butenes isomerize thermally below 80°C. In addition,  $\text{TiCl}_3$  is the only effective isomerization catalyst for the compounds listed, with the exception of isobutene. All butenes except isobutene were found to approach an equilibrium mixture of butene-1, *cis*-butene-2, and *trans*-butene-2 (see Table VI). An approach to the same isomer distribution from butene-2 was greatly accelerated in the presence of  $(\text{C}_2\text{H}_5)_3\text{Al}$  against  $\text{TiCl}_3$  as compared to  $\text{TiCl}_3$  alone, shown in Tables I and V.

Table VI shows the time-isomerization relation of *trans*-butene-2 in the presence of  $\text{Al}(\text{C}_2\text{H}_5)_3$ - $\text{TiCl}_3$  catalyst ( $\text{Al}/\text{Ti} = 2$ ).

### DISCUSSION

As can be seen from Table I, butene-1 polymerizes much faster than butene-2 in the presence of the Natta catalyst, but isobutene does not polymerize. The polymerization activities decrease with decreasing molar ratio in  $\text{Al}/\text{Ti}$  and with increasing substitution of chloride component in organoaluminum compounds of the catalyst systems which were known to result in an increased cationic nature. Similar results were observed on addition of pyridine to the Natta catalyst.

All of the resulting polymers except those formed from isobutene were confirmed by their infrared spectra of x-ray diffraction spectra<sup>4</sup> and their physical properties to consist of polybutene-1, not a copolymer of butene-1 and -2. From this result, it was clear that butene-2, which was known not to be polymerized due to the steric effect of the substituents could be used as a new monomer of high polymerization.

From Table I, butene-1 was found not to be isomerized in the presence of the Natta catalyst as compared with butene-2. This result might be understood from the fact that the polymerization of butene-1 takes place faster than its isomerization, i.e., in the presence of  $\text{TiCl}_3$ , which does not initiate the polymerization of butene-1, isomerization to butene-2 was observed (Table V). However, from the gas chromatographic determination of the isomer distribution of butenes recovered after polymerization, the isomerizations from one butene-2 to the other butene-2 and to butene-1 was observed. In this case, it was found that the rates of polymerization by the catalyst systems used in this study were proportional to the isomerization rates, indicating that the isomerization from butene-2 to butene-1 must occur before the polymerization.

The isomerization of the butenes takes place in the presence of the catalyst systems consisting of  $\text{TiCl}_3$  to approach an equilibrium mixture of *trans*-butene-2, *cis*-butene-2, and butene-1. Since no methyl rearrangement occurred in these catalyst systems, no isobutene was produced and no isomerization relating to isobutene was found.

No isomerization of the butenes was observed with organoaluminum compounds alone, but it was clear that triethylaluminum could cocatalyze the isomerization of butene-2 by  $\text{TiCl}_3$  and produce, at the same time, an active center for the polymerization of butene-1. Recently, Reinhart and Fuest<sup>11</sup> have found that the butenes are isomerized by alcoholic rhodium or ruthenium chloride solution. Although in the present study only  $\text{TiCl}_3$  could act as a catalyst of butene isomerization, it was observed that some other transition metal salts could also serve as a catalyst; this will be reported in detail in the next paper.<sup>12</sup> Of course, these catalysts could not induce the polymerization of butene-1 and butene-2 without the addition of the Natta catalyst, indicating that there are two different active centers for isomerization and polymerization.

From the gas chromatographic determinations of the isomer distribution of the butenes, the concentration of the respective butene isomers in an equilibrium mixture was determined as shown in Table VII. Since the

TABLE VII  
Isomerization and Polymerization of  $\beta$ -Olefins by  $(\text{C}_2\text{H}_5)_3\text{Al-TiCl}_3$   
Catalyst (Al/Ti = 2) for 28 hr. at 80°C.

$\beta$ -Olefin	Polymer yield, %	Structure of polymer obtained <sup>a</sup>	Concn. of isomeric $\alpha$ -olefin in equilibrium mixture, %	
			Observed	Calcd.
<i>cis</i> -Butene-2	18.0	Butene-1	3.5	5.1
<i>trans</i> -Butene-2	17.5	Butene-1	3.1	5.1
<i>n</i> -Pentene-2	5.1	<i>n</i> -Pentene-1	2.7	3.1
<i>n</i> -Hexene-2	1.9	<i>n</i> -Hexene-1	3.0	1.8
3-Methylbutene-2	0	—	0	0.5
4-Methylpentene-2	0	—	0	0.5
3-Methylpropene-2	0	—	0	0.04

<sup>a</sup> Confirmed by infrared spectra of the polymers.

equilibrated concentration of the butene isomers was controlled by their thermodynamic stabilities, it was observed that their concentrations observed were in fairly good agreement with those calculated by the free energies of their formations as shown in Table VII, in which data on the other  $\beta$ -olefins are also given.

As can be seen from Table VII, the equilibrium concentration of butene-1 is quite low (3–5%), indicating that butene-1 is less stable than butene-2. Since butene-1 has, however, less steric hindrance caused by the substituents than butene-2, its polymerizability toward the Natta catalyst is expected to be more superior than butene-2, as shown in Table I.

From the fact that the isomerization of butene-2 is proportional to the polymerizability toward the Natta catalyst, the concentration of butene-1 produced by isomerization of butene-2 in the neighborhood of the active center for the polymerization may be enough to give a high molecular

weight polymer. If these conditions are satisfied, it is concluded that butene-2 isomerizes to butene-1 which has less steric hindrance and then polymerizes as butene-1 through an ordinary vinyl polymerization by a coordinated anionic mechanism.

If this consideration is general for the other  $\beta$ -olefins and the equilibrium concentration of the respective isomeric  $\alpha$ -olefin exists over this range ( $>2-5\%$ ), such  $\beta$ -olefins can be expected to polymerize with isomerization to the corresponding  $\alpha$ -olefins to give a high molecular weight polymer having the recurring unit of the  $\alpha$ -olefin. As shown in Table VII, it was found that *n*-pentene-2 and *n*-hexene-2 could polymerize to high molecular weight polymers of *n*-pentene-1 and *n*-hexene-1, respectively. However, no isomerization and polymerization of 3-methylbutene-2, 4-methylpentene-2, and 3-phenylpropene-2 were observed.<sup>13</sup>

In the cationic polymerization of some branched  $\alpha$ -olefins including 3-methylbutene-1, 4-methylpentene-1, and 3-phenylpropene-1, Kennedy et al.<sup>8</sup> and Ketley et al.<sup>9</sup> found that the growing cations were isomerized with the migration of a hydride ion to give a more stable carbonium ion in the propagation reaction. This type of isomerization was more favored in branched  $\alpha$ -olefins than in the corresponding linear  $\alpha$ -olefins.

In the coordinated anionic polymerization of  $\beta$ -olefins, it was clearly shown from Table VII that  $\beta$ -olefins were isomerized to the corresponding  $\alpha$ -olefins and then polymerized as only  $\alpha$ -olefins to give polymers the same as those from  $\alpha$ -olefins. In general,  $\beta$ -olefins were more stable thermodynamically, as indicated in Table VII, and had more steric hindrance than the respective  $\alpha$ -olefins. Since  $\beta$ -olefins did not copolymerize with  $\alpha$ -olefins with the Natta catalyst, these results might indicate that only the steric effect of the substituent in the monomer was an important factor for these olefins to polymerize.

As described above, the isomerization of butene-2 to butene-1 occurred first in the butene-2 polymerization. In this case an equilibrated concentration of  $\alpha$ -olefin isomerized from  $\beta$ -olefin must be kept, at least, enough for formation of high polymer to take place in the neighborhood of the active center for polymerization. Accordingly, a large difference in thermodynamic stabilities between  $\alpha$ - and  $\beta$ -olefins, which was more favored in branched  $\beta$ -olefins than in unbranched  $\beta$ -olefins, would lead to a decrease in the equilibrated concentration of  $\alpha$ -olefin; hence no polymerization of such  $\beta$ -olefins were observed, as understood from Table VII.

Two different mechanisms for olefin isomerizations in the presence of transition metal compounds have been presented:<sup>14</sup>  $\sigma$ -complex formation and  $\pi$ -allyl complex formation.

(1)  *$\sigma$ -Complex Formation Mechanism.*<sup>14,15</sup> Even though the catalyst system consisted of metal hydride, this mechanism can be explained by both geometrical and positional isomerizations.

(2)  *$\pi$ -Allyl Complex Formation Mechanism.*<sup>5,11</sup> In this mechanism, the initial catalyst system has no need of a hydride and only positional isomerization must be observed.



Recently Reinhart and Fuest<sup>11</sup> have stated that isomerization of the butenes by alcoholic rhodium and ruthenium chloride solutions takes place via the  $\pi$ -allyl complex formation. However, the results listed in Table VI show that *cis*-butene-2 was produced at the same time with butene-1 from *trans*-butene-2. This indicated that there was concurrent geometrical and positional isomerization of butene-2 in the presence of the above catalyst systems (consisting of  $\text{TiCl}_3$ ). Accordingly, at the present time it is concluded that butenes were isomerized by the  $\sigma$ -complex formation mechanism under the present conditions.

### References

1. G. Natta, G. Dall'asta, G. Mazzanti, I. Pasquon, A. Valvassori, and A. Zambelli, *J. Am. Chem. Soc.*, **83**, 3343 (1961).
2. H. Z. Friedlander, in *Macromolecular Chemistry (J. Polymer Sci. C, 4)*, M. Magat, Ed., Interscience, New York, 1964, p 1291.
3. H. Z. Friedlander, *Chem. Eng. News*, **42**, No. 6, 42 (Feb. 10, 1964).
4. A. Shimizu, T. Otsu, and M. Imoto, *J. Polymer Sci. B*, **3**, 449 (1965).
5. A. Iwamoto and S. Yuguchi, paper presented at the 13th Annual Meeting of Polymer Science of Japan, June 1964.
6. R. O. Symcox, *J. Polymer Sci. B*, **2**, 947 (1964).
7. A. Shimizu, T. Otsu, and M. Imoto, *Bull. Chem. Soc. Japan*, **38**, 1535 (1965).
8. J. P. Kennedy et al., *Makromol. Chem.*, **53**, 28 (1962); *ibid.*, **64**, 1 (1963); *J. Polymer Sci. A*, **2**, 1441, 2093 (1964); *ibid.*, **3**, 367, 381 (1965).
9. A. D. Ketley et al., *J. Polymer Sci. B*, **1**, 313 (1963); *ibid.*, **2**, 827 (1964); *J. Polymer Sci. A*, **2**, 4461 (1964).
10. J. W. S. Hearle, *Skinner's Silk Rayon Record*, **30**, 354 (1956).
11. R. E. Reinhart and R. W. Fuest, *Chem Eng. News*, **43**, No. 7, 40 (Feb. 15, 1965).
12. A. Shimizu, T. Otsu, and M. Imoto, *J. Polymer Sci.*, in press.
13. A. Shimizu, T. Otsu, and M. Imoto, *J. Polymer Sci. B*, **2**, 1031 (1964).
14. T. A. Manuel, *J. Org. Chem.*, **27**, 3941 (1962).
15. G. L. Karapinka and M. Orchin, *J. Org. Chem.*, **26**, 4187 (1961).

### Résumé

Un essai de préparation de polybutène-1 isotactique de poids moléculaire élevé au départ de *cis*- ou de *trans*-butène-2 a été effectué. On a remarqué que la polymérisation ne se passe pas par suite de l'effet stérique des constituants. En présence d'un catalyseur  $\text{TiCl}_3\text{-Al}(\text{C}_2\text{H}_5)_3$  les deux monomères butène-2 polymérisent à une vitesse plus lente que le butène-1 et fournissent des polymères consistant en unités périodiques de butène-1. Au départ de déterminations par chromatographie gazeuse, de la distribution isomérique du butène récupéré après polymérisation, on a trouvé que le butène s'isomérisé en présence du système catalytique contenant le  $\text{TiCl}_3$  et s'approche du mélange à l'équilibre thermodynamique du butène-1, *cis*-butène-2 et *trans*-butène-2. On a également trouvé que les vitesses de polymérisation du butène-2. On a également trouvé que les vitesses de polymérisation du butène-2 en présence du système catalytique utilisé était proportionnel aux vitesses d'isomérisation. Ces résultats montrent que le butène-2 isomérisé tout d'abord en butène-1 qui a moins d'empêchements stériques et polymérise ensuite comme butène-1 au moyen d'une polymérisation vinylique ordinaire par un mécanisme anionique coordinatif. Ce type de polymérisation a été observé avec certaines autres—oléfines linéaires tels que le pentène-2 normal et l'hexène-2 normal.



### Zusammenfassung

Ein Versuch zur Darstellung eines hochmolekularen isotaktischen Polybuten-1 aus *cis*- oder *trans*-Buten-2 wurde unternommen. Es wurde festgestellt, dass wegen der sterischen Effekte der Substituenten keine Polymerisation auftrat. In Anwesenheit von  $\text{TiCl}_3\text{-Al}(\text{C}_2\text{H}_5)_3$  als Katalysator polymerisierten bei den Buten-2-Monomeren mit geringerer Geschwindigkeit als Buten-1 und lieferten Polymere mit Buten-1-Bausteinen. Durch gaschromatographische Bestimmung der Isomerenverteilung der nach der Polymerisation zurückgewonnenen Butene wurde festgestellt, dass in Gegenwart des  $\text{TiCl}_3$ -haltigen Katalysatorsystems eine Isomerisierung der Butene in Richtung auf die thermodynamische Gleichgewichtsmischung von Buten-1, *cis*-Buten-2 und *trans*-Buten-2 auftritt. Weiters wurde gefunden, dass die Polymerisationsgeschwindigkeit von Buten-2 mit dem verwendeten Katalysatorsystem der Isomerisierungsgeschwindigkeit proportional war. Diese Ergebnisse zeigen, dass Buten-2 zuerst zu Buten-1 isomerisiert, welches eine geringere sterische Hinderung besitzt, und dann als Buten-1 durch die normale Vinylpolymerisation über einen anionischen Koordinationsmechanismus polymerisiert. Dieser Polymerisationstyp wurde bei einigen anderen  $\alpha$ -Olefinen, wie *n*-Penten-2 und *n*-Hexen-2 beobachtet.

Received October 24, 1965

Revised November 6, 1965

Prod. No. 4995A

## Heterogeneous Polymer Systems. IV. Mechanism of Rubber Particle Formation in Rubber-Modified Vinyl Polymers

GUNTHER E. MOLAU, *Plastics Department Research Laboratory,*  
and HENNO KESKKULA, *Polymer and Chemicals Research*  
*Laboratory, The Dow Chemical Company, Midland, Michigan*

### Synopsis

A mechanism for the formation of rubber particles in the polymerization of solutions of rubber in vinyl monomers is presented. A polymeric oil-in-oil emulsion is formed in the first phase of the polymerization. This polymeric oil-in-oil emulsion is transformed into a solid dispersion of rubber in vinyl polymer in the second phase of the polymerization. A phase inversion takes place in the emulsion in the first phase of the polymerization. Rubber solution droplets are formed at the phase inversion point. These droplets harden as the polymerization proceeds and are gradually transformed into the solid, crosslinked rubber particles of the final polymer.

### Introduction

Rubber-modified polystyrene is one of the most important thermoplastic materials. It combines the rigidity of polystyrene with an improved toughness, which makes this material more resistant to impact breakage than unmodified polystyrene. The improvement in impact resistance is obtained by incorporation of fine particles of rubber into a matrix of polystyrene. This incorporation of rubber into polystyrene can be achieved by several methods, whereby the quality of the final product depends to a large extent upon the method of preparation.

Amos et al.<sup>1</sup> have described the preparation of rubber-modified vinyl polymers by polymerization of solutions of unvulcanized rubber in vinyl monomers and have demonstrated that agitation of the polymerizing mixtures during the first 40% conversion of the monomers is of vital necessity, if a final product of high quality is to be obtained. They also pointed out that the rubber is grafted with the vinyl monomers during the polymerization. The grafting of natural rubber was studied by Merrett<sup>2</sup> and other authors of the British Rubber Producers' Research Association. Merrett<sup>2</sup> polymerized solutions of natural rubber in mixtures of styrene or methyl methacrylate with benzene and isolated the grafted rubber by fractionated precipitation with methanol. He noticed that a colloidal dispersion of rubber particles was obtained after addition of a certain fraction of metha-

nol and explained<sup>3</sup> this phenomenon by stating that the grafted side chains of poly(methyl methacrylate) or polystyrene are still soluble at the point of precipitation of the rubber and thus hold the collapsed rubber trunks in colloidal solution. The grafting and crosslinking of various rubbers and the structure of the grafted and crosslinked materials were studied by Blanchette and Nielsen,<sup>4</sup> who polymerized solutions of rubber in styrene and fractionated their materials by solvent-nonsolvent techniques. Claver and Merz<sup>5</sup> used phase-contrast and electron microscopy for the investigation of mechanical blends of various polymers and Merz et al.<sup>6</sup> studied the morphological and physical properties of mechanical blends of rubber and polystyrene. Traylor<sup>7</sup> described a sample preparation technique for the investigation of rubber-modified polymers by phase-contrast microscopy. The topic of this paper will be the mechanism of formation of the reinforcing rubber particles in rubber-modified vinyl polymers prepared by polymerization of solutions of unvulcanized rubbers in vinyl monomers. The mechanism of particle formation and other phenomena occurring during the polymerization of solutions of rubbers in vinyl monomer will be discussed, the polymerization of a solution of a polybutadiene rubber in styrene being used as a typical example.

### Phenomenology

The investigation of a rubber-modified polystyrene under a phase-contrast microscope reveals that such a material is a heterogeneous polymer system.<sup>5,6</sup> The morphological structure of such a system depends on the method of preparation, and the colors of the phases in the microscopic image depend on the type of phase-contrast microscope used.

In a phase-contrast microscope, a two-phase system appears black and white. The phase with the higher refractive index appears black, and the phase with the lower refractive index appears white in a dark phase-contrast microscope. Examination of a 1–2  $\mu$  slice from a rubber-modified polystyrene prepared according to Amos et al.,<sup>1</sup> i.e., by polymerization of a solution of rubber in styrene with agitation, under a dark phase-contrast microscope shows that this material consists of a solid dispersion of rubber particles in a matrix of polystyrene. Because of the refractive indices of the two phases, rubber and polystyrene, the rubber phase appears light and the polystyrene phase appears dark in positive dark phase-contrast photomicrographs.

The question arises: How are the rubber particles formed during the polymerization of a solution of rubber in styrene?

A solution of a pure synthetic rubber in styrene looks like mineral oil and has a similar consistency, depending on the concentration of the rubber. When such a solution is heated to a temperature high enough for polymerization to occur, it becomes turbid after a short time. The viscosity increases as the polymerization proceeds, and, finally, a solid, opaque polymer is formed which looks quite uniform to the naked eye, but is heterogeneous as microscopic investigation reveals. If two polymerizations are carried



Fig. 1. Rubber particles (white) in a continuous phase of polystyrene (black), prepared by polymerization of a solution of polybutadiene rubber in styrene with agitation (final polymer).

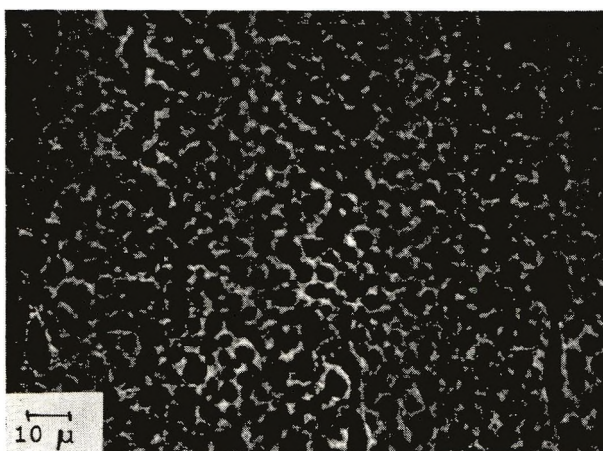


Fig. 2. Pools of polystyrene (black) in a continuous phase of polybutadiene rubber (white) prepared by polymerization of a solution of polybutadiene rubber without agitation (final polymer).

out, one with agitation and one without agitation, microscopic investigation of thin cross sections cut from the final polymer reveals that only the sample prepared with agitation (Fig. 1) contains the rubber dispersed in the form of discrete particles in a continuous polystyrene phase; the sample prepared without agitation contains the rubber in an entirely different form which can be described as a continuous phase of rubber with a disperse phase of polystyrene or as a spongy, interwoven network of two continuous phases, namely a continuous rubber phase and a continuous polystyrene phase (Fig. 2). This difference gives rise to another question: What is the role of the agitation in the formation of the rubber particles?



Since the samples shown in Figures 1 and 2 were prepared by polymerization of rubber solutions, and since polystyrene is formed as a second polymer during such a polymerization, certain properties of solutions containing more than one polymer must be considered here. From the classic paper of Dobry and Boyer-Kawenoki<sup>8</sup> it is known that a solution of two different polymers in a mutual solvent generally separates into two phases. A few exceptions to this rule have been observed in systems in which strong interaction occurs between the two dissolved polymers.<sup>8</sup> Thermodynamic treatments of the phenomenon of phase separation have been presented by Scott<sup>9</sup> and by Allen et al.<sup>10</sup> Phase equilibrium data have been obtained for solutions of natural rubber and polystyrene in benzene by Dobry and Boyer-Kawenoki<sup>8</sup> and for solutions of polybutadiene rubber and polystyrene in various solvents by Paxton.<sup>11</sup> At low polymer concentrations and low molecular weights of the two polymers, both phases consist of both polymers plus the solvent. At sufficiently high concentrations and molecular weights of the polymers involved, the immiscibility of the polymers is practically complete so that each phase is a solution of essentially only one of the polymers in the mutual solvent. Scott<sup>9</sup> has referred to this case as the complete immiscibility approximation. During the polymerization of a solution of rubber in styrene, phase separation occurs as soon as a sufficient amount of polystyrene has been formed and the complete immiscibility approximation holds at a rather low degree of conversion; so that the two phases can be denoted the rubber phase and the polystyrene phase.

In the first paper in this series,<sup>12</sup> a new class of emulsions has been introduced. These emulsions have been named "polymeric oil-in-oil emulsions" (POO-emulsions) because they consist of immiscible polymer solutions which are emulsified with graft copolymers as emulsifying agents. A mechanism of stabilization of POO-emulsions has been proposed in a preceding paper.<sup>13</sup> The second phase and the emulsifying graft copolymer can be generated *in situ* when a solution of one polymer in another monomer is polymerized. The occurrence of phase separation during such a polymerization is often not obvious, particularly when no phase contrast microscope is employed, because POO-emulsions are often extremely stable so that the formation of two layers of polymer solutions cannot be readily observed. To avoid confusion, the term phase separation has been used only for the thermodynamical phenomenon of polymer incompatibility and the term demixing has been used for the colloidal phenomenon of separation into two layers.<sup>12</sup>

### Phase Inversion

The polymerization of a solution of an unsaturated rubber in a vinyl monomer leads to the formation of a polymeric oil-in-oil emulsion, because a second phase, namely the vinyl polymer phase, is generated, and the rubber is grafted<sup>2,4</sup> with the vinyl monomer during the polymerization. The formation of the grafted rubber begins as soon as vinyl monomer is converted into vinyl polymer.<sup>2</sup> The amount of grafted rubber formed

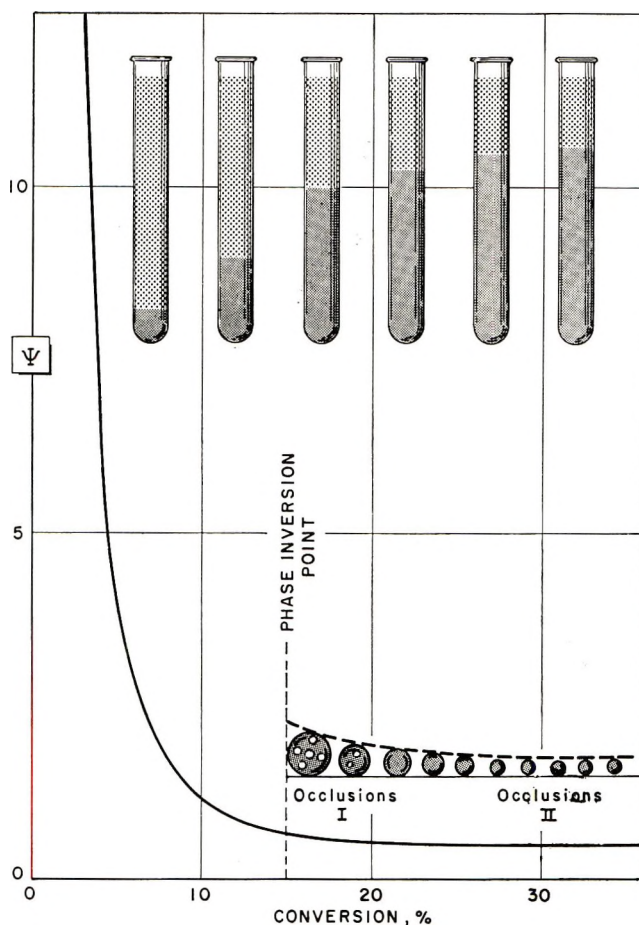


Fig. 3. Phase-volume ratio as a function of the degree of conversion for the polymerization of a solution of polybutadiene rubber in styrene.

early in the polymerization is large enough to make the formed POO-emulsions so stable that they can be coagulated only by extended centrifugation in an ultracentrifuge.

A very important parameter in the polymerization of a solution of rubber in a vinyl monomer is the ratio of the volumes of the two phases. This ratio is denoted here by  $\Psi$  and is defined as the ratio of the volume of the rubber phase to the volume of the vinyl polymer phase. The determination of the phase volume ratio as a function of the degree of conversion would require the coagulation of samples taken at various degrees of conversion during a polymerization. This method is inconvenient, because the coagulation of such samples is difficult and often impossible because of the extraordinarily high stability of POO-emulsions containing rubber. An alternative is the preparation of "simulated samples" by making solutions which are equal in composition to samples taken during a polymeriza-



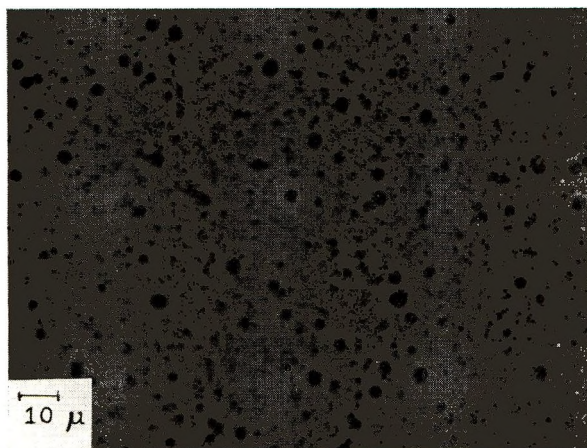


Fig. 4. POO-emulsion before the phase-inversion point in the polymerization of a solution of polybutadiene rubber in styrene.

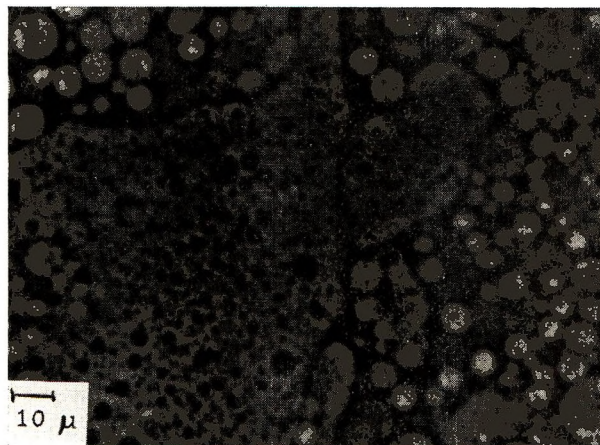


Fig. 5. POO-emulsion at the phase-inversion point in the polymerization of a solution of polybutadiene rubber in styrene.

tion, except that they contain no grafted rubber. Such simulated samples demix readily without centrifugation because they contain no POO-emulsifier, and allow a fast determination of the phase-volume ratio. Figure 3 shows a typical phase-volume ratio curve for the polymerization of a solution of rubber in polystyrene. The test tubes in the upper portion of Figure 3 show the phases in the demixed simulated samples. The rubber phase is the upper phase, and the polystyrene phase is the lower phase. The phase-volume ratio varies somewhat with the type and quantity of the rubber as well as of the vinyl polymer, but the shape of the curve is the same in all systems.

The phase-volume ratio is an important parameter in the polymerization of a rubber solution, because it determines the type of the formed POO-



Fig. 6. POO-emulsion after the phase-inversion point in the polymerization of a solution of polybutadiene rubber in styrene.

emulsion. In a system containing rubber and polystyrene, either the rubber phase or the polystyrene phase can be the disperse phase of the POO-emulsion. Before the critical point, only one phase exists, and a phase-volume ratio is not defined. At the critical point, i.e., at the onset of phase separation, a very small polystyrene phase comes suddenly into existence. This polystyrene phase must necessarily be the disperse phase, because it is much too small to be the continuous phase. As Figure 3 shows, the volume of the polystyrene phase increases rather rapidly as the polymerization proceeds. Finally, a point is reached at which the volume of the polystyrene phase is too large for this phase to be the disperse phase and the volume of the rubber phase is too small for this phase to be the continuous phase of the POO-emulsion. At this point, an inversion of the phases occurs. (Agitation of the system is necessary for this phase inversion to occur for reasons which will be discussed later in this paper.) The polystyrene phase becomes then the continuous phase and the rubber phase becomes the disperse phase. A similar behavior can be observed in systems containing dissolved polymers other than rubber.<sup>12</sup>

The phase inversion can easily be observed by phase-contrast microscopic investigation of samples taken at intervals of a few per cent conversion during the polymerization of a solution of rubber in styrene. Figures 4-6 show some of the phase contrast photomicrographs taken from such a series of samples. The rubber phase is always white and the polystyrene phase is always black in these pictures.

Figure 4 shows the state of the POO-emulsion before the phase-inversion point; droplets of a polystyrene solution are dispersed in a continuous phase of a rubber solution. Figure 5 shows the system at the phase-inversion point. Figure 6 shows the emulsion after the inversion point; droplets of the rubber solution are dispersed in a continuous phase of the polystyrene solution.

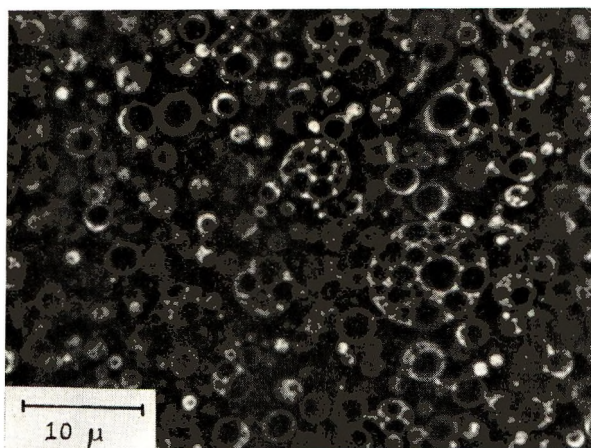


Fig. 7. Multiple emulsions formed at the phase-inversion point during the polymerization of a solution of polybutadiene rubber in styrene preserved in the final polymer (black type I occlusions of polystyrene in white rubber particles).

In a given system, the phase inversion occurs always at the same degree of conversion or, which is the same, at the same phase-volume ratio. The exact position of the inversion point depends on the system, i.e., on the type and concentration of rubber and on the type of the vinyl polymer/vinyl monomer. The type and concentration of the rubber are less influential than the type of vinyl polymer/vinyl monomer part of the system. In the concentration range of 0–20% rubber, the phase inversion occurs at 15–18% conversion of the styrene during the polymerization of a solution of rubber in styrene. In a given system, the inversion point is usually reproducible within a range of 2–3% conversion of the monomer.

The phase inversion is reversible. A re-inversion occurs when the system after the phase-inversion point is diluted with enough of the original rubber solution to obtain a total composition corresponding to a degree of conversion before the inversion point. The inversion and re-inversion can be repeatedly achieved by alternating polymerization and dilution steps. A POO-emulsion made by dilution cannot be microscopically distinguished from a POO-emulsion made by polymerization. Summarizing, one can say that the position of the phase-inversion point is reproducible and that, at conversions at which both phases are still liquid, the phase inversion is reversible and the emulsion state depends only on the composition of a system and is independent of the way by which this composition has been achieved.

An interesting phenomenon which is caused by the phase inversion is the formation of multiple emulsions at the phase-inversion point. Multiple emulsions are emulsions in emulsions. In the system discussed here, the droplets of the rubber solution after the inversion point can contain occluded droplets of the polystyrene solution. The interior of such rubber droplets is essentially a rudiment of the emulsion state of the system before



the inversion point (Fig. 7). As a consequence of the occlusion of a portion of the polystyrene phase inside the droplets of the rubber phase, the "effective" volume of the rubber phase (rubber phase plus occlusions of the polystyrene phase) is not identical with the "real" volume of the rubber as given by the phase-volume ratio.

Multiple emulsions in oil-water systems have been described and photographed by Seifriz,<sup>14</sup> and multiple emulsions in oil-oil systems have been described in a previous paper.<sup>12</sup> The reasoning<sup>15</sup> that the occurrence of multiple emulsions in oil-water systems is a consequence of the phase inversion should apply to POO-emulsions as well.

### Formation of the Rubber Particles

A necessary prerequisite for the formation of the reinforcing rubber particles is agitation of the polymerizing solution of rubber in the vinyl monomer during the first 40% conversion.<sup>1</sup> The mechanism of the formation of the rubber particles and the reason for the necessity of agitation in the described stage can be understood from the preceding discussion of the phase inversion.

The rubber particles come into existence at the phase-inversion point. At this point, the rubber phase and the polystyrene phase are still liquid, i.e., they are solutions of rubber or of polystyrene, respectively, in styrene. However, the viscosity of the rubber phase is considerably higher than the viscosity of the polystyrene phase and, as a consequence of the high viscosity of the rubber phase, the phase inversion does not readily occur unless the system is agitated.

The reversibility of the phase inversion and the fact that the inversion occurs always at the same degree of conversion suggest that the inversion point is a constant of a given system in the same sense as, e.g., the boiling point of a mixture of liquids is a constant of that system. Both the phase-inversion point of a polymerizing POO-emulsion and the boiling point of a mixture of liquids depend only on the composition of a given system, but not on the way that composition is reached.

This consideration is important for the understanding of the role of the agitation with respect to the phase inversion. Agitation is necessary for the phase inversion to occur, but it is not the cause of the phase inversion. The factors which cause the inversion must be inherent in the system rather than be introduced into the system from the outside. Inherent factors which have an influence on the position of the phase inversion point are the phase-volume ratio and the amount of grafted rubber present in the system. Rather than causing the occurrence of the phase inversion, the agitation acts like a catalyst: it increases the rate with which the inversion takes place.

Because of the high viscosity of the rubber phase the rate of inversion is too slow when a solution of rubber in styrene is polymerized without agitation. Before the phase inversion can take place, the polymerization has proceeded far enough that the system has solidified in the emulsion state

before the inversion point. The rubber remains in the continuous phase and forms a spongy network, as shown in Figure 2. This rubber network can be broken down by extrusion of the final polymer, but only irregularly shaped pieces of rubber rather than round particles can be obtained in this manner.

In an agitated system, the phase inversion is fast enough that it takes place within a range of less than 3% conversion, because the agitation increases the rate of inversion. The reason for this quasi-catalytic effect of the agitation is simply that an agitated emulsion is a dynamic system in which coalescence and re-formation of droplets occurs incessantly. An agitated emulsion comes much closer to being in equilibrium than a non-agitated emulsion, in which coalescence and re-formation of droplets can occur only by thermal motion. Particularly in POO-emulsions, agitation is necessary to keep a system in equilibrium, because the rather high viscosity of polymer solutions has an impeding effect on the coalescence and re-formation of the droplets. Since rubber solutions are particularly viscous, the retarding effect of the viscosity on the phase inversion becomes so high in POO-emulsions with a continuous rubber phase as to inhibit the phase inversion entirely.

Multiple emulsions are observed in most systems in samples taken immediately after the phase-inversion point. If the agitation is not too vigorous, the multiple emulsions survive the further polymerization and form occlusions of polystyrene in the rubber particles of the final polymer. The occlusions are round and will be referred to as type I occlusions (Fig. 3).

Figure 7 shows type I occlusions of polystyrene inside the rubber particles of a material which was prepared under such conditions that the multiple emulsions formed at the phase-inversion point survived the further polymerization. The perfectly round peripheries of the occlusions as well as of the rubber particles in Figure 7 are noteworthy, because they indicate that both the occlusions and the particles have been formed at a time when both phases of the system were still liquid enough that the occlusions and the rubber particles could assume the round shape of drops. The presence of type I occlusions in a final polymer indicates that the material has been made by polymerization of a solution of rubber. However, the absence of type I occlusions is not necessarily indicative of a preparation of the material in question by a process not involving polymerization of a rubber solution, because multiple emulsions can be destroyed by vigorous agitation.

Immediately after the inversion point, the droplets of the rubber solution are larger than the rubber particles in the final polymers. The droplets shrink very rapidly during a few per cent conversion after the phase inversion point and reach a constant size, namely the size of the final rubber particles, at about the same degree of conversion at which the phase-volume ratio becomes nearly constant. This behavior has been illustrated schematically in Figure 3. At the point of constant drop size and constant phase-volume ratio, the rubber phase is still liquid: it is a concentrated



Fig. 8. Electronphotomicrograph of type I and type II occlusions of polystyrene in rubber particles; final polymer formed by polymerization of a solution of polybutadiene rubber in styrene.

solution of rubber in monomer. This monomer, which serves as the solvent, forms polystyrene within the rubber phase, as the overall polymerization proceeds, and gives rise to phase separation within the rubber phase. This newly formed polystyrene is present in the rubber phase in the form of a polystyrene solution in monomer, so that the solvent monomer disappears in two ways from the rubber phase: as polystyrene and as solvent for this newly formed polystyrene. Because of the extremely high viscosity of the rubber at the rubber concentrations involved, the newly formed polystyrene solution can no longer leave the rubber phase: it forms a second type of occlusions in the rubber particles. These type II occlusions (Fig. 3) are so small as to be invisible under a phase-contrast microscope, but they can be made visible with an electron microscope. An electron photomicrograph of type I and type II occlusions in a rubber particle is shown in Figure 8. (The technique for the preparation of electron photomicrographs in rubber-modified systems will be reported elsewhere.<sup>16</sup>) The characteristic feature of this type of polystyrene occlusion is the irregular shape of the periphery, which indicates that these occlusions were formed at a time where the phases were no longer liquid enough to assume the round shape of droplets.

As the polymerization proceeds, all monomer in the rubber phase as well as in the polystyrene phase is converted into polymer, so that both phases harden gradually until at substantially complete conversion of the monomer the final system is a solid dispersion of rubber particles in a matrix of polystyrene. Such a polymer can be dissolved in solvents like benzene or



toluene, because the polystyrene matrix is soluble and the rubber particles can swell to such an extent that the resulting system appears to the naked eye as a true solution, particularly on sufficiently high dilution. In contrast to such an "inverted" polymer (Fig. 1), an uninverted polymer (Fig. 2), in which the rubber has crosslinked in the form of a spongy network, cannot be dissolved, because a matrix of crosslinked rubber is insoluble. Thus, the solubility of the final polymers can be used as a simple test of the morphological structure of the materials, as has been described previously.<sup>1</sup>

### Conclusions

The polymerization of a solution of a rubber in a vinyl monomer consists of two phases. In the first phase (0–40% conversion), in which the system is liquid, a polymeric oil-in-oil emulsion is formed, and the size of the rubber particles is established. In the second phase (40–100%) this polymeric oil-in-oil emulsion hardens gradually to a solid dispersion of rubber particles in a matrix of the vinyl polymer, whereby the structure of the POO-emulsion is retained and no significant morphological changes occur.

The rubber particles are formed by the phase inversion which occurs in the first phase of the polymerization.\* At the phase-inversion point, the rubber phase is dispersed in the form of droplets in the vinyl polymer phase. The formation of multiple emulsions can occur at this point. The droplets of the rubber phase harden gradually by polymerization of the monomer and by crosslinking of the rubber and become finally solid rubber particles. The rubber particles contain irregularly shaped, tiny occlusions of vinyl polymer caused by polymerization of the portion of the monomer which was the solvent in the rubber phase. In addition, the rubber particles can contain larger occlusions with round peripheries stemming from multiple emulsions formed at the phase-inversion point. Since the high viscosity of rubber solutions has an impeding effect on the phase inversion, agitation is necessary in the first phase of the polymerization in order to overcome the inertia of the system and achieve the phase inversion before the POO-emulsions can solidify in the uninverted state.

\* After the manuscript of this paper had been completed, a publication appeared,<sup>17</sup> in which the dispersion of rubber by a phase inversion was also described. Bender's observations are in mutual agreement with the observations presented in this paper and in the first paper<sup>12</sup> in this series.

The authors are indebted to Mr. P. A. Traylor and Mr. H. L. Garrett for the preparation of the photomicrographs.

### References

1. J. L. Amos, J. L. McCurdy, and O. R. McIntire (to The Dow Chemical Company), U.S. Pat. 2,694,692, (November 16, 1954).
2. F. M. Merrett, *Trans. Faraday Soc.*, **50**, 759 (1954).
3. F. M. Merrett, *Ric. Sci.*, **25**, 279 (1955).
4. J. A. Blanchette and L. E. Nielsen, *J. Polymer Sci.*, **20**, 317 (1956).
5. G. C. Claver and E. H. Merz, *Offic. Dig. Federation Paint Varnish Production Clubs*, **28**, 858 (1956).

6. E. H. Merz, G. C. Claver, and M. Baer, *J. Polymer Sci.*, **22**, 325 (1956).
7. P. A. Traylor, *Anal. Chem.*, **33**, 1629 (1961).
8. A. Dobry and F. Boyer-Kawenoki, *J. Polymer Sci.*, **2**, 90 (1947).
9. R. L. Scott, *J. Chem. Phys.*, **17**, 279 (1949).
10. G. Allen, G. Gee, and J. P. Nicholson, *Polymer*, **1**, 56 (1960).
11. T. R. Paxton, *J. Appl. Polymer Sci.*, **7**, 1499 (1963).
12. G. E. Molau, *J. Polymer Sci. A*, **3**, 1267 (1965).
13. G. E. Molau, *J. Polymer Sci. A*, **3**, 4235 (1965).
14. W. Seifriz, *J. Phys. Chem.*, **29**, 738 (1925).
15. W. Clayton, in *Theory of Emulsions*, C. G. Sumner, Ed., Blakiston, New York, 1954.
16. H. Keskkula and P. A. Traylor, to be published.
17. B. W. Bender, *J. Appl. Polymer Sci.*, **9**, 2887 (1965).

### Résumé

Un mécanisme de formation de particules de caoutchouc dans la polymérisation de solutions de caoutchouc dans les monomères vinyliques est présenté. Une émulsion polymérique huile dans huile est formée dans la première phase de la polymérisation. Cette émulsion huile-huile est transformée en une dispersion solide de caoutchouc dans le polymère vinylique dans la seconde phase de la polymérisation. Une inversion de phase se place dans l'émulsion au cours de la première phase de la polymérisation. Les gouttelettes de solution de caoutchouc se sont formées au point d'inversion de phase. Ces gouttelettes durcissent lorsque la polymérisation progresse et sont graduellement transformées en solide, constitué de particules caoutchouteuses pontées du polymère final.

### Zusammenfassung

Ein Mechanismus für die Bildung von Kautschukteilchen bei der Polymerisation von Lösungen von Kautschuk in Vinylmonomeren wird vorgeschlagen. In der ersten Phase der Polymerisation wird eine "polymere Öl-in-Öl"-Emulsion gebildet. Diese "polymere Öl-in-Öl"-Emulsion wird in der zweiten Phase der Polymerisation in eine feste Dispersion von Kautschuk im Vinylpolymeren umgewandelt. In der ersten Phase der Polymerisation findet eine Phasenumkehr in der "polymeren Öl-in-Öl Emulsion" statt. Am Phasenumkehrpunkt entstehen Tröpfchen einer Kautschuklösung. Diese Tröpfchen erhärten mit fortschreitender Polymerisation und gehen allmählich in die festen vernetzten Kautschukteilchen des Endprodukts über.

Received October 12, 1965

Revised November 15, 1965

Prod. No. 5006A

## Stereoregular Polymerization of Methyl Vinyl Ether with Fluoro Aluminum Initiators

R. J. KERN and J. D. CALFEE, *Monsanto Company, St. Louis, Missouri*

### Synopsis

The reactions of HF, BF<sub>3</sub>, or certain organic fluorine compounds with AlCl<sub>3</sub>, (C<sub>2</sub>H<sub>5</sub>)<sub>3</sub>Al, or ethylaluminum chlorides in chlorinated hydrocarbons give rise to gels which exhibit pronounced stereoregular polymerization initiating ability toward methyl vinyl ether. The active sites are believed to involve species of the type RAlF<sub>4</sub>. Polymeric products having a wide range of stereoregularities are obtained. Several polymerization variables were examined. The reaction systems exhibit a variety of appearances and interesting rheological sequences. These are the consequences of differential solubility behaviors of the various stereoregular fractions. The most highly stereoregular fractions may be fabricated as fibers, films, or molded objects. Fractions of intermediate stereoregularity exhibit interesting emulsion-forming properties. Stereoregularity is shown to afford a novel control over degree of water absorption in films.

The Lewis acid-promoted polymerization of alkyl vinyl ethers is widely recognized. Initiation of vinyl ethers by BF<sub>3</sub>·(C<sub>2</sub>H<sub>5</sub>)<sub>2</sub>O provided one of the earliest examples in which high polymer stereoisomerism was experimentally recognized.<sup>1</sup> It has now become apparent that the degree of stereoregularity developed in poly(alkyl vinyl ethers) initiated by most common Friedel-Crafts type catalysts is only marginal. Products exhibiting markedly greater stereoregularity have been described by Vandenberg,<sup>2</sup> who used transition metal-containing initiators, and ourselves.<sup>3</sup> Details regarding our catalyst and polymerization systems not previously described are presented here.

Polymer chemists have come to appreciate more fully that stereoregular polymerization systems must be characterized not only by the properties of the most unique fraction isolated but also by the stereoregularity distribution throughout the total polymeric product formed. Neglecting this point leads to considerable distortion of the overall picture. This has been particularly true of alkyl vinyl ether polymerizations.

Methods for measuring the degree of stereoregularity were treated previously.<sup>3</sup> It is sufficient here to say that an index derived from the ratio of the 12.40 μ/12.65 μ absorption bands has proven a most convenient and useful way to compare the stereoregularity of one product (of a given species) with another. This method does not in itself furnish the ultimate index for completely isotactic material.

## NATURE OF THE POLYMERIZATION SYSTEM

### Catalysts

Three related catalyst preparations are described in the Experimental Section. While all three types give rise to similar qualitative results, the following descriptions and data specifically pertain to type III ( $C_2H_5AlCl_2 + CH_3CHF_2$ ).

### Media

Bulk polymerization of pure liquid methyl vinyl ether (VME) is difficult to control. In our hands it also gave rise to low molecular weight and stereoregularity levels. Use of diluents avoids these shortcomings (see monomer concentration).

Polymerization does not proceed in hexane. Solution polymerization occurs in chloroform.<sup>4</sup> By employing combinations of hexane and chloroform (or methylene chloride), diluent mixtures can be obtained which afford control over the nature of product precipitation (self-fractionation) which occurs in the polymerization mixture. Fractions of higher stereoregularities separate in a wide variety of physical forms while lower fractions remain in solution. In appearance the reaction mixtures therefore range from viscous solutions through slurries of highly solvated solids to nonsolvated solids. Solids may be finely divided powders, shreds, long strands, or burrlike spheres from which spiked protrudances extend. Control over product fractionation by diluent composition and other variables is of direct process significance. This system provides an interesting case study of how reaction mixture morphology changes as a function of common polymerization variables.

### Temperature

Polymerization proceeds from at least  $-70$  to  $+40^\circ C$ . at atmospheric pressure. At the higher temperatures, products become more soluble, as shown by the decreasing conversion to polymer insoluble in the reaction mixture (Fig. 1) and self-fractionation accordingly becomes more rigorous (Fig. 2). However, the overall stereoregularity built into the total product does not change markedly. For poly(methyl vinyl ether) (PMVE) fractions (A and B) of known indexes (IR), eq. (1) was demonstrated to be valid:

$$(IR)_A \times \text{wt. fraction A} + (IR)_B \times \text{wt. fraction B} + \dots = (IR)_{\text{composite}} \quad (1)$$

It was found that the sum of the products of individual polymer weight fractions and their respective infrared indexes was essentially unchanged for runs conducted from  $-35$  to  $+40^\circ C$ .

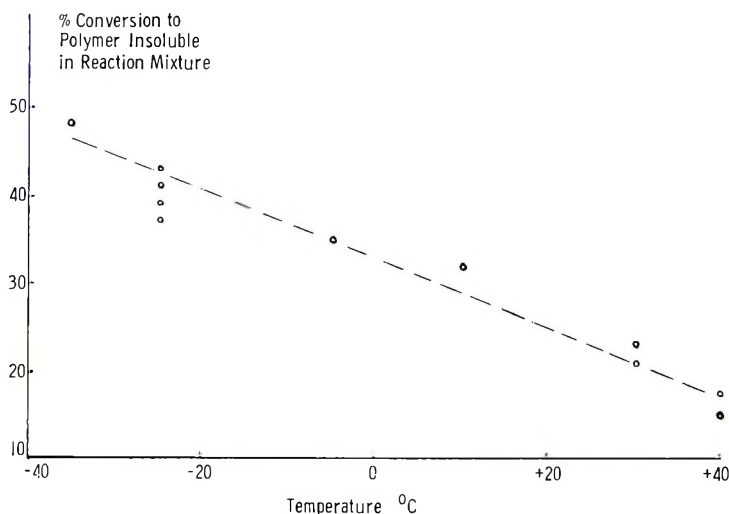


Figure 1.

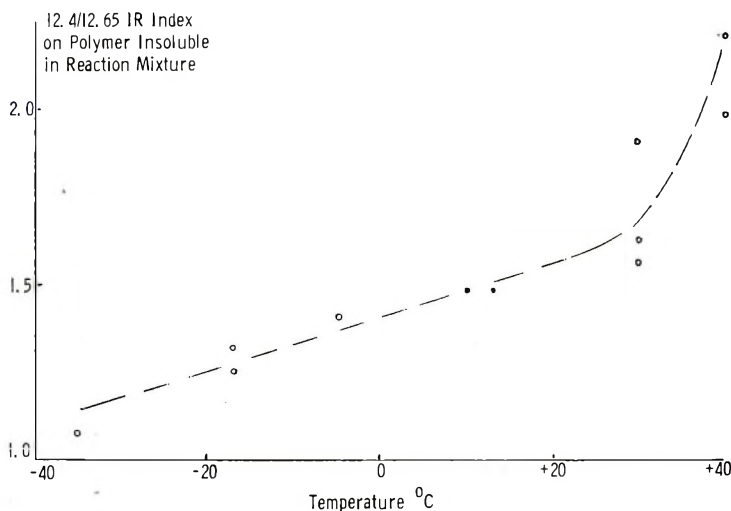


Figure 2.

### Order of Component Addition

Addition of the monomer to a catalyst-diluent mixture led to formation of finely divided, sandy solids of comparatively low IR index. The reverse procedure, adding catalyst to monomer-diluent mixture, resulted in shreds or cottonlike fibrous material of higher IR index. This reflects more intensive self-fractionation, with the monomer itself acting as solvent.

This change in solvent power due to monomer consumption also probably explains the observed change in physical nature of the solids formed throughout any given run. Solids formed toward the end of the reaction



possess a lower IR index and a lower degree of organization. Accentuating this phenomenon is the selective absorption of  $\text{CH}_2\text{Cl}_2$  by the insoluble polymer formed during the early stages of reaction. Thus, polymer formed later actually sees a diluent richer in nonsolvent hexane. Liquors isolated after appreciable conversions had taken place were found to consist of hexane/ $\text{CH}_2\text{Cl}_2$  ratios of 4-8 compared to an initial ratio of 3.

### Monomer Concentration

On mixing diluent, monomer, and catalyst in that order, it was found that lower monomer concentrations led to higher IR indexes (Fig. 3) and higher viscosity (molecular weight) (Table I).

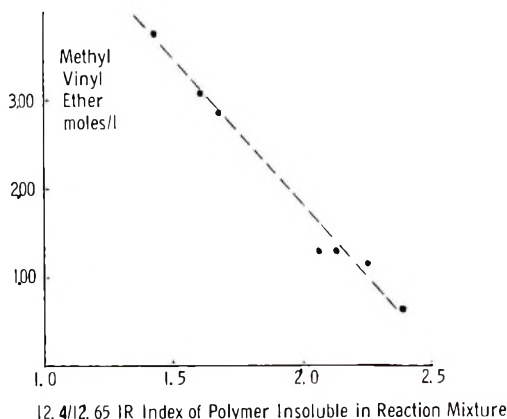


Figure 3.

More vigorous fractionation in monomer-rich (acting as solvent) environment which would lead to higher IR indexes at higher monomer concentrations is eclipsed by another complication. Just what this effect is due to is not clearly understood. It is difficult to believe chain transfer to monomer is the only cause, because purified diethyl ether can be employed as polymerization diluent (in place of hexane- $\text{CH}_2\text{Cl}_2$ ) without severe attenuation of molecular weight and stereoregularity. More regarding this point appears below.

TABLE I  
Product Viscosity versus MVE Concentration in Hexane- $\text{CH}_2\text{Cl}_2$  (3:1) at 0°C.

Methyl vinyl ether concn., mole-%	$\eta_{sp}$ (0.1% in $\text{CHCl}_3$ , 25°C.)
10	0.69 (acetone-insoluble fraction)
23	0.40 " " "
42	0.11 " " "
100	0.04 whole polymer (none acetone-insoluble)

### Product Fractionation

Fractionation of the total polymeric product may be conducted in a wide variety of solvents (see Table II). Invariably, the greater the weight fraction dissolved, the greater the IR index of the remaining insoluble portion.

TABLE II  
Fractionation Data<sup>a</sup>

Solvent	Typical IR index, insoluble fraction	$\eta_{sp}$ of insoluble fraction <sup>b</sup>
Water	0.9	0.06-0.15
Acetone	1.2	0.10-0.25
Benzene	1.9	0.20-0.30
Water	0.6 (soluble fraction)	0.03-0.06

<sup>a</sup> Polymerization at 0°C., 33 mole-% MVE in 3:1 hexane-chloroform.

<sup>b</sup> In CHCl<sub>3</sub>, 0.1% (w/v), 25°C.

In fact a way to characterize a stereoregular polymerization catalyst is to plot weight per cent of total polymer insolubles in a given liquid against the IR index of that insoluble fraction (Fig. 4).<sup>3</sup>

From a practical viewpoint, as implied above, polymerization conditions were adjusted to achieve one step of product fractionation directly during polymerization. Insolubles (A) were isolated by filtration. The soluble

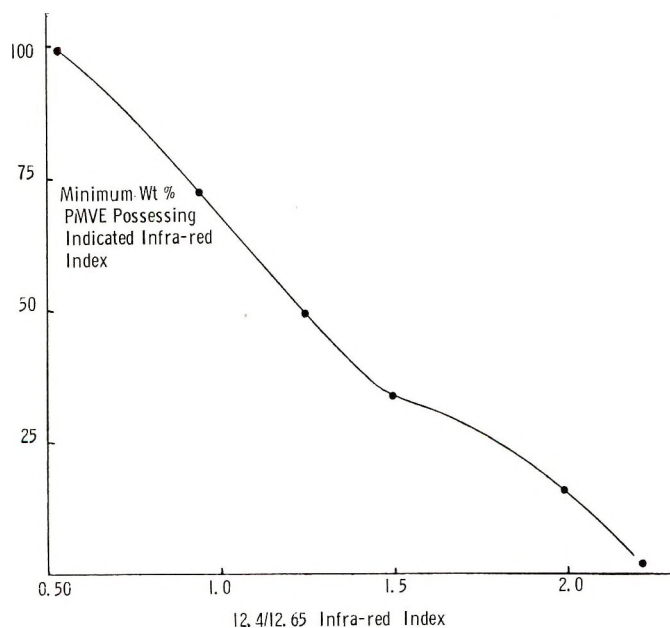


Figure 4.

portions remaining were isolated from solvent and extracted with cold water, thus yielding a water-insoluble fraction (B) and a water-soluble fraction (C).

### NATURE OF THE POLYMER

The poly(methyl vinyl ether) fraction (A) which is insoluble in the reaction mixture and obtained in 30–50% yield is remarkable by contrast to the mechanical properties of its atactic analog (fraction C). PMVE having specific viscosity of 0.2–0.3 can be molded, melt-spun into fibers, and ex-

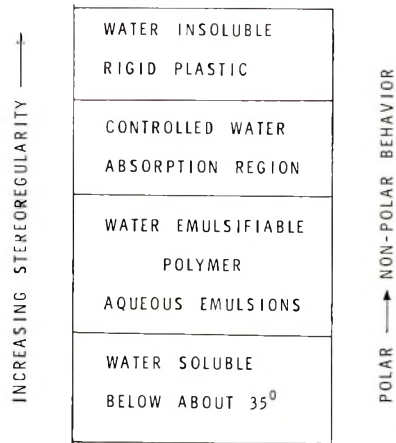


Fig. 5. Behavior of poly(methyl vinyl ether) with water.

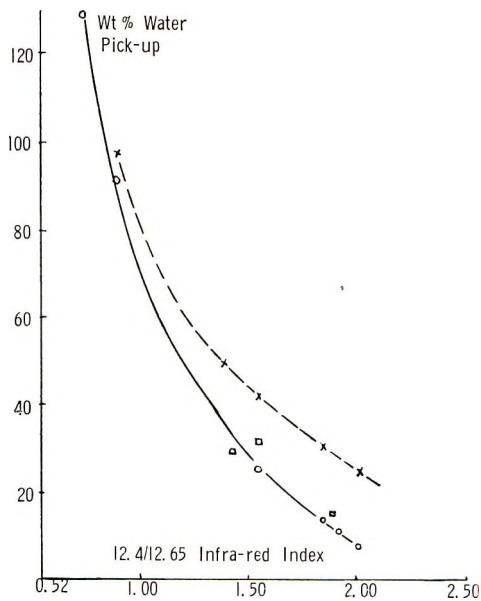


Fig. 6. Water pick-up of films: (X) molded; (O) cast from CH<sub>2</sub>Cl<sub>2</sub>; (□) blown.

trusion-blown into film. The film exhibits interesting properties in the subjective area of human response to touching (feel). By employing empirically determined fractionation solvents, a series of PMVE fractions can be isolated and fabricated as films. The liquid water pick-up for these films is seen to be a function of the stereoregularity index (Fig. 6). Behavior varies from negligible water take-up to complete solubility. Stereoregularity here provides a novel control over the important property of water interaction. Other properties of highly stereoregular PMVE have been discussed previously (see Fig. 5).<sup>2,3</sup>

The water-soluble fraction (formed in 20–25% yield) consists of conventional atactic PMVE which has been well described elsewhere.<sup>5</sup> The intermediate fraction B, which is soluble in the reaction mixture but insoluble in water, forms emulsions if whipped with water in a blender. Such emulsions have been stable at room temperature for several years in our laboratory. They coagulate at 35°C., as do aqueous solutions of PMVE generally. One also encounters fractions which, while initially soluble in water, become water-insoluble after being isolated and dried. Some change in physical interaction evidently occurs during the drying process.

### Oxidation Susceptibility

PMVE exhibits the pronounced susceptibility to oxidation which is characteristic of ethers as a class. Nonstabilized products readily become cheesy and lose strength. PMVE baked in an air oven at about 150°C. proceeds through this cheesy stage to form thereafter a glossy, dark-brown, water-insoluble enamel within a few hours.

When stereoregular fractions of PMVE are heated in air one finds that the infrared stereoregularity index at first increases and then decreases with exposure time.<sup>6</sup> For example, the index of one sample at 100°C. in air increased from 2.05 to 3.30 in 4 hr., thereafter dropping steadily. At 150°C. this initial increase in index either did not occur or else did so so rapidly as not to be observed.

As chains are degraded, the more highly stereoregular blocks are released from the restrictions imposed by the less regular portions. They are then better able to enter a more ordered arrangement which is reflected by a more intense 12.4  $\mu$  band. Remembering that the IR index is a ratio of two band intensities (from certain base lines),<sup>3</sup> it is significant that the 12.65  $\mu$  component (denominator) does not change appreciably during 100°C. treatment. Similar increases in crystallinity resulting from the thermal oxidation of polyethylene have been reported.<sup>7</sup> Of twelve oxidation stabilizers tested, the most effective was found to be 4,4'-thiobis-(6-*tert*-butyl-*m*-cresol).

## CATALYST SYSTEM

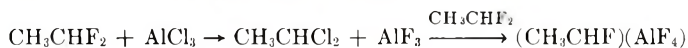
### Synthesis

Catalysts employed in this work were compositions found during an investigation of aluminum fluoride synthesis. Commercial aluminum fluo-

ride made by the action of HF or  $\text{H}_2\text{SiF}_6$  on aluminum oxide at elevated temperatures is very insoluble and intractible. This stands in marked contrast to materials formed by the reaction of aluminum compounds soluble in organic solvents with certain fluorine-containing compounds. These fluorinated aluminum products are readily water-soluble and enter into several reactions.

Trialkylaluminum compounds can react with HF or  $\text{BF}_3$  to produce aluminum fluoride in the form of white solids or a colorless gel, depending on the reaction medium employed. Aluminum fluoride formed in this way is without initiating ability. Additional coordinated HF or  $\text{BF}_3$  is required.  $\text{AlF}_3$  gel may be reversibly changed from being active to being inactive as regards initiation by cross-titrating with small amounts of  $\text{Et}_3\text{Al}$  and HF or  $\text{BF}_3$ .

When  $\text{AlF}_3$  gel in methylene chloride is reacted with certain organic fluorine compounds (such as ethylidene fluoride or dichlorodifluoromethane) heat is evolved, a reddish brown color forms, and pronounced stereoregular initiation ability toward alkyl vinyl ethers develops. Complexes of the type  $\text{RAlF}_4$  are believed to form. These same organic fluorine compounds also readily exchange fluorine for the chlorine atoms in aluminum chloride.<sup>8</sup> Thus, they may be employed to form active initiators directly from aluminum chloride without using HF or  $\text{BF}_3$  at all.



Mixed alkylaluminum chlorides may also be employed. In these cases  $\text{BF}_3$  is best employed to exchange F for alkyl groups on Al. Organic fluorine compounds exchange F for alkyls on Al only with difficulty but they exchange F for Cl on aluminum readily. In this regard they are much more effective than  $\text{BF}_3$ . Organic fluorine compounds vary markedly in their tendencies to undergo this chloro-exchange reaction. Hydrogen fluoride readily replaces both chloro and alkyl groups on aluminum.

### Concepts

The objective of this work was not to establish reaction mechanisms. Nevertheless, certain unifying concepts can be presented. Electrons are donated into the vinyl group of vinyl ethers. The extent to which this occurs is extreme compared to most vinyl monomers (highly negative  $e$  values). The charge separation in the coordination complex  $\text{RAlF}_4$  is viewed as being of just sufficient magnitude to allow attack on the polarized vinyl group. The charge separation is not sufficient to initiate less strongly polarized double bonds (in the sense of donating electrons into the vinyl group). This explains why these catalysts initiate vinyl ethers only. The simplest picture seems to be one of cationic propagation with the anionic counterions anchored in a gel structure (Fig. 7). In cases where counterions are viewed as being relatively fixed it has been popular to speak of monomer insertion processes, but this is largely a matter of semantics.



Aluminum fluoride exhibits a tendency to coordinate with unshared electron pairs not only on fluorine but also on organic nitrogen and to a lesser degree oxygen. Thus,  $\text{AlF}_3$  gel washed with acrylonitrile, tetrahydrofuran, or diethyl ether (and subsequently dried in vacuum at  $75^\circ\text{C}$ .) retains these liquids as ligands to the extents  $\text{AlF}_3\text{AN}$ ,  $(\text{AlF}_3)(\text{THF})_{0.4}$ , and  $\text{AlF}_3[(\text{C}_2\text{H}_5)_2\text{O}]_{0.3}$ . This suggests that a precoordination of vinyl ether molecules might occur on sites in the aluminum fluoride gel before they are incorporated into the chain. The resulting restrictions could well be important in determining polymer stereoregularity. This tendency of aluminum fluoride to coordinate also explains the observed deactivation by strongly polar groups such as  $-\text{C}\equiv\text{N}$ .

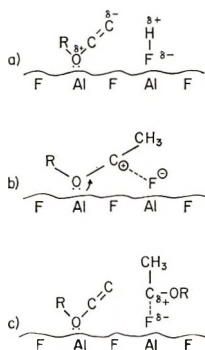


Figure 7.

While propagation through precoordinated monomer may occur, propagation directly from the liquid phase of monomer not precoordinated is also conceivable. The rate of propagation involving monomer directly from the liquid phase could have a greater concentration dependence than propagation which involves precoordination. The fact is that the dominant mode of polymerization does change to one of less stereoregularity, lower molecular weight, and higher polymerization rate as monomer concentration increases to high values.

## EXPERIMENTAL DETAILS

### Purification of Monomer

General Aniline methyl vinyl ether was passed through 40 cm. columns of calcium chloride and of potassium hydroxide pellets and finally through two bubble towers containing about 4% triethylaluminum in kerosene to remove acetaldehyde, methanol, and 1,1-dimethoxyethane. Condensed monomer contained small amounts of ethylene from the  $\text{Et}_3\text{Al}$  but they did not interfere. Condensed monomer was then stored in a 750-ml. steel tank and dispensed as needed measuring by weight differential.

### Polymerization

A typical polymerization was conducted as follows. A four-necked 3-liter round-bottomed flask was baked at 120°C., fitted with stirring motor and temperature indicator, and hooked to a nitrogen manifold. The flask was evacuated and vacuum released with dry nitrogen. Methylene chloride was refluxed over calcium hydride (until evidence of moisture condensing was gone) and then distilled. Methylene chloride contains usually about 1/2% ethanol which was not removed.

Dry commercial grade hexane (900–1200 ml.) and methylene chloride (300 ml.) were added to the flask and cooled to the desired temperature (at least 0°C.). Catalyst sufficient to give 1–10 mmole/l. Al was injected by syringe and needle after addition of monomer through a copper tube and adapter from the inverted monomer storage tank. A Dry Ice condenser is required if the polymerization is to be run above about 10°C. Polymerizations were conducted under a positive nitrogen pressure of about 5 mm. Polymerization times required were in the range of 2–4 hr.

### Work-Up Procedure

The variety of polymerization mixtures obtained as reaction conditions are changed requires each type to be treated differently. Generally, we filtered the cold reaction mixture directly through a 30-mesh brass sieve. The precipitate was covered with acetone and stirred slowly for about thirty minutes, filtered and the process repeated. The solids were filtered and then heated in boiling water to remove adsorbed methylene chloride. After overnight cold-water exposure solids were finally filtered and dried.

Original and acetone filtrates were combined and concentrated by evaporation on a steam bath. The dope was treated with boiling water until solvents were removed. The warm plastic mass remaining was then stretched out into a thin skin by hand and extracted (leached) with cold water with only occasional slow agitation. The remaining water insoluble solids also comprise the emulsifiable fraction of PMVE. Water solubles may easily be recovered by heating the aqueous extraction liquors to 40–50°C., whereon the polymer coagulates.

### Catalyst Synthesis

**Synthesis I. Reaction of  $(C_2H_5)_3Al$  and HF or  $BF_3$ .** Triethylaluminum (10 ml.) which had been recently distilled was diluted into 150 ml. of Phillips pure grade hexane in a nitrogen-purged 500-ml. polyethylene bottle. This hexane has substantially less benzene and olefin content than regular commercial hexane. Even small amounts of aromatic components (Ar) in the alkane medium lead to yellow product believed due to a species  $ArH^+ AlF_4^-$ . The 500-ml. bottle was fitted with magnetic stirrer, external cooling apparatus, an inlet dip tube for HF introduction a nitrogen port, and an exit port leading to a simple bubble indicator. The

apparatus was constructed entirely of polyethylene except the glass exit bubble-indicator body.

Nitrogen and a slow stream of HF gas were introduced to the stirred mixture at about 0°C. until a dense cloud of smoke emitted from the exit bubbler (20–30 min.). The HF was turned off and the cooling bath replaced with a 40°C. water bath for 30 min. The system was then purged with N<sub>2</sub> at room temperature. The whitish solids were centrifuged, rinsed with fresh dry hexane, and stored under hexane. For the reaction of BF<sub>3</sub> with (C<sub>2</sub>H<sub>5</sub>)<sub>3</sub>Al a similar glass apparatus was used. BF<sub>3</sub> was introduced into a hexane solution by means of an 8-in. No. 17 hypodermic needle through an orifice capped by a soft rubber plug. The resulting slurry of white solids was heated to 50–60°C. Solids were separated, rinsed with hexane, and stored under hexane or methylene chloride until used.

**Synthesis II. Reaction of AlCl<sub>3</sub> with CH<sub>3</sub>CHF<sub>2</sub> in Methyl Chloride.** Methyl chloride, passed through drying towers of CaH<sub>2</sub> and molecular sieves, was condensed (50 ml.) onto about 5 g. of resublimed AlCl<sub>3</sub>. This mixture was magnetically stirred briefly and the supernatant methyl chloride poured off and discarded. Then another 325 ml. (liquid) of the methyl chloride was distilled (condensed) in. Stirring was conducted 15–30 min. to saturate this portion of methyl chloride with AlCl<sub>3</sub>. This saturated solution was decanted into another chilled N<sub>2</sub>-purged vessel. The dissolved AlCl<sub>3</sub> content is very close to 1.0% (w/v).

Another 25–30 ml. of methyl chloride was distilled and condensed into a 50-ml. flask followed by about 2 mole of ethylidene fluoride/mole of AlCl<sub>3</sub> dissolved above. This ethylidene fluoride–methyl chloride solution was then distilled into the magnetically stirred AlCl<sub>3</sub>/CH<sub>3</sub>Cl solution, above. A cherry-red gel dispersion develops in about 30 min. If ethylidene fluoride droplets are condensed directly into the CH<sub>3</sub>Cl/AlCl<sub>3</sub> solution dark brown balls of soft solids form which hasten flocculation of the gel dispersion. A severalfold excess of CH<sub>3</sub>CHF<sub>2</sub> does not appear to alter the chemical nature of the reaction. The gel dispersion may be employed as polymerization initiator as such. If filtered under nitrogen and dried *in vacuo*, brick-red solids result. They turn brilliant purple, then white, on exposure to the open atmosphere.

Ethyl chloride may be employed instead of methyl chloride. Although the solubility of AlCl<sub>3</sub> is greater (about 5%, w/v), as much as 5–8% of a resinous organic by-product also forms.

**Synthesis III. Reaction with Ethylaluminum Dichloride.** A 250-ml. centrifuge bottle modified with a 24/40 female joint was fitted with a male joint which had been closely joined to a 4-mm. T-type stop-cock. The straight portion of the T easily accepts an 8-in. No. 17 gauge hypodermic needle. The perpendicular arm of the T was connected to a nitrogen source. After baking and evacuating the apparatus, followed by release of the vacuum with nitrogen, 100 ml. of dry, alcohol-free methylene chloride was injected, and the solvent then cooled to 0 to –20°C. Alcohol was removed from CH<sub>2</sub>Cl<sub>2</sub> by water-washing or by molecular sieves. C<sub>2</sub>H<sub>5</sub>-

$\text{AlCl}_3$ , 1.0 ml. (10 mmole) was then injected using a warm syringe and needle ( $\text{C}_2\text{H}_5\text{AlCl}_2$  freezes at about  $30^\circ\text{C}$ .).

Anhydrous gaseous reactants were passed through 30-cm. columns of 5A molecular sieves and  $\text{CaH}_2$  and then introduced through a 17-gauge hypodermic needle of appropriate length while employing magnetic agitation. A 1-ml. syringe cut off along the barrel serves well as connector between gas tubing and needle.  $\text{BF}_3$  was introduced at a rapid bubble-by-bubble rate for about 1 min. until dense white fumes evolved from the reactor. The temperature was allowed to rise to ambient. After about 30 min., a colorless to straw-colored gel developed. An organic fluorinating agent (ethylene fluoride or dichlorodifluoromethane) was then introduced for a minute or so. The gel became brownish-red after times ranging from a few minutes to several hours. Heat evolution accompanied the color formation. Gel products were usually centrifuged, supernatant liquors decanted under nitrogen, the process repeated and the gel dried *in vacuo* ( $25^\circ\text{C}/0.5$  mm.) for several hours for analysis. As polymerization initiators, the slurries of gels in  $\text{CH}_2\text{Cl}_2$  were dispersed directly via syringe and needle.

### References

1. C. E. Schildknecht, A. O. Zoss, and F. Grosser, *Ind. Eng. Chem.*, **41**, 2891 (1949).
2. E. J. Vandenberg, in *First Biannual American Chemical Society Polymer Symposium*, (*J. Polymer Sci. C*, **1**), H. W. Starkweather, Jr., Ed., Interscience, New York, 1963, p. 207.
3. R. J. Kern, J. J. Hawkins, and J. D. Calfee, *Makromol. Chem.*, **66**, 126 (1963).
4. S. Okamura, S. Higashimura, and H. Yamamoto, *J. Polymer Sci.*, **33**, 510 (1958).
5. C. E. Schildknecht, *Vinyl and Related Polymers*, Wiley, New York, 1952, p. 602.
6. E. H. Mottus, these laboratories, unpublished results.
7. F. H. Winslow, C. J. Aloisio, W. L. Hawkins, W. Matreyek, and S. Matsuoka, *Chem. Ind. (London)*, **1963**, 1465.
8. W. T. Miller, E. W. Fager, and P. H. Griswall, *J. Am. Chem. Soc.*, **72**, 705 (1950).

### Résumé

Les réactions de HF,  $\text{BF}_3$ , et de certains dérivés organiques fluorés avec  $\text{AlCl}_3$ , le triéthylaluminium ou le chlorure d'éthylaluminium dans des hydrocarbures chlorés donnent lieu à la formation de gels qui manifestent un pouvoir initiateur de polymérisation très stéréorégulier à l'égard des éthers méthylvinyles. Des sites actifs sont attribués à des espèces du type  $\text{RAlF}_4$ . Des produits fortement stéréoréguliers ont ainsi pu être obtenus. Les différentes variables relatives à ces polymérisations ont été examinées. Ces systèmes montrent une grande variété d'apparences et de conséquences rhéologiques intéressantes. Celles-ci sont les conséquences des différences de solubilité des différentes fractions stéréorégulières. Les fractions les plus hautement stéréorégulières peuvent être utilisées à la fabrication de fibres, films ou d'objets moulés. Des fractions de stéréorégularités intermédiaires manifestent des propriétés émulsifiantes intéressantes. La stéréorégularité est ainsi montrée être apte à permettre un contrôle nouveau du degré d'absorption d'eau au sein de films.

### Zusammenfassung

Die Reaktion von HF,  $\text{BF}_3$  oder gewissen organischen Fluorverbindungen mit  $\text{AlCl}_3$ ,  $(\text{C}_2\text{H}_5)_3\text{Al}$  oder Äthylaluminiumchloriden in chlorierten Kohlenwasserstoffen liefert Gele, welche eine ausgeprägte Fähigkeit zur Initiierung der stereoregulären Polymerisa-

tion von Methylvinyläther zeigen. Es wird angenommen, dass die aktiven Stellen Spezies vom Typ  $\text{RAIF}_4$  enthalten. Polymere Produkte mit einem weiten Bereich an Stereoregularität werden erhalten. Mehrere Polymerisationsvariablen werden untersucht. Die Reaktionssysteme zeigen eine Vielfalt von Erscheinungen und interessante rheologische Sequenzen. Diese sind die Folgen des verschiedenen Löslichkeitsverhaltens der verschiedenen stereoregulären Fraktionen. Die Fraktionen mit der höchsten Stereoregularität können zu Fasern, Filmen oder geformten Gegenständen verarbeitet werden. Fraktionen mit mittlerer Stereoregularität zeigen interessante emulsionsbildende Eigenschaften. Die Stereoregularität liefert eine neuartige Kontrolle des Grades der Wasserabsorption in Filmen.

Received September 1, 1965

Revised November 17, 1965

Prod. No. 5008A



## A New Series of Organoboranes. VII. The Preparation of Poly-*m*-carboranylenesiloxanes\*

STELVIO PAPETTI, B. B. SCHAEFFER, A. P. GRAY, and T. L. HEYING, *Chemicals Division, Olin Research Center, New Haven, Connecticut*

### Synopsis

This paper describes the preparation of the first members of a new series of polysiloxanes characterized by having *m*-carborane nuclei in the backbone of the polymers. Although neither hydrolysis of 1,7-bis(chlorodialkylsilyl)-*m*-carborane monomers nor catalytic dehydration of the corresponding dihydroxy compounds would proceed to give the type of polysiloxanes desired, the polymers were readily prepared by the ferric chloride-catalyzed elimination of an alkyl halide from equimolar mixtures of dichloro- and dialkoxysilanes. This technique allowed the systematic introduction of dialkylsiloxy groups between *m*-carborane nuclei. Characterization of the polymers is described as well as differential scanning calorimetry studies which show the prime members of the series to be thermally stable to 500°C. and oxidatively stable to about 350°C.

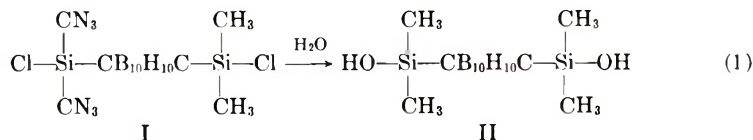
Papers IV<sup>1</sup> and V<sup>2</sup> of this series have described the propensity for bisilyl-*o*-carboranes† to enter into the formation of cyclic compounds containing either one *o*-carborane nucleus participating in a five-membered ring or two *o*-carborane nuclei in a six-membered ring. This extreme tendency can be explained in terms of the geometry of the *ortho* or 1,2 arrangement of the carbon atoms of the carborane nucleus which are ideally situated for participation in such exocyclic rings. (Assignments of the structures of the isomeric *ortho*, *meta*, and *para* carboranes have been presented in a number of articles.<sup>4-6</sup>) The analogy to the ready formation of phthalic anhydride from *o*-phthalic acid is obvious.

Since the formation of these cyclic molecules did not permit the formation of carboranylene-based polymers, we turned our attention to the isomeric derivatives of *m*-carborane which, because of the 1,7 orientation of carbon atoms, should have little tendency to participate in small rings and should allow the formation of linear polymers; here we draw analogy to isophthalic acid. The required derivatives were readily prepared, and although we established that indeed there was no tendency to form cyclic

\* Presented at the 150th Meeting, American Chemical Society, Atlantic City, New Jersey, September 17, 1965.

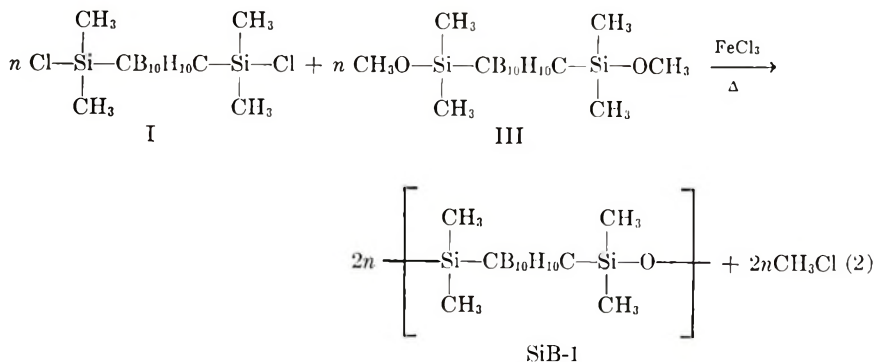
† Numbering and nomenclature of the dicarboclovododecaboranes (carboranes) are discussed by Adams<sup>3</sup>; subsequent structural analysis has established the use of *meta* to designate the 1,7 isomer.

derivatives, there was also little tendency to form polymers by generally reliable reactions.<sup>7</sup> For example, hydrolysis of 1,7-bis(chlorodimethylsilyl)-*m*-carborane (I) under a variety of conditions gave only 1,7-bis(hydroxydimethylsilyl)-*m*-carborane (II) in quantitative yield [eq. (1)]. This behavior has been ascribed to the influence of the extremely electro-



negative carborane nucleus.<sup>8</sup> Attempts to promote the polymerization of the bishydroxyl compound II were fruitless.

Since the oxygen atoms of II were so firmly bound to the silicon atoms we considered methods of preparing the desired polysiloxanes which would not require a disruption of this bond. The chlorine atoms of I are rather reactive, and we reasoned that the above criterion could be met in a copolymerization of I and bis(methoxydimethylsilyl)-*m*-carborane (III) in the presence of an appropriate catalyst with the evolution of methyl chloride.<sup>9</sup> according to eq. (2).



On bulk heating of equimolar quantities of I and III in the presence of a catalytic amount of ferric chloride at 140–165°C., approximately 60% of the theoretical quantity of methyl chloride was evolved, whereupon the mixture solidified. The temperature was gradually brought to 175–190°C., whereupon gas evolution resumed and was complete. The polysiloxane which we have designated SiB-1 is the first example of a polymer having a *m*-carboranylene unit in the backbone. More detailed study of this reaction has shown that the above conditions are essentially optimum for a high yield (nearly quantitative) of high molecular weight material. About 2 mole-% of ferric chloride is preferred and other similar catalysts which have been examined have not been as effective.

After it is freed from catalyst, SiB-1 is a white crystalline solid. Its structure is supported by elemental analysis, by the regular evolution of the required methyl chloride and by the correspondence of its infrared spectrum

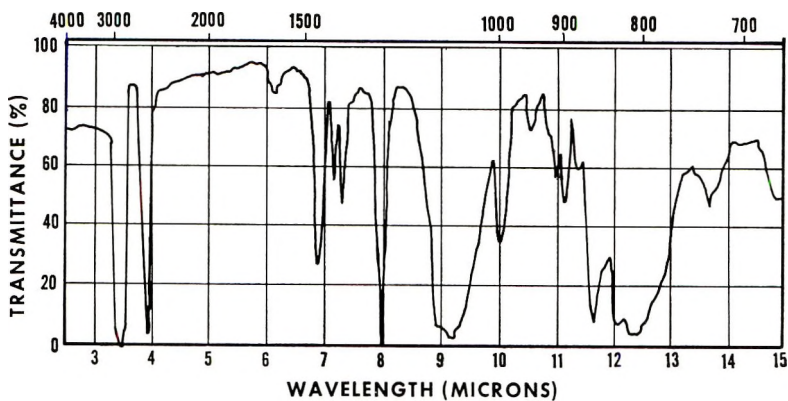


Fig. 1. Infrared spectrum of SiB-1, mineral oil mull.

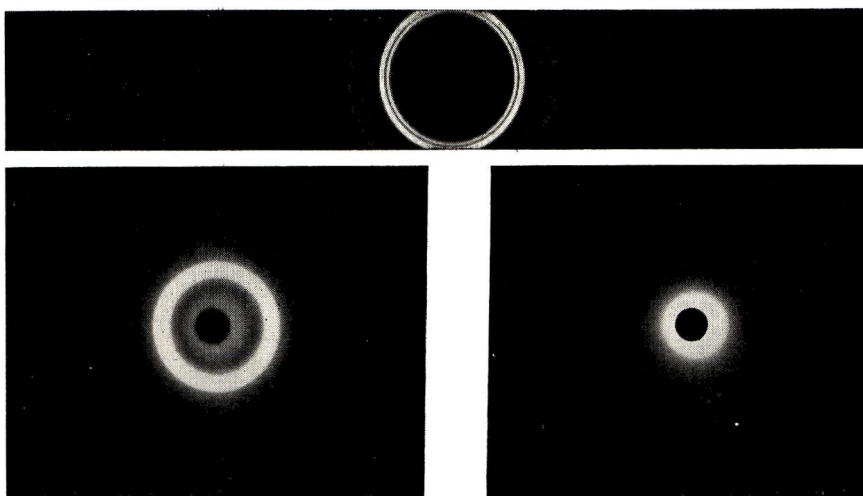
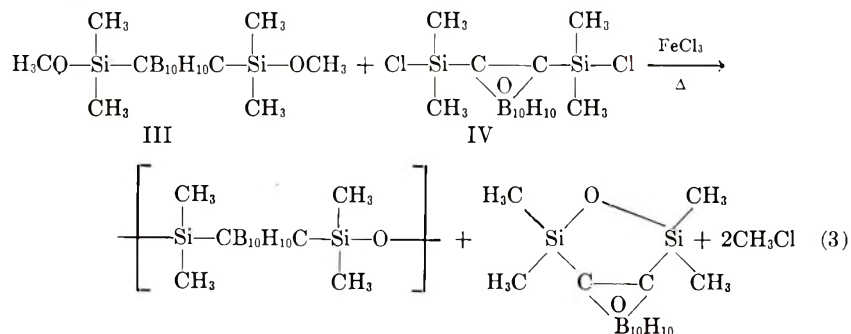


Fig. 2. X-ray diffraction patterns of (top) Sib-1; (left) Sib-2; (right) Sib-3.

(Fig. 1) to that expected. It is soluble in hot *N*-methyl-2-pyrrolidone, Decalin, chlorobenzene, *o*-dichlorobenzene, bromobenzene, and xylene. Molecular weights to 16,000 have been measured at 100 and 130°C. in *o*-dichlorobenzene by the differential vapor pressure technique (osmometer). Material above 16,000 is too poorly soluble for accurate molecular weight measurement. The molecular weights of some lower polymers has been corroborated by endgroup (chlorine) analysis. SiB-1 can be recrystallized on cooling a hot xylene solution, and no appreciable difference in molecular weight is found on such treatment. Its x-ray diffraction pattern (Fig. 2a) is typical of that of a crystalline organic polymer which is also apparent under a polarizing microscope. There is slight variation depending on molecular weight but a melting range of  $\sim 235\text{--}255^\circ\text{C}$ . is usually observed.

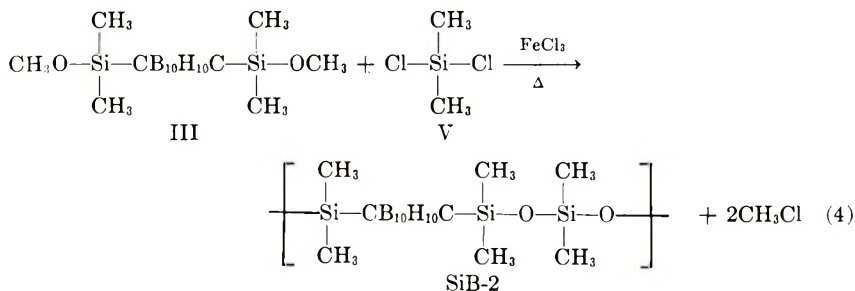
Now having the polymer at hand for comparison, we reinvestigated alternate routes of synthesis and did find that extremely low polymers (MW 1000–2000) could be formed in low yield on prolonged heating of the bis-hydroxy compound (II) in Decalin (with or without catalyst) or by heating the bischloro compound (I) in acetonitrile with mercuric oxide (HgO); no polymerization occurred on reacting I and II in the presence of a hydrogen chloride acceptor.

Consideration of the success of this polymerization scheme prompted us to attempt to prepare an analogous alternating *ortho-meta* carborane polymer by reacting III with bis(chlorodimethylsilyl)-*o*-carborane (IV). Instead of obtaining such a polymer, the reaction in eq. (3) occurred quantitatively.



The course of this reaction is open to several interpretations which we will not elaborate upon here.

This ferric chloride-catalyzed polymerization scheme lends itself to the systematic introduction of dimethylsiloxyl groups between the *m*-carborane nuclei. We therefore adapted this procedure to prepare the next polymer of the series having a second —Si—O— unit in the repeating unit by using dichlorodimethylsilane (V) in place of the bischloro compound I, as shown in eq. (4). The reaction proceeded as desired; we suspected that the

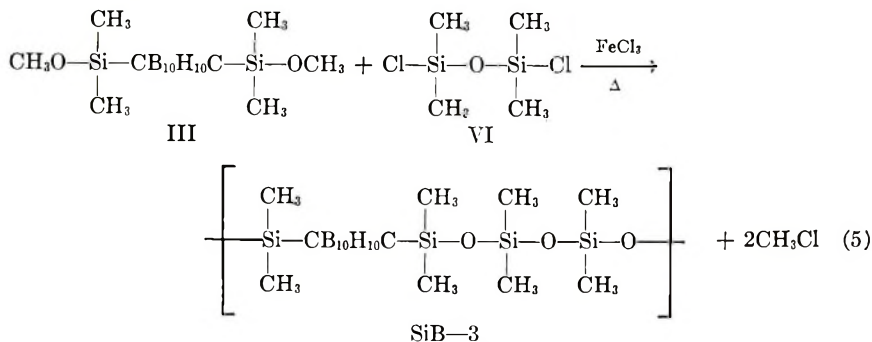


presence of the additional —Si—O— unit would tend to provide a polymer lower melting than SiB-1, but instead SiB-2 is highly elastomeric.

The structure of SiB-2 has been confirmed in the manner of SiB-1. Examination of its x-ray diffraction pattern (Fig. 2b) and under a polarizing microscope shows some crystallinity. Polymers below a molecular weight of 10,000 will dissolve in the solvents listed for SiB-1; above 10,000 there

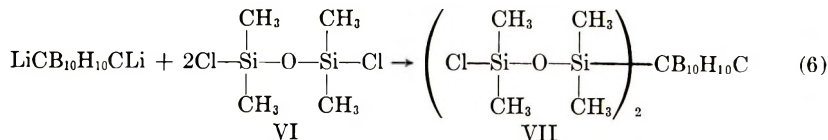
is little if any solubility in these solvents, but some solubility in hexamethyl phosphoramide. Catalyst can be removed by treatment with acetone or acetone-water in a blender; the elastomer is readily milled to a white crepe which will accept a variety of fillers and can be cured.\*

The next member of this homologous series of polymers was achieved in a similar manner from the dichlorosiloxane VI according to eq. (5).

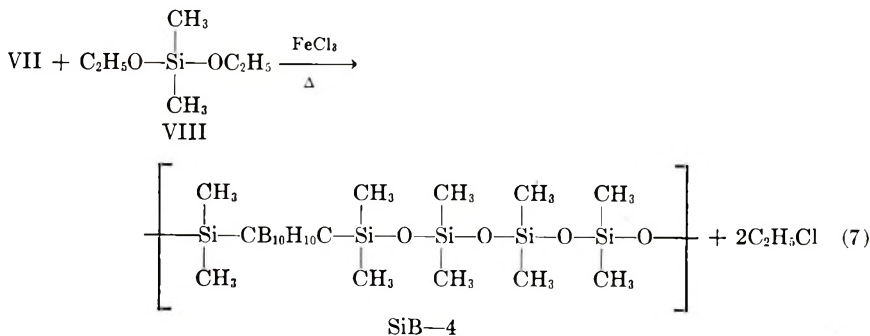


SiB-3 is very similar to SiB-2; its x-ray pattern shows no crystallinity (Fig. 2c), and this is reflected in the fact that formulation studies have shown it to be a more "snappy" rubber remaining flexible at lower temperatures.

It was necessary to approach the next homolog, SiB-4, in a slightly different manner. We first prepared the dichloro monomer VII by the reaction of dilithio-*m*-carborane with dichlorotetramethyldisiloxane (VI) in the standard manner<sup>7</sup> [eq. (6)]. SiB-4 was then prepared by copolymerizing VII with diethoxydimethylsilane (VIII) in the established man-



ner according to eq. (7). This polymer is more rubbery than SiB-3 at low

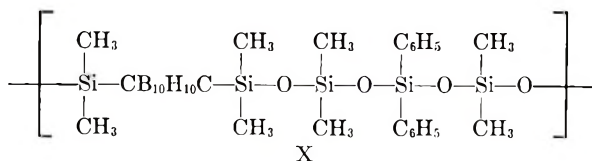
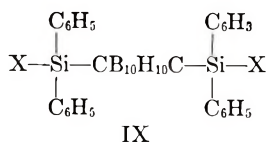


temperature, but is otherwise quite similar.

\* A detailed treatment of the practical development of these elastomers will be presented elsewhere.



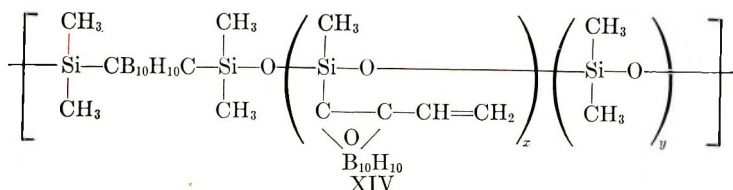
The foregoing discussion has described the preparation of the SiB-1 through SiB-4, in which all appendages to the silicon atoms are methyl groups. The system, however, has allowed a study of the effect that a wide variation of substituents could have on chemical and physical properties as well as to provide desired sites for curing in applications studies. Only a few of the more interesting derivatives will be mentioned here. First it will suffice to say that other alkyl or phenyl groups were readily substituted for the methyl groups of the various polymers by using the appropriate corresponding monomers. In general these products were of no particular additional interest, except that the precept developed that monomers having phenyl substituents on the silicon atoms attached to the *m*-carborane carbon atoms (IX)<sup>7</sup> would not enter into such polymerizations. The introduction of phenyl groups generally lessened the rubbery



characteristics of the polymers, but, as expected, improved oxidation resistance at elevated temperatures. The SiB-4 type polymer X deserves special mention in this regard, since this polymer is still quite elastic and is notably more oxidation-resistant.

Although the polymers already described could be cured by free-radical hydrogen abstraction and subsequent coupling of the methylene fragments, it was found that this process was markedly aided by substituting vinyl groups for some of the pendant methyl groups. This was readily achieved by substituting dichloromethylvinylsilane (XI) for a portion of the non-*m*-carboranyl monomer, usually dichlorodimethylsilane (V). Replacement of about 0.2–8 mole-% of V for this purpose was quite effective.

We were similarly able to replace some of the methyl groups by *o*-carboranyl by preparing and appropriately using the new monomers dichloro(1-methylcarboran-2-yl)methylsilane (XII) and dichloro(1-methylcarboranyl-2-yl)phenylsilane (XIII). Success in these attempts allowed us to progress to the preparation of variations on the polymer type shown as XIV by utilizing the newly synthesized monomer dichloro(1-vinylcarboran-2-yl)-methylsilane (XV).



From previous work in these<sup>2</sup> and other laboratories it was known that the various carborane nuclei were quite stable at elevated temperatures and that, ostensibly due to the fact that these units have many resonant forms which can act as energy sinks, they will impart such stability to nearby units to a greater or lesser degree. It was considered, therefore, that any polymer obtained in this work regardless of its physical nature, would maintain its chemical and physical integrity at elevated temperatures. To establish whether this was the case, samples of the various polymers were heated out of contact with air for various periods at 400°C.; with the exception of melting of SiB-1, no gross changes were observed.

To study their thermal and oxidative behavior more exactly, the polymers were subjected to differential calorimetry studies both in air and under nitrogen. SiB-1, SiB-2, and SiB-3 of the structural formulae shown above were found to be stable up to 500°C. in an inert atmosphere. In air, however, only the first, which contains one Si(CH<sub>3</sub>)<sub>2</sub> group attached directly to the carbon atoms of the *m*-carborane nucleus, remained inert. The other two, containing three and four Si(CH<sub>3</sub>)<sub>2</sub> groups per repeat unit reacted in a two-stage fashion, as shown, with exothermic heats of 180 and 396 kcal./repeat unit, respectively. The fact that the ratio of reaction heats is approximately 1:2 and not 3:4 indicates that it is only the Si-(CH<sub>3</sub>)<sub>2</sub> groups bonded to oxygen which are unstable, since it is only these groups that are present in this ratio. This conclusion is supported by the magnitude of the heat effect, which is consistent with that calculated from the known mechanism of decomposition for such groups, and by the magnitude of the weight loss, which indicated a crosslinking of adjacent polymer chains through a —Si—O—Si— bond replacing the original structure —Si—CH<sub>3</sub> CH<sub>3</sub>—Si—.

The analysis of SiB-4 gave results which were not in accord with the above explanation, but the validity of the determination was clouded by the physical behavior nature of the heated polymer which did not allow sufficient contact with the atmosphere (see Experimental). Analysis of the phenyl-modified SiB-4 (X) which physically behaved more like SiB-2 and SiB-3 on heating, gave results in agreement with the above hypothesis. It should also be noted that the substitution of the two phenyl groups (X) for two methyl groups of SiB-4 raised the temperature of incipient oxidative degradation from 325 to 370°C.

Additional work on the scientific and practical aspects of these polymers is in progress and will be reported subsequently.

## EXPERIMENTAL

## Monomers

Monomers other than carboranes were obtained from commercial sources and were thoroughly purified before use. Preparation of all carborane-containing monomers specifically mentioned in this paper are given, even though some are not shown in specific polymerization examples below. All analyses were by the Olin Microanalytical Section.

**1,7-Bis(chlorodimethylsilyl)-*m*-carborane(I).** Preparation was in accord with that described by Papetti and Heying.<sup>7</sup> Alternatively, 1,2-Bis(chlorodimethylsilyl)-*o*-carborane<sup>1</sup> is gradually heated under nitrogen to its reflux temperature and allowed to remain at this temperature overnight. The pressure is reduced and I distills at 108–110°C./0.1 mm. The only losses are mechanical.

**1,7-Bis(methoxydimethylsilyl)-*m*-carborane (III).** Preparation was in accord with that described by Papetti and Heying.<sup>7</sup>

**Compound VII.** Dilithio-*m*-carborane was prepared from 48.59 g. (0.334 mole) *m*-carborane in the standard manner<sup>7</sup> and dissolved in 300 ml. of dry ether. Under nitrogen it was slowly added to an ice-cooled solution of 150.54 g. (0.74 mole) dichlorotetramethyldisiloxane (VI) in 400 ml. of ether. The mixture was stirred and allowed to come to and remain at room temperature for 2.5 hr.; after filtering, the filtrate was concentrated and the remaining liquid was distilled at 128–128.5°C./0.08 mm. to give 65% of compound VII.

ANAL.: Calc'd. for  $C_{10}H_{34}B_{10}O_2Si_4Cl_2$ : C, 25.14%; H, 7.17%; B, 22.64%; Si, 23.51%; Cl, 14.84%; Found: C, 25.03%; H, 7.11%; B, 23.01%; Si, 23.72%; Cl 15.10%.

**Dichloro(1-methyl-*o*-carboran-2-yl)methylsilane (XII).** A solution of 1-lithio-2-methyl-*o*-carborane<sup>10</sup> was prepared from 1-methyl-*o*-carborane (55.27 g.; 0.35 mole) in 100 ml. ether and 0.35 mole of *n*-butyllithium in hexane. This was added to a cooled solution of methyl trichlorosilane (57.37 g., 0.38 mole) in 200 ml. of ether. After the addition was complete, the mixture was stirred at room temperature for 2 hr. and filtered; the filtrate was concentrated, and the residue was distilled under reduced pressure to give 62% of XII which solidified on standing (m.p. 35.5–37.5°C.).

ANAL. Calc'd. for  $C_4H_{16}B_{10}Cl_2Si$ : C, 17.70%; H, 5.94%; B, 39.88%; Cl, 26.13%; Si, 10.35%. Found: C, 17.6%; H, 6.00%; B, 39.38%; Cl, 25.80%; Si, 9.87%.

**Dichloro(1-methyl-*o*-carboran-2-yl)phenylsilane (XIII).** This was prepared in a manner identical with that for XII above from 79.1 g. of 1-methyl-*o*-carborane and 116.3 g. of phenyl trichlorosilane. The product XIII was obtained by distillation (b.p. 155.7°C./0.06 mm.) in 74% yield and solidified on standing (m.p. 53–54.5°C.).

ANAL.: Calc'd for  $C_9H_{18}B_{10}Cl_2Si$ : Calc'd.: C, 32.42%; H, 5.44%; B, 32.45%; Cl, 21.27%; Si, 8.42%; Found: C, 32.90%; H, 5.44%; B, 32.22%; Cl, 21.35%; Si, 8.29%.

**Dichloro(1-vinyl-*o*-carboran-2-yl)methylsilane (XV).** 1-Vinyl-*o*-carborane<sup>11</sup> (42.62 g.; 0.25 mole) in 300 ml. of ether was converted to its lithium derivative by addition of 0.25 mole *n*-butyllithium in hexane. As in the preparation XII above, it was added to 0.30 mole methyl trichlorosilane in 450 ml. ether. After the usual isolation, 57% pure XV was obtained by distillation under reduced pressure; XV solidified on standing (m.p. 40–42°C.).

ANAL. Calc'd. for  $C_6H_{16}B_{10}Cl_2Si$ : C, 21.19%; H, 5.69%; B, 38.18%; Cl, 25.03%; Si, 9.91%. Found: C, 21.02%; H, 5.61%; B, 38.30%; Cl, 25.15%; Si, 9.62%.

### Polymers

**Preparation of the Polysiloxane SiB-1.** In a typical experiment, 1,7-bis-(methoxydimethylsilyl)-*m*-carborane (III) (21.16 g., 0.066 mole), 1,7-bis-(chlorodimethylsilyl)-*m*-carborane (I) (21.77 g., 0.066 mole), and 2 mole-% of anhydrous ferric chloride (based on the total number of moles of the two neocarborane starting materials added) were mixed in a 150-ml. single-necked flask which was equipped with a stirring bar and a nitrogen inlet line for flushing the apparatus. The reaction flask was also connected to a vacuum line having a bubble-off and an outlet for sampling volatile products. A wet-test meter was connected to the bubble-off to measure methyl chloride evolution.

The flask was placed on an oil bath and heat was applied. Gas evolution began at 175°C., and the reaction was completed after 30 min., at which time the temperature was 225°C. The crude polymeric product was a solid material which was recrystallized from xylene and dried under vacuum at 150°C. for 90 min. A total of 34.8 g. of the purified polymer product was recovered (96.5% of the theoretical amount). The molecular weight was determined and found to be 16,500 by the osmometric method; this sample was observed to melt over the range 233–240°C.

ANAL. Calc'd. for:  $C_6H_{22}B_{10}OSi_2$ : C, 26.24%; H, 8.07%; B, 39.40%; Si, 20.46%. Found: C, 25.51%; H, 7.71%; B, 38.92%; Si, 20.40%.

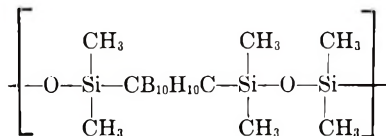
**Preparation of the Polysiloxane SiB-2.** In a typical experiment, 1,7-bis-(methoxydimethylsilyl)-*m*-carborane (47.35 g., 0.1476 mole), dichlorodimethylsilane (19.0468 g., 0.1476 mole), and 1 mole-% of anhydrous ferric chloride (based on the number of moles of the *m*-carborane starting material added) were mixed in a 300-ml. single-necked flask which was attached to the apparatus described for the preparation of SiB-1.

The flask was placed on an oil bath and heated at a temperature between 100 and 120°C. Although the reaction was vigorous at first, after about 30 min. the reaction ceased. A second portion of ferric chloride catalyst was added (about 1 mole-% based on the weight of the *m*-carborane starting material), and the reaction mixture was heated at a temperature of 180–



185°C. until the reaction had gone to completion, as evidenced by the total amount of methyl chloride evolved. The resulting product was a rubbery material which was not soluble in the common organic solvents. Elimination of ferric chloride from the product was achieved by thoroughly washing the milled gum first with acetone, then with 10% water solution in acetone, and finally again with acetone. With this technique, the iron content of the thus treated rubbery product was reduced to about 0.01% by weight. The yield of polymeric product was essentially quantitative.

The infrared spectrum was in accord with that expected for a product having recurring units of the formula:

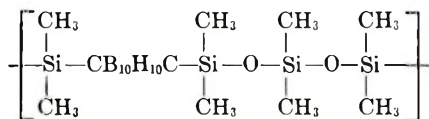


ANAL. Calc'd. for:  $\text{C}_8\text{H}_{28}\text{B}_{10}\text{O}_2\text{Si}_3$ : H, 8.09%; B, 31.02%; Si, 24.16%; Found: H, 7.76%; B, 31.59%; Si, 24.59%.

**Preparation of the Polysiloxane, SiB-3.** In a typical experiment, 1,7-bis-(methoxydimethylsilyl)neocarborane (22.638 g., 0.07059 mole), which had been purified by recrystallization and tetramethyldichlorodisiloxane (14.346 g., 0.07059 mole) which had been purified by redistillation, and 2 mole-% of anhydrous ferric chloride, (based on the number of moles of the *m*-carborane compound utilized) were reacted in the same manner as described in Example I. After 2.70 liter of gaseous methyl chloride had been evolved, a semisolid polymeric product formed. After holding this product at 180°C. for 2 hr. there was obtained a polymeric gum, very similar to SiB-2 which was not soluble in common organic solvents. SiB-3 was recovered in 85.5% yield (after removal of catalyst as above) based on the weight of the *m*-carborane starting material.

ANAL. Calc'd. for:  $\text{C}_{10}\text{H}_{34}\text{B}_{10}\text{O}_3\text{Si}_4$ : C, 28.40%; H, 8.10%; B, 25.58%; Si, 26.57%; Found: C, 28.25%; H, 8.13%; B, 26.16%; Si, 25.88%.

Based on this elemental analysis and on an infrared analysis it was determined that the product consisted essentially of recurring units of the formula:



The polymeric gum softened somewhat when heated to a temperature above 260°C., but even at 350°C. it remained a rubbery material.

**Preparation of the Polysiloxane, SiB-4.** Compound VII (29.58 g., 0.062 mole), diethoxydimethylsilane (9.18 g., 0.062 mole), and 2 mole-% of anhydrous ferric chloride (based on the total number of moles of the *m*-carborane compound employed) were placed in a 300-ml. single-necked flask



equipped as above. There was a considerable amount of ethyl chloride evolution when the oil bath was at a temperature of 100–150°C. When this first gas evolution ceased, the product was a dark viscous liquid.

An additional 1 mole-% of anhydrous ferric chloride was added to this liquid, which was then heated at 180°C. After 35 min. the product had become rubbery. After the usual washings the polymer was quite similar to SiB-3 in appearance and behavior.

ANAL. Calc'd. for  $C_{12}H_{40}B_{10}O_4Si_5$ : C, 29.00%; Y, 8.11%; B, 21.77%; Si, 28.25%. Found: C, 28.61%; H, 8.18%; B, 21.13%; Si, 29.14%.

#### Preparation of a Representative Vinyl-Modified SiB-2 Polysiloxane.

Bis(methoxydimethylsilyl)-*m*-carborane (16.10 g., 0.05 mole), dichlorodimethylsilane (6.15 g., 0.0477 mole), methylvinylchlorosilane (0.35 g., 0.0025 mole), and 2 mole-% of anhydrous ferric chloride which was added in two equal increments (based on the total number of moles of *m*-carborane compound) were reacted in the same manner as in the preparation of SiB-2.

The product, a rubbery material which exhibited a slight tackiness, was washed first with acetone and then with acetone and water to eliminate the catalyst. The yield of the elastomer was essentially quantitative. The infrared spectrum clearly showed the presence of the pendant vinyl groups; their presence is also clearly indicated in curing studies now in progress.

**Preparation of a Phenyl-Modified SiB-4 Polysiloxane.** According to the previous SiB-4 procedure, compound VII (16.35 g., 0.034 mole), diphenyl dimethoxysilane (8.35 g., 0.034 mole), and 1 mole-% of anhydrous ferric chloride (based on the total number of moles of the *m*-carborane compound) were placed in a 100-ml. single-necked flask equipped as usual. The flask was placed in oil bath and heated to 140°C., where a rapid gas evolution occurred. After the gas evolution subsided considerably, another 1 mole-% of anhydrous ferric chloride was added and the mixture was heated to 180°C. On cooling, the product was a viscous liquid which was dissolved in ethyl ether; it was treated with water and the ether layer taken to dryness. The residue was a light brown, transparent, viscous liquid. The molecular weight was determined by the differential vapor pressure technique at 100°C. in chlorobenzene and was found to be of 3398.

This product placed under vacuum above 200°C. for a short time and then at atmospheric pressure at 250°C. to give the elastomeric material very similar to SiB-4.

ANAL. Calc'd. for:  $C_{22}H_{44}B_{10}O_4Si_5$ : C, 42.54%; H, 7.14%; B, 17.40%; Si, 22.61%. Found: C, 41.58%; H, 7.47%; B, 17.54%; Si, 22.90%.

#### Differential Calorimetry Investigation

All determinations were conducted with a Perkin-Elmer differential scanning calorimeter (Model DSC-1) operating at a linear heating rate of 18°C./min. The upper temperature limit is 500°C. It should be kept in mind that transitions and reactions which occur slowly may actually occur at somewhat lower temperatures when investigated under isothermal

conditions. No attempt was made to refine the numbers obtained for  $\Delta H$  by repetition of the experiments, choice of optimum sample size, etc., but the results are felt to be precise within  $\pm 10\%$ , which is usually adequate for a preliminary investigation.

**SiB-1.** This material melts in air in a manner characteristic of polymers, beginning at  $\sim 208^\circ\text{C}$ ., rising slowly to a maximum at  $248^\circ\text{C}$ ., and dropping to zero at  $253^\circ\text{C}$ . under the conditions of the experiment. The heat of fusion was approximately 13 cal./g. (endothermic), which is normal. Originally, the sample was taken to  $450^\circ\text{C}$ . only. It was found that up to this temperature, the samples recrystallized on cooling and could be remelted and recrystallized indefinitely. On heating from 450 to  $500^\circ\text{C}$ ., a complex thermal transition occurs which is mainly endothermic, but is usually accompanied by a small, but sharp, exothermic deflection of the pen near the beginning of the change. No strong maximum occurs, the transition having the appearance of a step in the heat capacity curve rather like a second-order transition in solid polymers. On cooling, the material no longer crystallizes, and it has a glassy character. Examination of the infrared spectra before and after the change indicates that the change affects principally the silicon-containing portion of the molecule. No attempt was made to analyze the spectra in detail, although this may be of interest. The weight loss of the sample was about 1%. In nitrogen, no change other than melting occurred to  $500^\circ\text{C}$ .

**SiB-2.** On heating in air, this material undergoes a large exothermic reaction, commencing abruptly at  $335^\circ\text{C}$ . The rate of the reaction reaches a maximum at  $350^\circ\text{C}$ ., drops to a lesser rate of about 2/3 the maximum at  $380^\circ\text{C}$ ., and then reaches a second maximum at  $408^\circ\text{C}$ . The existence of this double peak with intermediate minimum in the rate was confirmed on three separate samples. The reaction is terminated near  $435^\circ\text{C}$ . The heat of the reaction was 195 kcal./repeat unit. The product was greyish white as compared to the original brown elastomer and appeared to retain some elastomeric character, although it could be shredded between the fingers. When a sample was run under nitrogen, no transition occurred up to  $500^\circ\text{C}$ . The weight loss under nitrogen was zero. The same sample was rerun in air, and the exothermic reaction occurred, with a weight loss of  $3.2 \pm 0.5\%$ .

**SiB-3.** In air, this sample behaved much like SiB-2. The exothermic reaction again began abruptly at  $335^\circ\text{C}$ . but rose to a steady maximum rate, which persisted to  $420^\circ\text{C}$ . The rate diminished to zero at  $450^\circ\text{C}$ . The heat of this reaction was 430 kcal./repeat unit. The measured weight loss was about 5%.

Upon completion of the runs, a small amount of greasy material was found to have been deposited on the interior of the cover over the sample holder assembly. The infrared spectrum of this indicated that it was a member of the polymer family under investigation and evidently represented a volatile portion of one of the samples. Again, no attempt was made to determine the origin or specific nature of this substance.

**SiB-4.** The sample was studied in air under the same conditions. The exothermic decomposition initiated at 325°C. rose to a maximum rate at 340°C., moderated somewhat between 350 and 380°C., rising to a second small maximum at 390°C. after which the rate rose to a strong, sharp maximum at 422°C. and dropped thereafter to a negligible rate. The total exothermic heat was 77.1 cal./g. or 38.2 kcal./repeat unit. This is a low value compared to the previous samples, where it was assumed that roughly 180 kcal./repeat unit corresponded to dissociative reaction of one  $\text{Si}(\text{CH}_3)_2$  group per repeat unit (see Discussion). On this assumption, the heat found corresponds to a low percentage of such groups reacting per repeat unit. However, other factors may be controlling in this case, which remain to be investigated; for example, with the sample being a dense, viscous mass, it may be that only the surface of the sample is sufficiently exposed to the atmosphere to permit complete oxidative reaction and the remainder of the material may degrade by a different route or remain unreacted. Further experiments can be designed to check out such a possibility. After heating to 500°C. in air, the material had not changed greatly in appearance, although it appeared to be less viscous.

**Phenyl-Modified SiB-4.** The thermal oxidative decomposition of this sample did not begin until 370°C. and did not reach a substantial rate until 395°C. The decomposition continued up to and presumably beyond 500°C., although the shape of the curve indicates the reaction is nearing completion at this instrumental upper limit. The area corresponds to a heat of 170 kcal./repeat unit, which, on the basis of the previous postulate, would correspond to the reaction of two  $\text{Si}-\text{CH}_3$  per repeat unit. The product, after heating in air, was yellow and brittle.

This work was supported by the Office of Naval Research.

### References

1. S. Papetti and T. L. Heying, *Inorg. Chem.*, **2**, 1105 (1963).
2. S. Papetti, B. B. Schaeffer, H. J. Troscianiec, and T. L. Heying, *Inorg. Chem.*, **3**, 1444 (1964).
3. R. Adams, *Inorg. Chem.*, **2**, 1087 (1963).
4. H. Schroeder and G. D. Vicker, *Inorg. Chem.*, **2**, 1317 (1963).
5. S. Papetti and T. L. Heying, *J. Am. Chem. Soc.*, **86**, 2295 (1964).
6. J. A. Potenza and W. N. Lipscomb, *Inorg. Chem.*, **3**, 1673 (1964).
7. S. Papetti and T. L. Heying, *Inorg. Chem.*, **3**, 1448 (1964).
8. M. F. Hawthorne, T. E. Berry, and P. A. Wegner, *J. Am. Chem. Soc.*, **87**, 4746 (1965).
9. P. C. Servais, U.S. Pat. 2,485,928 (1949).
10. T. L. Heying, J. W. Ager, S. L. Clark, R. P. Alexander, S. Papetti, J. A. Reid, and S. I. Trotz, *Inorg. Chem.*, **2**, 1097 (1963).
11. T. L. Heying, J. W. Ager, S. L. Clark, D. J. Mangold, H. L. Goldstein, M. Hillman, R. J. Polak, and J. W. Szymanski, *Inorg. Chem.*, 1089 (1963).

### Résumé

Cet article décrit la préparation des premiers membres d'une nouvelle série de polysiloxanes caractérisée par la présence de nouaux *m*-carboranes dans la chaîne principale

des polymères. Bien que ni l'hydrolyse de 1,7-bis-chloro-dialkylsilyl-*m*-carborane monomère, ni la déshydratation catalytique des composés dihydroxylés correspondants ne puissent fournir le type de polysiloxane désiré, les polymères ont été facilement préparés par l'élimination d'halogénures d'alcyle, catalysé par du chlorure ferrique au départ de mélanges équimoléculaires de silanes dichlorés et dialkoxylés. Cette technique permettait l'introduction systématique de groupes dialkyles siloxylés entre les noyaux *m*-carborane. La caractérisation des polymères est décrite de même que la colorimétrie différentielle; celle-ci montre que le premier membre de la série est stable thermiquement jusqu'à 500°C et stable à l'oxydation jusque environ 350°C.

### Zusammenfassung

In der vorliegenden Mitteilung wird die Darstellung der ersten Glieder einer neuen Reihe von Polysiloxanen beschrieben, welche durch *m*-Carborankerne in der Hauptkette des Polymeren charakterisiert sind. Weder die Hydrolyse von 1,7-Bis(chlordialkylsilyl)-*m*-carboranmonomeren noch die katalytische Dehydratation, der entsprechenden Hydroxyverbindungen verlief unter Bildung des gewünschten Polysiloxantyps. Die Polymeren konnten jedoch leicht durch die Ferrichlorid-katalysierte Eliminierung von Alkylhalogenid aus äquimolaren Mischungen von Dichlor- und Dialkoxysilanen dargestellt werden. Diese Verfahren erlaubte die systematische Einführung von Dialkylsiloxygruppen zwischen die *m*-Carborankerne. Die Charakterisierung der Polymeren wird beschrieben, sowie eine differential-kalorimetrische Untersuchung, welche zeigte, dass die ersten Glieder der Reihe bis zu 500°C thermisch stabil und bis etwa 350°C oxydativ stabil sind.

Received November 8, 1965

Revised November 24, 1965

Prod. No. 5013A

## NOTES

*Reaction of Dichlorocarbene with cis-1,4-Polyisoprene\**

The reaction of carbenes with olefins to form cyclopropane derivatives has attracted intensive interest during the past few years.<sup>1</sup> In the field of polymers, we have previously suggested<sup>2</sup> modification of the properties of unsaturated rubbers by reaction with carbenes. More recently, the addition of halocarbenes to *cis*-1,4-polyisoprene and *cis*-1,4-polybutadiene has been reported<sup>3</sup> by Pinazzi and Levesque. In this communication, we wish to present data on some physical properties of the reaction product of dichlorocarbene with *cis*-1,4-polyisoprene. Natsyn,† a *cis*-1,4-polyisoprene rubber with an inherent viscosity of 3.6 dl./g. (0.1% solution in benzene), was extracted with acetone to remove antioxidants and any low molecular weight extractable material. A solution containing 13.6 g. of the dried rubber (0.2 mole) in about 600 ml. of dry heptane was mixed with 25 g. of chloroform (0.209 mole) in a 1-liter flask. The solution was agitated and under a nitrogen atmosphere 24 g. of potassium *tert*-butoxide (0.214 mole) was added

TABLE I  
A Comparison of the Low Temperature Properties<sup>4</sup> of *cis*-1,4-Polyisoprene  
and a *cis*-1,4-Polyisoprene-Dichlorocarbene Adduct

	Relative modulus values	<i>cis</i> -1,4-Polyisoprene	<i>cis</i> -1,4- Polyisoprene- dichlorocarbene adduct
T <sub>2</sub> <sup>a</sup>	2	+1°C	+5°C.
T <sub>5</sub>	5	-53	-30.5
T <sub>10</sub>	10	-57	-41
T <sub>100</sub>	100	-61	-52

<sup>a</sup> T<sub>2</sub>, T<sub>5</sub>, T<sub>10</sub>, T<sub>100</sub> are temperatures in °C. at which the relative modulus values are 2, 5, 10, and 100, respectively.

in small portions. The reaction temperature was maintained at 5°C. After 45 min., the reaction mixture was allowed to warm up to room temperature. After 3 days, the reaction product was precipitated in isopropyl alcohol, washed repeatedly with water, and finally was suspended in a 1:1 (by volume) isopropyl alcohol-water mixture for 3 days. This product, hereafter designated as adduct A, was dried under 2 Torr to constant weight. It had an inherent viscosity of 3.4 dl./g. and contained 15.55% chlorine. The chlorine analysis indicates that about 18% of the double bonds had been reacted with dichlorocarbene to form, presumably, dichlorocyclopropane ring structures.

\* Contribution No. 341 from the Research Laboratories, The Goodyear Tire & Rubber Co., Akron, Ohio.

† Registered trademark of the Goodyear Tire & Rubber Co.



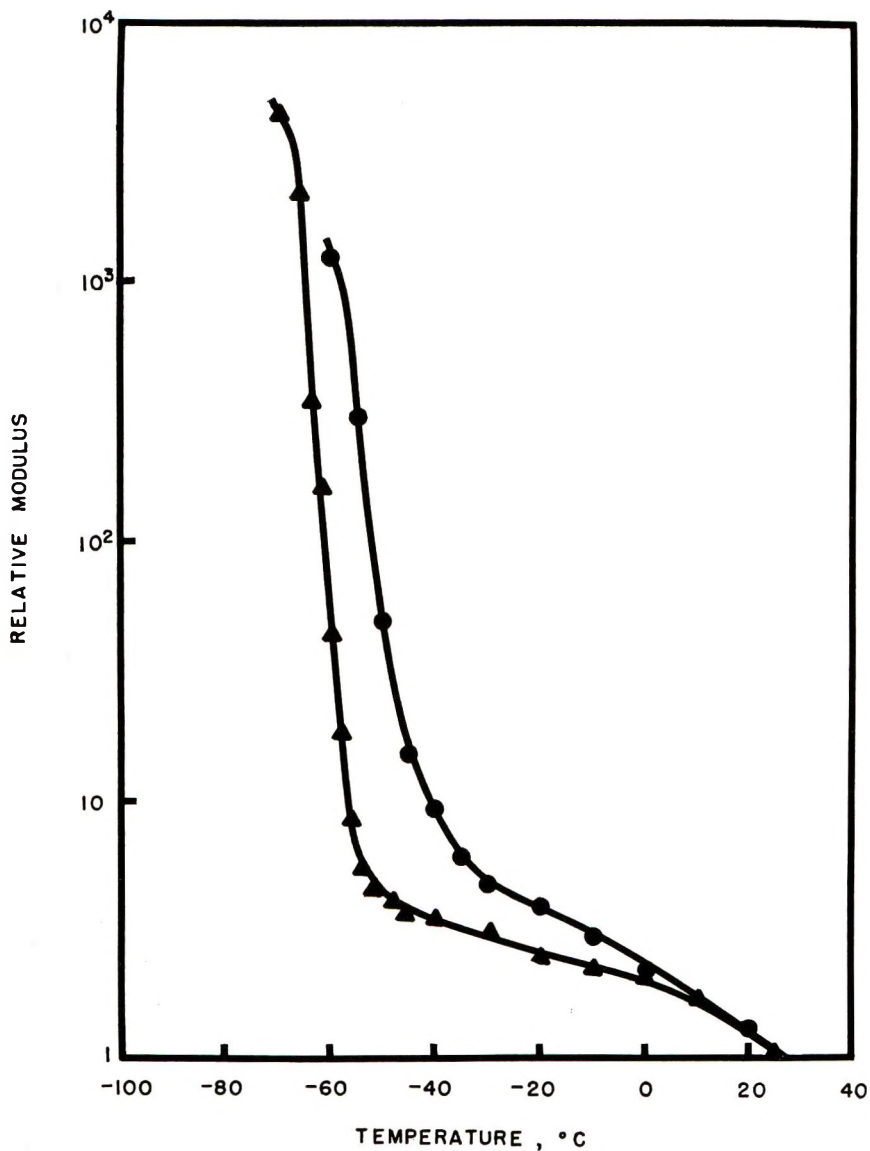
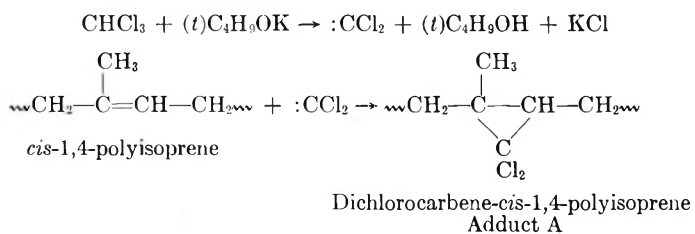


Fig. 1. Relative modulus of *cis*-1,4-polyisoprene (▲) and dichlorocarbene-*cis*-1,4-polyisoprene adduct A containing 15.6% chlorine (●) as a function of temperature.

TABLE II  
 A Comparison of Physical Properties of Gum Vulcanizates<sup>a</sup> of *cis*-1,4-Polyisoprene and a *cis*-1,4-Polyisoprene-Dichlorocarbene Adduct B

Compound	Cure time, min.	Tensile strength, psi	Elongation at break, %	300% modulus, psi	Shore A hardness	Swelling ratio <sup>b</sup>	Solubility, <sup>c</sup> %
<i>cis</i> -1,4-Polyisoprene	10	3695	865	200	42	4.60	5.0
<i>cis</i> -1,4-Polyisoprene-dichlorocarbene adduct B	20	3430	705	345	45	3.57	3.9
	10	1945	707	396	47	4.45	3.4
	20	1600	637	418	47	4.32	3.3

<sup>a</sup> Cure temperature: 127°C.

<sup>b</sup> Grams of benzene solvent per gram of the vulcanizate at 25°C.

<sup>c</sup> Benzene, 25°C.

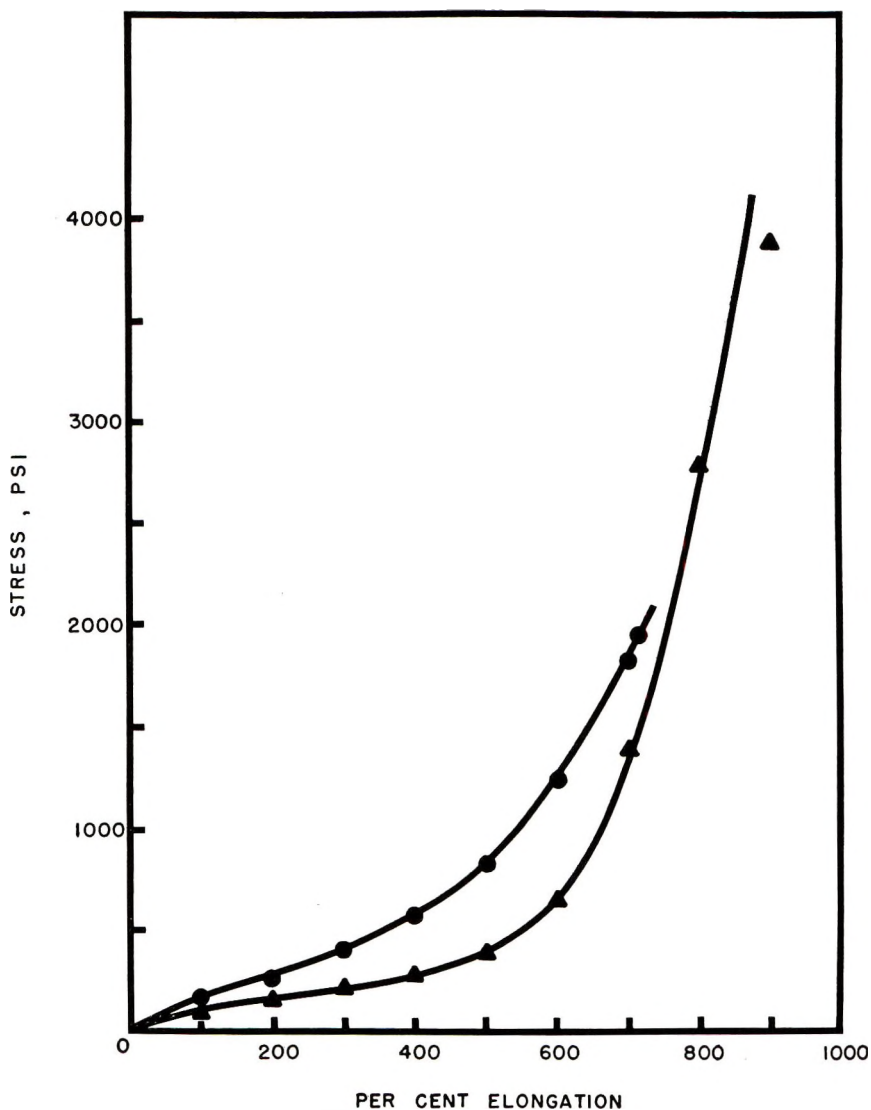


Fig. 2. Stress-strain behavior at 25°C. for gum vulcanizates of *cis*-1,4-polyisoprene (▲) and dichlorocarbene-*cis*-1,4-polyisoprene adduct B (●).

A molded, unstretched sample of adduct A was shown to be amorphous by x-ray diffraction. The stretched sample flowed considerably and it was not possible to obtain an x-ray diffraction in the stretched state. On storage at  $-25^{\circ}\text{C}$ . for about 72 hrs., it did not show any sign of crystallization.

The relative modulus versus temperature data on adduct A were obtained by the low temperature torsion flex test and are shown in Figure 1 together with corresponding data for the unreacted *cis*-1,4-polyisoprene. The relative modulus is defined as the ratio of the modulus at any given temperature to the modulus at  $25^{\circ}\text{C}$ . The values of the low temperature parameters are given in Table I. The adduct A was far less rubbery than expected from its  $T_{10}$  temperature of  $-41^{\circ}\text{C}$ . Presumably, it was a mixture of polymers

of different compositions and its chlorine content reflected only the average composition.

Stress-strain properties were determined on another preparation, adduct B. This adduct was prepared at 15°C. under conditions similar to those used for adduct A except that the chloroform was added last to the agitated mixture of a *cis*-1,4-polyisoprene solution and potassium *tert*-butoxide.

Adduct B was compounded as follows with all ingredients expressed as weight in parts per 100 parts of the adduct: zinc oxide, 6; stearic acid, 4; sulfur, 3.5; mercaptobenzothiazole, 0.5; and tetraethylenepentamine, 1. The physical properties of the gum vulcanizates are given in Table II together with the corresponding data from the *cis*-1,4-polyisoprene vulcanizates for comparison. The stress-strain data are also shown in Figure 2. The presence of dichlorocyclopropane ring structures in adduct B disrupts the regularity of the *cis*-1,4-polyisoprene. As a result, its vulcanizates fail to crystallize on stretching. Presumably this factor is responsible for tensile strength values lower than those obtained from the vulcanizates of *cis*-1,4-polyisoprene. Due to the limited data, the effect of the modification of the *cis*-1,4-polyisoprene chain with dichlorocyclopropane ring structures on the swelling ratio of the vulcanizates cannot be determined. Differences in crosslink density of the vulcanizates and molecular weights of the rubbers are other important considerations in such a comparison.

#### References

1. W. Kirmse, *Carbene Chemistry*, Academic Press, New York, 1964.
2. J. Lal and W. M. Saltman, French Pat. 1,387,425 (January 30, 1964).
3. C. Pinazzi and G. Levesque, *Compt. Rend.*, **260**, 3393 (1965); "Addition of Carbenes to *cis*-1,4-Polyisoprene and to Analogous Polymers," Preprint No. P625, International Symposium on Macromolecular Chemistry, Prague, 1965.
4. ASTM D 1053-61, *Am. Soc. Testing Mater. ASTM Std.*, **1964**, Part 28, 524.

JOGINDER LAL  
WILLIAM M. SALTMAN

The Goodyear Tire and Rubber Company  
Research Division  
Akron, Ohio

Received December 3 1965

### *The Blue Complexes of Iodine with Poly(vinyl Alcohol) and Amylose*

Very little is known about the molecular structure of the blue complexes of poly(vinyl alcohol) with iodine, while the mechanism of the amylose-iodine reaction has been well elucidated.

Some of the essential features of the latter reaction are as follows:<sup>1</sup> (1) Amylose exists in aqueous solution in the shape of a loose, locally disturbed helix.<sup>2</sup> (2) When iodine is added and iodide ions are present, a channel inclusion compound is formed in which the helix structure is tightened and a linear polyiodide chain becomes nested inside the channel of the amylose helix. (3) One turn of the helix consists of six glucosane residues and envelopes one molecule of iodine.<sup>3</sup>

The wavelength of the absorption maximum of the complex is a function of the length of the polyiodide chain,<sup>4</sup> and this again depends upon the degree of polymerization of the host molecule, at least up to a certain molecular weight. Thus, the absorption maximum would lie at 540  $m\mu$  for an amylose hydrolyzate with a DP of 41 and move up gradually with increasing chain length, reaching 630  $m\mu$  for a native amylose.<sup>5</sup> Above a DP of 300, however, the correlation between the length of the amylose chain and the wavelength of the absorption maximum breaks down,<sup>6</sup> and other factors seem to influence the length of the polyiodide chain. By a suitable choice of the experimental conditions, the absorption maximum of an amylose complex can be moved up to 675  $m\mu$ .<sup>7</sup>

It appears that high molecular weight amylose prefers to form several shorter helices instead of one very long one.<sup>2</sup> These helices, being part of one molecular chain, may tend to associate laterally, which would be in accordance with a recent finding of Yamashita,<sup>8</sup> who showed that helices belonging to the same molecule are backfolded upon themselves in amylose monocrystals. In solution the loops between the amylose-iodine helices can be broken enzymatically, the helices themselves remaining intact.<sup>2</sup>

The mechanism of the poly(vinyl alcohol)-iodine reaction is much less clear. Considerably higher concentrations of the reactants are necessary to bring about the blue coloration,<sup>3</sup> which in itself is not surprising. For a randomly coiled PVA molecule assuming an ordered shape so that it can accommodate and stabilize a linear polyiodide chaining should be accompanied by a much larger entropy decrease than that in the case of amylose. Thus, other factors being equal, the free-energy change of the reaction of iodine with poly(vinyl alcohol) could be expected to be considerably lower than for amylose. That the ordered shape of the PVA chain may be that of a helix has repeatedly been suggested,<sup>9,10</sup> but no real proof has been presented so far.

The absorption maximum of the PVA-iodine complex has variously been reported to lie somewhere between 595 and 620  $m\mu$ <sup>11-14</sup> in the absence of boric acid, and at 670  $m\mu$  in its presence.<sup>15</sup> If, as in the case of amylose, the wavelength of the absorption maximum is here also a function of the length of the linear polyiodide chain, it means that boric acid causes the polyiodide chain to become longer. One would then expect this lengthening of the polyiodide chain by boric acid to proceed in a continuous fashion, instead of in a jump from a length corresponding to 620  $m\mu$  to one corresponding to 670  $m\mu$ .

In our studies of the PVA-iodine complexes<sup>16</sup> we have found that the absorption maximum of these complexes can be shifted continuously from 580 up to 700  $m\mu$ . This can be done, in a series of reaction mixtures, by decreasing the concentration of iodide ions, and increasing that of boric acid, while leaving the iodine concentration constant.

With increasing boric acid concentration, the color intensity rises considerably; this testifies for the increasing degree of iodine binding by the polymer.<sup>17</sup> Spectrophotometric titrations of poly(vinyl alcohol) solutions, in the presence of sufficient iodine, give typical, sigmoidal curves when the extinction at the absorption maximum is plotted versus boric acid concentration, a shape which is often associated with a coil-helix transition.<sup>18</sup>



We had also noted that a poly(vinyl alcohol) molecule can reach a saturation value of iodine binding without coming out of solution. "Saturation value" is here defined as the point for a given polymer concentration at which no further increase in color intensity can be brought about by increasing the iodine or boric acid concentration. The highest extinction coefficient per base mole of PVA that could be attained was approximately 1840. Taking 44,000 as the molar extinction coefficient of iodine in a polyiodide chain, as is found in the case of amylose,<sup>17</sup> the limiting stoichiometry of vinyl alcohol residues per iodine molecule would be  $44000/1840 \approx 24$ . With the aid of Stuart models, one can demonstrate that 24 vinyl alcohol residues can snugly envelope one iodine molecule by forming two turns of a poly(vinyl alcohol) helix.

In this spatial arrangement, the role of the boric acid may be to stabilize the helical structure by holding on to two OH-groups belonging to two successive turns of the helix which have become close neighbors due to the helical conformation of the polymer.

In the absence of boric acid, there exists an iodine concentration threshold below which no blue staining will occur. Above it the color development is slow; the intensity peak is reached only after several days.<sup>14</sup> By that time, the complex is no longer in equilibrium with its surrounding solution, and subsequent dilution to below the threshold concentration does not cause the complex to decompose again, at least not for a very long time.

These and other irreversible phenomena in the PVA-iodine interaction can be qualitatively understood by assuming that the reaction proceeds via a process of short helix formation at a number of places along the polymer chain, rapidly followed by intramolecular helix association. After that, a relatively slow process of "recrystallization" of the helix cluster sets in, during which the channels become long and regular enough for short iodine chains to link up and develop the blue color.

In the absence of boric acid different PVA products of similar molecular weights often display, under identical reaction conditions, large differences in staining intensities. This can be ascribed to differences in the stereoregularity of the respective polymers.<sup>11</sup> A poly(vinyl alcohol) with a more random conformation seems to have greater difficulty in assuming the peculiar shape necessary for complex formation with iodine and, thus, will display lower color intensities than more regularly built molecules in the same chemical environment.

Recently Tebelev et al.<sup>19</sup> rightly pointed out that beside steric randomness, disturbances in the PVA chain regularity such as acetate rests, branching, and others<sup>20</sup> can likewise diminish the strength of iodine binding by poly(vinyl alcohol).

The same authors also reported a marked increase in iodine binding when the PVA concentration was raised from 0.1 to 1.0%. They interpreted this to mean that complexed iodine is taken up into the interstices between aggregated molecules. This conclusion seems to us difficult to sustain. Our own experiments had indicated that below  $10^{-2}$  base mole per liter ( $\sim 0.05\%$ ) there was essentially no dependence of the degree of iodine binding per vinyl alcohol group on polymer concentration. Therefore, if during complex formation helices grow and associate, they will do so intramolecularly. On the other hand, if polymer concentrations are progressively increased a point will be reached eventually where the domains of individual polymer molecules will begin to interpenetrate. In such a situation a newly forming helix may join any aggregate of helices either from the same or from any other molecule in close proximity. Because of the additional stability of the complex believed to be derived from such an association, the relative degree of iodine binding may, from this point on, also become a function of polymer concentration.

The concentration at which domain interpenetration commences can be estimated by a number of methods.<sup>21,22,23</sup> Relating directly to poly(vinyl alcohol), Kuhn and Balmer<sup>24</sup> have shown experimentally that in crosslinking the transition from a purely intramolecular to an intermolecular reaction occurs at a polymer concentration around 0.2% ( $\sim 4 \times 10^{-2}$  base mole/l.). It is quite likely, therefore, that in other processes involving poly(vinyl alcohol), where either an intra- or an intermolecular interaction

is possible, the transition from the one to the other may also occur at concentrations somewhere between 0.1 and 1.0%, which is the region Tebelev and co-workers had studied. The dependence on polymer concentration which they observed in no way constitutes any evidence, however, for the actual location of the iodine molecules in a PVA complex.

Finally, it is worth recalling that Kuhn<sup>24</sup> found the effect of the intramolecular reaction in poly(vinyl alcohol) to increase with the square root of the degree of polymerization. A qualitatively analogous dependence on the degree of polymerization has been observed by Imai and Matsumoto<sup>11</sup> in the PVA-iodine complex formation.

### References

1. Senti, F. R., and S. R. Erlander, in *Non-Stoichiometric Compounds*, Academic Press, New York, 1964, p. 568.
2. Hollo, J., and J. Szejtli, *Brauwissenschaft*, **13**, 358, 380 (1960).
3. Rundle, R. E., J. F. Foster, and R. A. Baldwin, *J. Am. Chem. Soc.*, **66**, 2116 (1944).
4. Ono, S., S. Tsuchihashi, and T. Kuge, *J. Am. Chem. Soc.*, **75**, 3601 (1953).
5. Ohashi, K., *Nippon Nogei Kagaku Kaishi*, **33**, 576, 580 (1959); *Chem. Abstr.*, **58**, 1619d, 2561c (1963).
6. Greenwood, C. T., in *Advances in Carbohydrate Chemistry*, Vol. 11, Academic Press, New York, 1956, p. 370.
7. Foster, J. F., and E. F. Paschall, *J. Am. Chem. Soc.*, **74**, 2105 (1952).
8. Yamashita, Y., *Chem. High Polymers Japan*, **21**, 103 (1964).
9. Schildknecht, C. E., Abstract 138th Meeting of the American Chemical Society, New York 1960, 12T-26.
10. Brown, J. F., *Sci. Am.*, **207**, 82 (1962).
11. Imai, K., and M. Matsumoto, *J. Polymer Sci.*, **55**, 335 (1961).
12. Yoda, T., *Nippon Shashin Gakkai Kaishi*, **23**, 179 (1960).
13. Rosen, H., G. H. McCain, A. L. Endrey, and C. L. Sturm, *J. Polymer Sci. A*, **1**, 951 (1963).
14. Glikman, S. A., S. M. Ushakov, E. P. Korchagina, and E. Lavrientieva, *Dokl. Akad. Nauk SSSR*, **154**, 372 (1964).
15. West, C. D., *J. Chem. Phys.*, **17**, 219 (1949).
16. Zwick, M. M., *J. Appl. Polymer Sci.*, **9**, 2393 (1965).
17. Murakami, H., *J. Chem. Phys.*, **22**, 367 (1954).
18. Peticolas, W. L., *Nature*, **197**, 898 (1963).
19. Tebelev, L. G., G. F. Mikulskii, E. P. Korchagina, and S. A. Glikman, *Vysokomolekul. Soedin.*, **7**, 123 (1965).
20. Zwick, M. M., and C. van Bochove, *Textile Res. J.*, **34**, 417 (1964).
21. Weissberg, S. G., R. Simha, and S. Rothman, *J. Res. Natl. Bur. Stand.*, **47**, 298 (1951).
22. Jacobson, H., and W. H. Stockmayer, *J. Chem. Phys.*, **18**, 1600 (1950).
23. Kuhn, W., and H. Majer, *Makromol. Chem.*, **18/19**, 239 (1955).
24. Kuhn, W., and G. Balmer, *J. Polymer Sci.*, **57**, 311 (1962).

M. M. ZWICK

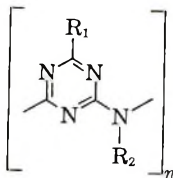
Spinning Research Department  
Central Laboratory T.N.O.  
Delft, The Netherlands

Received October 8, 1964

Revised November 12, 1965

**Preparation and Properties of a New  
Poly-*s*-Triazinylene Imide**

Polymers of the type



with  $R_1$  being  $-\text{C}_6\text{H}_5$ ,  $-\text{CH}_3$ ,  $-\text{OC}_6\text{H}_5$ ,  $-\text{NHC}_6\text{H}_5$ , or  $-\text{Cl}$ , and  $R_2$  being  $-\text{H}$ ,  $-\text{CH}_3$ ,  $-\text{C}_2\text{H}_5$ , or  $-\text{C}_8\text{H}_5$ , have been described earlier.<sup>1</sup>

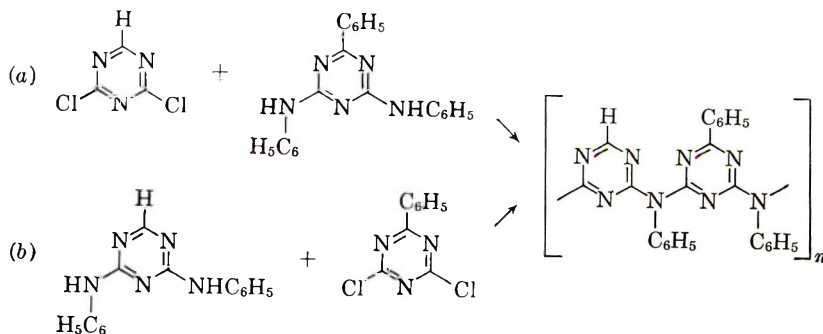
It seemed to be of interest to study briefly the *s*-triazinylene imide system with  $R_1$  being hydrogen, since it allowed closer packing of the polymer chains, and higher rigidity and thermal stability could be expected.

Starting materials used for this approach were 2,4-dibromo-*s*-triazine hydrobromide and 2,4-dichloro-*s*-triazine.\* The extreme sensitivity of these two compounds towards moisture pointed to a high reactivity in general, with the possibility of obtaining polymers of higher molecular weight than found previously.<sup>1</sup>

2,4-dibromo-*s*-triazine hydrobromide was synthesized by brominating *s*-triazine,<sup>2,3</sup> which in turn was prepared by pyrolysis of formamidine hydrochloride.<sup>4,5</sup> 2,4-dichloro-*s*-triazine has been obtained through trimerization of cyanogen chloride with hydrogen cyanide in the presence of dry hydrogen chloride.<sup>6,7</sup> Procedure and purification of this compound were rather troublesome, and only a few grams of pure 2,4-dichloro-*s*-triazine were finally available. 2,4-dianilido-*s*-triazine was prepared by adding aniline to an ether suspension of 2,4-dichloro-*s*-triazine and heating, under evaporation of the ether, to 140°C. This compound, which had been obtained previously from 2,4-dibromo-*s*-triazine hydrobromide in only 10.2% yield,<sup>2</sup> and also from reduction of 2,4-dianilido-6-chloro-*s*-triazine, was synthesized in 35% yield.

All of the condensation reactions of 2,4-dibromo-*s*-triazine hydrobromide with 2,4-dianilido-6-phenyl-*s*-triazine and other aliphatic and aromatic diamines, in melt and in solution, led to partial or total decomposition of 2,4-dibromo-*s*-triazine. Only unreacted diamines or their hydrobromide salts could be isolated from the reaction mixtures. The dibromotriazine hydrobromide itself starts to decompose at 160°C., under evolution of bromine and hydrogen bromide.

A polymer can be obtained, however, from the melt reaction of 2,4-dichloro-*s*-triazine with 2,4-dianilido-6-phenyl-*s*-triazine as well as 2,4-dianilido-*s*-triazine with 2,4-dichloro-6-phenyl-*s*-triazine:

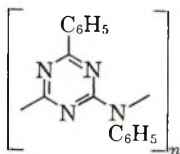


\* Synthesized by Wyandotte Chemicals Corporation, Wyandotte, Michigan, under Air Force contract.

The components were reacted under nitrogen, at temperatures between 200 and 220°C. for 24–40 hr., until the evolution of hydrogen chloride ceased.

From both reactions, practically the same polymer has been obtained. It is a light brown powder, soluble in *m*-cresol and tetrahydrofuran. Its molecular weight estimated from the inherent viscosity of 0.05 is probably in the order of 2000. While Cl end-group analysis would indicate molecular weights of either 4000 or 8000, a lower molecular weight seems to be more realistic since some of the original Cl endgroups might have been hydrolyzed.

The IR spectrum is very similar to poly-6-phenyl-*N*-phenyl-2,4-*s*-triazinylene imide<sup>1</sup>



except for an additional band in the 13 $\mu$  region. Onset of softening under load occurs at about 100°C., with a major penetration around 200°C., somewhat higher than the above described polymer. The highest rate of weight loss during thermogravimetric analysis is in about the same temperature range as that of the homopolymer, however the residue at 900°C. is considerably higher. Differential thermal analysis indicates a melting endotherm between 177 and 182°C. and a decomposition exotherm at 404°C. Elemental analysis gave the following results:

ANAL. Calcd. for the pentamer (10 triazine units, molecular weight 2117): C, 68.0; H, 3.8; N, 26.5; Cl, 1.7. Found (approach *a*) C, 68.2; H, 4.0; N, 26.3. Found (approach *b*) C, 66.0; H, 4.0; N, 25.7; Cl, 1.3.

Trials to synthesize the homopolymer from 2,4-dichloro-*s*-triazine (m.p. 47°C.) and 2,4-dianilido-*s*-triazine (m.p. 307°C.) failed due to the difference in melting points and extensive sublimation. A solution polymerization also gave unsatisfactory results.

#### References

1. G. F. L. Ehlers, and J. D. Ray, *J. Polymer Sci. A*, **2**, 4989 (1964).
2. C. Grundmann, and A. Kreutzberger, *J. Am. Chem. Soc.*, **76**, 632 (1954).
3. C. Grundmann, and A. Kreutzberger, *J. Am. Chem. Soc.*, **77**, 44 (1955).
4. F. C. Schaefer, I. Heckenbleikner, G. A. Peters, and V. P. Wystrach, *J. Am. Chem. Soc.*, **81**, 1466 (1959).
5. C. Grundmann, H. Schroeder, and W. Ruske, *Ber.*, **87**, 1865 (1954).
6. I. Heckenbleikner, *J. Am. Chem. Soc.*, **76**, 3032 (1954).
7. U. S. Pat. 2,762,794 (1956).

G. F. L. EHLERS  
J. D. RAY\*

Air Force Materials Laboratory  
Wright Patterson Air Force Base, Ohio

Received December 2, 1965

\* 1960–1964 University of Dayton Research Institute, Dayton, Ohio. Present address: Emerson Electric of St. Louis, St. Louis, Mo.

## ERRATA

### Terpolymers of Ethylene and Propylene with *d*-Limonene and $\beta$ -Pinene

(article in *J. Polymer Sci. A*, **3**, 3815, 1965)

By RALPH W. MAGIN, C. S. MARVEL, and EDWARD F. JOHNSON  
*Department of Chemistry, University of Arizona, Tucson, Arizona*

Sample I-49, listed in Table I, should be deleted from consideration in the further study of this paper.

### Ringed Spherulites and Multiple-Order Light Scattering from Ringed Spherulites

(article in *J. Polymer Sci. A*, **3**, 4093, 1965)

By ROBERT S. MOORE  
*Bell Telephone Laboratories, Murray Hill, New Jersey*

On page 4111 Figures 14c and 14d should be interchanged and each should be inverted.

### Studies on Alcohol-Modified Transition Metal Polymerization Catalysts. I. Infrared Studies

(article in *J. Polymer Sci. A*, **3**, 3713, 1965)

By R. H. MARCHESSAULT, H. CHANZY, S. HIDER, W. BILGOR,  
and J. J. HERMANS  
*Cellulose Research Institute and Chemistry Department,  
State University College of Forestry, Syracuse, New York*

The captions for Figures 9 and 10 should read as follows:

Fig. 9. High-resolution infrared spectra of 0.1*M* solutions of *n*-propanol and  $\text{TiCl}_4$  in  $\text{CCl}_4$  before and after addition of 0.1*M* triethyl aluminum: (A) 3:1 ratio of *n*-propanol/ $\text{TiCl}_4$ ; (B) 3:1:1 ratio of *n*-propanol/ $\text{TiCl}_4$ / $\text{Al}(\text{Et})_3$ .

Fig. 10. High-resolution infrared spectra of mixtures containing 3 moles of *n*-propanol per mole of  $\text{TiCl}_4$  at various dilutions in  $\text{CCl}_4$ .



**Studies in Cyclopolymerization. II. Relative Rates of Addition  
in the Copolymerization of Acrylonitrile with Certain 1,4-Dienes**

(article in *J. Polymer Sci. A*, **3**, 4205, 1965)

By GEORGE B. BUTLER and RADHAKRISHNA B. KASAT

*Department of Chemistry, University of Florida,  
Gainesville, Florida*

On pages 4207 and 4209 Figures 1 and 2 should be interchanged.